Evaluation of Severe Accident Risks: Quantification of Major Input Parameters

Expert Opinion Elicitation on In-Vessel Issues

Prepared by
F. T. Harper, R. J. Breeding, T. D. Brown, J. J. Gregory,
A. C. Payne, E. D. Gorham, C. N. Amos

Sandia National Laboratories
Operated by
Sandia Corporation

Evaluation of Severe Accident Risks: Quantification of Major Input Parameters

Expert Opinion Elicitation on In-Vessel Issues

Prepared by
F. T. Harper, R. J. Breeding, T. D. Brown, J. J. Gregory,
A. C. Payne, E. D. Gorham, C. N. Amos[1]

Sandia National Laboratories
Albuquerque, NM 87185

[1]Science Applications International Corporation, Albuquerque, NM

ABSTRACT

This report records part of the vast amount of information received during the expert judgment elicitation process that took place in support of the NUREG-1150 effort sponsored by the U.S. Nuclear Regulatory Commission. The results of the In-Vessel Expert Panel are presented in this part of Volume 2 of NUREG/CR-4551. The In-Vessel Panel considered six issues:

1. Temperature-Induced pressurized water reactor (PWR) Hot Leg or Surge Line Failure Before Vessel Breach;

2. Temperature-Induced Steam Generator Tube Rupture (SGTR) Before Vessel Breach;

3. Boiling water reactor (BWR) In-Vessel Hydrogen Production;

4. BWR Bottom Head Failure;

5. PWR In-Vessel Hydrogen Generation;

6. PWR Bottom Head Failure.

The report begins with a brief discussion of the methods used to elicit the information from the experts. The information for each issue is then presented in five sections: (1) a brief definition of the issue, (2) a brief summary of the technical rationale supporting the distributions developed by each of the experts, (3) a brief description of the operations that the project staff performed on the raw elicitation results in order to aggregate the distributions, (4) the aggregated distributions, and (5) the individual expert elicitation summaries. The individual expert elicitation summaries were written soon after the elicitation and were sent to the experts for review. They represent the raw results as received directly from the experts.

CONTENTS

FIGURES

FIGURES (Continued)

FIGURES (Continued)

FIGURES (Continued)

TABLES (Continued)

FOREWORD

This is one of many documents that constitute the technical basis for the NUREG-1150 document produced by the NRC Office of Nuclear Regulatory Research. This document's purpose is to give the results of the In-Vessel Expert Panel. The document consists of the distributions and associated technical rationale provided by the expert panels for the phenomenological questions posed by the NUREG-1150 analysts.

Figure 1 identifies all the documents that present the results of the accident progression analysis, the source term analysis, the consequence analysis, and the overall risk integration. Three interfacing programs performed this work: the Accident Sequence Evaluation Program (ASEP), the Severe Accident Risk Reduction Program (SARRP), and the PRA Phenomenology and Risk Uncertainty Evaluation Program (PRUEP). Table 1 is a list of all of the original primary documentation (published in 1987) and the corresponding revised documentation that supports the current version of NUREG-1150.

The current NUREG/CR-4551 covers the analysis included in the original NUREG/CR-4551 and NUREG/CR-4700. The accident progression event trees (APETs) originally documented in NUREG/CR-4700 are now documented in the appendices of Volumes 3 to 7 of NUREG/CR-4551.

Originally, NUREG/CR-4550 was published without the designation "Draft for Comment." Thus, the final revision of NUREG/CR-4550 is designated Revision 1. The label Revision 1 is used consistently on all volumes, including Volume 2, which was not part of the original documentation. NUREG/CR-4551 was originally published as a "Draft for Comment"; the Revision 1 designator is used to maintain consistency with NUREG-4550 documents.

There are several other reports published that are closely related to NUREG/CR-4551. These are:

NUREG/CR-5380, SAND88-2988, S. J. Higgins, "A User's Manual for the Post Processing Program PSTEVNT," Sandia National Laboratories, Albuquerque, NM, 1989.

NUREG/CR-5360, SAND89-0943, H.-N. Jow, W. B. Murfin, and J. D. Johnson, "XSOR Codes User's Manual," Sandia National Laboratories, Albuquerque, NM, 1989.

NUREG/CR-4624, BMI-2139, R. S. Denning et al., "Radionuclide Release Calculations for Selected Severe Accident Scenarios," Volumes I-V, Battelle Columbus Division, Columbus, OH, 1986.

NUREG/CR-5062, BMI-2160, M. T. Leonard et al., "Supplemental Radionuclide Release Calculations for Selected Severe Accident Scenarios," Battelle Columbus Division, Columbus, OH, 1988.

NUREG/CR-5331, SAND89-0072, S. E. Dingman et al., "MELCOR Analyses for Accident Progression Issues," Sandia National Laboratories, Albuquerque, NM, 1989.

NUREG/CR-5253, SAND88-2940, R. L. Iman, J. C. Helton, and J. D. Johnson, "A User's Guide for PARTITION: A Program for Defining the Source Term/Consequence Analysis Interfaces in the NUREG-1150 Probabilistic Risk Assessments," Sandia National Laboratories, Albuquerque, NM, 1989.

NUREG/CR-5382, SAND88-2695, J. C. Helton et al., "Incorporation of Consequence Analysis Results into the NUREG-1150 Probabilistic Risk Assessments," Sandia National Laboratories, Albuquerque, NM, 1989.

NUREG/CR-5174, SAND88-1607, J. Michael Griesmeyer and L. N. Smith, "A Reference Manual for the Event Progression Analysis Code (EVNTRE)," Sandia National Laboratories, Albuquerque, NM, 1989.

NUREG/CR-5262, SAND88-3093, R. L. Iman, J. D. Johnson, and J. C. Helton, "A User's Guide for the Probabilistic Risk Assessment Model Integration System (PRAMIS)," Sandia National Laboratories, Albuquerque, NM, May 1990.

SUPPORT DOCUMENTS TO NUREG-1150
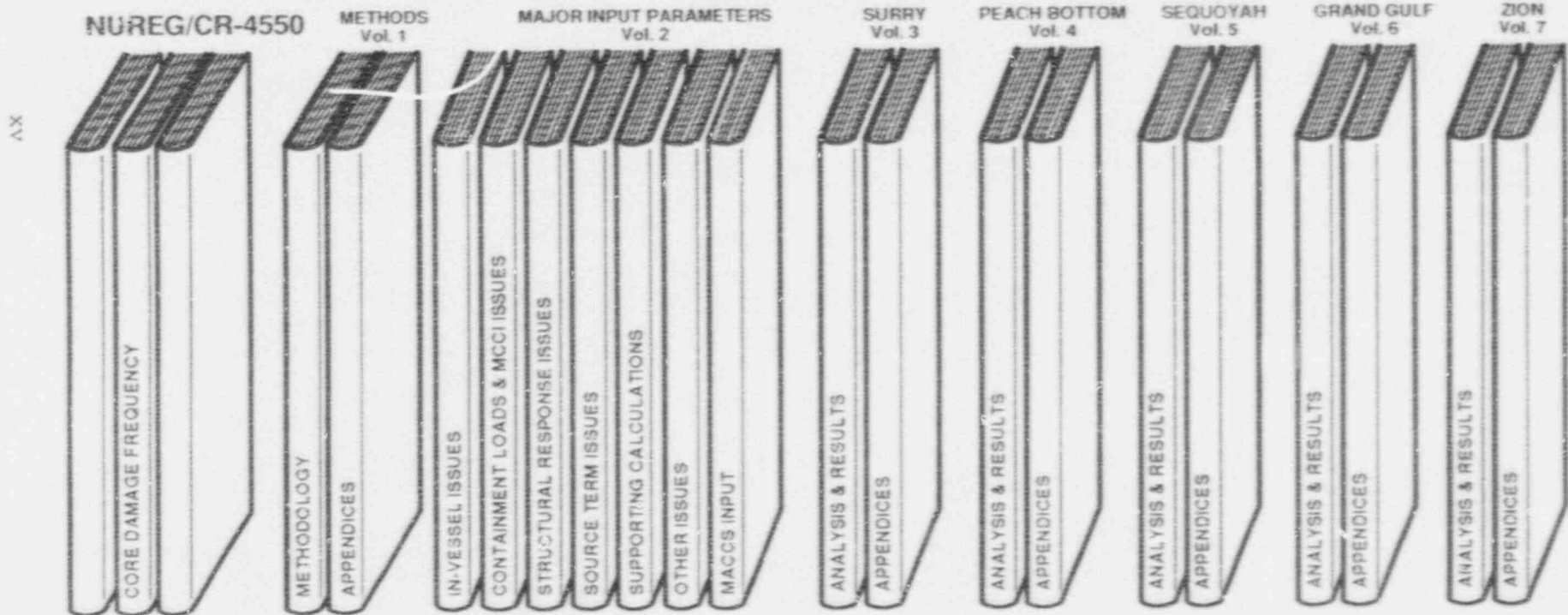
Figure 1. Back-End Documentation for NUREG-1150.

Table 1. NUREG-1150 Analysis Documentation

Original Documentation

NUREG/CR-4550	NUREG/CR-4551	NUREG/CR-4700
Analysis of Core Damage Frequency From Internal Events	Evaluation of Severe Accident Risks and the Potential for Risk Reduction	Containment Event Analysis for Potential Severe Accidents

Vol.			Vol.			Vol.		
1	Methodology		1	Surry Unit 1		1	Surry Unit 1	
2	Summary (Not Published)		2	Sequoyah Unit 1		2	Sequoyah Unit 1	
3	Surry Unit 1		3	Peach Bottom Unit 2		3	Peach Bottom Unit 2	
4	Peach Bottom Unit 2		4	Grand Gulf Unit 1		4	Grand Gulf Unit 1	
5	Sequoyah Unit 1		5	Zion Unit 1				
6	Grand Gulf Unit 1							
7	Zion Unit 1							

Revised Documentation

NUREG/CR-4550, Rev. 1, Analysis of Core Damage Frequency | NUREG/CR-4551, Rev. 1, Eval. of Severe Accident Risks

Vol.				Vol.		
1	Methodology			1	Part 1, Methodology; Part 2, Appendices	
2	Part 1	Expert Judgment Elicit. Expert Panel		2	Part 1 In-Vessel Issues	
	Part 2	Expert Judgment Elicit. Project Staff			Part 2 Containment Loads and MCCI Issues	
					Part 3 Structural Issues	
					Part 4 Source Term Issues	
					Part 5 Supporting Calculations	
					Part 6 Other Issues	
					Part 7 MACCS Input	
3	Part 1	Surry Unit 1 Internal Events		3	Part 1 Surry Analysis and Results	
	Part 2	Surry Unit 1 Internal Events App.			Part 2 Surry Appendices	
	Part 3	Surry External Events				
4	Part 1	Peach Bottom Unit 2 Internal Events		4	Part 1 Peach Bottom Analysis and Results	
	Part 2	Peach Bottom Unit 2 Int. Events App.			Part 2 Peach Bottom Appendices	
	Part 3	Peach Bottom Unit 2 External Events				
5	Part 1	Sequoyah Unit 1 Internal Events		5	Part 1 Sequoyah Analysis and Results	
	Part 2	Sequoyah Unit 1 Internal Events App.			Part 2 Sequoyah Appendices	
6	Part 1	Grand Gulf Unit 1 Internal Events		6	Part 1 Grand Gulf Analysis and Results	
	Part 2	Grand Gulf Unit 1 Internal Events App.			Part 2 Grand Gulf Appendices	
7	Zion Unit 1 Internal Events			7	Part 1 Zion Analysis and Results	
					Part 2 Appendices	

ACKNOWLEDGMENTS

ACRONYMS AND INITIALISMS

ADS   automatic depressurization system
AICC   adiabatic isochoric complete combustion
AIChE   American Institute of Chemical Engineers
ANL   Argonne National Laboratory
ANS   American Nuclear Society
APET   accident progression event tree
ASME   American Society of Mechanical Engineers
ATWS   anticipated transient without scram

BNL   Brookhaven National Laboratory
BWR   boiling water reactor

CCI   core-concrete interaction
CDF   cumulative distribution function
CRD   control rod drive

DBA   design basis accident
DCH   direct containment heating
DDT   deflagration-to-detonation transition
DF   decontamination factor
DMP   dump
DOE   Department of Energy

FCI   fuel-coolant interaction
FAI   Fauske and Associates, Inc.
FSAR   final safety analysis report

GP   gravity pour

HPME   high-pressure melt injection

IC   ice condenser
IDCOR   Industry Degraded Core Rulemaking
INEL   Idaho National Engineering Laboratory

LOCA   loss-of-coolant accident
LMFBR   liquid-metal fast breeder reactor
LMR   liquid-metal reactor
LSD   least significant difference
LWR   light water reactor

MAAP   Modular Accident Analysis Program
MCCI   molten core-coolant interactions

ORNL   Oak Ridge National Laboratory

PORV   power-operated relief valve
PRA   probabilistic risk analysis
PWR   pressurized water reactor

RCP	reactor coolant pump
RCS	reactor coolant system
RPV	reactor pressure vessel
RV	reactor vessel
SAIC	Science Applications International Corporation
S&W	Stone and Webster
SG	steam generator
SRV	safety relief valve
TVA	Tennessee Valley Authority
UHI	upper head injection
USC	University of Southern California
UCHB	unconditional hydrogen burn
UP	upper plenum

1. INTRODUCTION

The United States Nuclear Regulatory Commission (NRC) has prepared NUREG-1150[1] to examine the risk of accidents in a selected group of nuclear power plants. The three main objectives of NUREG-1150 are given below.

1. Prepare a current assessment of the severe accident risks of five nuclear power plants which will:

   - Provide a "snapshot" of risks reflecting plant design and operational characteristics, related failure data, and severe accident phenomenological information extant in March 1988;

   - Update the estimates of NRC's 1975 risk assessment, the Reactor Safety Study;

   - Include quantitative estimates of risk uncertainty, in response to a principal criticism of the Reactor Safety Study; and

   - Identify plant-specific risk vulnerabilities, in context of the NRC's individual plant examination process.

2. Summarize the perspectives gained in performing these risk analyses, with respect to:

   - Issues significant to severe accident frequencies, consequences, and risks;

   - Uncertainties for which the risk is significant and which may merit further research;

   - Comparisons with NRC's safety goals;

   - The potential benefits of a severe accident management program in reducing risk; and

   - The potential benefit of other plant modifications in reducing risk.

3. Provide a set of methods for the prioritization of potential safety issues and related research.

In support of NUREG-1150 and as part of the Accident Sequence Evaluation Program (ASEP) and the Severe Accident Risk Reduction Program (SARRP), Sandia National Laboratories (SNL) has directed the production of Level 3 probabilistic risk assessments (PRAs) for the Surry, Sequoyah, Peach Bottom, and Grand Gulf nuclear power plants. (Level 1 PRAs contain accident sequence analyses developed to the point of core damage; Level 2 PRAs include Level 1 and accident progression analyses; and Level 3 PRAs include Level 1, Level 2, and consequence analyses.) A PRA for the fifth NUREG-1150 plant, Zion, has been prepared by EG&G Idaho, Inc., of the Idaho National Engineering Laboratory (INEL) (Level 1) and Brookhaven National Laboratory (BNL) (Levels 2 and 3). Two of these analyses (Surry and Peach Bottom) include external events.

Expert judgment elicitation is an integral part of the methods used to produce the PRAs in support of NUREG-1150. Expert judgment is used where applicable experimental data or complete analyses are inadequate. Such situations are common in analysis of rare events and complicated severe accident phenomena. The purpose of this report is to provide the results and technical rationale obtained from the In-Vessel Expert Panel. The expert judgment methodology is presented in detail in NUREG/CR-4551 Volume 1.

Expert judgments are expressions of opinion, based on knowledge and experience, that experts make in responding to technical problems. Specifically, the judgments represent the expert's state of knowledge at the time of response to the technical question. Expert judgment is not restricted to the experts' answer but includes the experts' mental processes (definitions, assumptions, and algorithms) for arriving at answers.

Expert judgment is necessarily used in all technical fields. Because these judgments are often implicit, they are sometimes not acknowledged as being expert judgments. For example, expert judgment is frequently used implicitly, even unconsciously, when researchers make decisions about defining problems, establishing boundary conditions, or screening data. By contrast, expert judgment can also be obtained explicitly, through formal processes.

Risk assessment frequently needs explicit expert judgment as a source of data, particularly if one or more of the following situations exist:

1. No other data (analytical or experimental) for predicting the outcome of phenomena are available;

2. High variability characterizes the data;

3. Experts question the applicability of the data;

4. Existing data needs to be supplemented, interpreted, or incorporated with model or code calculations;

5. Analysts need to determine the state of knowledge about what is currently known, what is not known, and what is worth learning.

The issue selection process consisted of accumulating an extensive list of potential issues by plant or across plants and then evaluating the significance of each issue. Expert panel members participated in the issue selection by reviewing the issues selected and rejected for the expert judgment process and recommending the addition, deletion, or modification of issues from the initial list.

There were six in-vessel issues that were considered important enough to be the subject of a formal expert judgment elicitation. Table 1 lists these issues.

Section 2 of this report briefly outlines the expert selection process and gives a short biograp'ical sketch of each expert. Section 3 describes the fundamental expert judgment elicitation methodology. Section 4 lists the meetings held for the in-vessel issues and the people who gave presentations at the meetings. Section 5 constitutes the bulk of this report and contains a description of each issue considered, a summary of the technical rationale applied by the experts to the issue, a description of the method used to aggregate the expert's distributions, the aggregated distributions, and written accounts of each individual response to the question. The individual expert's narrative includes the distributions and the detailed rationale behind the distributions. Each account was written by the substantive expert who assisted with the elicitation. In all cases the experts were given ample opportunity to review these written accounts and approve them. In a few cases, the experts did not respond and were informed that their lack of response would be assumed to be tacit approval of the written account.

Table 1-1
In-Vessel Issues Considered for Expert Judgment Elicitation

Issue	Applicable Plants
1. Temperature-Induced PWR Hot Leg or Surge Line Failure Before Vessel Breach	All PWRs
2. Temperature-Induced Steam Generator Tube Rupture (SGTR) Before Vessel Breach	All PWRs
3. BWR In-Vessel Hydrogen Production	All BWRs
4. BWR Bottom Head Failure	All BWRs
5. PWR In-Vessel Hydrogen Generation	All PWRs
6. PWR Bottom Head Failure	All PWRs

REFERENCE

1. U.S. Nuclear Regulatory Commission, "Severe Accident Risks: An Assessment for Five U. S. Nuclear Power Plants," NUREG-1150,Vol.1, Office of Nuclear Regulatory Research, June 1989. (Second Draft for Peer Review)

2. EXPERT CREDENTIALS

The objective for selecting the panel members was to obtain experts with maximum expertise in the fields of in-vessel phenomena. The project attempted to include a wide diversity of expertise that encouraged alternative points of view. The selection of experts would preclude stakeholders in the findings of NUREG-1150 from participating as members of the expert panel. This led to several criteria in selecting the experts:

1. Experts would demonstrate experience by authoring publications, demonstrating hands-on experience, and consulting or managing research in the areas related to the issues;

2. Experts would have a wide variety of experience obtained in universities, consulting firms, laboratories, nuclear utilities, or government agencies;

3. The experts would represent as wide a perspective of the issues as possible;

4. The experts would be willing to be elicited under the methodology to be used.

To ensure proper representation, letters were sent to many organizations requesting nominations for experts to serve on the in-vessel, containment loads, molten core/containment interaction, structural response, and source term panels. Some of the organizations that received these letters are listed below:

Atomic Energy of Canada LTD.
Battelle Columbus Division
Bechtel Western Power Company
Brookhaven National Laboratory
Commonwealth Edison
Electric Power Research Institute
General Electric
Idaho National Engineering Laboratory, (EG&G Idaho, Inc.)
Illinois Department of Nuclear Safety
International Technology Corporation
MHB Technical Associates
New York Power Authority
NUMARC
Oak Ridge National Laboratory
Philadelphia Electric Co.
Sandia National Laboratories
Stone and Webster Engineering Corporation
Systems Energy Resources, Inc.
Tennessee Valley Authority
U.S. Nuclear Regulatory Commission
Virginia Electric Power Co.
Westinghouse Electric Corp.

It was impossible to satisfy each criterion entirely for every expert/ issue combination. Nevertheless, we were pleased with the high quality and objectivity of the experts. The experts chosen for the containment loads (CL) and molten core/containment interaction (MCCI) issues were:

Peter Bieniarz   Risk Management Associates
William Camp   Sandia National Laboratories
Vern Denny   Science Application International Corporation
Richard Hobbins   Idaho National Engineering Laboratory
Steve Hodge   Oak Ridge National Laboratory
Robert J. Lutz, Jr.   Westinghouse Electric Corporation
Michael Podowski   Rensselaer Polytechnic Institute
Garry Thomas   Electric Power Research Institute
Robert Wright   Nuclear Regulatory Commission

Brief biographical sketchs of the experts are presented below:

In-Vessel Expert Panel

PETER P. BIENIARZ. Peter Bieniarz is President of Risk Management Associates, Inc., (RMA). He has been heavily involved in the severe accident analysis field from both the probabilistic risk analysis (PRA) and fission product behavior ends. As part of his work, Mr. Bieniarz has been either involved in, or directed, several PRAs and has developed several analytical methods for calculating the progression of severe accidents. Before establishing RMA, Mr. Bieniarz was the General Manager of the Albuquerque Office of Energy, Inc., and Senior Technical Consultant with Pickard Lowe and Garrick, Inc.

WILLIAM CAMP. Dr. Camp is Department Manager of the Mathematics and Computational Science Department, 1420, at Sandia National Laboratories (SNL) where he provides the mathematical and computational resources necessary to carry out leading-edge research on the application of large-scale parallelism to difficult problems in science and engineering.

At Sandia, Dr. Camp has been a staff member in the High-Temperature Science Division, Solid State Theory Division, a visiting staff member in the Systems Analysis Division at SNL in Livermore, CA, and the supervisor of the Reactor Safety Theoretical Physics Division. He has (a) managed the development of VICTORIA, a computer model for the determination of chemical equilibrium for an arbitrary number of elements; (b) managed the development of several large computer codes for multiphase flow, heat transfer, and radiation transport, in which state-of-the-art methods are utilized or extended; (c) managed the development of CHARM, an advanced model for aerosol behavior in complex flows; (d) instituted and directed research on computational analysis of non-linear instability problems encountered in partial differential equations for fluid dynamics (Rayleigh-Taylor Instabilities); and (e) instituted and directed the development of MELPROG/TRAC, a system-level model of reactor primary systems during severe accidents. His current research involves "exact" numerical simulation of

nonlinear instabilities in fluid dynamics, extraction of fractal and multifractal behavior in such instabilities and development of models for the transition to chaotic behavior.

VERNON DENNY. Vernon Denny is a senior technical staff member in the Thermal Sciences Division of Science Applications International Corporation in Los Altos, California. He received a B. S. in Chemical Engineering from the University of Minnesota in 1953 and a Ph.D., also from the Unversity of Minnesota, in Chemical Engineering and Applied Mathematics in 1961. He has over 20 years of experience in chemical, mechanical, and nuclear engineering and has been an educator, consultant, and a scientist for a number of years. His research and consulting experience includes both theoretical and experimental work in thermal and fluid sciences, with emphasis on such topics as laminar/turbulent condensation in the presence of noncondensables, vorticity transport in high Reynolds number recirculating flows, free convection in enclosures at large Rayleigh numbers, interaction of free-stream turbulence and chemical reactions with high-speed boundary layer flows, transport of heat and mass-species in porous catalyst pellets, transport processes in reverse osmosis, evaporation of thermally radiated and convectively heated liquid droplets in high-temperature surroundings, gas-controlled heat pipes, semiconductor switching devices for laser hardening, and open-channel flows. Since joining SAIC in July 1979, Dr. Denny has assumed increasing responsibility for the thermal/hydraulics program at the Palo Alto/Los Altos office. He has authored a bounding model for analyzing the integrity of piping in the vicinity of LMFBR superheater/evaporators following a design basis leak in the heat exchange tubes, served as consultant to EG&G in response to NRC needs for simulant calculations following the TMI-2 incident, developed a computer code for predicting peak temperatures in Mark I suppression pools during steam blowdown transients, and assisted the EPRI analytical program on consequence calculations for LWR degraded core accidents. In addition, he was a principal (with A. T. Wassel) in the development of direct-contact evaporator/condenser designs for the Solar Energy Research Institute's OTEC program. Recently, Dr. Denny has devoted considerable effort to the development of a mechanistic computer code (CORMLT) for predicting the progression of core meltdown accidents in LWRs. The major objective of the work is to provide best estimate calculations of the thermal/hydraulics response of LWR containments to core degrading events.

RICHARD R. HOBBINS. Richard Hobbins is a Principal Scientist with EG&G Idaho, Inc., [Idaho National Engineering Laboratory (INEL)]. He holds a bachelor's degree in Chemistry from Princeton University and a doctorate in metallurgy from the University of Delaware. Dr. Hobbins has been engaged in research on fuel and fission product behavior at the INEL for 19 years. He has actively participated in planning, conducting, and interpreting results from experimental programs on severe accidents including the Severe Fuel Damage tests in the Power Burst Facility (PBF), the FP-2 test in the Loss-of-Fluid Test (LOFT) reactor, and the TMI-2 core examination. Dr. Hobbins has served on a number of NRC advisory panels including the Kouts Panel on Review of Research on Uncertainties in Estimates of Source Terms from Severe Accidents in Nuclear Power Plants and the National Research Council Panel on Chemical Processes and Products in Severe Nuclear Reactor Accidents. Following the Chernobyl accident, Dr. Hobbins was a member of the DOE Design Review of the N reactor at Hanford and the Savannah River

Plant reactors, and served as a consultant to the International Atomic Energy Agency (IAEA) on reactivity initiated accidents.

STEVEN A. HODGE. Steve Hodge is the program manager for the Boiling Water Reactor Severe Accident Technology (BWRSAT) Program at Oak Ridge National Laboratory (ORNL). Dr. Hodge and those under his technical direction are often called upon to provide advice to the NRC and to serve upon committees addressing special problems associated with postulated BWR severe accidents. Much of the BWRSAT program effort involves long-term cooperative endeavors with other national laboratories in BWR code development and experimental analyses. Upon graduation from the University of Texas in 1961, Dr. Hodge spent the next 13 years as a Naval Officer, with duty in destroyers, nuclear power school and prototype training, and nuclear submarines. After leaving the Navy in 1974, he obtained a masters degree in mechanical engineering from the University of Texas, then came to Oak Ridge National Laboratory in 1977 to complete his PhD thesis. He was awarded the PhD degree and became a Laboratory employee in 1979.

ROBERT J. LUTZ, JR. Bob Lutz is a fellow engineer in the Nuclear Safety Department of the Power Systems Division of Westinghouse Electric Corporation (WEC). He has over 18 years experience in the field of commercial nuclear power safety analysis and has spent the last eight years investigating severe reactor accidents and developing methodologies for the realistic analysis of severe reactor accidents. He is presently involved in the investigation of the progression of severe accidents and the development of strategies to mitigate their consequences. Mr. Lutz has presented over 20 technical papers on thermal hydraulic aspects of severe reactor accidents. He has been a consultant to electric power utilities in the United States and in several European countries, including Sweden, Switzerland, and Italy. He was also a consultant to DOE and NRC on the Chernobyl accident in 1986. Mr. Lutz has been a member of several study committees for the Atomic Industrial Forum (now called NUMARC).

MICHAEL Z. PODOWSKI. Michael Podowski is a professor in the Department of Nuclear Engineering and Engineering Physics at Rensselaer Polytechnic Institute (RPI), Troy, New York. His research activities include two-phase flow and boiling heat transfer, reactor thermal-hydraulics and safety, and reactor dynamics and stability. In particular, he has been involved in the modeling and analysis of severe reactor accidents, including experiments, development of theoretical models, and their numerical implementation as the APRIL computer code. Dr. Podowski has published several articles, reports and books on the abovementioned subjects. He has been a consultant to private industry, government, Korean Advanced Energy Research Institute (KAERI), and the IAEA. Dr. Podowski is a member of various technical/ scientific societies, including American Society of Mechanical Engineers (ASME), American Nuclear Society (ANS), American Institute of Chemical Engineers (AIChE), and American Society of Electrical Engineers (ASEE).

GARRY R. THOMAS. Garry Thomas is a Program Manager in the Safety Technology Department of the Nuclear Power Division at the Electric Power Research Institute (EPRI). He has 22 years experience evaluating nuclear fuel behavior in off-normal to severe accident conditions--the 14 most recent years in light water reactors (LWRs) at EPRI and the previous eight years with General Electric (GE) in liquid metal breeder reactors

(LMBR). Included in this experience is the performance and analysis of 25 irradiation experiments studying fuel behavior under severe power conditions. For 1-1/2 years he was EPRI's representative to the Organization of Economic Cooperation and Development (OECD) Halden Reactor Project in Norway. Since the accident at TMI-2 in March 1979, Mr. Thomas has been actively involved in understanding the actual severely degraded core behavior t'at occurred at TMI-2 and how this behavior should be translated into generic pressurized water reactor (PWR) and BWR severely degraded core accident modeling. As part of this effort, he has been a member of several working groups studying severe accident behavior (the most recent being the TMI-2 Accident Evaluation Advisory Group); and he has directed the development of codes for describing the early phases of severe core degradation for both PWRs and BWRs and for predicting fission product release from a degrading core. His evaluation of the adequacy of these codes and other industry and NRC-sponsored core degradation modeling codes always has been based on the understanding gained from the actual severely degraded core behavior that occurred at TMI-2.

ROBERT WRIGHT. No biographical sketch available.

3. METHODOLOGY

3.1 Introduction

This section contains a summary of the methodology used to elicit expert judgment from the expert panels. An in-depth discussion of the methodology is contained in Volume 1 of NUREG/CR-4551.

The methodology used in the expert judgment process for NUREG-1150 was designed to obtain subjective estimates of unknown physical quantities and frequencies in a manner that best uses the available expertise and accurately reflects the collective uncertainty about these values. Several principles guided the development of the methods:

1. The assessments should be limited to issues where alternative sources of information such as experimental or observational data, or validated computer models are not available.

2. The issues analyzed using expert judgment should have the potential to make a significant impact on the estimates of risk and uncertainty in risk.

3. The decomposition of complex issues into simpler assessments is made in order to improve the quality of the resulting information.

4. Issues should be presented to the experts without ambiguity and without the potential for preconditioning or biasing responses.

5. Experts should be trained in the practice of expressing knowledge and beliefs as probability distributions.

6. Discussion of issues and alternative beliefs should take place in structured and controlled meetings that encourage the exploration of alternative beliefs while inhibiting pressure to conform.

7. Elicitation of expert opinion should be conducted using techniques and instruments that reflect the state of the art in subjective probability assessment.

8. The aggregation of judgments from various experts should preserve the uncertainty that exists among alternative points of view. Equal weight should be assigned to the assessment for each expert to represent the uncertainty completely.

NUREG-1150 does not attempt to reduce uncertainty in risk analysis, nor is it an attempt to find a best estimate. It is an attempt to produce an unbiased picture of uncertainty in risk. The study tries to discover the range in risk inherent in the range of plausible assumptions about phenomenology and initial and boundary conditions. The risk corresponding to the most (subjectively) plausible assumptions has a higher likelihood of being accepted by a randomly chosen expert in accident phenomena. The risk

corresponding to less plausible assumptions nevertheless has some likelihood of being accepted by any expert, and may indeed be the most acceptable for some experts. Experts are sometimes wrong, and the "true" risk could lie outside the ranges found in this study.

3.2 Steps to Elicit Expert Judgment

The principles identified above, the criticism of the draft NUREG-1150 expert judgment efforts, and the findings of precursor studies employing expert judgment[1,2] provided guidance for the design of the NUREG-1150 expert judgment elicitation process. The process evolved into ten steps:

1. Selection of issues;
2. Selection of experts;
3. Elicitation training;
4. Presentation and review of issues;
5. Preparation of expert analyses by panel members;
6. Discussion of analyses;
7. Elicitation;
8. Recomposition and aggregation;
9. Review by the panel of experts;
10. Documentation.

The methodology was implemented in a three-meeting format, with much additional work being accomplished between meetings. Steps 1 and 2 were accomplished before the first meeting of the expert panel. Step 3, elicitation training, took place in the first meeting which lasted one-half day. The presentation and review of issues, Step 4, was done during the second meeting which, in order to reduce travel costs, took place immediately after the first meeting. Step 5 was accomplished between the second and third meetings (in some cases the expert panels met for additional discussions during this time). Discussion and elicitation, Steps 6 and 7, were discussed in the third meeting, which usually took place three months after the first and second meetings (the accident sequence frequency group and the structural response group met two months after the first two meetings). The final steps, 8, 9, and 10, were accomplished after the third meeting.

3.3 Selection of Issues

The NUREG-1150 program attempts to show the range and distribution of risk due to uncertainty in the inputs. Some of that uncertainty is phenomenological, some is stochastic, and some is due to limited background of data. There are an enormous number of input points, and all are uncertain to some extent. It was thus impossible to treat all questions and issues with the same degree of thoroughness. The criteria used to select issues for detailed uncertainty analysis were:

- **High impact on risk**. If an issue was highly uncertain, but variation across its entire range would not cause a big change in risk, there would be little need for a detailed treatment. The likely impact on risk was determined by the outcome seen in the draft version of NUREG-1150, by smaller scale side calculations, by the opinions of the expert panels, and by examination of previous PRAs.

- *Interest within the reactor safety community.* Some issues were thought not to be major determinants of uncertainty in risk, but had nevertheless been the subject of intense investigation and debate. The reason for including these issues in the analysis was to confirm this opinion.

- *To improve on the treatment in Draft NUREG-1150.* Some issues had not appeared to be important in the draft version; however, it was recognized that the treatment there was less than optimum. Such issues were included to determine whether an improved treatment would change those insights.

- *The issue was uncertain.* Even if an issue is important for the magnitude of risk, if the outcome is certain there is no impact on the uncertainty in risk.

Issues meeting any of these criteria were listed by the NUREG-1150 staff. The preliminary list of issues was presented to a panel of experts, along with reasons for their inclusion. A list of other issues was also presented, along with reasons for their exclusion. The expert panel was asked to review the list of issues, and to add or delete issues. The expert panels were the same ones that would be asked for quantification of the uncertain issues. An understanding of the limited time and resources available generally militated against an unwarranted or overly generous expansion of the issues.

Those issues that were selected for quantification by the external expert panels fell into three broad classes: uncertain issues affecting the sequence frequency calculation, uncertain issues affecting the response of the containment and its systems, and uncertain issues affecting the radiological source term. There were more issues affecting containment than for the other classes, and there was a further breakdown into issues related to the in-vessel phenomenology, containment loads, structural response, and molten core-concrete interactions. Tables 3-1 through 3-5 show the issues presented to the containment and radiological source term expert panels, along with the reasons for including the issue.

Table 3-1
Issues Presented to the In-Vessel Panel

Issue No.	Title	Reason for Inclusion
1	Temperature-induced PWR hot leg failure	Large hot leg failure could preclude direct containment heating; depressurize RCS and preclude SGTR
2	Temperature-induced PWR SGTR	SGTR gives direct path to environment, with large release of radionuclides
3	In-vessel hydrogen production in BWRs	Hydrogen burning has potential for causing release to environment
4	Temperature-induced bottom head failure in BWRs	Mode of bottom head failure determines subsequent accident progression
5	In-vessel hydrogen production in PWRs	Hydrogen burning has potential for causing release to environment
6	Temperature-induced bottom head failures in PWRs	Mode of bottom head failure determines subsequent accident progression

Table 3-2
Issues Presented to the Containment Loads Panel

Issue No.	Title	Reason for Inclusion
1	Hydrogen phenomena at Grand Gulf	Early failure of drywell or wetwell has potential for causing large source term
2	Hydrogen burn at vessel breach at Sequoyah	Early failure of containment or bypass of ice condenser has potential for causing large source term
3	BWR reactor building failure due to hydrogen burns	Bypass of reactor building has potential for increasing source terms
4	Loads at vessel breach at Grand Gulf	Failure of containment at vessel breach has potential for causing large source terms
5	Loads at vessel breach at Sequoyah	Same as Issue 4
6	Loads at vessel breach at Surry.	Same as Issue 4
7	Loads at vessel breach at Zion	Same as Issue 4

Table 3-3
Issues Presented to the Structural Response Panel

Issue No.	Title	Reason for Inclusion
1	Static failure pressure and mode at Zion	Containment failure is the most important determinant of source terms
2	Static failure pressure and mode at Surry	Same as Issue 1
3	Static failure pressure and mode at Peach Bottom	Same as Issue 1
4	Reactor Building bypass at Peach Bottom	Bypass of Reactor Building has potential for allowing large release of radionuclides
5	Static failure pressure and mode at Sequoyah	Same as Issue 1
6	Ice condenser failure due to detonations at Sequoyah	Failure or bypass of ice condenser has potential for large source terms
7	Drywell and wetwell failure due to detonations at Grand Gulf	Failure of drywell bypasses suppression pool. Failure of wetwell allows large release to environment
8	Pedestal failure due to erosion at Grand Gulf	Pedestal failure is a major factor in subsequent accident progression

Table 3-4
Issues Presented to the Molten Core-Concrete Interaction Panel

Issue No.	Title	Reason for Inclusion
1	Mark I drywell melt-through at Peach Bottom	Drywell meltthrough bypasses suppression pool; controversial issue
2	Mark III containment failure via pedestal failure at Grand Gulf	Pedestal failure could lead to early containment failure; controversial issue

Table 3-5
Issues Presented to the Source Term Panel

Issue No.	Title	Reason for Inclusion
1	In-vessel fission product release and retention	Release and retention are major determinants of source term
2	Ice condenser deconta-mination factor (DF) at Sequoyah	Ice condenser is principal decontamination mechanism in blackouts
3	Revolatilization from RCS/RPV	Revolatilization could negate effects of high retention; highly uncertain issue
4	CCI release	If in-vessel release is low, CCI release could be high; uncertain issue
5	Release of RCS and CCI species from contain-ment	Aerosol agglomeration may be major source of cleanup in blackout; highly uncertain issue
6	Late sources of iodine at Grand Gulf	Appeared as important issue in Draft NUREG-1150
7	Reactor Building DF at Peach Bottom	Natural decontamination processes could reduce source term; uncertain and controversial issue
8	Release during direct containment heating	Uncertain and controversial issue; direct heating is also associated with early containment failure

3.4 Selection of Experts

Experts were chosen to ensure a balance of viewpoints. To this end, experts from industry groups, engineering and consulting firms, the Federal Government, and the national laboratories were included in the panel. A brief summary of their credentials has been presented in Section 2.

3.5 Elicitation Training

Training in probability assessment techniques is an integral part of the expert opinion methodology used in NUREG-1150. Each panel of experts that participated in the expert opinion process attended a half-day training session. This session constituted the first meeting of each panel. The training was given by consultants from the field of probability assessment and decision analysis. The trainer for the In-Vessel Panel was Professor Steve Hora of the University of Hawaii at Hilo.

The purpose of training in probability assessment is to facilitate the elicitation process. Experts in various fields of science are often not trained in probability theory and the techniques of probability elicitation. The expertise possessed by the scientists and engineers on the panels is called substantive expertise and thus they are called substantive experts. Expertise about probability elicitation is called normative expertise and the participants in the expert opinion process schooled in probability assessment are known as normative experts. Both substantive expertise (knowledge of the problem domain being studied) and normative expertise (knowledge of techniques for encoding beliefs into probability distributions) are required for a successful expert opinion process.

During probability training, experts are exposed to various techniques for probability elicitation and the difficulties that accompany probability elicitation. Once trained, substantive experts are better able to express their knowledge in the form of probabilities and the resulting elicitations will be of a better quality. The resulting assessments are better calibrated in the sense that they accurately reflect the expert's knowledge and uncertainty. A by-product of the training is that the experts become more comfortable with the concept of subjective probability and more confident in expressing their beliefs in probability distributions.

Another benefit of training is that the time spent by the experts preparing for the issues is used more effectively because the experts can direct their analyses to the questions that must be addressed in the elicitation sessions. Furthermore, the elicitation sessions run smoothly since the normative and substantive experts are working with the same definitions and the same understanding of the desired product.

3.5.1 Training Topics

The training sessions conducted for NUREG-1150 covered several related topics. These topics included the expert opinion process itself and the need for expert opinion, the elicitation techniques for the probabilities of various types of quantities and events or phenomena, the psychological aspects of probability assessments, and the decomposition of complex issues.

Each training session began with an overview of the goals of the expert opinion process and background material on the development of that process. The process was reviewed in some detail so that the substantive experts would be aware of what would be required of them and how their elicitations would be used. Because the formalized use of expert opinion was new to many of the participants, some were initially uneasy with the concept of expert opinion and the uses that it might be put to. Gaining the confidence of these experts through familiarization with the process was essential to the success of the expert opinion effort.

There are many different types of assessments that might be required of the experts. The type of assessment depends upon the nature of the physical quantity or phenomena under study. During the training sessions, the experts were introduced to assessment instruments for continuous quantities, discrete quantities, zero-one events, and dependent events. At appropriate points in the training, the experts were asked to make

assessments using the methods under discussion. Using practice assessments develops confidence and ensures that the substantive experts understand the tasks that they will be required to perform. In order to make the training more interesting and more relevant, examples were used that reflected nuclear power risk issues.

Since many of the assessments would require the development of a probability distribution for a continuous quantity, the experts were given training in both the direct assessment techniques (assessing probabilities of given intervals of values) and bisection techniques (assessing values of the variable having given cumulative probabilities) for continuous variables. Later, in the elicitation sessions, these techniques would be used interchangeably by the normative experts.

A discussion of stochastic and parametric uncertainties and how they are differentiated in an uncertainty analysis was also provided. The concept of calibration of experts and calibration functions was also introduced. However, mathematical calibration of experts was not attempted in the NUREG-1150 expert opinion process.

Psychological aspects of probability elicitation received much attention in the training because failure to recognize and deal with psychological biases can impair the quality of the resulting assessments. One of the psychological aspects discussed is the tendency to give subjective probability distributions that are too narrow and thus understate the uncertainty or, conversely, overstate knowledge. This phenomenon is often called "overconfidence" since the effect is that the probability distribution expresses greater certainty than is warranted. Other psychological aspects of subjective probability assessment that were discussed include anchoring, which is the tendency to assume an initial position and fail to give sufficient credit to other sources of information; representativeness, which is the tendency to give too much credit to other situations that are similar in some aspects but not others; the tendency to overestimate the probabilities of rare events; and and problems with group behavior such as personality dominance. Whenever possible, examples of these difficulties were presented and the experts being trained were asked to participate in demonstrations.

At the end of the training session the participants were given an assessment training quiz containing 16 assessment tasks using the direct and bisection methods of assessment. The participants were asked to complete the training quiz during that evening and return the next morning to discuss the results. The purpose of the training exercise was twofold: to give the substantive experts experience with the elicitation instruments and to provide feedback on the quality of the individual's assessments. As expected, most participants found that their assessed distributions expressed overconfidence. Once aware of this tendency, it is easier for the substantive experts to correct for this bias.

Problem decomposition was the last major segment of the training session. Problem decomposition has been used in the NUREG-1150 expert judgment process as a mechanism to improve the quality of the subjective assessments. Problem decomposition improves the quality of assessments by structuring the analysis so that the expert is required to make a series of

3.9

simpler assessments rather than one complex assessment. Experimental studies[3,4] have shown that decomposition often improves the accuracy of assessments. Improvement occurs because the experts are responding to questions that are less difficult to answer. The experts must state their reasoning explicitly by being more introspective about their assumptions of the analysis and thus consider alternatives that they might otherwise ignore. Some improvement may be due to cancellation of errors which occurs when errors of underestimation are offset by comparable errors of over-estimation. Decomposition also provides a form of self documentation since the expert's thought process is made explicit in the decomposition.

Training in decomposition was conducted by presenting examples of decompositions that had been developed for the NUREG-1150 study. Several types of decompositions were shown and the process of recombining the assessments was discussed. Comments from the participants indicated that the use of problems from the nuclear safety area enhanced the value of the decomposition training.

3.6 Presentation of Issues

During the second part of the second meeting, plant analysts presented the issues to the expert panel. The purposes of the presentations were to ensure that there was a common understanding of the issue being addressed; ensure that the experts would be responding to the same elicitation question; permit unimportant issues to be excluded and important issues to be included; allow modification or decomposition of the issue; and provide a forum for the discussion of alternative data sources, models, and forms of analysis.

Each presentation included a suggested decomposition of the problem. Plant analysts usually presented the suggested decompositions without the suggested probabilities or distributions to avoid preconditioning or bias-ing the experts. For many of the issues, the proposed decomposition brought about lively discussions that illuminated the alternative approaches to analyzing the issue. The plant analyst also presented data sources, models, and reports that were relevant to the issue, and provided references to other sources of information. The list of documents that were provided to the In-Vessel Panel is included as Appendix B.

Capturing uncertainty in the experts' opinion quires that the various experts be permitted to follow alternative an_ _s. Since the process was designed to take advantage of the diversity of approaches, experts were encouraged to seek their own decompositions or to modify decompositions that were suggested by the analysts. Criticism of the decompositions was encouraged and the experts were assisted in producing decompositions that better matched their interpretations of the issues.

3.7 Preparation and Discussion of Analyses

Two or three months were allowed between the initial presentations of the issues and the elicitation sessions. During this period, the experts studied the issues. Some experts chose to alter the proposed decompositions or create new decompositions and made preliminary evaluations of the subjective probabilities represented in their decompositions of the issues.

The elicitation meeting provided a forum for discussion of alternative views of the issue. Presentations from both the panel members and invited observers of the meetings were encouraged. These sessions generated a substantial amount of discussion and interchange of information which often led the experts to make revisions of their prepared analyses. In some instances, the panel members prepared documentation that amounted to brief reports. It became apparent in the elicitation sessions that this interchange was an important source of information for the experts.

3.8 Elicitation

The discussion of each issue was followed by elicitation meetings between the experts and a team composed of one normative analyst and one substantive analyst (an analyst familiar with the risk implications of the issue. Documentation of the experts' assumptions and reasoning was produced during the elicitation meetings. Normally, each meeting consisted of three participants (one panel member, a normative expert, and a substantive expert) and lasted about two hours. However, in a few cases where there were more experts to be elicited than available normative experts, two experts were elicited in a single session.

The elicitation sessions served several purposes. The first was to obtain from the experts the decomposition and assessments of the problems. The experts were required to explain their thinking to the assessment team of one normative and one substantive expert. During the discussion of the elicitation process, the expert being elicited was questioned about stated beliefs and asked to reflect on, and explain the reasoning behind, the values that he or she had provided. In many cases, the resulting decompositions and probability distributions differed somewhat from the initial assessments.

The role of the normative experts was to assist the expert in codifying the experts' beliefs and to ensure that the assessment was complete and consistent in a probabilistic sense so that the assessments could be recomposed at a later time. Normative experts have the ability to draw from the experts the important details being elicited. Their talent for becoming involved in the technical aspects of issues, which are not their basic area of expertise, is a crucial factor in facilitating the experts' abilities to develop logically consistent assessments. Such individuals are necessary in any expert judgment elicitation process.

The role of the substantive expert was to assist the expert by answering questions related to the issue and to ensure that technical reasoning was complete and to the point. He also served as a technical advisor to the normative expert to assist him in questioning the expert in a direction consistent with the technical needs and constraints of the plant analysis teams.

Much of the documentation of the experts' assumptions and reasoning was completed during the assessment meetings. However, some follow-up work was necessary after the elicitation sessions to fill in voids in the logic provided by the experts, or to obtain values that were incomplete.

Documentation of the elicitations is provided in Section 5 of this report. Note that while the experts participating for each issue are identified, the individual assessments are kept anonymous, and the experts are identified as Experts A, B, C, etc.

3.9 Recomposition and Aggregation of Results

Each member of the expert panels produced a distribution for each case of each issue. For some issues, several dependent variables were requested, and a separate distribution was elicited for each variable. If all the experts had worked with identical case structures and if all had produced the' results in the same form, the task of aggregation would have been simply a matter of taking the numerical average of all the distributions for each case. However, some experts used idiosyncratic case structures. On some issues, the experts expanded the case structure beyond what was tractable in the accident progression event trees (Section 4) or the XSOR codes (Section 5). On some issues, experts gave their results in different forms.

For the purposes of aggregation it was absolutely required that the case structure be small enough to fit into the containment event trees and XSOR codes and that the case structure and dependent variables be the same between experts. If the case structure was impractically large and complex, it was reduced if possible by an analysis of variance (ANOVA). The ANOVA compared the variance in the dependent variable attributable to the differences between cases and the variance attributable to the differences among experts to the unexplained variance in the dependent variable. For many issues it was found that the differences between cases were not significant compared to the differences between experts, that is, that the large and complex case structure had little effect on the dependent variable. A mathematical procedure was then used to determine which of the cases could be safely combined.

If different experts used different cases, they were first encouraged to resolve their differences; if they failed to do so it was necessary to find some common ground. The cases common to all experts were of course retained. The remaining cases were inspected, and the most important ones were retained. If an expert did not have one of these cases, but did have a closely analogous case, the analog was used for the missing case. If the expert did not have a case closely related to the missing case, then the average of the case for all other experts was used for his missing case. It was recognized that this procedure would reduce the range of uncertainty, so the substitution was resorted to as little as possible. For some issues, missing data could be filled in by interpolation or ratios of existing cases.

If the experts produced different dependent variables, some analysis was required to put all the outputs into the same form. Whenever this was done the experts involved might find the final form of their data difficult to reconcile with what had been produced in the elicitation. Therefore, analytical alteration of results was resorted to as little as possible, and attempts were made to explain the reasons for and methods of analysis to the experts.

3.12

After each of the experts' distributions were put in the same format, they were aggregated by averaging. The experts' outputs were almost always in the form of cumulative distribution functions (CDFs), that is, curves or tables of the probability that the independent variable would be no greater than some specific value. The aggregation was carried out by averaging all the experts' probability values for each value of the independent variable. The aggregated results were thus also CDFs.

3.10 Review

Following the recomposition of the assessments and the modification of the documentation accompanying each assessment, the written analyses of each issue were returned to each panel expert, normative expert, and substantive expert associated with the issue for review. This review process ensured that potential misunderstandings were identified and resolved and that the documentation, which is given in Section 5 of this report, correctly reflects the judgment of the experts involved.

3.11 Documentation

Clear, comprehensive documentation is crucial for ensuring that the expert opinion process is accepted as credible. There must be no question as to the openness and impartiality of the process. Users and reviewers of the results must be able to trace the development of aggregated assessments from the information presented to the experts, to the rationale which motivates each expert to generate his particular assessments, and through the process of aggregating the individual assessments into a final result, including any manipulation of the assessments needed for aggregation. To this end, the issue discussions were recorded on video cassette. Such recording provides evidence of the exact conversations and presentations made before the panel. Written notes were taken by both the normative and substantive experts. Each expert was encouraged to personally document his rationale for his elicitation immediately at the end of the session. By far the most important documentation is each expert's in-depth discussion of his reasoning for his assessments. The discussion should contain the technical foundation of information (experience, issue presentation, existing data or analyses) from which the rationale for the assessment is derived.

References

1. A. Mosleh, V. M. Bier, and G. Apostolakis, "Methods for the Elicitation and Use of Expert Opinion in Risk Assessment," Pickard, Lowe & Garrick, Inc., NUREG/CR-4962, PLG-0533, August 1987.

2. A. Tversky and D. Kahneman, "Judgment under Uncertainty: Heuristics and Biases," _Science, 185_, pp. 1124-31 (1974).

3. J. S. Armstrong, _Long-Range Forecasting: From Crystal Ball to Computer_, John Wiley & Sons, New York, 1985.

4. J. S. Armstrong, W. B. Denniston and M. M. Gordon, "The Use of the Decomposition Principle in Making Judgments," _Organizational Behavior and Human Performance, 14_, pp. 257-63, (1975).

4. ELICITATION MEETINGS

The first two meetings (the elicitation training and the presentation and review of the technical issues) for the In-Vessel Expert Panel were held from November 11 to 13, 1988. Presentations to the In-Vessel Panel were made by the following people:

Nestor Ortiz, SNL
Steven Hora, University of Hawaii at Hilo
Frederick Harper, SNL
Eric Haskin, SNL
Walt Murfin, Technadyne
John Kelly, SNL
Robert Lutz. Jr., Westinghouse
Vern Denny, SAIC
Mark Kenton, FAI
Chris Amos, SAIC
Richard Hobbins, INEL
Randy Summers, SNL
Michael Podowski, RPI
Garry Thomas, EPRI
Ariel Sharon, FAI
Randy Gauntt, SNL
Steve Hodge, ORNL
Peter Cybulskis, BNL
Marty Pilch, SNL

The elicitation meeting for the In-Vessel Expert Panel was held on April 12 to 15. Presentations at these meetings were made to the panel by the following people:

Elaine Gorham, SNL
Ralph Keeney, University of Southern California (USC)
Allen Camp, SNL
Roger Breeding, SNL

Normative experts for Source Term elicitation sessions were:

Ralph Keeney, USC
Detlof von Winterfeldt, USC
Richard John, USC.

5. RESULTS OF THE ELICITATION ON EACH IN-VESSEL ISSUE

The results of the expert panel elicitations are presented in detail here. A brief description of each issue is given, the individual expert assessments and rationale for the assessments are discussed, and the aggregated results or resolutions for each issue are presented.

5.1 Issue 1. Temperature-Induced PWR Hot Leg or Surge Line Failure Before Vessel Breach

Summary and Aggregation of In-Vessel Issue 1:
Temperature-Induced Pressurized Water Reactor (PWR) Hot Leg or
Surge Line Failure Before Vessel Breach

Experts Consulted. William J. Camp, Sandia National Laboratories; Vern E. Denny, Science Applications International Corporation; Robert J. Lutz, Westinghouse Electric Corporation.

Issue Description

What distributions characterize the uncertainty in the conditional probability of occurrence of a large temperature-induced failure of the hot leg or the surge line? The pipe breaks in question are induced by temperatures much higher than design temperatures. These temperatures may occur in reactor accidents after core degradation. The nuclear steam supply systems of the Surry, Sequoyah, and Zion power plants are sufficiently similar so that a separate quantification of this issue for each plant is not deemed necessary. The cases to be considered include:

Case 1: Steam generators dry, no failure of reactor coolant system (RCS) pressure boundary--Classic TMLB' sequence. There is no source of makeup coolant. The initial RCS pressure is 2500 psia, and steam temperature may range from saturation (668°F) to very high superheat. Gross flow exits from the core region into the hot leg containing the pressurizer, out of the power-operated relief valve (PORV).

Case 2: Auxiliary feed water failed, early induced pump seal loss-of-coolant accident (LOCA). Maximum leak rate from the pump seals is 900 gpm. RCS pressure minimum is 1200 psia, and repressurization to full setpoint pressure of 2500 psia might occur when the steam generators dry out. Gross flow is initially out the cold legs, through the pump seals, but after repressurization, flow occurs out of the PORV.

Case 3: Auxiliary feed water operating, pump seal LOCA initiator. Maximum leak rate from the pump seals is 900 gpm. RCS pressure is about 1200 psia, and no repressurization occurs. The steam generators act as a heat sink. Gross flow is out the cold leg pump seals, and there may be natural recirculation through the steam generators.

The experts felt that hot leg failure was extremely unlikely in Case 3 because of the reduced effectiveness of natural circulation and the lower loop stress on the pipe. Distributions were not provided for Case 3.

Summary of Experts' Rationale/Methodology

To evaluate Case 1, Expert A reviewed a series of MELPROG and TRAC/MELPROG calculations for Surry TMLB', that he had performed. He also referred to the results of CORMLT/PSAAC calculations for Surry and Zion in a TMLB' scenario, the RELAP5/SCDAP analysis of Surry TMLB', the Westinghouse natural circulation experiments with simulants, and the results of COMMIX analysis of the Westinghouse experiments. He gave the highest credibility to the MELPROG/TRAC calculations, next highest to the CORMLT/PSAAC calculations, and lower credibility to the SCDAP calculations.

Classic TMLB' sequence calculations indicate the gas temperature leaving the core is very close to the surface temperature of the core. Natural circulation maintains a nearly constant temperature over the core. There is a very high probability that natural circulation cells occur in the hot legs. These cells eventually disappear due to hydrogen in the steam generators and stratification. The cells make about 50° difference in the temperature of the hot leg.

There is a race between temperatures in the core and temperatures in the hot leg. As the core gets hotter, the grid spacers make holes in the cladding which prevents path blockages by clad ballooning. The Expert felt that ballooning does not have a significant impact on hot leg failure. However, blockages can occur near the bottom after liquified core material has relocated downward. The Expert feels that the issue can be reduced to the likelihood that structures reach a temperature of 1000 to 1200 K before natural circulation shuts down. Expert A's calculations show that either the nozzle, the hot leg pipe, or the surge line fails before natural circulation stops.

The Expert based his analysis of Case 2 on a MELPROG calculation. In this case, the pressures are lower causing natural circulation to be less effective, and heat transfer less efficient. The frequency of temperature induced hot leg LOCA is less than for Case 1.

Expert B reviewed the documentation that was supplied by the NUREG-1150 analysts, and performed some unpublished CORMLT/PSAAC calculations. Expert B also used insights gained from extensive knowledge of the MAAP code and MAAP calculations.

Expert B considered a decomposition for Case 1, that included the time from core uncovery to vessel breach, the time that the hardware in question (hot leg piping, surge line, or nozzle) is at creep temperature, and the time required at creep temperature for failure. The decomposition did not include dependency upon natural circulation within the RCS because the Expert felt that it is not necessary to have natural circulation in order to get a structural failure in a TMLB' sequence.

The creep rupture criterion used by Expert B was 1100 K. Distributions were provided for failure of the hot leg nozzle, the hot leg piping, and the pressurizer surge line in terms of the time sustained at a temperature of 1100 K.

The only information that Expert B was able to use for Case 2 was the MELPROG calculation performed by Expert A. The Expert felt that for this case, the only potential for hot leg failure would be during the heat-up before the loop seals clear. The frequency of failure was felt to be small.

Expert C placed primary reliance on MAAP runs that were made for Ringhals 3 and Seabrook. He also considered RELAP/SCDAP, MELPROG, and CORMLT calculations. Creep rupture as a function of time and temperature for the hot leg and the surge line was taken from the curves in NUREG-1265.

Expert C considered surge line failure in his hot leg assessment. The MAAP calculations indicated that the hot leg would fail before the surge line. Other code calculations showed that the surge line temperatures were higher than the hot leg temperatures.

Because the steam density is a strong function of pressure, Expert C concluded that the strong natural circulation necessary to create high temperatures in the hot leg could occur only when the RCS is at or near the PORV setpoint pressure. Any previous break in the RCS pressure boundary will preclude a temperature-induced hot leg failure during core melt. If the auxiliary feedwater system has operated, Expert C felt that the high temperatures required for a hot leg break will not be reached in the primary system due to reflux cooling in the steam generators. Expert C concluded that only Case 1 would result in system setpoint pressure in the RCS and only quantified that Case.

Expert C decomposed the problem into two questions: how much hydrogen has been produced in the reactor vessel, and how much time is there between core slump into the bottom head and failure of the vessel? The hydrogen production is one of the major parameters impacting primary system temperatures and includes consideration of relocation temperature, mode of core slump, and formation of core blockages. The core slump timing question can be interpreted as a division between vessel failures due to penetration failures, which occur in less than 10 min, and other vessel failure modes, e.g., circumferential bottom head failures, which take longer than 10 min.

Expert C felt that the RCS would either fail before vessel breach or that the vessel would breach without subsequent RCS failure by creep rupture. He felt that failure of the hot leg or surge line was likely to occur before vessel breach for events that exhibit the following characteristics:

1. RCS pressure at or near the pressurizer PORV setpoint;
2. Dry steam generators at the time the core melts; and
3. No significant and prolonged forced flows in the RCS during core melting.

Method of Aggregation

Case 1

Expert A provided a continuous distribution for conditional probability of hot leg LOCA. The distribution had discontinuities at probabilities of zero and 100%, indicating some belief on the part of Expert A that induced hot leg failure could either never occur or would always occur. Table 1-1 and Figure 1-1 show the Expert's distribution for Case 1.

Expert B provided a single probability for occurrence of induced hot leg LOCA. In Expert B's view, induced hot leg LOCA might or might not occur, but if the phenomenology is such as to cause occurrence, there would always be a hot leg LOCA. Conversely, if the phenomenology is such as to prevent occurrence, there would never be a hot leg LOCA. Expert B believed that there was a 65% probability of occurrence.

Expert C provided 5th, 50th, and 95th percentiles for probability of induced LOCA for several subcases, each of which depended on the fraction of zirconium oxidized in-vessel and on the mode of vessel breach. He stated that the probabilities for the latter events should be taken from the aggregated results for in-vessel Issues 5 and 6. Expert C believed that there was no possibility of an induced hot leg LOCA for Case 2.

Because Expert C's distribution for probability of hot leg LOCA depended on the extent of zirconium oxidation, his distribution was correlated with in-vessel Issue 5. The correlation coefficient was 0.43, indicating that 18.6% of the variance in Issue 1 could be attributed to Issue 5. Figure 1-1 shows Expert C's distribution for Case 1. Salient points of the distribution are given in Table 1-2.

Because of the correlation in Expert C's distribution, a simple numerical averaging was not appropriate. Instead, a Monte Carlo procedure was used in which each expert was equally represented. This is equivalent, in effect, to numerical averaging, but Expert C's results could be correlated with Issue 5 while Expert A and B were uncorrelated. An overall correlation coefficient was then calculated for the aggregate.

The analysis showed that the aggregated distribution was only weakly correlated (r = 0.06) with Issue 5. The reasons for the weak correlation are that Expert C's distribution was not very strongly correlated to start with, and Experts A's and especially B's results for probability of hot leg LOCA were uncorrelated and also were mostly either zeroes or ones, which further diluted the correlation. The aggregate is shown in Figure 1-1.

The aggregated distribution shows that there is approximately a 14% probability that an induced hot leg LOCA will never occur, and a 44% probability that hot leg LOCA will always occur. The probability of an induced hot leg LOCA is approximately 99%.

Case 2:

Expert A also provided a continuous distribution for this case. However, the Expert's opinion was that hot leg LOCA was much less likely than for Case 1. He believed that there was a 50% probability that there would never be a hot leg LOCA. If an induced LOCA occurred, the median probability would only be about 12%. Table 1-4 shows this Expert's distribution for Case 2.

Expert B provided a single probability for hot leg LOCA in this case, and gave only a 0.3% probability of occurrence. Expert C believed that there was no chance whatever for a hot leg LOCA to occur for Case 2. Figure 1-2 shows the aggregated distributions for Case 2. The aggregate is also shown in Table 1-5. There is an 83% probability that hot leg LOCA will never occur. If a LOCA is induced, the median probability will be about 10%. The aggregate thus reflects the view of all three experts that hot leg LOCA would be either impossible or unlikely for Case 2.

Aggregated Results

Table 1-1
Expert A's Distribution for Case 1

Probability, F	Probability of Not Exceeding F
0.0	0.1
0.10	0.15
0.50	0.20
0.80	0.275
0.90	0.35
1.00	0.50

Table 1-2
Expert C's Distribution for Case 1

Probability, F	Probability of Not Exceeding F
0.25	0.01
0.50	0.05
0.75	0.19
0.90	0.34
0.95	0.45
0.99	0.65
1.00	0.80
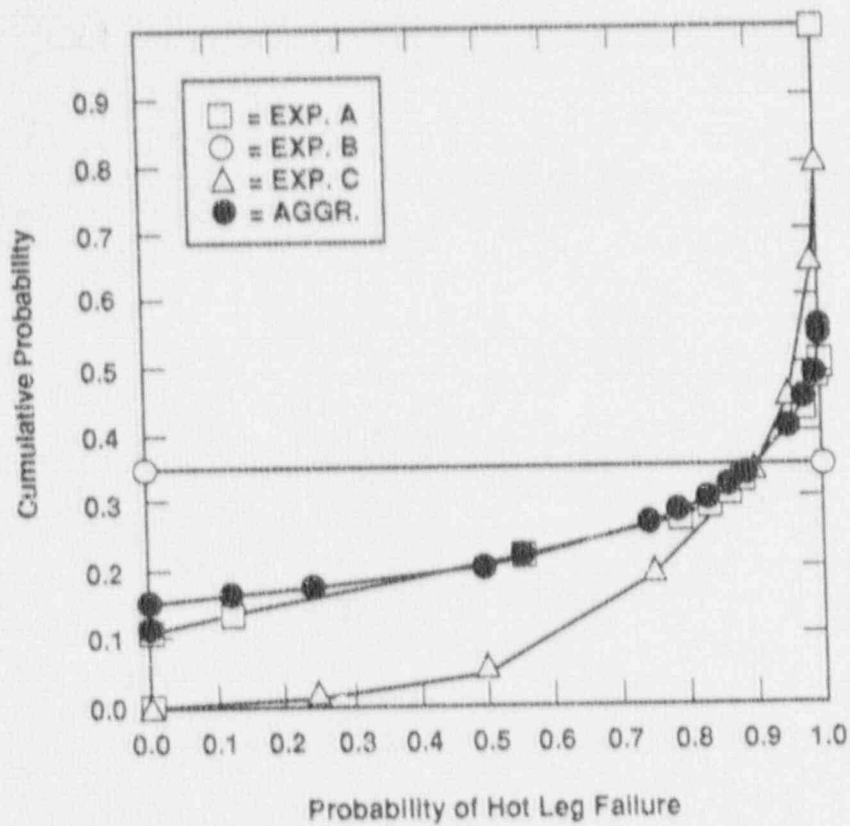
Figure 1-1. Case 1: Induced Hot Leg Failure in PWRs.
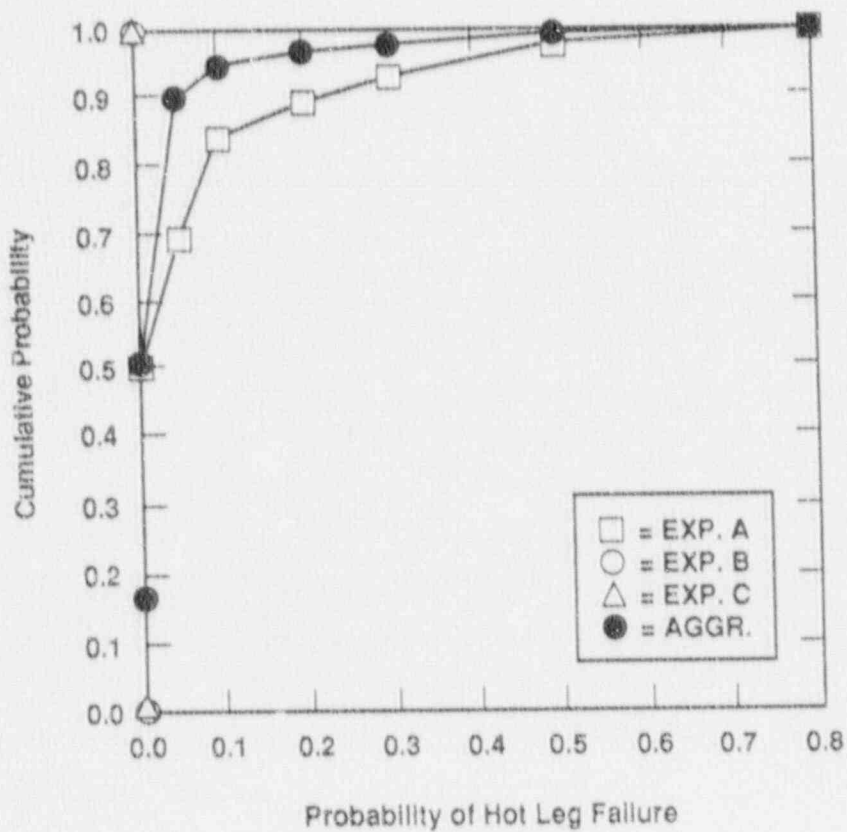
Figure 1-2. Case 2: Induced Hot Leg Failure in PWRs.

5.1-6

Table 1-3
Aggregated Distribution for Case 1

Probability, F	Probability of Not Exceeding F
0.00	0.14
0.05	0.16
0.50	0.21
0.75	0.27
0.90	0.35
0.95	0.39
0.99	0.50
1.00	0.56

Table 1-4
Expert A's Distribution for Case 2

Probability, F	Probability of Not Exceeding F
0.00	0.50
0.05	0.69
0.10	0.84
0.20	0.89
0.30	0.93
0.50	0.98
0.80	1.00

Table 1-5
Aggregated Distribution for Case 2

Probability, F	Probability of Not Exceeding F
0.00	0.83
0.05	0.90
0.10	0.95
0.20	0.96
0.30	0.98
0.50	0.99
0.80	1.00

Individual Elicitations for In-Vessel Issue 1

Expert A's Elicitation

Issue 1. Temperature-Induced PWR Hot Leg or Surge Line Failure Before Vessel Breach

Description of Expert A's Rationale/Methodology

Case 1

The Expert had reviewed a series of MELPROG and TRAC/MELPROG calculations for Surry TMLB', which he himself had carried out. He was also familiar with the results of CORMLT/PSAAC calculations for Surry and Zion in a TMLB' scenario, RELAP5/SCDAP analysis of Surry TMLB', The Westinghouse natural circulation experiments with simulants, and the results of COMMIX analysis of the Westinghouse experiments. He gave the highest weight to his own calculations, then to the CORMLT/PSAAC calculations, and lower weight to the SCDAP calculations.

He first considered the classic TMLB' scenario. In this sequence, the calculations indicate the gas temperature leaving the core is very close to the surface temperature of the core. Natural circulation maintains a nearly constant temperature over the core. There is a very high probability (80 to 90%) of natural circulation cells occurring in the hot legs. These cells would disappear in time because of hydrogen in the steam generators and stratification. The effect of natural circulation cells on the hot leg LOCA would be of the order of 10%, because the cells would only make about 50° difference in the temperature of the hot leg.

A complicating factor is that there is a race between temperatures in the core and temperatures in the hot leg. As the core gets hotter, the grid spacers make holes in the cladding which prevents ballooning. In fact, this experts discounts the possibility that ballooning could have any great effect on hot leg failure. When the temperature is high enough, the $Zr-H_2O$ reaction becomes autocatalytic. During oxidation, part of the material liquifies and runs down, forming a blockage near the bottom. Eventually, the material falls down, after which the only heat for the gas is that which leaks through. He believes that natural circulation within the vessel will heat and melt steel in the upper structures before natural circulation shut down. In his calculations, the structures in the failure locations (nozzle, hot leg pipe, and surge line) always fail before natural circulation stops.

The structures that could cause a hot leg failure would have a fair probability of failure at 1000 K, and would certainly fail at 1200 K. The question of the probability of hot leg LOCA can be reduced to the likelihood that structures reach this temperature before natural circulation shuts down. He believes it is very likely that the failure will occur first at the hottest location; therefore, it is only necessary to consider what the temperature would be at any location, and all locations can be aggregated for this issue.

Case 2

A calculation with MELPROG indicated a bulk temperature of 900 K for this case. The Expert believed that, on the basis of this calculation, a normally distributed temperature with a mean of 900 K and a standard deviation of 50 K would be reasonable. There would thus be a possibility of failure at the upper end of the band. Differential stress could enhance the probability of failure. However, there is no possibility of failure until the accumulator dumps.

After the accumulators dump, the core will be in a film boiling condition, and most of the water can get in before the accumulators isolate. The situation would then be like a classic cold leg LOCA. Eventually, the loop seals will dry out, which will allow more natural circulation. However, the pressures are now lower, natural circulation is less effective, and heat transfer will be less efficient. There is thus a lower probability of failure for the second temperature peak (after accumulators dump) than for the first. Thus, the probability of failure on the first temperature peak bounds the problem.

The Expert stated that his results did not apply to Sequoyah, because of upper head injection (UHI) at that plant. However, since the elicitation, Sequoyah has received permission not to use UHI, so that the differences between plants are now minimal.

Results of Expert A's Elicitation

Case 1

Table A-1 shows a cumulative distribution function (CDF) for mean structural temperature (for at least six minutes) at the hottest of the three locations of interest. It would be possible for the temperature to exceed 1200 K. However, the expert believes that at 1200 K a hot leg LOCA is certain, so that higher temperatures are not relevant.

Table A-2 shows probability of failure as a function of mean structural tempeature (for at least six minutes). Figure A-1 shows the convolution of Tables A-1 and A-2. As a check on Figure A-1, the Expert had made a holistic estimate of 67 to 75% for the probability of failure for case 1. Figure A-1 indicates a probability of approximately 10% that there is no chance at all of an induced hot leg LOCA, a probability of about 20% that the probability of hot leg LOCA does not exceed 20%, and a probability of about 55% that hot leg LOCA is absolutely certain. The Expert's preliminary estimate is thus in reasonable agreement with the results of his decomposition.

Case 2

A normal distribution with a mean of 900 K and a standard deviation of 50 K for the temperature of the structures of interest was combined with the probabilities of failure of Table A-2, to give the distribution of Figure A-2. Figure A-2 indicates a 50% probability of no LOCA at all, and approximately a 5% probability that the probability of induced LOCA was as

high as 50%. This compares with the Expert's preliminary holistic estimate of a 10% probability of induced LOCA for Case 2.

Sources of Uncertainty

There is relatively little uncertainty for Case 1 that high temperatures will develop in some part of the structure. Whether natural circulation cells develop in the hot leg structure is not subject to question. Flow of high temperature fluids out the cycling PORV completely overwhelm the uncertainty as to whether natural circulation cells are developed. However, there is uncertainty in timing; whether the structures are heated to a high enough temperature to fail before blockages cut off circulation to the core.

For Case 2, on the other hand, there is great uncertainty. The distribution of Figure A-2 is based on a single calculation. More calculations should be performed to determine how sensitive the results are to details of timing of the pump seal LOCA. The Expert indicated that he would also feel more secure about this case if other calculations were performed. A very great determinant for the temperature distribution is the observation that the loop seals dry out. If this did not happen, the results could be very different. The Expert was also uncomfortable with such apparently small leaks causing such a great difference in the results.

Suggested Methods for Resolving Uncertainties

None provided.

Table A-1
Cumulative Distribution Function for Structural
Temperatures, Case 1

Temperature (K)	Probability That Structural Temperature is No Greater Than Indicated Temperature
800	0.00
900	0.10
1000	0.20
1200	0.50
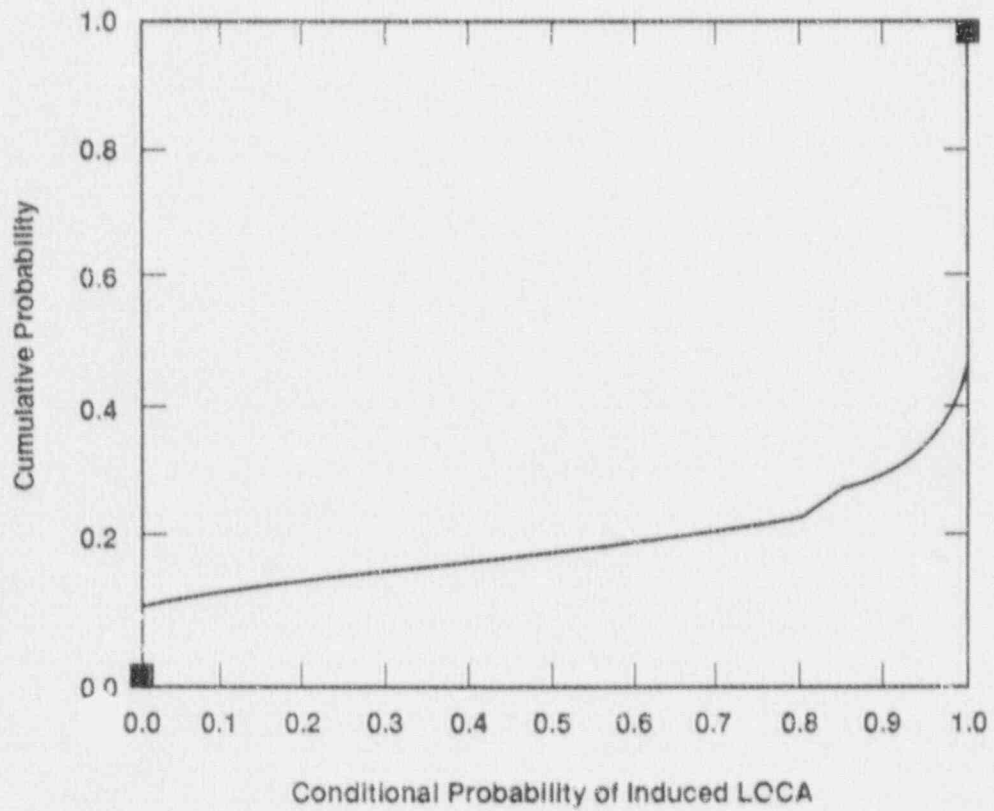
Figure A-1. Induced Hot Leg LOCA, Case 1

Table A-2
Failure Probability as a Function of Temperature

Temperature (K)	Failure Probability
900	0.00
950	0.10
1000	0.50
1050	0.80
1100	0.90
1200	1.00
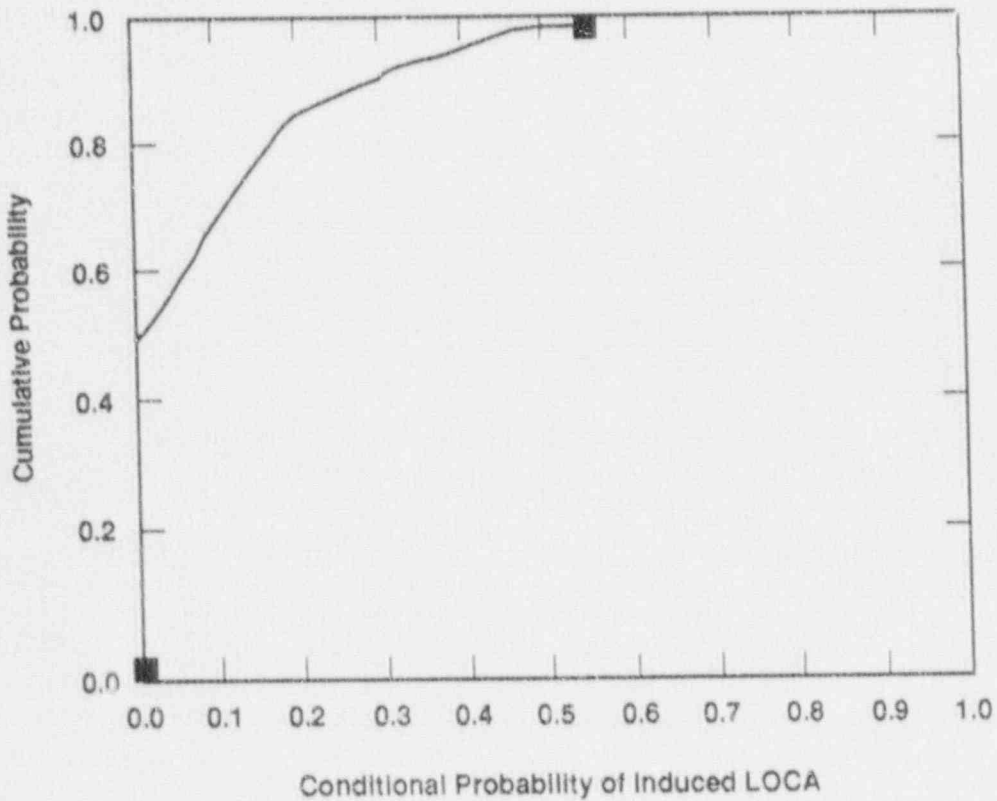
Figure A-2.   Induced Hot Leg LOCA, Case 2

Expert B's Elicitation

Issue 1. Temperature-Induced PWR Hot Leg or
Surge Line Failure Before Vessel Breach

Description of Expert B's Rationale

Expert B reviewed the documentation[B-1 to B-6] that was supplied initially with the issue paper and also performed and used some unpublished CORMLT/PSAAC calculations. Results and comments made by Experts A and B were considered in formulating the assessment. Expert B possesses extensive knowledge of the MAAP code and MAAP calculations and has many years experience in rendering and reviewing work related to this subject.

In order to include effects of all three PWR plants in the CORMLT/PSAAC calculations that were performed, the upper plenum mass for the three separate reactors was averaged. The upper plenum mass is important for the effect of its heat capacity on the temperature histories of the upper vessel and hot leg piping structures. Expert B compiled a decomposition for Case 1, which reflects a joint correlation between time to vessel failure and overall system response. For the other cases, this correlation is not necessarily true--there are intervening events which affect the entire process.

Results of Expert B's Elicitation

Case 1

The decomposition for Case 1 included the time from core uncovery to vessel breach, the time that the hardware in question (hot leg piping, surge line, or nozzle) is at creep temperature, and the time required at creep temperature for failure. The decomposition is as follows:

Core Uncovering (t=0)	Time to VB (min) t_1	Time @ creep Temp (min) t_2	Failure Criterion (min) t_3
	>180		
	150		
	120		
	90		
	<60		
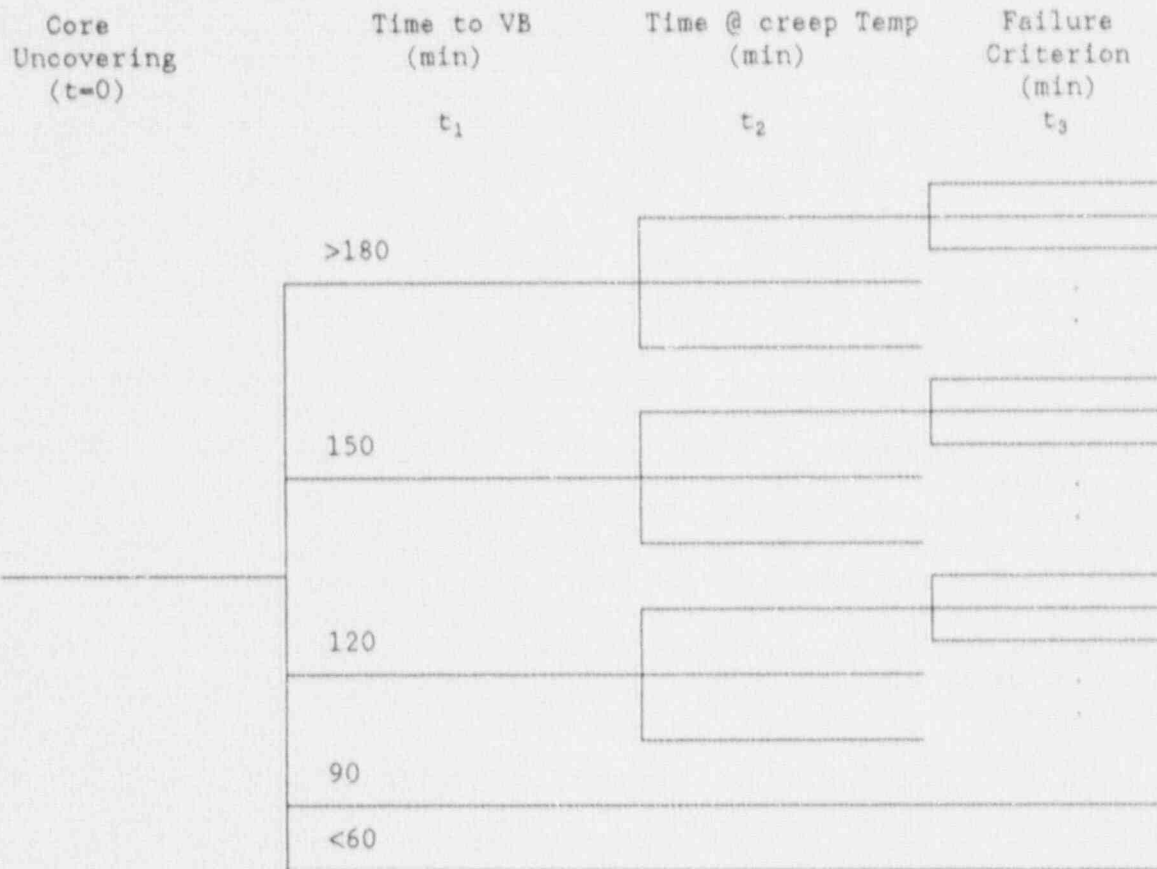
The first two steps in the decomposition were identical for all hardware, and the final two steps were assessed separately for the three pieces of hardware.

Core uncovering is assumed when 100% of the core is exposed. Vessel breach is defined as the initial pathway for rejection of core material from the vessel to containment such that the boundary of the vessel is compromised. Three Mile Island-2 (TMI-2) for instance, did not demonstrate vessel breach, because the core material that followed a pathway along the instrument tubes resolidified within the tubes, thereby plugging them and containing all the core material within the primary boundary.

The decomposition does not include dependency upon natural circulation within the reactor coolant system because the Expert felt that it is not necessary to have natural circulation in order to get a hot leg break in a TMLB' sequence. This is because with a cycling PORV, induced flow in the system already exists, and material is being transported within the system regardless of natural circulation loops.

A time dependency at a predefined creep temperature was included in the decomposition, rather than simply considering a threshhold temperature. A component might reach a threshhold temperature, and then its temperature could decrease due to phenomena such as the formation of blockages which limit heat transfer to the upper vessel structures because circulation has

decreased. Simply considering that a piece of hardware experiences a threshhold failure temperature is not sufficient when assessing creep-rupture of that component.

A value of 1200 K was used in the initial decomposition for the creep temperature. This value was obtained from the information provided by W. Murfin in the issue paper; however, in discussion, Expert A proposed that creep rupture failure occurred when the hot leg piping maintained a temperature of 1000 K for 6 minutes. The creep rupture criterion of this assessment, therefore was adjusted to correspond to the time at which the hardware was at 1100 K.

The decomposition also included a failure criterion consideration. The criterion was specified for the piece of hardware in which the hot leg failure occurs. The hardware included the hot leg nozzle, the hot leg piping and the pressurizer surge line. Distributions were provided for failure of each piece of hardware in terms of the time sustained at a temperature of 1100 K.

For the first branch in the tree, time to core uncovering, the probability is 1.0. The time between core uncovering and vessel breach, t_1, was determined by looking at various calculations. The value of t_1 was judged to be in the 120 to 150-minute regime, but lower failure times were included for cases of auto-catalytic burn of localized melt. In order to get times greater than 180 minutes, there would have to be uniform and symmetrical heat transfer to the entire system. The best estimate is 120 minutes and the distribution between the lower and upper bounds is relatively flat, due to the degraded core geometries where uncertainties are greatest. The distribution was provided as follows:

t_1 (min)	< 60	90	120	150	> 180
Cumulative Probability	0.01	0.25	0.50	0.75	0.99

The time at creep temperature, t_2, is for the component specified. In MELPROG calculations, the surge line attains higher temperatures, and in some calculations it is predicted to be the hot leg piping (SCDAP/RELAP5, MAAP). For small times to vessel breach, i.e., for times $t_1 <$ 100 min., there would be virtually no possibility for the hardware to attain creep temperatures for any extended period of time; thus, there were no hot leg failures for the two lower branches. The larger the value of t_1, the larger the spread in time at creep temperature, t_2.

The times at creep temperature were provided for the surge line, and the creep temperature was defined to be 1100 K. The original supporting CORMLT/PSAAC calculations had been done assuming 1200 K as the creep temperature. To adjust for the change from 1200 K to 1100 K, Expert B reviewed the calculations and adjusted the times by adding 4 min. to t_2. For the other hardware, the times at creep temperature would be less, because the piping and the nozzle are more thermally massive structures. In the support calculations, the piping temperature lags the surge line temperature by about 200 to 300 K, corresponding to a time of about 10 min. The lag time for the nozzle is about 20 min. Thus, for these two pieces of hardware, the time at creep temperature is decreased by these lag times.

The distributions for t_2 for the different hardware conditional on t_1 are as follows:

Cum. prob.   .01   .25   .50   .75   .99

Pressurizer surge line

t_1 (min)			t_2 (min)		
120	6	13	20	27	34
150	20	31	42	53	64
>180	34	49	64	79	94

Hot leg piping

t_1 (min)			t_2 (min)		
120	0	3	10	17	24
150	10	21	32	43	54
>180	24	39	54	69	84

Hot leg nozzle

t_1 (min)			t_2 (min)		
120	0	0	0	7	14
150	0	11	32	33	44
>180	14	29	44	59	74

The decomposition was concluded by assessing CDFs for the three pieces of hardware conditional upon time at creep temperature (t_3) and no previous failure. For the piping and nozzle failures the time distributions were identical for both pieces of hardware. A finite probability was assessed at 0 min. (1%) to account for creep temperatures less than 1100 K. The distributions for failure are as follows:

Cum. prob.	.01	.05	.50	.90	.99

Pressurizer surge line

t_3 (min)	0	3	6	10	20

Cum. prob.	.01	.05	.50	.80	.99

Hot leg piping and hot leg nozzle

t_3 (min)	0	6	12	20	30

The results of the aggregration of these distributions is 65.0% failure of the hot leg before vessel breach. The failure location is the surge line for all occurrences. Failure is possible in the hot leg piping and nozzle, but their failure is conditional upon failure of the surge line. Because it is the same phenomena dictating failure for the three pieces of hardware and the surge line maintains creep temperature longer than the other two components, the failure always occurs in the surge line. Although it is not included in the assessment, the cycling PORV is liable to stick open after thermal effects take their toll; high temperatures affect the actuation process. If this occurred, the sequence would be changed entirely.

The distribution associated with this assessment will be sampled in a zero/one type of mode in which 35% of the samples will be assessed as no failure and 65% of the samples will be assessed as failure. The distribution is shown graphically:

Cumulative Probability

1.0

.35

0.0

0.0   1.0

Frequency of Failure
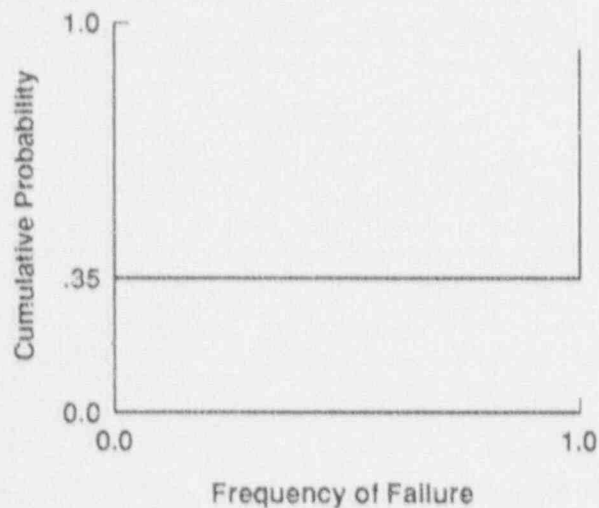
Case 2

For this case, the only information Expert B was able to draw upon was the MELPROG calculation that Expert A had done. The only failure location in this case will be in the surge line, and it will be during the initial (Phase 1) heat-up before the loop seals clear. After they clear, the energy is distributed evenly throughout the entire system, and the time to vessel failure is longer than in Case 1. The surge line was judged to be the only piece of hardware that will be at creep temperature for any period of time during Phase 1 heat-up. During Phase 2 heat-up, failure of all three pieces of hardware was deemed possible.

During Phase 1 heat-up, the probability of hot leg failure is small, but during Phase 2 heat-up, the probability is even smaller--by about 2 orders of magnitude. Thus, phase 1 only was considered in assessing the distribution. It was judged that the decomposition in the issue paper was adequate for this case:

| Gas Temp | Surge line Temp | Surge line failure (yes/no) |
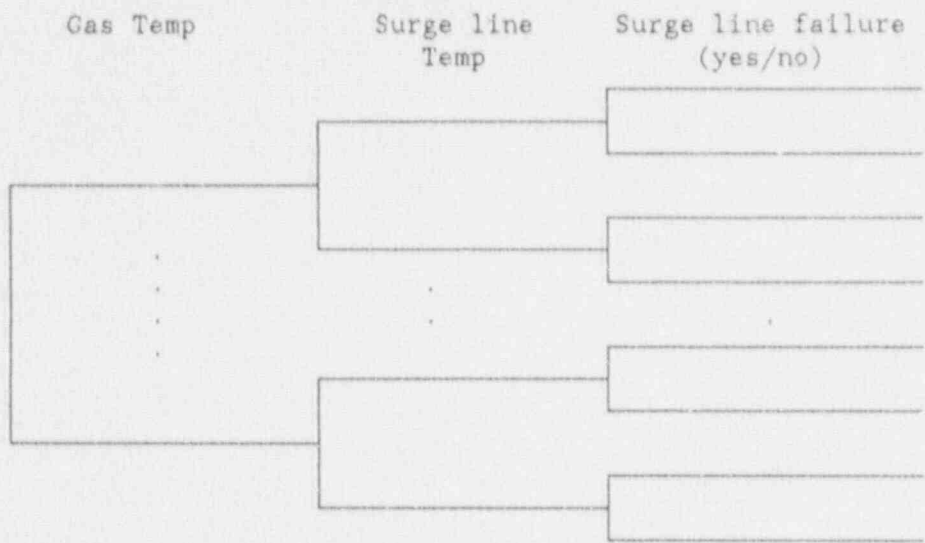
The distribution for gas temperature is the following:

Cum. prob.	.01	.20	.50	.99
Gas Temp (K)	630	1000	1200	1400

The assessed distribution of the surge line temperature conditional on the gas temperature is (uniform over distribution):

Cumulative Probability	.01	.99

Gas Temp (K)	Surge line Temp (K)	
<1000	630	700
1000-1200	650	800
1200-1400	750	950

The probability of surge line failure conditional on surge line temperature is:

Cum. prob.	0.0	0.0	.02	.10
Surge line Temp (K)	630	800	900	950

The results of the aggregration of these distributions is 0.3% failure of the hot leg surge line before vessel breach. For this case, Expert B felt that without Expert A's calculation, cooling of the entire system would have been misjudged, and originally the probability of hot leg failure would have been considered higher. The loop seal clearing is very important in consideration of this case.

Case 3

Expert B felt there was not enough quantitative information available in reference to this case, therefore no distributions were assessed.

Sources of Uncertainty

There are many uncertainties involved in the phenomenological modelling in
the codes that are used to quantify the phenomena involved in this issue.
One uncertainty affecting the distribution is the assumptions involved in
the formation of blockages. In the MAAP code, blockages form at the onset
of change in core geometry. These blockages then hamper natural
circulation and temperatures in the upper plenum and hot leg sometimes
decrease as a result. MELPROG and CORMLT/PSAAC allow blockages to form
which can remelt. It is the assumptions that are made in the codes--when
the core geometry is changing--that lead to a large part of the uncertainty
in the assessment.

There is uncertainty associated with the partitioning of the energy
throughout the entirety of the RCS. Uniformly distributed energy would
cause lower temperatures in the hot leg structures. Energy transport
throughout the system is the main component of this uncertainty, which may
not be accurately modelled in the codes.

Another contributor to the uncertainty in this issue is the creep failure
mode in itself. The time at which a piece of hardware must be at an
elevated temperature before failure is not well known. There is another
uncertainty associated with the possibility of local failures. Many of the
hot leg structures are riddled with small tubes and penetrations. It is
not clear how the temperature fields in these spots might affect local
failures. The effect would decrease the lower bound that a structure could
be at creep temperature because the components are smaller. This failure
mode would not affect the upper bound.

Suggested Methods for Reducing Uncertainty

None provided.

REFERENCES

B-1.   V. Denny, and B. R. Sehgal, "PWR Primary System Temperatures During Severe Accidents," ANS Transactions, 47 (317-319), 1984.

B-2.   V. E. Denny, "The Role of Natural Circulations in Severe Accident Analysis," Proceedings of the Topical Meeting on Thermal Reactor Safety, 2:699-719, September 1986.

B-3.   B. R. Sehgal, W. A. Stewart, V. E. Denny, and B. C-J Chen, "Effects of Natural Circulation Flows on PWR System Temperatures During Severe Accidents," Transactions ASME, National Heat Transfer Conference (223-234), June 1985.

B-4.   J. T. Han, Natural Circulation in Reactor Coolant System, Chapter 2 of Uncertainty Papers on Severe Accident Source Terms, NUREG-1265, U.S. Nuclear Regulatory Commission, Washington, DC, 1987

B-5.   J. E. Kelly, R. J. Henninger, and J. F. Dearing, "MELPROG-PWR/MOD1 Analysis of a TMLB' Accident Sequence," SAND86-2175, NUREG CR-4742, Sandia National Laboratories, 1987.

B-6.   P. D. Bayless "Natural Circulation During a Severe Accident: Surry Station Blackout," EGG-SSRE-7858, EG&G Idaho, Inc. (Idaho National Engineering Laboratory), Idaho Falls, ID, 1987.

Expert C's Elicitation

Issue 1. Temperature-Induced PWR Hot Leg or
Surge Line Failure Before Vessel Breach

Description of Expert C's Rationale/Methodology

Expert C has provided a document which contains his reasoning in some detail, and which contains plots of the code results he used as the basis for his conclusions.[C-1] Expert C placed primary reliance on MAAP runs that were made for Ringhals 3[C-2] and Seabrook.[C-3,C-4] Ringhals 3 is a three-loop plant with a NSSS similar to Surry's, and Seabrook is a four-loop plant with an NSSS similar to those of Sequoyah and Zion. He also used results from RELAP/SCDAP,[C-5] MELPROG,[C-6] and CORMLT.[C-7] Creep rupture as a function of time and temperature for the hot leg and the surge line were taken from the curves in NUREG-1265.[C-8]

Expert C defined the term "hot leg" to include the surge line as well. As both are large pipes and result in large LOCAs as defined in NUREG-1150, no differentiation is made hereafter. The MAAP runs all indicated that the hot leg would fail before the surge line. Some results with other codes, however, showed that the surge line temperatures were higher than the hot leg temperatures. Because the steam density is a strong function of pressure, Expert C concluded that the strong natural circulation necessary to create high temperatures in the hot leg could occur only when the RCS is at, or near, the PORV setpoint pressure. Thus, any previous break in the RCS pressure boundary, such as a major failure of the reactor coolant pump seals or the deliberate opening of the PORVs by the operators, will preclude a temperature-induced hot leg failure during core melt. Additionally, if the auxiliary feedwater system is operating, the high temperatures required for a hot leg break will not be reached in the primary system due to reflux cooling in the steam generators. Expert C concluded that only the first case would have the RCS at system setpoint pressure, and that is the only case that he quantified.

Expert C was certain that the second case would not result in core melt with the RCS at 17 MPa (2500 psia) or thereabouts. Case 3 has core melt at or below 8 MPa (1200 psia) by definition. Hot leg failure before vessel breach requires that the RCS be at the PORV setpoint pressure for two reasons. First, the reduced pressure severely reduces the effectiveness of natural circulation. As it is natural circulation which is transferring the heat from the core to the hot leg, this results in lower temperatures. Second, the lower pressures result in lower hoop stress on the pipe. Taken together, these reasons make hot leg or surge line failure not credible if there is a pump seal failure or any other event which significantly reduces the pressure below the PORV setpoint pressure.

In the Seabrook MAAP runs,[C-3,C-4] the assumptions about core blockage, clearing of the loop seals, and the time between core slump and vessel failure were varied. The combinations are ranked below, with the combination that gave the highest hot leg and surge line temperatures at the top:

1. No core blockage, loop seal present;
2. Core blockage, loop seal present, long time to vessel failure;
3. Core blockage, loop seal cleared, long time to vessel failure;
4. Core blockage, loop seal present, short time to vessel failure;
5. Core blockage, loop seal cleared, short time to vessel failure.

That is, hot leg temperatures were higher when the core steam flow channels were not blocked by refreezing core debris during the relocation process than for any combination of the other two factors when the center of the core was blocked.

In the Surry MELPROG runs, the assumptions about natural circulation and the time of fuel rod relocation were varied. It was actually the temperature at which the clad relocates which was varied, but this has a direct effect on the time of fuel relocation as it takes longer to achieve a higher temperature. The combinations are ranked below, with the combination that gave the highest hot leg temperatures at the top:

1. Natural circulation, delayed fuel rod relocation;
2. Natural circulation, early fuel rod relocation;
3. No natural circulation.

In the Ringhals MAAP runs, the assumptions concerning core blockage and the time between core support plate failure and reactor vessel failure were varied. The combinations are given below, with the combination giving the highest hot leg temperatures at the top:

1. Delayed RV failure, no core blockage;
2. Delayed RV failure, core blockage;
3. Early RV failure, core blockage;
4. Early RV failure, no core blockage

Results of Expert C's Elicitation

Figure C-1 shows Expert C's decomposition tree. The first question or top event is hydrogen production in the reactor vessel, expressed in terms of the fraction of zirconium inventory reacted prior to the time the core slumps into the bottom head. Although some hydrogen could be produced from other metal-water reactions, the total hydrogen produced is translated into a percentage of equivalent zirconium inventory reacted. The hydrogen production is one of the major parameters impacting primary system temperatures and includes the considerations of relocation temperature, mode of core slump, and the formation of core blockages.[C-1]

The other question on the tree illustrating Expert C's decomposition concerns the time between the core slump into the bottom head and the failure of the vessel. This can be interpreted as a division between vessel failures due to penetration failures, which occur in less than 10 min, and other vessel failure modes, e.g., circumferential bottom head failures, which take longer than 10 min (some as long as 1 h).
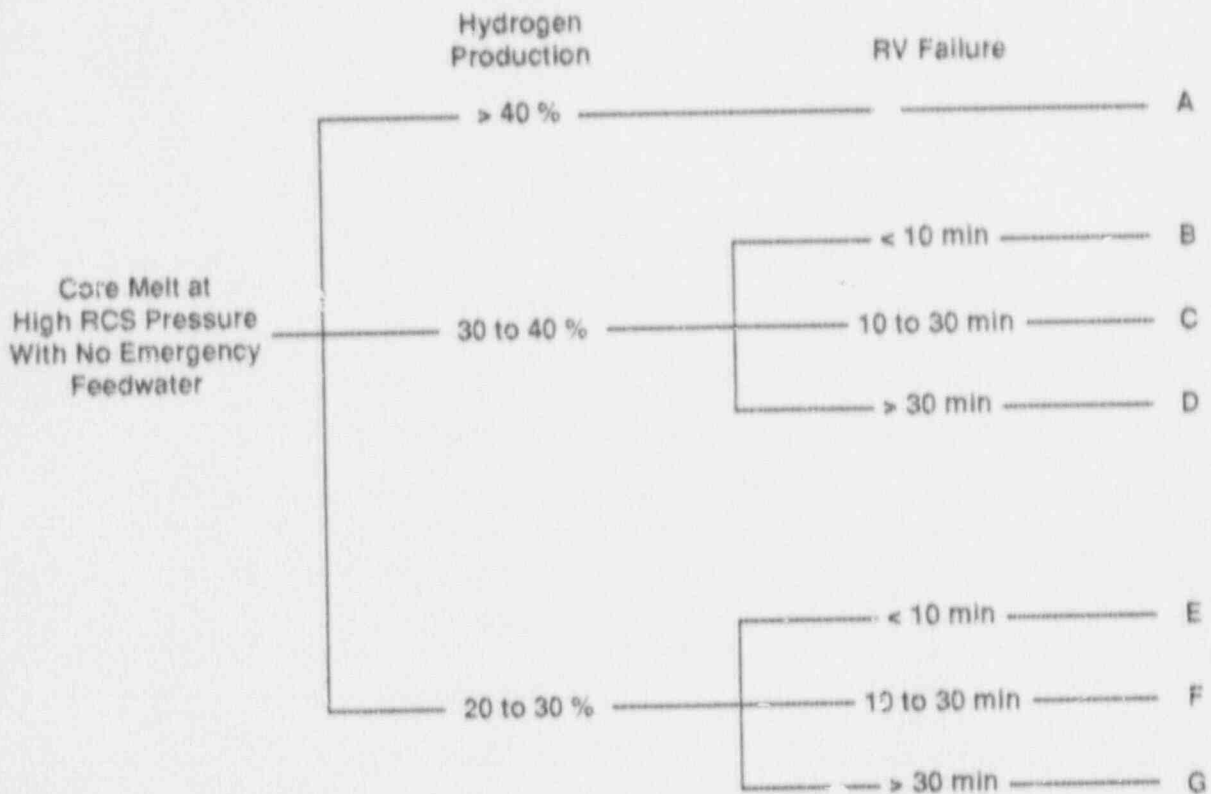
Figure C-1. Expert C's Decomposition Tree.

Expert C obtained the creep rupture leg failure probability for each of the seven endpoints on the tree from one or more MAAP, MELPROG, RELAP/SCDAP, or CORMLT analyses as shown in Tables C-1 and C-2. In Expert C's view, each path of the tree would always result in either;

1. RCS failure prior to vessel failure; or
2. Vessel failure without RCS failure by creep rupture.

The probability assignments represent the uncertainty in the specification of which event will occur. However, in the opinion of Expert C, failure of the hot leg or surge line was more likely to occur prior to vessel breach than vessel failure without creep rupture failure of the RCS pressure boundary for events which exhibit the following characteristics:

1. RCS pressure at or near the pressurizer PORV setpoint;
2. Dry steam generators at the time the core melts; and
3. No significant and prolonged forced flows in the RCS during core melting.

Table C-1
Summary of Analyses to Investigate
RCS Piping Failure Before RV Failure

Analysis	Peak Hot Leg Temperature	Peak Surge Line Temperature	Time With Temperature Greater Than 1100 K
Seabrook			
Base Case	1035 K	875 K	N/A
No Core Block	1600 K	--	> 30 min
Loop Seal Clear	940 K	--	N/A
Ringhals 3			
Base Case	900 K	900 K	N/A
4-h EFW	800 K	750 K	N/A
No Core Block	980 K	900 K	N/A
Delayed RV Failure	1050 K	900 K	N/A
High Relocation Temperature; Delayed RV Failure	1150 K	900 K	> 10 min
Surry			
RELAP/SCDAP	1200 K	1400 K	> 30 min
MELPROG	1250 K	--	> 30 min
Zion			
PSSAC/CORMLT	--	1475 K	> 30 min

Table C-2
Summary of Hydrogen Production From Analyses
To Investigate RCS Piping Failure Before RV Failure

Analysis	Case	Hydrogen Production (% Zr-Water)
Seabrook	Base Case	Not Reported
	No Core Blockage	Not Reported
	Loop Seal Clear	Not Reported
Ringhals	Base Case	18 %
	4-h EFW	19 %
	No Core Blockage	19 %
	Delayed RV Failure	19 %
	High Relocation Temperature;	
	Delayed RV Failure	27 %
Surry	RELAP/SCDAP	Not Reported
	MELPROG	38 %
Zion	PSSAC/CORMLT	Not Reported

The distribution for the hydrogen production and the time between core slump and and vessel breach should come, in Expert C's view, from In-Vessel Issues 5 and 6. The assignment of values to the endpoints of the tree by Expert C are given in Table C-3.

Based on the MAAP results, which showed the hot leg to be hotter than the surge line in all cases, Expert C concluded that the hot leg would always fail before the surge line. However, this is not a critical point in the evaluation since either hot leg or surge line failure would completely depressurize the RCS before vessel failure.

Sources of Uncertainty

Different codes make different assumptions about the time from core slump to vessel failure; these times are usually dependent upon the mode of vessel failure. For example, MAAP assumes that if the failure mode is penetration failure, it will happen within a few minutes after slump whereas bottom head failure may take 30 to 60 min from slump. Obviously these times affect the time available for hot leg failure to occur.

There are also uncertainties in the creep rupture correlation, the material properties, the natural circulation models used, heat losses from the pipes, and the neglect of pipe wall heating by deposited fission products. However, Expert C concluded that these uncertainties are relatively small compared with those accounted for by the variations in the MAAP runs, and he did not take these factors into account explicitly. Other weak points

In the RCS pressure boundary are the nozzle between the hot leg and the vessel, the convection thermal sleeve, and the welds joining the parts of the hot leg and surge line together. Expert C concluded that it was sufficient to treat the homogeneous pipe sections of the hot leg and the surge line, and that any uncertainties introduced by these other portions of the pressure boundary were small compared to those in the core degradation model, the fuel-rod relocation time, etc.

Table C-3
Uncertainty Distributions For Logic Diagram

	Percentile		
End Point	5th	50th	95th
A	0.9	0.99	1.0
B	0.5	0.90	0.99
C	0.5	0.95	0.99
D	0.9	0.99	1.0
E	0.25	0.75	0.95
F	0.5	0.90	0.95
G	0.5	0.95	0.99

Correlations With Other Variables

The core degradation model used in the computer code directly affects both this issue and Issue 5--Hydrogen Production. The amount of zirconium oxidized in the vessel before breach directly controls the amount of hydrogen produced. Since zirconium oxidation is exothermic, a high hydrogen production case also results in high hot leg temperatures. In the sampling, it would be inconsistent to take a low core temperature case for hot leg break (Issue 1) and a high zirconium oxidation case for hydrogen production (Issue 5).

Whether hot leg failure occurs has implications for hydrogen production and fission product behavior. If hot leg failure does occur, the steam flow rate in the core will increase due to flashing as the pressure drops. The amount of increase depends on how much core blockage is assumed. Thus, if the zirconium oxidation has been steam-limited up to this time, zirconium oxidation may increase dramatically after the break. The increased steam flow may also greatly reduce the amount of fission product deposition that occurs within the RCS and thus affect the source term.

Applicability

The results of the considerations of hot leg and surge line creep rupture failure are based on analyses of the Westinghouse PWR design. In the opinion of Expert C, the results are applicable to all Westinghouse PWRs with a vessel and RCS configuration similar to Surry and Zion. Because creep rupture failure is highly correlated to natural circulation flows, the results are not directly applicable to CE or B&W designs without further evaluation.

REFERENCES

C-1. R. J. Lutz, Jr., "Creep Rupture Failure of Primary Coolant Piping Prior to Reactor Vessel Failure for Severe Accidents," WCAP-11910, Westinghouse Nuclear Technology & Systems Division, Pittsburgh, PA, July 1988.

C-2. R. J. Lutz, Jr. et al., "Ringhals Unit 3 Severe Accident Analyses to Support Development of Severe Accident Procedures," WCAP-11607, Westinghouse Nuclear Technology & Systems Division, Pittsburgh, PA, 1987.

C-3. M. G. Plys et al., "Seabrook Steam Generator Integrity Analysis," FAI/86-39, Fauske & Associates, Burr Ridge, IL, 1986.

C-4. K. N. Fleming et al., "Risk Management Actions to Assure Containment Effectiveness at Seabrook Station," PLG-0550, Pickard, Lowe and Garrick, Newport Beach, CA, 1987.

C-5. P. D. Bayless, "Natural Circulation During a Severe Accident: Surry Station Blackout," EGG-SSRE-7858, Idaho National Engineering Laboratory (EG&G Idaho, Inc.), Idaho Falls, ID, 1987.

C-6. J. E. Kelly et al., "MELPROG-PWR/MOD1 Analysis of a TMLB' Accident Sequence," NUREG/CR-4742, U.S. Nuclear Regulatory Commission, Washington, DC, 1987.

C-7. V. E. Denny, "The Role of Natural Circulations in Severe Accident Analysis," _Proceedings of the Topical Meeting on Reactor Physics and Safety_, 2:699-719, September 1986.

C-8. J. T. Han, "Natural Circulation in Reactor Coolant System, Chapter 2 in Uncertainty Papers on Severe Accident Source Terms," NUREG-1265, U.S. Nuclear Regulatory Commission, Washington, DC, 1987.

(Figures 2-7, 2-8, and 2-9 in this report were taken from B. L. Harris et al., Creep Rupture of Three Components of the Reactor Primary Coolant System during the TMLB' Accident, EGG-EA-7431, Idaho National Engineering Laboratory [EG&G Idaho, Inc.] Idaho Falls, ID, 1986.)

Issue 2. Temperature-Induced Steam Generator Tube Rupture (SGTR) Before Vessel Breach

Summary and Aggregation of Issue 2:
Temperature-Induced SGTR before Vessel Breach

Experts Consulted: Robert W. Wright, Nuclear Regulatory Commission; Vern E. Denny, Science Applications International Corporation; Robert J. Lutz, Westinghouse Electric Corporation.

Issue Description

What distributions characterize the uncertainty in the conditional probability of occurrence of temperature-induced SGTRs at Surry, Zion, and Sequoyah? The case to be considered is that in which the reactor coolant system pressure is at or near the PORV setpoint and the secondary side of the steam generators is dry. This is the classic TMLB' sequence in which gross flow exists from the core region, out the PORV in the hot leg containing the pressurizer. Steam temperature may range from saturation (668°F) to very high superheat.

Summary of Experts' Rationale/Methodology

The judgment of Expert A was highly influenced by the consideration of defective steam generator tubes. When defective tubes were not considered, this Expert believed that given an induced LOCA, 98.5% of the time hot leg failure will occur before an SGTR, and 1.5% of the time an SGTR failure will occur first. When defective tubes are considered, however, the distribution for frequency of SGTR failure before failure of the hot leg is 0.3% at the 5th percentile, 3% at the 50th percentile and 10% at the 95th percentile. This Expert believed that the phenomena that drive hot leg and SGTR failures are the same, and therefore the SGTR frequency distribution is perfectly correlated to the hot leg failure frequency distribution.

Expert B believed that induced SGTR requires the same therm hydraulic conditions that lead to induced hot leg failure. To get an SGTR, one needs to have the conditions for hot leg failure but not have hot leg failure before an SGTR. The Expert assigned a multiplier that would be used to determine the frequency of an SGTR if hot leg failure did not occur. In order to incorporate the dependency of both failure modes to the thermal-hydraulic conditions (the modes are perfectly correlated), the multiplier of 0.004 is applied to the hot leg nonfailure frequency multiplied by the hot leg failure conditions. The Expert obtained the value of 0.004 by considerating the frequency of tube defects that exceed 75% of the wall thickness.

In agreement with the other two experts, Expert C believed that the conditions that drive the induced hot leg failure mode also drive the the frequency of induced SGTR. The frequency of an SGTR, however, is small because of the large time lag between temperatures in the hot leg and those

in the steam generator tubes. Even considering tube defects, the frequency of SGTR is so small that it can be expressed as a constant value. Expert C provided a value of 10^{-4} for the conditional probability of an SGTR.

For incorporation into the containment event tree, hot leg failure becomes conditional upon SGTR failure, because of the stipulation of Expert A. The probability distributions for each failure, must be perfectly correlated, as stipulated by all three experts.

Method of Aggregation

The probability of SGTR was aggregated by averaging the three distributions. The three distributions for SGTR failure were determined as follows:

Expert A:

  5th percentile: $f_{SGTR} = f_{HL}/.997 * .003$,
  50th percentile: $f_{SGTR} = f_{HL}/.97 * .03$,
  95th percentile: $f_{SGTR} = f_{HL}/.9 * .1$.

Expert B:

  $f_{SGTR} = f_{CHL} * f(HLNF) * .004$,

where

  f_{CHL} = probability for conditions of hot leg failure, and
  $f(HLNF)$ = hot leg nonfailure probability distribution:

    50th percentile: $f(HLNF) = .01$
    95th percentile: $f(HLNF) = .10$

Expert C:

  $f_{SGTR} = .0001$,

where

  f_{SGTR} is probability of SGTR, and
  f_{HL} is the aggregate probability of hot leg failure (Case 1), and
  f_{CHL} can be approximated by f_{HL}.

The distributions are provided in Figure 2-1. Tabular aggregate values are provided in Table 2-1. The distribution for probability of SGTR is correlated to the distribution of probability for hot leg failure.
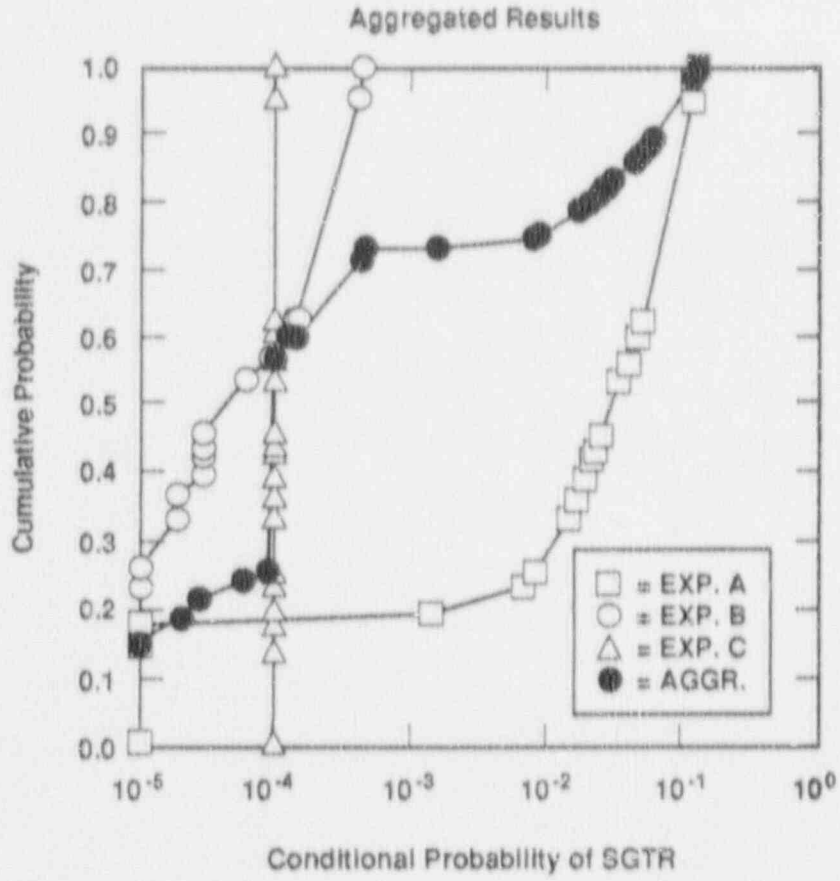
Figure 2-1.   PWR Temperature-Induced SGTR

Table 2-1
Probability of SGTR

Frequency	Cumulative Probability
0.00000	0.0000
0.00000	0.1200
0.00001	0.1400
0.00002	0.1768
0.00003	0.2068
0.00006	0.2336
0.00009	0.2438
0.00010	0.5649
0.00012	0.5906
0.00014	0.5973
0.00040	0.7086
0.00044	0.7254
0.00141	0.7300
0.00703	0.7433
0.00859	0.7500
0.01509	0.7767
0.01715	0.7867
0.01997	0.7967
0.02203	0.8067
0.02356	0.8100
0.02509	0.8167
0.03385	0.8433
0.03982	0.8533
0.04717	0.8667
0.05116	0.8733
0.11110	0.9833
0.12080	1.0000

Individual Elicitations for Issue 2

Issue 2.   Temperature-Induced SGTR before Vessel Breach

Description of Expert A's Rationale/Methodology

Expert A saw the hot leg, surge line, and steam generator (SG) tube temperatures as being closely coupled.   The hot gas which is responsible for the elevated surge line and SG tube temperatures must flow through the hot leg.   The high surge line temperatures are largely caused by the net outward gas flow through the line when the PORV is open.

Expert A concluded that if the hot leg or surge line failed first, SGTRs would not occur because of the reduced pressure in the RCS.   Thus Expert A proceeded by determining the failure temperatures for the SG tubes, the hot leg, and the surge line, and then determining to what temperatures these three portions of the RCS pressure boundary are subjected for what periods of time.   The entire analysis is based on the assumption that the reactor coolant pump seals have not failed so that the RCS is at the PORV setpoint pressure (around 16 MPa).

One of the difficulties with this approach is in determining the temperatures, as there are only a few code runs available that treat this part of the RCS.   Another difficulty is in taking the effects of existing SG tube defects into account.   Finally, the vastly different wall thickness of the hot leg, the surge line, and the SG tubes must be considered. Because the hot leg pipe wall is 2 to 2.5 in. thick, the temperature of the outer surface will be significantly cooler than the inner surface during the rapid oxidation temperature transient.

In determining the relative temperature of the hot leg, the surge line, and the steam generator tubes (SGTs), Expert A placed his primary reliance on the RELAP/SCDAP results of Bayless.[A-1]   The preliminary CORMLT/PSAAC results presented by Vern Denny at the elicitation meeting showed similar values and trends.   This made the RELAP/SCDAP results more believable. Both sets of results showed that the temperature in the surge line leads the temperature in the SG tubes by significant amounts.   This is largely due to the cycling PORV, and it confirms the counter-current flow in the hot leg.

For failure temperatures, Expert A used Figures A-1 and A-2.[A-2]   No similar plot for the surge line was available.   The surge line was believed to be made of 316 stainless steel instead of the 304 stainless steel shown in Figure A-2.   He assumed that the surge line failure curves were similar to those shown in Figures A-1 and A-2.   The time period of interest on these curves is around 0.1 h (6 min).   The SG tubes are so thin that the inner and outer wall temperatures are essentially the same.

To estimate how long it takes for a given temperature change to propagate from the inside wall of the hot leg to the outside wall, Expert A used the MELPROG result shown in Figure A-3,[A-2] checked by a hand thermal diffusion
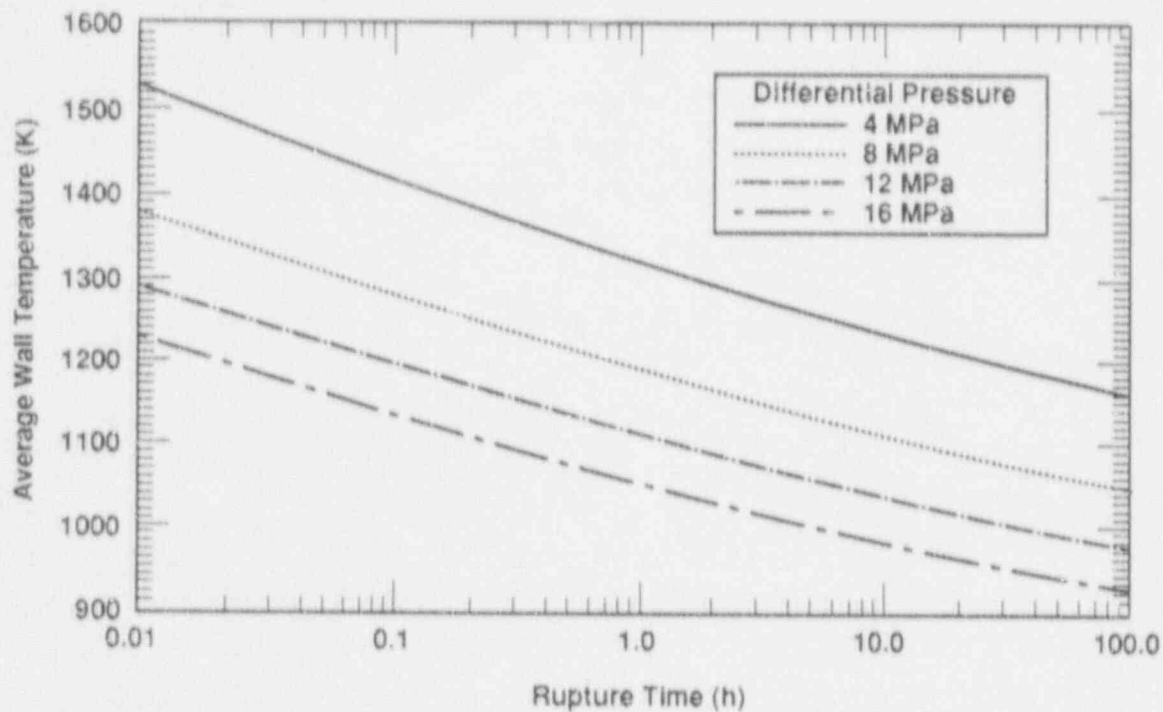
Figure A-1. Average Wall Temperature Versus Rupture Time for Steam Generator Tube.
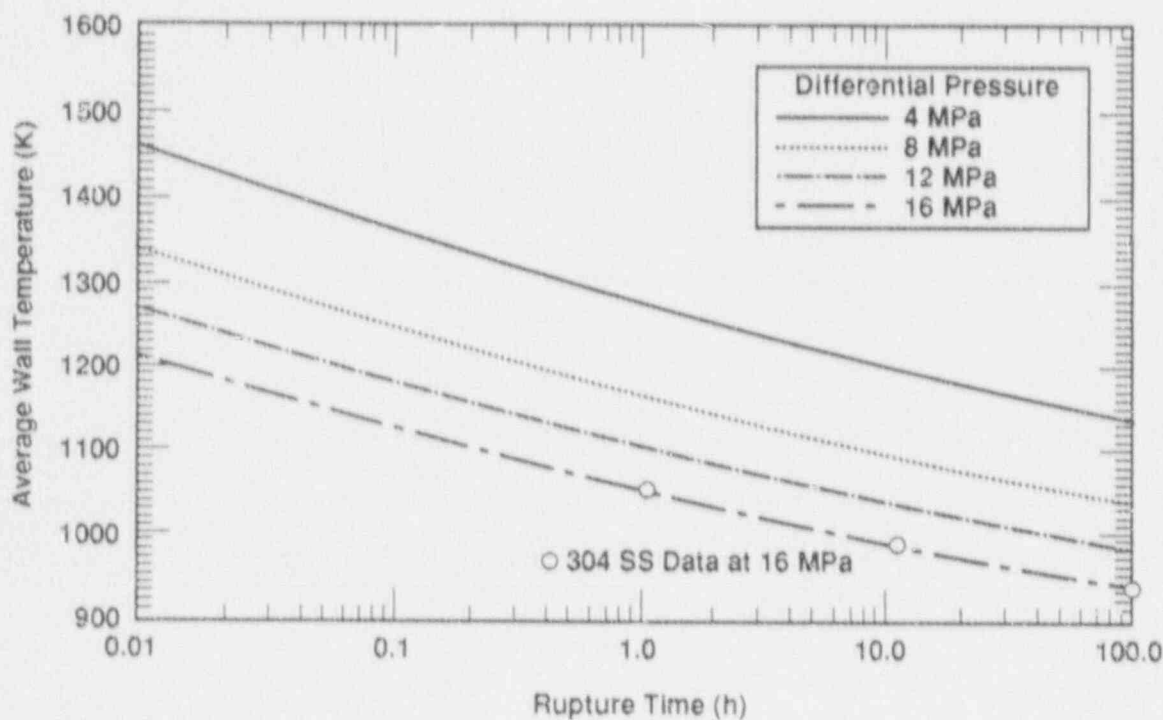
Figure A-2. Average Wall Temperature Versus Rupture Time for Hot Leg Pipe.
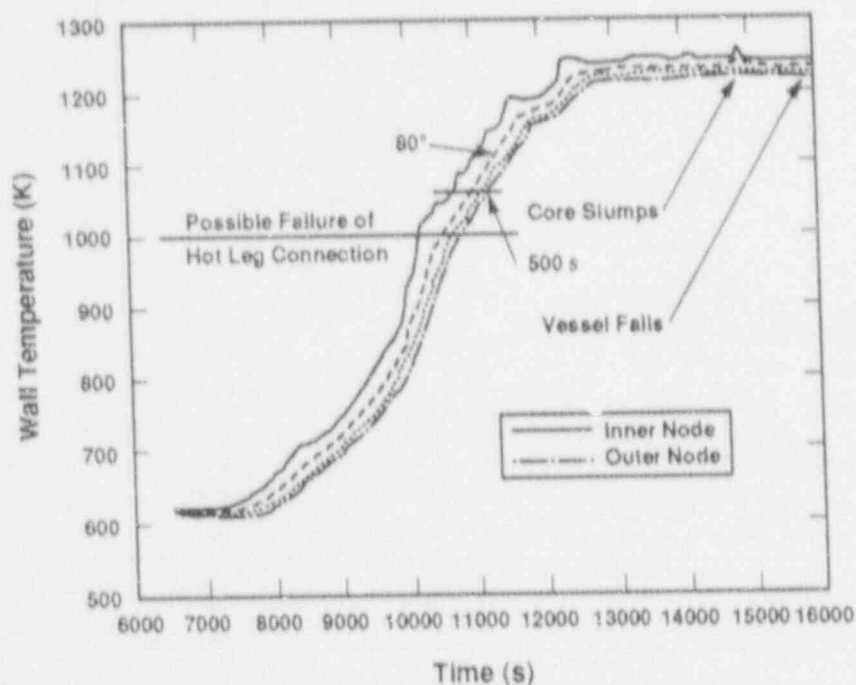
Figure A-3. Temperatures Through Hot Leg Wall at Nozzle--Hot Leg Connection.

calculation. He concluded that the time was about 500 s (8.3 min) and that the difference between the inner and outer wall temperatures was around 80 K. Thus, in comparing the hot leg and SG tube temperatures in Bayless's results, shown in Table A-1, for the time of molten zircaloy relocation in SCDAP, 80 K should be subtracted from the hot leg temperature to get the outer wall temperature, and 50 K should be subtracted to get an average effective temperature for creep rupture considerations. The right column of Table A-1 gives 731 K for the SG tube temperature and 829 K for the hot leg temperature; but this is the temperature of the inner wall of the hot leg. The effective temperature for creep rupture considerations in the hot leg will be about 779 K.

The surge line temperature in Table A-1, however, is 1001 K, and the surge line wall is much thinner than that of the hot leg, so the outer wall temperature would certainly be over 960 K. Thus we have a 230 K or more temperature difference between the outer wall of the surge line and the SG tube temperature. The CORMLT/PSAAC results showed the surge line temperatures leading the SG tube temperatures by similar or larger amounts. Thus Expert A concluded that the surge line was much more likely to fail than an undamaged SG tube.

Table A-1
Conditions When Zircaloy Relocation Begins

Parameter	Once-Through	In-Vessel	Hot Leg and In-Vessel
Time (min)	160.5	167.3	178.3
Hydrogen generated (kg)	96.9	47.2	33.7
Maximum middle channel fuel cladding temperature (K)	--	1747	1546
Maximum upper plenum structure temperature (K)	1100	1248	1153
Hot leg nozzle temperature (K)	633	789	829
Maximum surge line temperature (K)	637	973	1001
Maximum steam generator tube temperature (K)	624	629	731
Reactor vessel liquid level (m)	3.26	2.59	2.11
Pressurizer liquid level (m)	4.03	3.07	1.99
Core outlet flow (kg/s)	1.2	10	11
Core return flow (kg/s)	--	8	8
Upper plenum recirculating flow (kg/s)	--	38	49

At each refueling outage, defective tubes are routinely detected and plugged in PWRs. The presence of defective tubes up to 50% depth in any given SG is therefore nearly certain. From Figure A-1, for 0.1 h, Expert A concluded that a 25% increase in stress is roughly equivalent to a 60 K decrease in the effective temperature for creep rupture failure. Thus he would expect a 50% SG tube defect to reduce the creep rupture failure temperature by about 120 K.

For a TMLB' accident in a Westinghouse PWR with no SG cooling and with the secondary system depressurized, the SCDAP results showed that the hot leg wall temperature would be about 100 K above the SGT temperature. About 50 K should be subtracted to get the average effective creep rupture temperature for the hot leg, which exceeds the SGT temperature by 50 K. As the 50% SGT defect reduces the creep rupture failure temperature by 120 K, the SGT with a 50% defect can be considered effectively about 70 K hotter

than the hot leg. Based on the CORMLT results, the hot leg wall temperature would be 150 K above the SGT temperature. To get the average hot leg temperature 50 K should be subtracted, so the average hot leg temperature exceeds the SGT temperature by 100 K. As the 50% SGT defect reduces the creep rupture failure temperature by 120 K, the SGT with a 50% defect is effectively about 20 K hotter than the hot leg (average) based on the CORMLT results.

Thus Expert A concluded that a SGT with a 50% defect is likely to fail before the hot leg. For a SGT with a 30% defect, he concluded that there was a 50% probability of the SGT failing before the hot leg (neglecting stress concentration, creep correction, etc.). This result is close to that of Murfin,[A.3] which is based on an analysis by Miller.[A.4] However, the discussion above has also showed that the surge line is much more likely to fail than either the hot leg or a SG tube.

Results of Expert A's Elicitation

Considering all the available evidence, Expert A concluded that while the failure of a defective SG tube might be about as likely or more likely than a hot leg failure, surge line failure is much more likely than either of them. Because there are so few code results, and because the codes are forced to make many assumptions and approximations, Expert A was unwilling to assign a probability as high as 99% for surge line failure first. He therefore settled upon a probability of 95% for surge line failure before either hot leg failure or SGTR. Given that the surge line did not fail, Expert A's conclusion, assuming that there were no defective SG tubes, was that the split would be 70% for hot leg failure first and 30% for SGTR first. Considering defective tubes, he doubled the probability of SGTR, to 60%. As there was only a 5% chance that the surge line would not fail first, this gave a 3% chance that an SG tube would fail before the hot leg or the surge line. He took this to be his median value.

Thus, taking defective tubes into account, Expert A gave the following distribution for failure of a SG tube before failure of the surge line or the hot leg:

    0.3% chance of SG tube failure first - 5% confidence
    3% chance of SG tube failure first - median value
    10% chance of SG tube failure first - 95% confidence

where the confidence level indicates Expert A's confidence that the "real" probability of the SG tube failing first does not exceed the value stated.

As hot leg failure and surge line failure are both large breaks and the accident progression analysis does not distinguish between them, there was no need for a distribution between hot leg and surge line failures.

Sources of Uncertainty

The fundamental uncertainties here involve the progression of the melting of the core and natural circulation in the SG tubes. Another source of uncertainty is that there are very few code results and they are all fairly recent. The fact that the preliminary CORMLT/PSAAC results show the same trends and roughly the same values as the RELAP/SCDAP results reduces the uncertainty considerably. There is also uncertainty in the extent of existing defects in the SG tubes.

REFERENCES

A-1 P. D. Bayless, "Natural Circulation During a Severe Accident: Surry Station Blackout," EGG-SSRE-7858, Idaho National Engineering Laboratory (EG&G Idaho, Inc.), Idaho Falls, ID, 1987.

A-2 J. T. Han, "Natural Circulation in Reactor Coolant System," Chapter 2 in Uncertainty Papers on Severe Accident Source Terms, NUREG-1265, U.S. Nuclear Regulatory Commission, Washington, DC, 1987.

(Figures 2-7, 2-8, and 2-9 in this report were taken from B. L. Harris et al., Creep Rupture of Three Components of the Reactor Primary Coolant System during the TMLB' Accident, EGG-EA-7431, Idaho National Engineering Laboratory [EG&G Idaho, Inc.], Idaho Falls, ID, 1986.)

A-3 W. B. Murfin, "Probabilistic Model for Induced Rupture of Steam Generator Tubes," Undated Informal Report, Sandia National Laboratories, Albuquerque, NM. (See Appendix A)

A-4 J. D. Miller, "Stress Analysis of an Inconel 600 Steam Generator Tube," Informal Letter Report, Sandia National Laboratories, Albuquerque, NM, 10 March 1988. (See Appendix A)

Expert B's Elicitation

Issue 2: Temperature-Induced SGTR before Vessel Breach

Description of Expert B's Rationale/Methodology

Expert B has explained his reasoning and provided copies of plots showing code results in a document prepared for his elicitation on these issues.[B-1] He agrees with the definition of the single case for this issue, that is, any prior break in the RCS pressure boundary, such as failure of the reactor coolant pump seals or the deliberate opening of the PORVs by the operators, or operation of auxiliary feedwater, will preclude a temperature-induced SGTR during core melt.

Expert B based his analysis on MAAP runs that were made for Ringhals 3[B-2] and for Seabrook.[B-3,B-4] Ringhals 3 is a three-loop plant with a NSSS similar to Surry's, and Seabrook is a four-loop plant with a NSSS similar to those of Sequoyah and Zion. He also used some RELAP/SCDAP results.[B-5] There were fewer relevant runs than for the hot leg issue since many of the analyses did not report the temperatures for the steam generators. None of the MELPROG runs were of use for that reason. All the code analyses assumed nondefective tubes.

From the temperature versus time to fail plot in NUREG-1265,[B-6] (Figure B.1), Expert B concluded that a nondefective tube would require 30 min at 1110 K to rupture for a 16 MPa pressure difference. This correspɔnds to the primary side of the steam generator at full pressure and the secondary side at atmospheric pressure. (If the secondary system had not been depressurized, the pressure difference would be about 8 MPa.)

The long-term blackout cases are likely to result in SG depressurization at Surry and Sequoyah. This depressurization is accomplished by manually opening valves. There are currently no instructions in the Emergency Operating Procedures at these two plants to close these valves after the steam-turbine-driven AFW fails. Thus it is likely that the pressure difference across the tubes will be 16 MPa for the long-term blackout sequence.

The MAAP results available[B-1] show the effects of varying whether the loop seal clears, the efficiency of natural circulation, core relocation temperature, and core blockage. None of these variations in the MAAP runs produced temperatures over 900 K in the SG tubes. MAAP may or may not be conservative, but the variations used, loop seals clear, for example, served to discount any nonconservatisms built in to MAAP. That is, Expert B feels that some of the variations made in the MAAP runs produced results which tend to overestimate the temperatures in the SG tubes. Therefore the conclusion that the SG tubes do not reach 900 K is not a result of the MAAP base case assumptions or the nature of the MAAP models. Since the creep rupture curve showed that a tube had to be at 1100 K for 30 min to fail, and none of the code results showed tube temperatures over 900 K, Expert B concluded that SGTR for nondefective tubes was not credible.
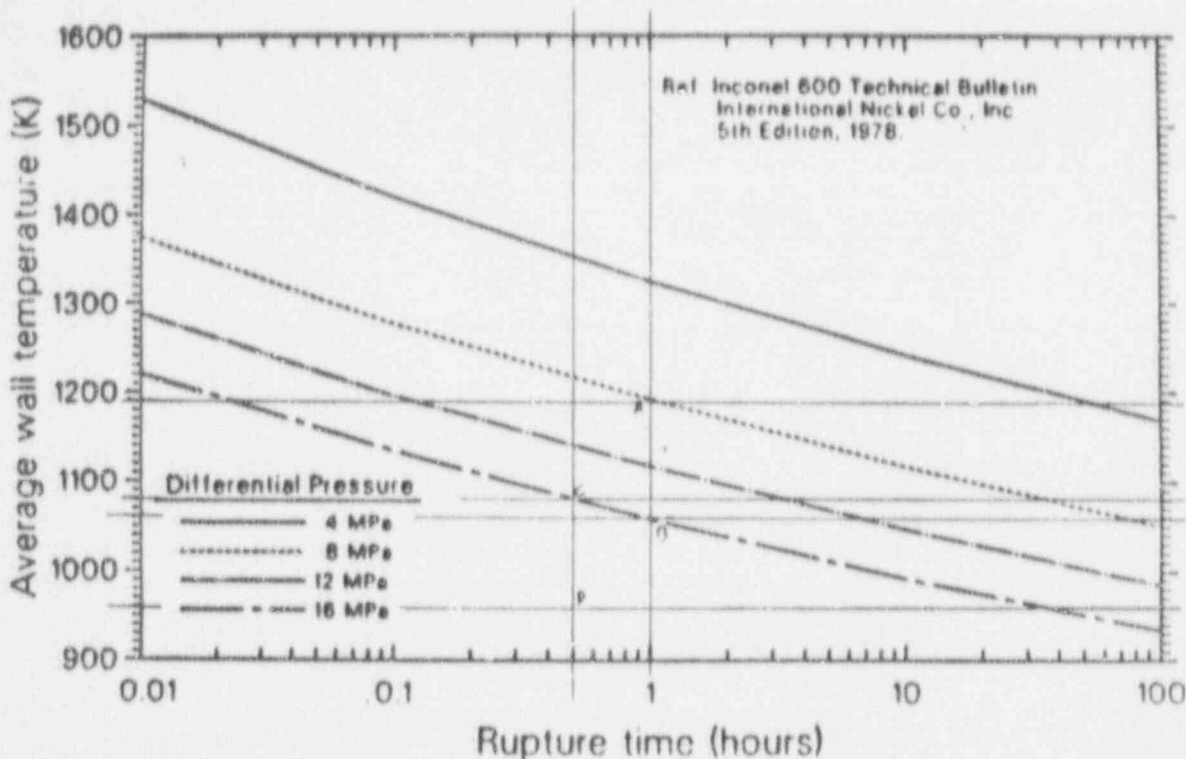
Figure B-1 Average Wall Temperature Versus Rupture Time For Steam
Generator Tube (Inconel 600). (Source: NUREG-1265.)

Expert B then turned to the problem of defective tubes. Steam generator
tube repair data indicates that the probability of having a tube with a
defect that exceeds 75% of the normal wall thickness is on the order of
0.4%. At this thickness, the creep rupture curve for SG tubes shows that a
temperature of over 850 K must be maintained for 30 min for failure to
occur. (The analyses presented in Reference B-1 show this to be an
unlikely event.) For those analyses in which the SG tube temperatures did
exceed 850 K, the hot leg temperatures exceeded the critical temperature
for creep rupture failure before the SG tubes exceeded 850 K.

Thus Expert B concluded that, for cases of hydrogen production exceeding
40% of the equivalent core zirconium inventory, or for vessel failure times
greater than 30 min, the probability of SG tube creep rupture is the
residual of the hot leg failure probability times the probability of there
being tubes with defects greater than 75% of the wall thickness. (The
residual of the hot leg failure probability is 1.0 minus the hot leg
failure probability.) Expert B expects the hot leg failure probability to
be quite high. For the mean value he took the hot leg failure probability
to be 99%, so the mean SG tube failure probability is 0.01 * 0.004 =
0.00004. At the 95% confidence level, he used a hot leg failure
probability of 90% to get a SG tube failure probability of 0.0004.

Results of Expert B's Elicitation

For nondefective tubes, Expert B felt that the evidence clearly showed that SGTR during core melt was not credible. For tubes with 50% wall thinning, the margin between the SG temperature computed in the MAAP runs and the temperature required to fail in 30 min was not so great, but it was still large enough to convince Expert B that SGTRs would not occur.

Expert B pointed out that only about 20% of the SG tubes, those that are directly above the hot leg junction with the SG intake plenum, carry hot gas away from the plenum and are exposed to the high temperatures. The rest of the tubes either have flow back from the outlet plenum or little or no flow. If a defect is to cause an SGTR, the defect must be located near the intake plenum in one of the tubes directly _above_ the hot leg junction. Thus, if a SG has a few defective tubes, the chances are that the defect will not be just above the inlet tubesheet in the 20% of the tubes that are exposed to the hot gases from the hot leg.

Furthermore, most of the SG tube failures, by far, are pinhole leaks. There have only been four actual ruptures, and these were due to something external like a stray bolt in the SG rubbing on a tube or increased stresses at the top bend on the inside tube. As the bulk of the tube wall will not be in the plastic strain region when the defective area fails to form a pinhole leak, the failure will not propagate and cause a rupture. Thus, even if a defective tube were to fail, Expert B would expect only a small leak to result, and the consequences of this are negligible unless many tubes are involved.

Sources of Uncertainty

Expert B feels that there is some uncertainty in the MAAP models and in the assumptions made in the input to MAAP. However, he feels that the variations run, and the sensitivity analyses conducted, adequately cover all the uncertainty about the accuracy of the models and the input. As no SG tube temperatures were observed that were over 900 K for different assumptions about natural circulation, the core degradation model, etc., he concluded that 900 K was at or above the upper end of the uncertainty range for SG tube temperature.

There are also uncertainties in the creep rupture correlation, the material properties, the natural circulation models used, and pipe wall heating by deposited fission products. However, Expert B concluded that these uncertainties are relatively small compared with those accounted for by the variations in the MAAP runs, and he did not take these factors into account explicitly.

REFERENCES

B-1. R. J. Lutz, Jr.,"Creep Rupture Failure of Primary Coolant Piping Prior to Reactor Vessel Failure for Severe Accidents," WCAP-11910, Westinghouse Nuclear Technology & Systems Division, Pittsburgh, PA, July 1988.

B-2. R. J. Lutz, Jr. et al., "Ringhals Unit 3 Severe Accident Analyses to Support Development of Severe Accident Procedures," WCAP-11607, Westinghouse Nuclear Technology & Systems Division, Pittsburgh, PA, 1987.

B-3. M. G. Plys et al., "Seabrook Steam Generator Integrity Analysis," FAI/86-39, Fauske & Associates, Burr Ridge, IL, 1986.

B-4. K. N. Fleming et al., "Risk Management Actions to Assure Contai Effectiveness at Seabrook Station," PLG-0550, Pickard, Low- Garrick, Newport Beach, CA, 1987.

B-5. P. D. Bayless, "Natural Circulation during a Severe Accident: Surry Station Blackout," EGG-SSRE-7858, Idaho National Engineering Laboratory (EG&G Idaho, Inc.) Idaho Falls, ID, September 1987.

B-6. J. T. Han, "Natural Circulation in Reactor Coolant System," Chapter 2 in Uncertainty Papers on Severe Accident Source Terms, NUREG-1265, U.S. Nuclear Regulatory Commission, Washington, DC, 1987.

(Figures 2-7, 2-8, and 2-9 in this report were taken from B. ... Harris et al., Creep Rupture of Three Components of the Reactor Primary Coolant System during the TMLB' Accident, EGG-EA-7431, Idaho National Engineering Laboratory [EG&G Idaho, Inc.], Idaho Falls, ID, 1986.)

Expert C's Elicitation

Issue 2. Temperature-Induced SGTR before Vessel Breach

Description of Expert C's Rationale/Methodology

Expert C reviewed the documentation,[C-1 to C-6] that was supplied initially with the issue paper, performed some CORMLT/PSAAC calculations and used some unpublished CORMLT/PSAAC calculations performed by Wassel at Science Applications International Corporation (SAIC). Comments of Experts A and B were taken into consideration for this assessment.

The PSAAC calculations have investigated somewhat mechanistically circulating flows in steam generator plena and tubes. The first 50 minutes of the accident are a key factor in determining the steam generator tube temperatures. At about 50 minutes, rapid breakaway zirconium oxidation occurs and core geometry begins to degrade; at this time hydrogen collects within the steam generator tubes, thus ending any natural circulation cells that may have been established.

For Westinghouse reactors, the heat sink mass in the upper plenum of the reactor is critical for assessing this problem. The difference in mass between any two reactors might be as high as a factor of four. This prompted a sensitivity study in which the lower bound was 16,000 kg and the upper bound was 75,000 kg. All structures were modelled in great detail-- heavy structures were multi-nodal, thin structures were single nodes. The structures included the upper core support system and control rod guide mechanisms. The results of the study show that for the upper bound, the curves are simply shifted in time; temperature profiles themselves do not decrease in magnitude for the larger thermal masses.

Results of Expert C's Elicitation

Temperatures in the hot leg will be sustained at creep temperatures long before the steam generator tubes will attain threshhold creep temperatures. The gas temperatures in the steam generator tubes lag the hot leg surge line structural temperature by ~400 K. The hot leg will fail before SGTR. In addition, the conditions that provide hot leg failure are exactly the ones that provide SGTR conditions, thus if the reactor coolant system pressure boundary is to fail, it will almost certainly be in the hot leg rather that in the SG tubes. In the worst case, at about 35 minutes into the accident (15 minutes before hydrogen generation), the gas temperatures in the steam generator plenum are ~800 K and the tubes are at ~700 K. At this temperature, there is a very low probability of failure (~10^{-4}). In the very unlikely event that SGTR occurs it is limited to the three loops (in a four-loop system).

The probability of SGTR of 10^{-4} applies given no pre-existing tube leakages. This probability also applies in cases where tubes are thinned or have defects. Without a pre-existing leak, natural circulation is not enough to raise the temperature in the steam generator tube structures to

creep temperatures before creep temperatures occur in the hot leg structures for extended times. The only exception would be to have a pre-existing leak which promoted forced circulation, or to have a defect such as a crack that might fail at a lower temperature. Without knowing the probability of the occurrence of such leaks or cracks (judged to be low), Expert C could not assess the probability of SGTR, based on this assumption. However, given a pre-existing crack or leak, the probability of failure would be very high (~.99)

The PSAAC code includes fission product self-heating within the coolant in the system--the current assumption is that 15 to 20% of the volatiles are released during the first 10 minutes. Higher temperatures than the PSAAC calculation predicted in the SG tube structures might occur if there were local depositions of high concentrations of volatiles in the SG tubes. Because the SG tube temperature is colder than other structural temperatures, this phenomenon would be promoted. But to attain creep temperatures, both this phenomenon (probability of ~10^{-2}), as well as a higher release of ~90% of volatiles (probability of ~10^{-2}) would have to occur. The resulting combined probability of this event is therefore also 10^{-4}.

The final assessment for conditional probability of induced SGTR, therefore, is 10^{-4}. It was assumed that if any defects were present in SG tubes, they would not be pre-existing leaks or cracks.

Sources of Uncertainty

Expert C feels that the main source of uncertainty in this issue is the possibility that there are pre-existing leaks or cracks at the onset of the accident. As far as modelling uncertainties are concerned, the large temperature difference of 400 K between the hot leg structures and the SG tube structures is too high for any mechanisms to be present to drop the difference significantly. If all the decay heat was dumped into the entire system uniformly, it would yet be unlikely that temperatures greater than 1200 K would be attained in the steam generators.

Suggested Methods for Reducing Uncertainty

None provided.

REFERENCES

C-1. V. Denny, and B. R. Sehgal, "PWR Primary System Temperatures During ... Accidents," ANS Transactions, 47 (317-319), 1984.

C-2. ... Denny, "The Role of Natural Circulations in Severe Accident Analysis," Proceedings of the Topical Meeting on Thermal Reactor Safety, 2:699-719, September 1986.

C-3. B. R. Sehgal, W. A. Stewart, V. E. Denny, and B. C-J Chen, "Effects of Natural Circulation Flows on PWR System Temperatures During Severe Accidents," Transactions ASME, National Heat Transfer Conference (223-234), June 1985.

C-4. J. T. Han, "Natural Circulation in Reactor Coolant System," Chapter 2 of Uncertainty Papers on Severe Accident Source Terms, NUREG-1265. Washington, DC: U.S. Nuclear Regulatory Commission, 1987.

C-5. J. E. Kelly, R. J. Henninger, and J. F. Dearing, "MELPROG-PWR/MOD1 Analysis of a TMLB' Accident Sequence," NUREG/CR-4742, SAND86-2175, Sandia National Laboratories, Albuquerque, NM, 1987.

C-6. P. D. Bayless, "Natural Circulation During a Severe Accident: Surry Station Blackout," EGG-SSRE-7858, EG&G Idaho, Inc., (Idaho National Engineering Laboratory), Idaho Falls, ID, 1987.

5.3   Issue 3. BWR In-Vessel Hydrogen Production

Summary and Aggregation of In-Vessel Issue 3:
BWR In-Vessel Hydrogen Production

Experts Consulted: Peter Bieniarz, RMA; Steve Hodge, Oak Ridge National Laboratory; Michael Podowski, Rensselaer Polytechnic Institute; Garry Thomas, Electric Power Research Institute.

Issue Description

Estimates of hydrogen production for various accident sequences are important in determining the amount of variables needed for the accident progression analysis (containment pressure loads, containment temperature, reactor building loads), and for the source term analysis. Hydrogen production is to be estimated in this issue for BWRs (Grand Gulf, LaSalle and Peach Bottom) using Peach Bottom as a surrogate. If the experts believe that there are differences between reactors, they can account for the differences by making appropriate adjustments to the Peach Bottom assessment.

The exact definition of the variable elicited was the percent of hydrogen produced relative to the maximum hydrogen production achievable by complete oxidation of all the in-core zirconium. Accounting for oxidation of other metals could lead to percentages larger than 100%. Experts could select an alternative variable (e.g., tons of hydrogen produced) as long as it could be translated into the elicitation variable.

The panel experts were asked to provide their answers in the form of cumulative probability distribution functions or fractiles of the probability density function over percent of hydrogen produced. The experts were to consider six cases:

Case 1a: Short term high pressure meltdown without recovery,
Case 1b: Short term high pressure meltdown with low pressure injection recovered prior to the breach of the reactor pressure vessel,
Case 2a: Short term low pressure meltdown without recovery,
Case 2b: Short term low pressure meltdown with low pressure injection recovered prior to the breach of the reactor pressure vessel,
Case 3a: High pressure meltdown with CRD injection without recovery,
Case 3b: High pressure meltdown with CRD injection with low pressure injection recovered prior to the breach of the reactor pressure vessel.

Panel experts were further requested to state the time history of hydrogen production, and to make estimates before and after bottom head failure.

Summary of Experts' Rationale/Methodology

Expert A identified four stages between the beginning of oxidation and vessel breach for Cases 1a and 1b, and estimated hydrogen production in terms of increments at each stage: stage 1, from beginning of oxidation to relocation of zirconium; stage 2, from beginning of relocation to the point at which debris drops onto the core plate; stage 3: from beginning of debris collection on the core plate to debris drop into the lower plenum, but before vessel breach; stage 4: after vessel breach.

In addition, Expert A identified two other phenomena that had a major impact on hydrogen production. The first phenomenon is blockage of the steam pathways through the core; blockage impairs steam flow and thereby significantly reduces hydrogen production. The Expert thought that the blockage effect was larger during early stages than during later stages when steam levels would be high. The second phenomenon is the time at which water was recovered. Water recovery leads to a temporary surge in steam and hydrogen production, after which further hydrogen production would cease. He felt that water recovery would lead to 2% additional hydrogen production at any stage of the process.

Expert A believed that there is relatively little hydrogen production in the first stage. The hydrogen production in the subsequent stages is more significant than the production in the first stage with production in stage 2 about twice that in stages 3 and 4. In stage 2, competing effects occur: higher temperatures lead to autocatalytic hydrogen production; at the same time the metals move down into the cooler regions, which reduces hydrogen production somewhat. In stage 3 much steam would be generated and quenching of the debris would produce additional steam and hydrogen. In stage 4 another steam surge would occur.

During the latter phase of hydrogen production, Cases 2a and 2b do not differ significantly from Cases 1a and 1b. During the first stage, Cases 2a and 2b produce more hydrogen than Cases 1a and 1b.

The Expert thought that the main difference between Cases 1a and 1b and 3a and 3b was the larger supply of steam. This increases hydrogen production by 5% throughout the process.

He did not see any differences among the three BWRs that would significantly influence his uncertainty about hydrogen production and he therefore assessed only one distribution for all plants.

Expert B's assessments were based on an analysis of Peach Bottom (BWR/4 Mark I) using the BWRSAR code.[3-1] For each of the Cases (1 to 3 with and without water recovery), BWRSAR was used to predict the total amount of hydrogen produced in the vessel. This value was then used as a "best" (median) estimate of in-vessel hydrogen production.

In order to account for uncertainty in this estimate, Expert B considered 14 separate sources of uncertainty and assessed how each of these would change his "best estimate" calculated by BWRSAR. The sources of uncertainty are listed below:

1. Oxidation of Relocating Control Blade and Channel Box Material.
2. Oxidation of Material Quenching above Core Plate.
3. Oxidation of Candling Clad (Shape Factor).
4. Effect of Blockage Formation by Relocated Material.
5. Amount of B_4C-Steam Reaction.
6. Mode of Core Plate Failure.
7. Oxidation of Solid Debris Relocating into Bottom Head.
8. Oxidation of Molten Debris Quenching in Bottom Head.
9. Collapse of Fuel Pellet Stacks.
10. Layering of Debris in Bottom Head.
11. In-Vessel Natural Circulation.
12. Metal Oxidation of Upper Debris During Boiloff.
13. Oxidation of Zr Metal During Blowdown.
14. Oxidation of Stainless Steel During Blowdown.

In some situations, correlations were considered and adjustments are made instead of simply adding uncertainty ranges.

Expert C based much of his rationale on APRIL[3-2] calculations. He assessed hydrogen production for eight situations. For each of the eight cases, the timing during which the hydrogen is produced was considered. The critical points in the accident sequence were defined as follows:

Time 0:   Water level is at the top of the active fuel (TAF) and dropping.

Time 1:   The water level drops to the core plate.

Time 2:   The time before vessel breach.

Time 3:   The end of blowdown (or the end of flow for low pressure cases).

Time 4:   End of the accident (or gross lower head failure whenever it occurs).

Expert C felt that the majority of the hydrogen is produced before core plate failure. Expert C did not consider the amount of hydrogen produced by each of the three BWRs individually.

Expert D relied on his experience in degraded core modeling (including code development, code applications, and detailed study of TMI-2) to assess BWR hydrogen production.

Expert D assessed hydrogen production in two ways which were then compared to reach a final assessment. The first of these was a direct assessment of the cumulative distribution function for the amount of hydrogen produced that was developed by Expert D in preparation for the elicitation session. The second assessment, during the elicitation, decomposed the production of hydrogen into two parts where hydrogen is first produced in-core and then produced in the bottom head.

With regard to the sequences in which cooling is eventually recovered, the Expert felt that hydrogen production would not occur if the upper one-third of the core remained uncovered.

Expert D felt the estimates for the fraction of equivalent zircaloy oxidation produced at Peach Bottom could be used for the other BWRs. Hydrogen production in other BWRs would then be in proportion to the ratio of total core zircaloy inventories.

Method of Aggregation

The operations performed on the results of the expert elicitation in order to obtain distribution for aggregation are discussed in this section.

Expert A:

This Expert combined distributions for extensive blockage and moderate blockage using a weighted average. He indicated that the likelihood of extensive blockage was 10% and, therefore, the likelihood of moderate blockage was 90%. The distribution weights used in this averaging process correspond to these possibilities.

Because of the large uncertainty associated with the timing of the various in-vessel stages, the early water recovery distributions (stage 1) were averaged with the late water recovery distributions (stage 2). In other words, there is a 50% chance of early injection and a 50% chance of later injection.

Expert B:

Total H_2 production curves are obtained from elicitation writeup. For the case with water injection recovery and anticipated transient without scram (ATWS) (Case 3a), there is no H_2 production in the bottom head because the vessel is assumed not to fail. The only cases which include bottom head H_2 production are Case 1a and Case 2a.

Case 1a. Uncertainty bounds for total H_2 production: 0.3 to 0.8 with a best estimate of 0.64. Uncertainty associated with in-core H_2 production is -0.29 to +0.16 on a best estimate of 0.323 or:

    low bound = 0.323-0.29 = 0.033
    upper bound = 0.323+0.16 = 0.483.

The distribution for H_2 production before vessel breach corresponds to the in-core H_2 production.

The distribution for H_2 production before vessel breach is obtained by applying a scaling factor to the total H_2 production distribution (multiply the amount of zirconium oxide from the total distribution by the scaling factor). The scaling factor is simply the ratio of the range in zirconium oxidation before vessel breach to the total range in zirconium oxidation:

$$SF = \frac{(0.483 - 0.033)}{(0.8 - 0.3)} = 0.9$$

$$Zr\ oxid_{BVB,2} = (Zr\ oxid_{TOT,2} - Zr\ oxid_{TOT,LB})\cdot SF + ZR\ oxid_{BVB,LB}$$

where subscript 2 refers to the point of interest and subscript LB refers to the low bound.

Case 2a. Uncertainty bound for total H_2 production is 0.1 to 0.6 with a best estimate of 0.27. Note: The actual uncertainty range is from 0.18 to 0.53 but the tails were extended to 0.1 and 0.6, respectively. The uncertainty is -0.09 and +0.26.

Uncertainty in In-Core Production. The uncertainty in in-core production is -0.09 and +0.19 with a best estimate of 0.262. The tails are divided based on relative contribution to the uncertainty in the in-core H_2 production. (The low bound on the uncertainty is only associated with in-core H_2 production; thus, the portion of the tail is added to the lower end of the distribution will only be included in the in-core releases.)

Upper tail: 0.6-0.53 = 0.07
Fraction attributed to in-core H_2 production:

$$[0.07]\left(\frac{0.19}{0.26}\right) = 0.051$$

lower bound: 0.1 = (0.262 - 0.09 - tail)
upper bound: 0.262 + .19 + 0.051 = 0.503

$$scaling\ factor = \frac{(0.503 - 0.1)}{(0.6 - 0.1)} = 0.806.$$

Expert C:

Consolidation of Case 3.

Expert C divided Cases 3a and 3b into 3xa, 3ya, and 3yb based on whether the flow rate is sufficient to cover the core plate. Because of the large uncertainty associated with the likelihood that the flow rate of water is sufficient to cover the core plate, it was assumed that Cases 3xa and 3ya were equally likely and were, therefore, averaged together. A similar approach was taken for the combustion of Cases 3xb and 3yb.

H_2 Production Before Vessel Breach

The Expert provided a distribution for the total amount of H_2 that would be produced in vessel. Then, given a specified level of hydrogen production for each case, the percentage produced in the various stages of the accident progression was estimated. The Expert divided the accident into four time regimes. For each time regime the Expert provided a distribution for the fraction of the total zirconium oxide

that would be oxidized by the end of that time regime. Time regime 2 corresponded with the time just before vessel breach.

To obtain the amount of H_2 produced up to the time of vessel breach (time regime 2), the total H_2 production distribution was convolved with the distribution that represented the fraction of H_2 produced before vessel breach. These two distributions were convolved numerically by using Latin Hypercube Sampling (LHS).

H_2 Production up to End of Blowdown

The distribution associated with time regime 3 for the fraction of H_2 produced was convolved with the total H_2 production curve.

H_2 Production During Blowdown

The H_2 production distribution for time regime 3 was subtracted from the distribution associated with before vessel breach (time regime 2) to give the amount produced during the blowdown. The fraction of H_2 produced before vessel breach was correlated (correlation of 1) with the fraction of H_2 produced up to the end of blowdown. The total H_2 production curve was sampled independently from these two distributions.

Expert D:

The distributions provided by Expert D corresponded with the H_2 production before vessel breach; no further operations were necessary.

Aggregated Results

The aggregated results for the in-vessel hydrogen production issue are given in Figures 3-1 to 3-6 for the cases defined earlier.
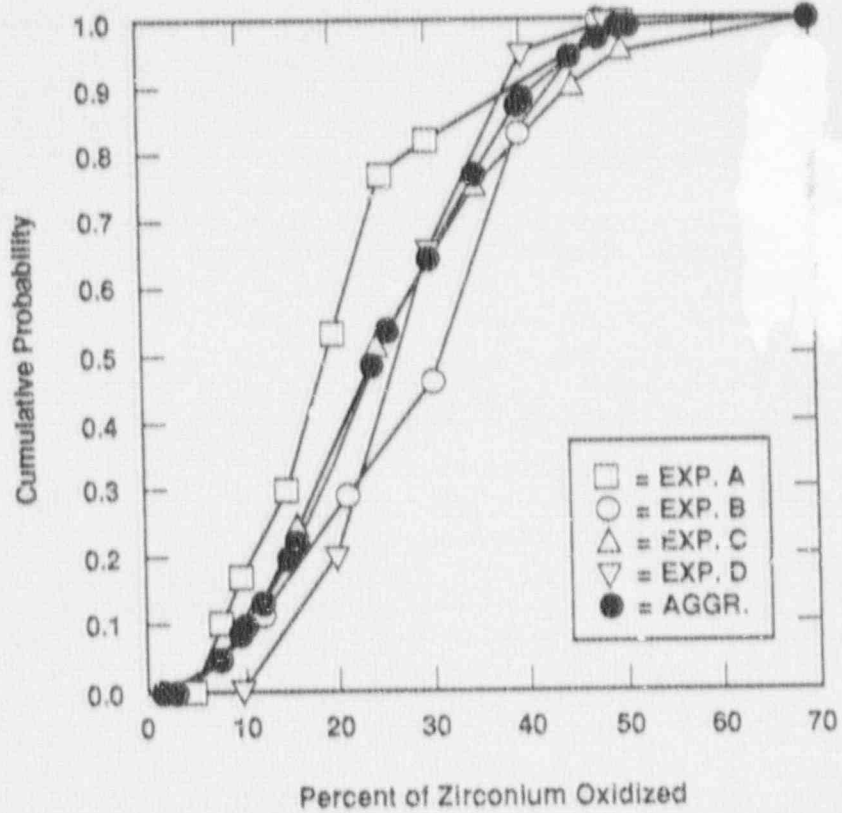
Figure 3-1.   Case 1a: Before Vessel Breach.
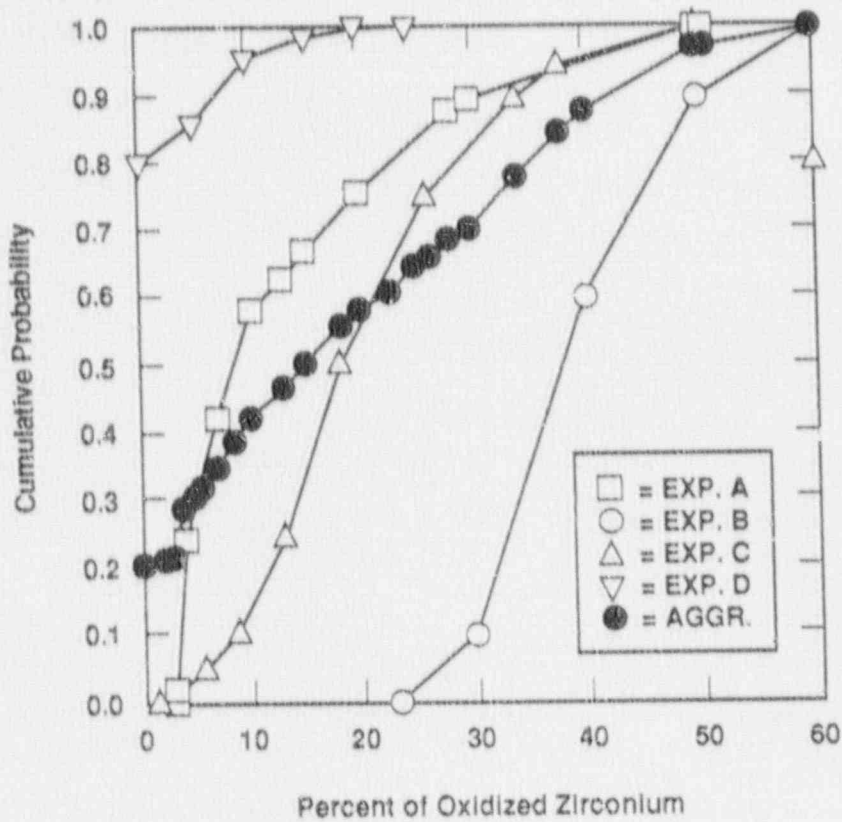
Figure 3-2.   Case 1b: Before Vessel Breach.
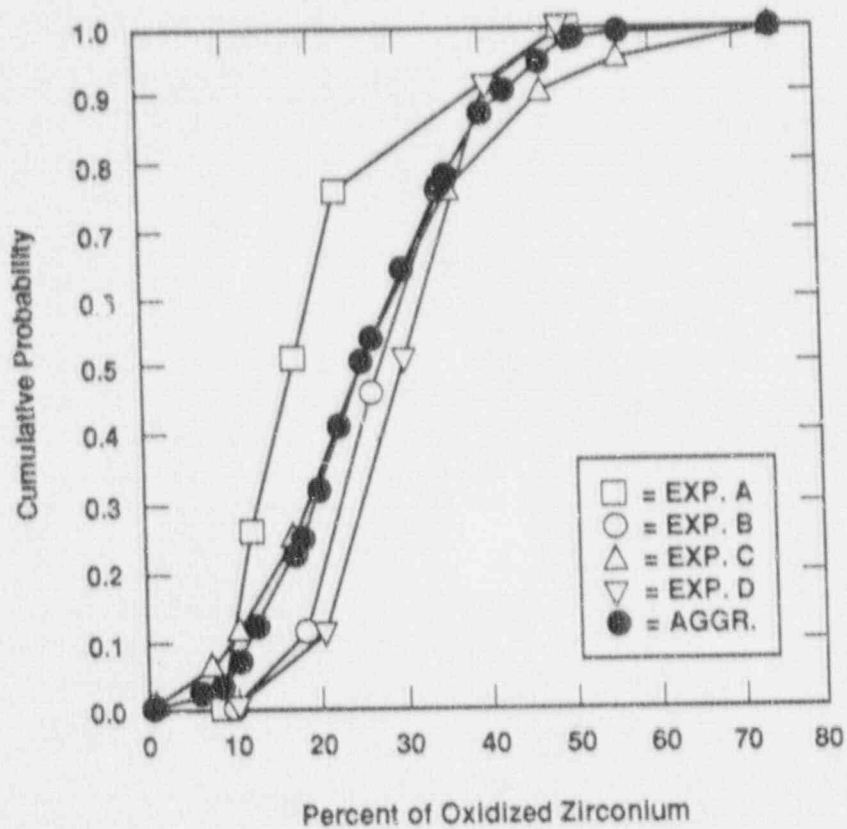
Figure 3-3.   Case 2a: Before Vessel Breach.
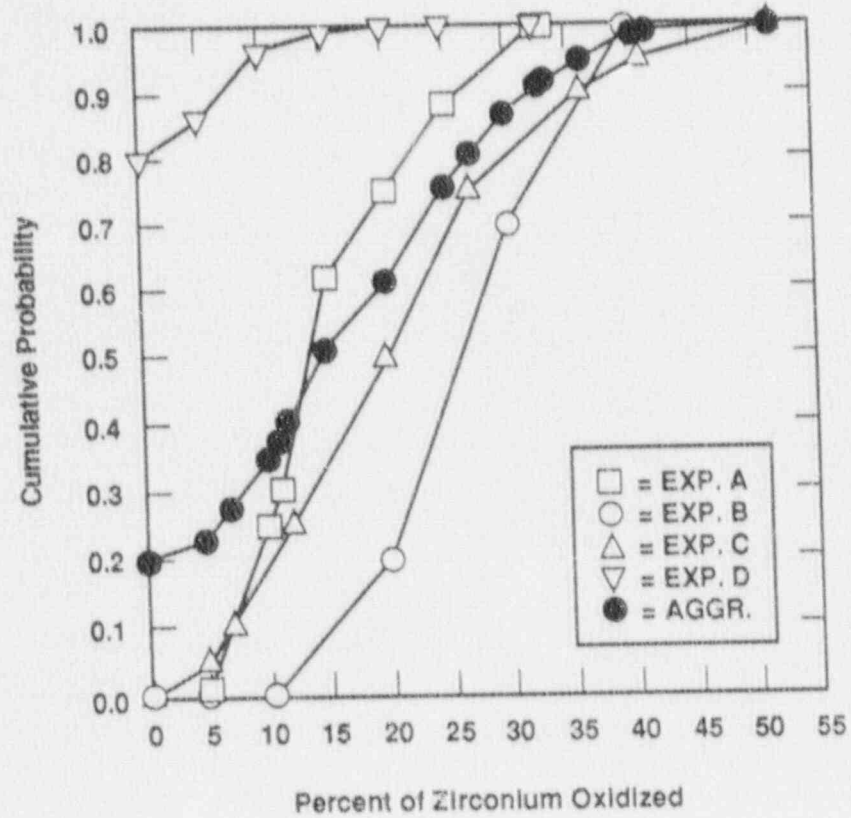
Figure 3-4.   Case 2b: Befor Vessel Breach.

5.
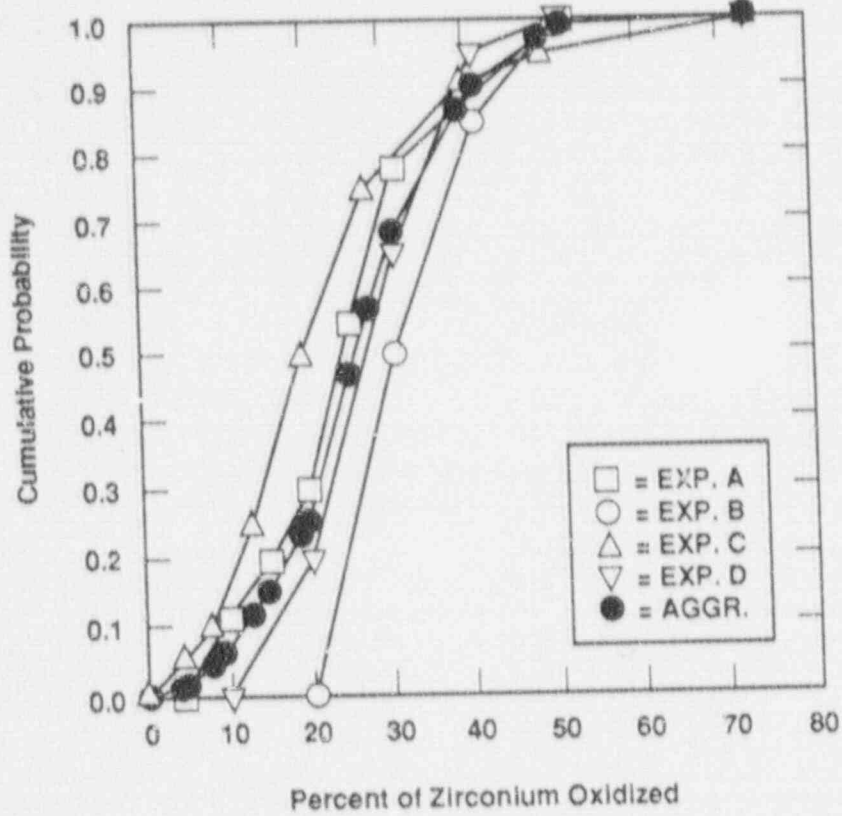
Figure 3-5.   Case 3a: Before Vessel Breach.
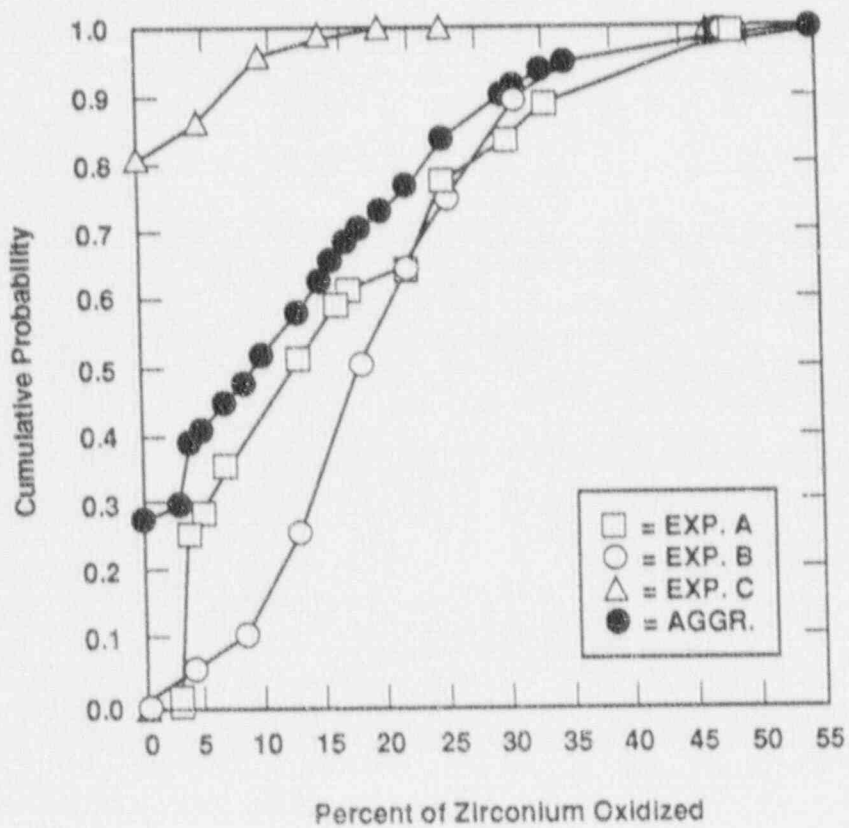
Figure 3-6.   Case 3b: Before Vessel Breach.

REFERENCES

3-1 L. J. Ott, "Advanced Severe Accident Response Models for BWR
     Applications," Proceedings of the USNRC 15th Water Reactor Safety
     Research Information Meeting, October 1987, NUREG/CP-0090.

3-2 S. H. Kim, D. H. Kim, B. R. Koh, J. A. O. Pessanha, El-K Si Ahmed,
     M. Z. Podowski, and R. T. Lahey, "The Development of APRIL, MOD2 --
     A Computer Code for Core Meltdown Accident Analysis of Boiling
     Water Nuclear Reactors," NUREG/CR-5157, 1988.

Individual Elicitations for In-Vessel Issue 3

Expert A's Elicitation

BWR In-Vessel Hydrogen Production

Expert A's approach to the elicitation task was to consider the phenomenology of in-vessel hydrogen production and to mentally walk through the accident progression. He identified four stages between the beginning of oxidation and vessel breach, described below, and estimated hydrogen production in terms of increments at each stage.

Case Structure and Decomposition

Expert A used the case structure proposed by the Sandia project team. He did not see any differences among the three BWRs that would significantly influence his uncertainty about hydrogen production and he therefore assessed only one distribution for all plants.

Figure A-1 shows Expert A's basic decomposition for Cases 1a and 1b. He separated the hydrogen production process into four main stages:

Stage 1: From beginning of oxidation to relocation of zirconium;

Stage 2: From beginning of relocation to debris dropping onto the core plate;

Stage 3: From beginning of debris collecting on the core plate to debri. dropping into the lower plenum, but before vessel breach;

Stage 4: After vessel breach.

In addition, Expert A considered two events that had, in his opinion, a major impact on hydrogen production. The first concerned whether extensive or complete blockage (significantly above 90%) would occur vs. moderate to high blockage (below 90%). Blockage is important because it impairs steam flow and thereby significantly reduces hydrogen production. The second event was the time at which water was recovered. Water recovery in stage 1 would lead to a temporary surge in steam and hydrogen production, after which further hydrogen production would cease. Water recovery in stage 2 would also lead to a surge in steam and hydrogen production, after which further hydrogen production would continue through stages 3 and 4.

Expert A assessed probabilities of 0.10 for extensive or complete blockage and 0.90 for moderate to high blockage. This assessment was mainly a result of the Expert's stringent definition of extensive or complete blockage, a state which he considered unlikely. No assessment of water recovery probabilities are made, as these events are considered part of the case structure.

Stage 1
From beginning
of oxidation to
relocation
      plate

Stage 2
From beginning
of relocation to
debris on core
breach

Stage 3
From core plate
to lower plenum,
before vessel

Stage 4
After vessel
breach

Water

Extensive
Blockage

Water

No Water

No Water

Water

Moderate
To High
Blockage

No Water
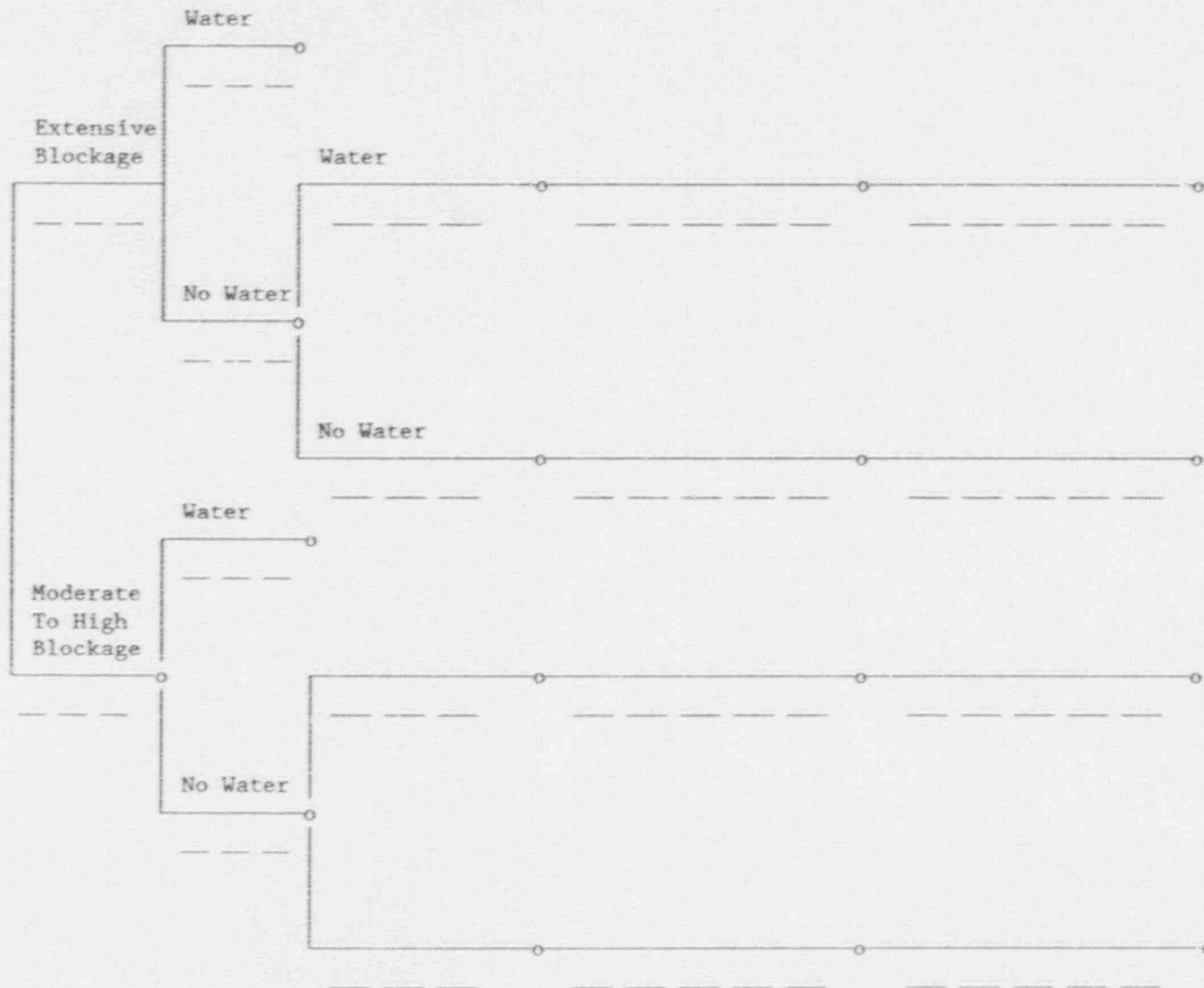
Figure A-1: Expert A's Decomposition for Cases 1a and 1b

Probability Distributions and Their Justification

Figure A-2 shows Expert A's fractiles for Cases la and lb. The percentages of zirconium oxidized at discrete fractiles are provided underneath the event lines in the event trees. If there are three numbers, they represent the 1st, 50th, and 99th fractile. If there are five numbers, they represent the 1st, 25th, 50th, 75th, 99th fractiles. For the first two stages, the Expert only gave the 1st, 50th and 99th fractile, since the medians and uncertainty bounds in those stages are fairly small. For the later stages he also provided the 25th and 75th fractiles. The estimates in Figure A-2 are cumulative meaning they include hydrogen produced up to the corresponding stage.

As can be seen, this Expert thinks that there is relatively little hydrogen production in the first stage. The 99th fractile is somewhat higher for the situation with moderate to high blockage (i.e., unblocked) due to uncertainties about the effects of the increased steam flow. Water recovery during the first stage will lead to a small surge in steam and some additional 2% of hydrogen production. In general, the Expert felt that water recovery would lead to 2% additional hydrogen production at all stages of the process.

The subsequent stages add about the same increments in hydrogen, with stage 2 contributing somewhat more (about 10% in the unblocked stage) than stages 3 and 4 (about 5% each in the unblocked state). In stage 2, two competing effects occur: higher temperatures lead to autocatalytic hydrogen production and at the same time the metals move down into the cooler regions, which would reduce hydrogen production somewhat. As a net result, the Expert does not feel that there would be a substantial amount of hydrogen produced at this stage. In stage 3 much steam would be generated and quenching of the debris would produce additional steam and hydrogen. This would add some 5% hydrogen. In stage 4 another steam surge would occur, adding some 5%.

Naturally, all estimates are higher in the unblocked state, because of higher steam circulation. However, the Expert thought that the blockage effect was larger during early stages than during later stages when steam levels would be high.

Figure A-3 shows the estimates for Cases 2a and 2b. In these cases the Expert did not distinguish among blocking states, because he thought that his uncertainties over other variables dominated the relatively minor blocking effect. While the later stage progression of hydrogen production does not differ that much from Cases la and lb, the Expert considers larger levels of hydrogen production in stage 1. In addition, the Expert did not expect any additional hydrogen production in stage 4.

Figure A-4 shows the estimates for cases 3a and 3b. The Expert thought that the main difference between cases la and lb and 3a and 3b was the larger supply of steam, which would add some 5% throughout the process.

Stage 1
From beginning
of oxidation to
relocation

Stage 2
From beginning
of relocation to
debris on core
plate

Stage 3
From core plate
to lower plenum,
before vessel
breach

Stage 4
After vessel
breach

Water

_3_ _4_ _7_

Extensive
Blockage

Water

_1_ _2_ _5_   _7_ _10_ _15_   _5_ _10_ _15_ _20_ _30_   _10_ _13_ _15_ _20_ _35_

No Water

_1_ _2_ _5_

No Water

_5_ _7_ _10_   _5_ _8_ _10_ _15_ _30_   _10_ _13_ _15_ _20_ _25_

Water

_3_ _4_ _10_

Moderate
To High
Blockage

Water

_1_ _2_ _8_   _10_ _18_ _25_   _5_ _13_ _20_ _28_ _50_   _10_ _20_ _25_ _35_ _60_

No   er

_1_ _2_ _8_

_8_ _15_ _20_   _5_ _15_ _20_ _25_ _50_   _10_ _20_ _25_ _35_ _60_

Figure A-2:   Expert A's Assessments for Cases 1a and 1b

5.3-16

Stage 1
From beginning
of oxidation to
relocation

Stage 2
From beginning
of relocation to
debris on core
plate

Stage 3
From core plate
to lower plenum,
before vessel
breach

Stage 4
After vessel
breach

Water

Extensive
Blockage

Water

No Water

No Water

Water

Moderate
To High
Blockage

_5 _10 _15

2 _5 _10

Water

_10 _15 _20
(8)   (25)

_11 _15 _20 _25 _33

_11 _15 _20 _25 _33

No Water

2 _5 _10

No Water

_5_ _10 _15_
(3)   (20)

_8 _12 _17 _22 _50

_8 _12 _17 _22 _50

Figure A-3: Expert A's Assessments for Cases 2a and 2b

Stage 1
From beginning
of oxidation to
relocation

Stage 2
From beginning
of relocation to
debris on core
plate

Stage 3
From core plate
to lower plenum,
before vessel
breach

Stage 4
After vessel
breach

Water

__3__ __4__ __7__

Extensive
Blockage

__1__ __2__ __5__

Water

__10__ __13__ __18__   __5__ __13__ __17__ __22__ __30__   __10__ __15__ __20__ __25__ __35__

No Water

__1__ __2__ __5__

No Water

__8__ __12__ __15__   __5__ __10__ __15__ __20__ __30__   __10__ __15__ __20__ __25__ __35__

Water

__3__ __4__ __16__

Moderate
To High
Blockage

__1__ __2__ __8__

Water

__15__ __20__ __28__   __5__ __22__ __25__ __33__ __50__   __10__ __25__ __30__ __40__ __60__

No Water

__1__ __2__ __8__

No Water

__12__ __17__ __25__   __5__ __20__ __25__ __30__ __50__   __10__ __25__ __30__ __40__ __60__

Figure A-4:   Expert A's Assessments for Cases 3a and 3b

Results of Expert A's Elicitation

Figure A-5 shows the calculated cumulative probability distribution functions (cdfs) for total hydrogen production through all four states. In it, we have averaged over the blocking vs. nonblocking states by using the Expert's probabilities assigned to these two states. We did not plot the case in which water recovery occurs in the second stage, since that case differs from the cases without water recovery only by a fairly constant increase in hydrogen of around 2 to 3%.

In total, there are six curves representing the six cases that were to be analyzed. Case 3a (high pressure meltdown, CRD injection without water recovery) shows the highest levels of hydrogen production overall. The range is substantial with a first fractile of 10% and a 99th fractile of 60%. Case 1a (short term, high pressure meltdown without water recovery) shows the next highest levels of hydrogen production. Case 2a (short term, low pressure meltdown without water recovery) is lowest of the three cases without water recovery.

In the cases with water recovery at the first stage, all estimates are fairly low, and uncertainty is small. Cases 1b and 3b are virtually identical with Case 3b showing more uncertainty at the upper end. Among the cases with water recovery, Case 2b has the highest hydrogen production estimates.
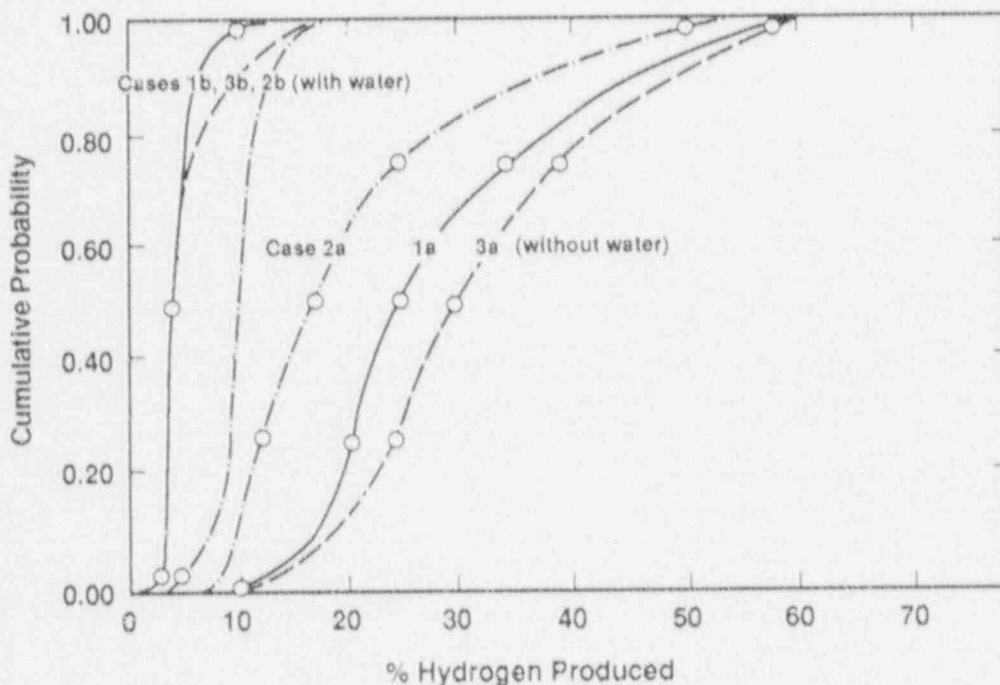
Figure A-5. Calculated Cumulative Probability
Distribution Functions For Total Hydrogen
Production Through All Four States.

Expert B's Elicitation

BWR In-Vessel Hydrogen Production

Expert B's assessments were based on an analysis of Peach Bottom (BWR/4 Mark I) using the BWRSAR code.[B-1] For each of the cases (1-3 with and without water recovery), BWRSAR was used to predict the total amount of hydrogen produced in the vessel. This value was then used as a "best" (median) estimate of in-vessel hydrogen production.

To account for uncertainty in this estimate, Expert B considered 14 separate sources of uncertainty and assessed how each of these would change his "best estimate" calculated by BWRSAR. Thus, for each source of uncertainty there is a range of hydrogen production levels. These ranges are added to create the overall range for hydrogen production. In some situations, correlations are considered and adjustments are made instead of simply adding uncertainty ranges.

Case Structure and Decomposition

Expert B considered the three cases defined by the Sandia team. He considered water recovery vs. no recovery for the first (short-term high pressure meltdown) and second (short-term low pressure meltdown) but not for the third case. Thus, he was elicited on a total of five cases. Expert B considered the three BWRs sufficiently similar to permit Peach Bottom to be used as a surrogate for the other two nuclear power plants, as suggested in the Sandia issue paper.

Expert B assumed that if injection is recovered before bottom head dryout, vessel breach will be averted. He also believed the time window between when injection will not avert the vessel breach and when vessel breach would occur without injection is sufficiently small and, therefore, Expert B assumes reflood will always avert vessel breach.

The basic difference between Cases 1 and 2 is that for Case 2 automatic depressurization system (ADS) is initiated, which results in rapid core-plate dryout and a steam-poor environment. Also, during blowdown there will be much less hydrogen produced in Case 2, because of the reduced amount of steam in the RPV as compared to Case 1.

For Case 3, ATWS and CRD injection (110 gpm), the core plate does not fail because the injection from the CRD flows over the core plate and keeps it relatively cool. The debris collects on the core plate, solidifies, and forms a "pan" above the core plate. Therefore, no hydrogen is produced in the bottom head for this case. If, however, the CRD water is turned off, the core plate will fail.

Hydrogen production in the bottom head is defined as that produced within the first 30 minutes after bottom head penetration failure. For Case 2, the upper limit for hydrogen production in the bottom head is determined by the amount of water in the downcomer region of the jet pumps. After vessel breach the debris in the bottom head heats and vaporizes the water (radiation) in the downcomer region. The steam formed during this process

passes through the debris bed in the bottom head and oxidizes some of the zirconium. For Case 2, the mass of water in the downcomer is approximately 30,000 lbs. Assuming an efficiency of 50%, the amount of hydrogen generated in the bottom head (beyond 30 minutes) is 1,681 lbs. Thus, the total equivalent fraction of initial zirconium inventory oxidized is 0.28. This will take <u>many</u> hours (approximately 75 lb $H_2 2$/h).

<u>Probability Distributions and Their Justifications</u>

Table B-1 shows the median estimates derived for the five cases from the BWRSAR code.

The cumulative probability distribution functions that were derived for each of the five cases considered 14 uncertainties surrounding this best estimate. These uncertainties are:

1. <u>Oxidation of Relocating Control Blade and Channel Box Material</u>. Oxidation of this material as it relocates is not modeled in BWRSAR. Oxidation of this material would increase the hydrogen production. Because Cases 2a and 2b occur in a steam-starved environment, an increase in hydrogen production for these cases is not expected.

2. <u>Oxidation of Material Quenching Above Core Plate</u>. This process is not modeled in BWRSAR. Oxidation of material quenching above core plate will result in an increase in the hydrogen production for Cases 1a, 1b, and 3a. Because Cases 2a and 2b occur in a steam-starved environment and core plate dryout occurs very rapidly after initiation of ADS, an increase in hydrogen production from the quenching material for these cases is not expected.

3. <u>Oxidation of Candling Clad (Shape Factor)</u>. A shape factor of 2 was used for the Peach Bottom calculations. Changing this parameter can either increase or decrease the amount of oxidation, however, its effect in the lower range is more uncertain.

4. <u>Effect of Blockage Formation by Relocated Material</u>. This process is not modeled in BWRSAR. Blockage will result in a steam starved environment and reduce the amount of hydrogen that is produced. Because Cases 2a and 2b are already steam-starved this process is not as important for these cases.

Table B-1
Summary: In-Vessel Hydrogen Production (NUREG-1150)

	Case				
	1a	1b	2a	2b	3a
Hydrogen production in the core region (lbs)	1959	2111	1592	1362	1694
Equivalent fraction of initial zirconium inventory oxidized	0.323	0.348	0.262	0.224	0.279
Hydrogen production in the bottom head (lbs)	1934	NA	48	NA	NA
Equivalent fraction of initial zirconium inventory oxidized	0.319	NA	0.008	NA	NA
Total In-vessel hydrogen production (lbs)	3893	2111	1640	1362	1694
Equivalent fraction of initial zirconium inventory oxidized	0.641	0.348	0.270	0.224	0.279

Note: 1. The initial zirconium mass is 137,385 lbs (81,238 in cladding, 50,291 in channel box walls, and 5856 in other structures). Using a conversion factor of 0.0442, the potential total hydrogen generation by zirconium oxidation is 6,072 lbs.

2. Hydrogen production in the bottom head is that produced within the first 30 minutes after bottom head penetration failure.

5. Amount of B4C-Steam Reaction. Oxidation will only occur in the core region. In BWRSAR, only 2% of the B4C is allowed to react. Increasing the amount of B4C that is allowed to react will increase the hydrogen produced.

6. Mode of Core Plate Failure. Each radial ring of the core plate fails due to loss of strength when its calculated temperature (debris and core plate mixed mean temperature) reaches 2000°F. This occurs after core plate dryout. When a particular radial ring of the core plate fails, the debris that is transported to the bottom head will affect the amount of steam production and hence hydrogen production. Because more debris relocates to the core plate in Case 1a (no ADS, and thus more water on core plate to boil-off) than Case 2a, the range for Case 1a is greater than

that for Case 2a. The ranges for the reflood cases are smaller than the ranges for the cases without reflood because there is less core plate failure with reflood.

7. <u>Oxidation of Solid Debris Relocating into Bottom Head</u>. This process is not modeled in BWRSAR. Oxidation of this material will increase the amount of hydrogen produced. The core plate does not fail in Case 3a and, therefore, the material does not relocate to the bottom head.

8. <u>Oxidation of Molten Debris Quenching in Bottom Head</u>. This process is not modeled in BWRSAR. Oxidation of this material will increase the amount of hydrogen produced. The core plate does not fail in Case 3a and, therefore, the material does not relocate to the bottom head.

9. <u>Collapse of Fuel Pellet Stacks</u>. The standing portions of the core fall into the lower plenum by radial column. Each column collapses when its average clad temperature reaches 4600°F (melting point of ZrO_2 is 4900°F). If the columns collapse at an earlier time (i.e., before core plate failure) the decay heat from the fuel pellets will cause an increase in steam production.

10. <u>Layering of Debris in Bottom Head</u>. In BWRSAR the control rods, channel boxes, and cladding melt relocate to the bottom head before the UO_2 is relocated. Thus, most of the metal is in the bottom layer (layer 1). The range of uncertainty accounts for the possibility that more metal is in the upper layers (layers 2 and 3) than is calculated by BWRSAR.

11. <u>In-Vessel Natural Circulation</u>. This process is not modeled in BWRSAR. Expert B does not believe that a natural circulation path will be set up, whereby water travels up through the core, down through the jet pumps, and back over to the core plate (water level must be below jet pump diffusers) as some have suggested. Expert B does, however, give some credit for a natural circulation loop that goes up through the fuel rods and then back down through the interstitial region (water level must be below core plate). This would increase the steam production, and hence hydrogen production.

12. <u>Metal Oxidation of Upper Debris During Boiloff</u>. Oxidation of this material would increase the amount of hydrogen produced.

13. <u>Oxidation of Zr Metal During Blowdown</u>. Expert B believes that BWRSAR calculates too much hydrogen during blowdown. He cites three factors in the BWRSAR modelling that may contribute to this over estimation:

13.1 A ZrO_2 layer does not build up on the debris as the zirconium is oxidized.

13.2 There is no channeling of steam. Channeling of steam through a particular path would reduce the amount of steam available in other regions of the bottom head and would reduce the amount of hydrogen produced.

13.3 The mass fraction of zirconium on the debris surface is the same as the mass fraction throughout the debris.

14. Oxidation of Stainless Steel During Blowdown. Stainless steel (SS) oxidation in the bottom head is not modeled in BWRSAR. BWRSAR oxidizes very little SS in the core region (~2%) and doesn't oxidize any SS in the bottom head or during blowdown. SS oxidizes very near its melting temperature. Thus, once the SS starts to oxidize in the core region it melts and relocates in the bottom head region where it refreezes. Thus, the majority of the SS is not oxidized, but rather is relocated. Once bottom head failure has occurred it remelts (with no oxidation) and relocates out of the RVP. Note: after vessel breach, a large amount of unoxidized SS will relocate to the pedestal cavity where it can be oxidized.

Note that uncertainties 1 through 6, 9, and 11 are in-core hydrogen production uncertainties, while the remaining ones concern bottom head failure. Because no hydrogen can be produced in the bottom head for Cases 1b and 2b and for Case 3a, the bottom head uncertainties only apply to Cases 1a and 2a without water recovery. Elicited uncertainty ranges are shown in Table B-2 in terms of deviations for the best-guess estimate.

For Cases 1a and 2a (without water recovery), it was noted that uncertainty about in-core hydrogen production would tend to be offset by bottom head hydrogen production. In other words, if less than the best estimate of hydrogen was produced in-core, more zirconium could be oxidized in the bottom head and vice versa. Qualitatively, this dependency should lead to tighter distributions over hydrogen production. In the first cut of estimates of uncertainty ranges, this dependency was ignored. For the final assessments of the probability distributions, a formula was used that allowed to calculate a revised uncertainty range based on the relative amount to in-core hydrogen production vs. bottom head hydrogen production and the uncertainty range in-core.

Results Expert B's Elicitation

Using Table B-2, the formula for adjusting bottom head uncertainties and additional judgment, the Expert provided cumulative probability distributions for the cases. These are shown in Figure B-1.

Time of hydrogen production was considered as follows: the best estimate plots of hydrogen production over time are shown in Figure B-2 to B-6. They were calculated using BWRSAR. Uncertainty bounds around these functions can be derived using Table B-3, which indicates which uncertainties would operate at which point in time of the accident progression.

Table B-2
Revised "Uncertainty" Ranges for BWR In-Vessel Equivalent
Hydrogen Generation Expressed As Deviations from Best Estimates

In-Core Uncertainties	1a		1b		2a		2b		3a	
1	0	+.01	0	+.01	0	0	0	0	0	+.01
2	0	+.02	0	+.02	0	0	0	0	0	+.02
3	-.04	+.01	-.02	+.01	-.04	+.01	-.02	+.01	-.04	+.01
4	-.05	0	-.05	0	-.02	0	-.02	0	-.01	0
5	0	+.03	0	+.03	0	+.03	0	+.03	9	+.03
6	-.01	+.02	-.05	+.01	-.03	+.01	-.02	+.01	0	+.10
9	-.10	+.05	0	+.10	0	+.10		+.10	0	+.05
11	0	+.02	0	0	0	+.04	0	0	0	0
Sub-Total	-.29	+.16	-.12	+.18	-.09	+.19	-.06	+.15	-.05	+.22

Bottom-Head Uncertainties	1a				2a	
7		+.01			0	+.01
8		+.03			0	+.05
10		+.02			0	0
12		+.01			0	+.01
13	-.15				0	0
14		+.02			0	0
Sub-Total	-.15	+.09			0	+.07

% Hydrogen Produced (equivalent % of zirconium oxide)
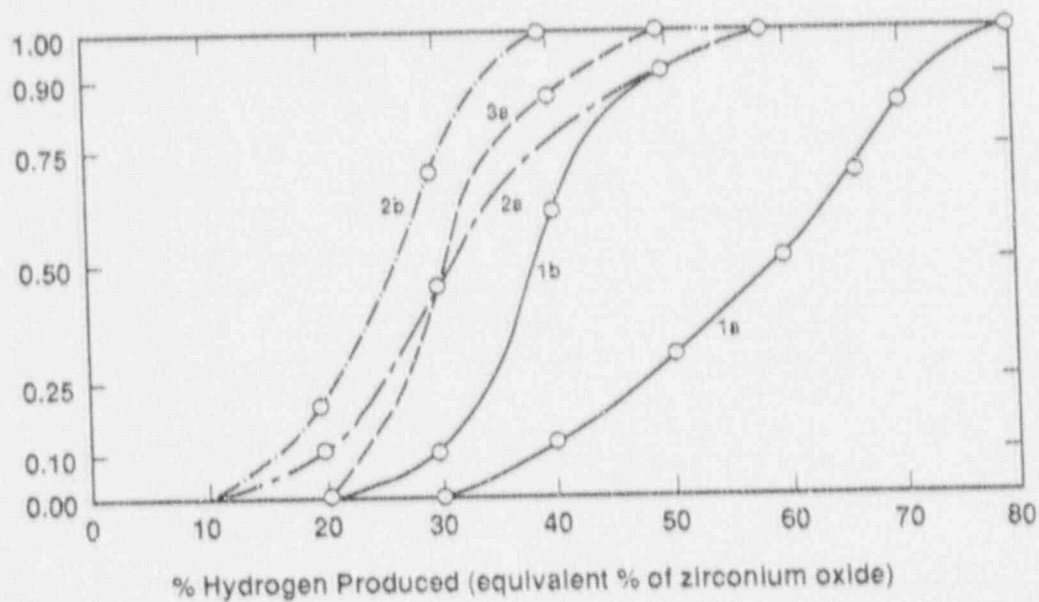
Figure B-1. Summary Results of Expert B.
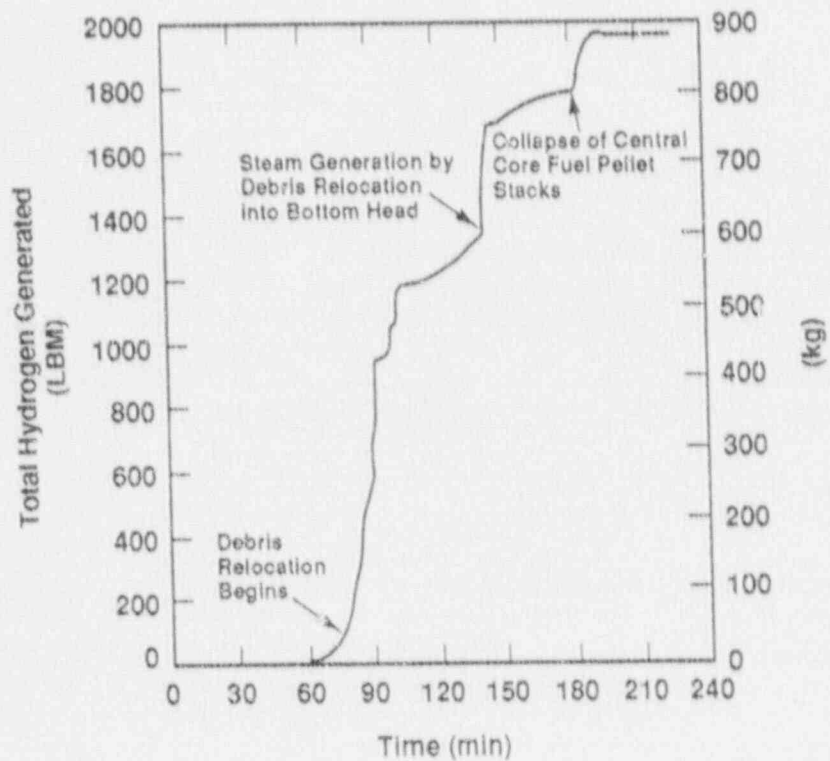
Figure B-2. Timing of Hydrogen Production for Case 1a.
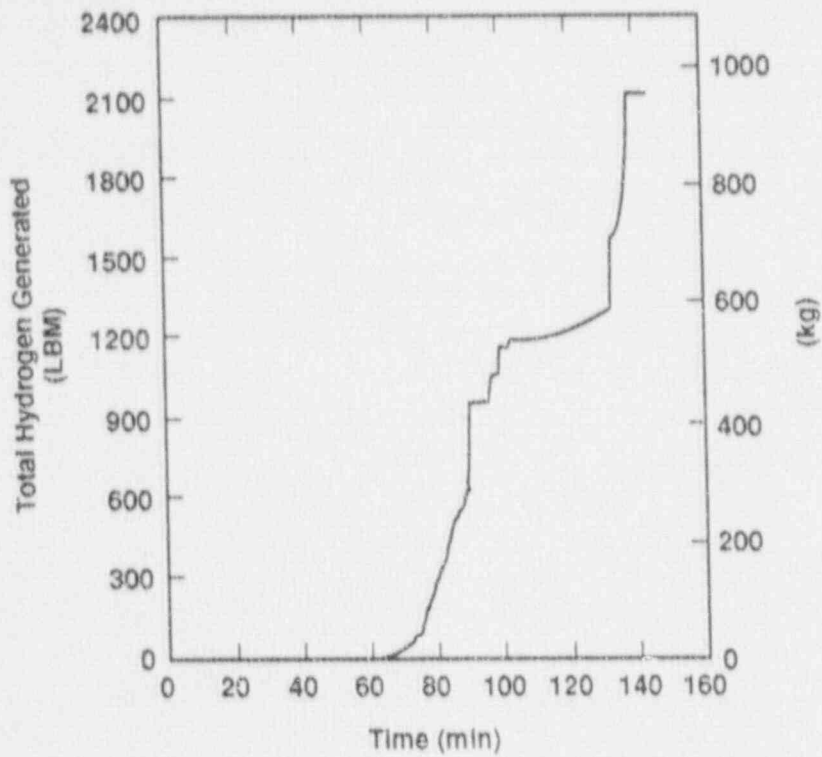
Figure B-3.   Timing of Hydrogen Production for Case 1b.
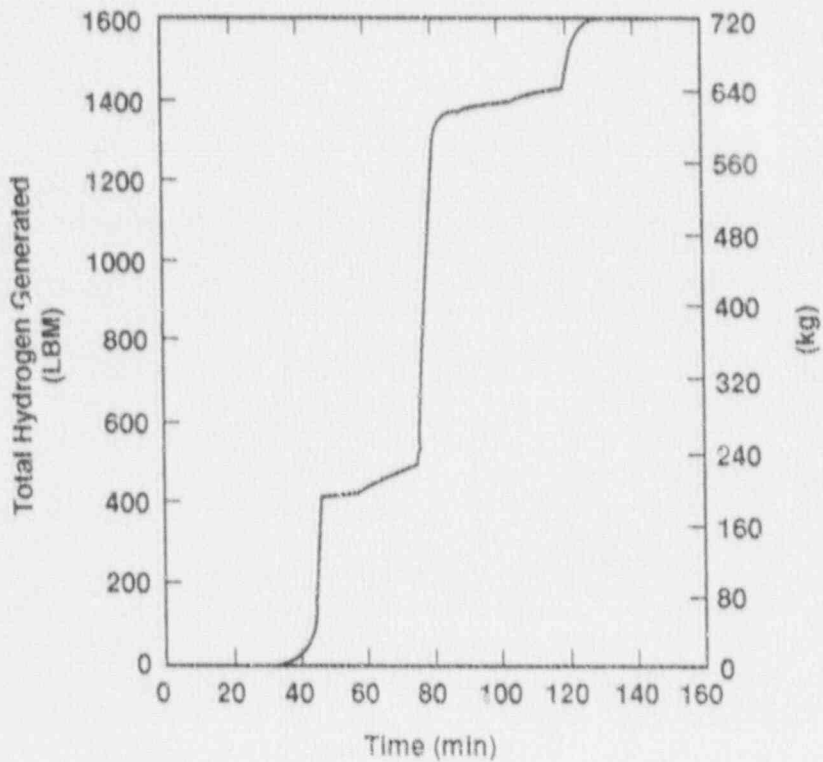
Figure B-4.   Timing of Hydrogen Production for Case 2a.
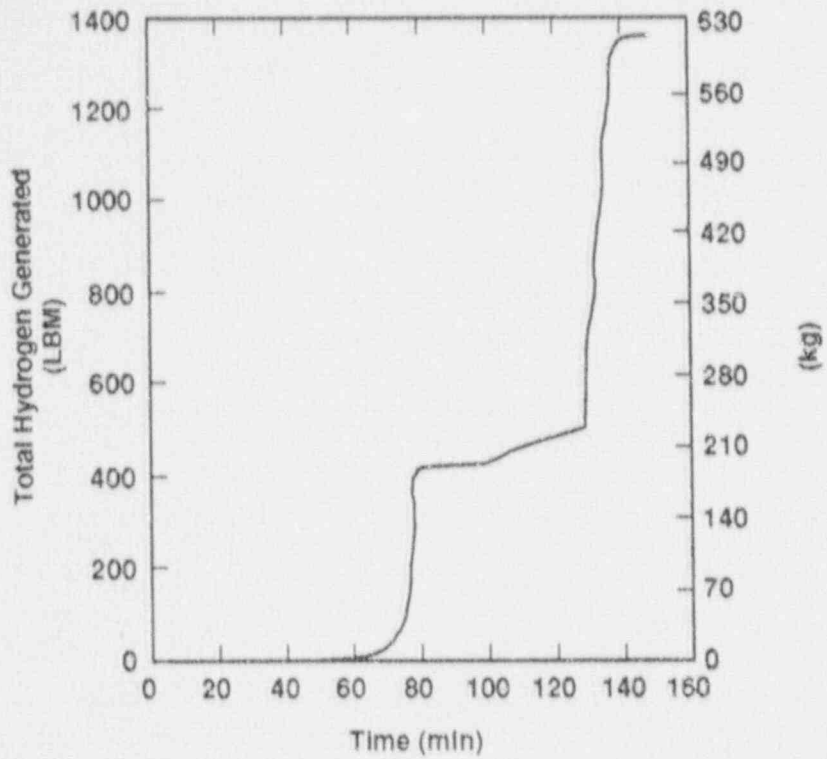
Figure B-5.   Timing of Hydrogen Production for Case 2b.
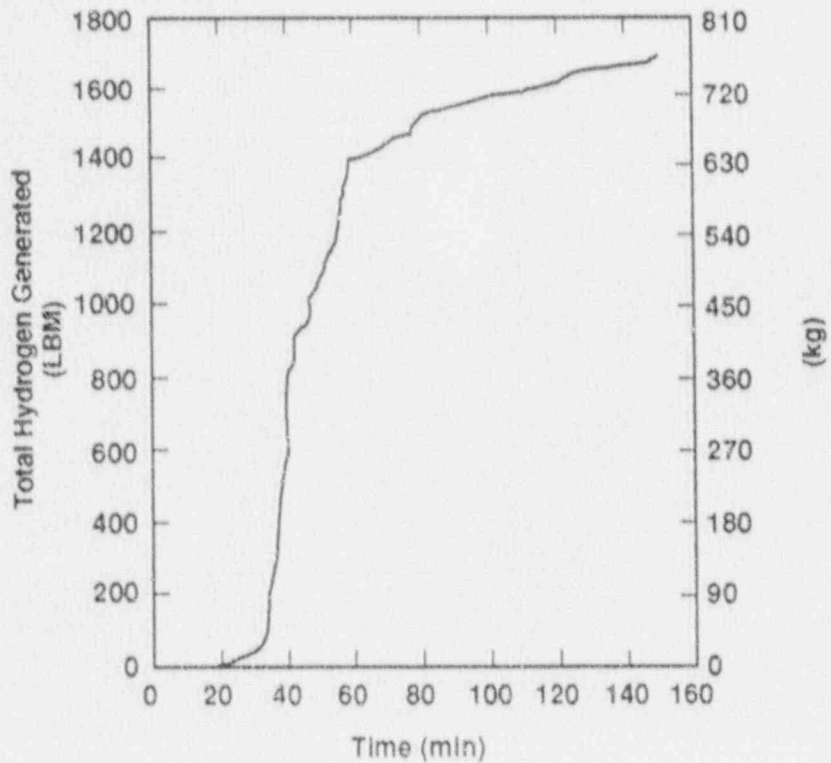
Figure B-6.   Timing of Hydrogen Production for Case 3a.

Table B-3
Timing of Hydrogen Uncertainties Production

Case 1		
Event	t(min)	Includes Uncertainties
Debris Relocation begins	75	1, 2, 3, 5
Core Plate Dryout	90	1, 2, 3, 4, 5, 6
Core Plate Failure	140	1, 2 3, 5, 6, 11
Cont. Core Fuel Stack Collapse	195	ALL

Case 2		
Event	t(min)	Includes Uncertainties
Begin Hydrogen Production	60	1, 2, 3, 5
15 Min Before 1st Local Core Plate Failure	115	1, 2, 3, 5, 6
1st Local Core Plate Fails	130	1, 2, 3, 4, 5, 6, 11
Fuel Pellet Stack Collapse	215	ALL

REFERENCE

B-1 L. J. Ott, "Advanced Severe Accident Response Models for BWR
     Applications," Proceedings of the USNRC 15th Water Reactor Safety
     Research Information Meeting, October 1987, NUREG/CP-0090.

Expert C's Elicitation

BWR In-Vessel Hydrogen Production

Expert C first carefully characterized the main factors in each of the long sequence of events that would result in the production of in-vessel hydrogen. Assessments of the possible amounts of hydrogen produced were estimated for each of the cases described below. Then, given a specified level of hydrogen production for each case, the percentage produced in the various stages of the accident progression was estimated.

Case Structure and Decomposition

For Cases 1 and 2, Expert C used the case structure proposed by the Sandia project team. For Case 3, there was a necessary alteration because the issue of whether the flow rate of water was sufficient to cover the core plate was important. Thus, Case 3 had four subcases pertaining to whether the flow rate of water was sufficient to cover the core plate and whether low pressure injection was recovered before the breach of the reactor pressure vessel.

In summary, assessments of hydrogen production were made for the following eight situations:

Case 1a: Short term high pressure meltdown without recovery,

Case 1b: Short term high pressure meltdown with low pressure injection recovered prior to the breach of the reactor pressure vessel,

Case 2a: Short term low pressure meltdown without recovery,

Case 2b: Short term low pressure meltdown with low pressure injection recovered prior to the breach of the reactor pressure vessel,

Case 3xa: High pressure meltdown with CRD injection where water flow rate is insufficient to cover the core plate without recovery,

Case 3xb: High pressure meltdown with CRD injection where water flow rate is insufficient to cover the core plate and low pressure injection is recovered prior to the breach of the reactor pressure vessel,

Case 3ya: High pressure meltdown with CRD injection where water flow rate is sufficient to cover the core plate without recovery,

Case 3yb: High pressure meltdown with CRD injection where water flow rate is sufficient to cover the core plate and low pressure injection is recovered prior to the breach of the reactor pressure vessel.

For each of the eight cases considered above, estimates were made of the time during the accident when the hydrogen is produced. This was done using descriptions of four points in the accident sequence that would occur after the initiation of the accident. The critical points in the accident sequence were defined as follows:

Time 0: Accident initiates when the water level is at TAF and begins dropping,

Time 1: The water level drops to the core plate,

Time 2: The time just before vessel breach,

Time 3: The end of blowdown (or the end of flow for low pressure cases),

Time 4: End of the accident (or gross lower head failure whenever it occurs).

Expert C believed that the present knowledge is insufficient to consider separately the amount of hydrogen produced by each of the three BWRs.

Probability Distributions and Their Justification

The first assessment was for Case 2a since this seemed to be easiest for Expert C to consider. Figure C-1 shows the resulting cumulative distribution of the probabil' y assessments in terms of the equivalent amount of zirconium oxidized measured in percent. The assessed points were first determined by appraising the relative likelihood of different ten percent intervals of zirconium oxidized. The most likely interval was the range from 30 to 40% zirconium oxidized. The second most likely interval was from 20 to 30% and the third most likely interval was 40 to 50%. These were followed by a tie in terms of relative likelihood between the intervals from 10 to 20% and from 50 to 60%. This was followed by the intervals from 60 to 70%, 0 to 10%, and 70 to 80% in that order. The likelihood of more than 80% of the zirconium being oxidized was very small according to Expert C. To get specific fractiles corresponding to those intervals, we began with the point where 40% was the equivalent amount of zirconium oxidized. Expert C felt there was a two-third chance of less than 40% being oxidized with Case 2a. He felt that there was a 0.4 chance of less than 30% being the equivalent amount of zirconium oxidized. The resulting assessments in Figure C-1 were completed in the same manner.

Case 2b was assessed by adjusting the results for Case 2a. Specifically, Expert C felt that Case 2b should produce two-thirds the amount of hydrogen than case 2a would produce for higher levels of zirconium oxidized. For lower levels of zirconium oxidized, the vessel breach time is shorter, so there is a slightly greater effect of low pressure injection. Hence, Expert C felt that a 40% reduction of the equivalent amount of zirconium oxidized would occur in situations where less than 30% of the equivalent amount of zirconium was oxidized for Case 2a. This produced the result shown in Figure C-1. However, in interpreting this

result, it is important to recognize that for these calculations the vessel was assumed not to fail.

Case 1a was assessed in exactly the same manner as Case 2a. The relative likelihoods of the hydrogen production being in the various 10% intervals from 0 to 10%, 10 to 20%, and so forth measured in terms of the equivalent amount of zirconium oxidized was 8, 5, 3, 1, 2, 4, 6, 7. The most likely interval for hydrogen production is thus between 30 to 40% and the next most likely was between 40 to 50%.
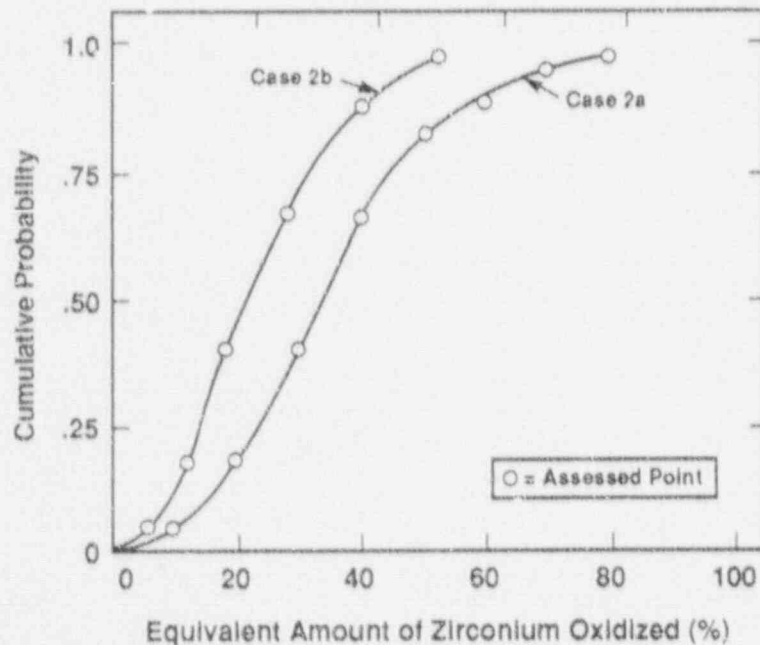
Figure C-1.   Case 2a Assessments of Hydrogen Production for Expert C.

This ranking also indicates that the likelihood for the equivalent amount of zirconium oxidized to exceed 80% is small. The resulting assessments are indicated in Figure C-2, including the 0.5 fractile, assessed as approximately 38%.

Case 1b hydrogen production was derived from Case 1a in exactly the same manner as Case 2b was derived from Case 2a described above. The reasons that pertain to this relationship are also the same as those concerning Case 2a.

The assessments for the various circumstances pertaining to Case 3 are indicated in Figure C-3. For Case 3xa, where the flow is insufficient to cover the core plate, Case 2a information and results apply. The initial oxidation phase of both of these is very similar. The rest of the hydrogen production depends on what happens in the lower plenum.

For Case 3ya, where the water flow is sufficient to cover the core plate, the median should be shifted by reducing it approximately one third from Case 3xa to 22% equivalent amount of zirconium oxidized. For higher level hydrogen productions, the shift should be greater. Specifically, Expert C felt that a reduction by half at the 0.9 fractile from Case 3xa to 30% equivalent amount of zirconium oxidized would be appropriate. At low levels of hydrogen production, the reduction of hydrogen produced from Case 3xa to Case 3ya should be very low (i.e., less than a 0.1 reduction). The resulting assessment for Case 3ya is indicated in Figure C-3.

For Case 3xb, the hydrogen production would be reduced relative to Case 3xa. Expert C felt it would be difficult to imagine all the possibilities for this case, but estimated that the results should be approximately half way between Cases 3xa and 3ya. This is indicated in Figure C-3. Finally, it was estimated that the hydrogen production from Case 3yb would be the same as that for Case 3ya.

Using Case 1a, it is indicated how the timing of the releases of hydrogen was addressed in the assessments. For each of the time points indicated in section 5.2, Expert C was asked to indicate a 0.1, 0.5 (i.e., median), and 0.9 fractile for the percentage of the hydrogen that was released by the indicated time point relative to the total amount of hydrogen that would be released by the end of the accident. First, Expert C indicated that he thought approximately 65% of the total hydrogen released with Case 1a would be released by time 1 where the water drops to the core plate. This was the median estimate. Because of the uncertainties about the timing of release, the 0.1 and 0.9 fractiles were assessed respectively as 30% and 85% of the hydrogen that would eventually be released. The corresponding assessments for time 2 defined as just before vessel breach indicated that the median amount of hydrogen that would be produced was 70% of the total produced. The 0.1 and 0.9 fractiles here were 40% and 90%. By time 3 at the end of the blowdown, the median amount of hydrogen released was estimated to be 95% with the 0.1 and 0.9 fractiles of 85% and 99%. By the end of the accident, by definition 100% of the hydrogen that would be released was released. The results of timing assessments for Case 1a are indicated in Figure C-4.

The assessments for the timing of hydrogen releases were similar for the remaining seven cases considered by Expert C. The results are given in Figure C-5.
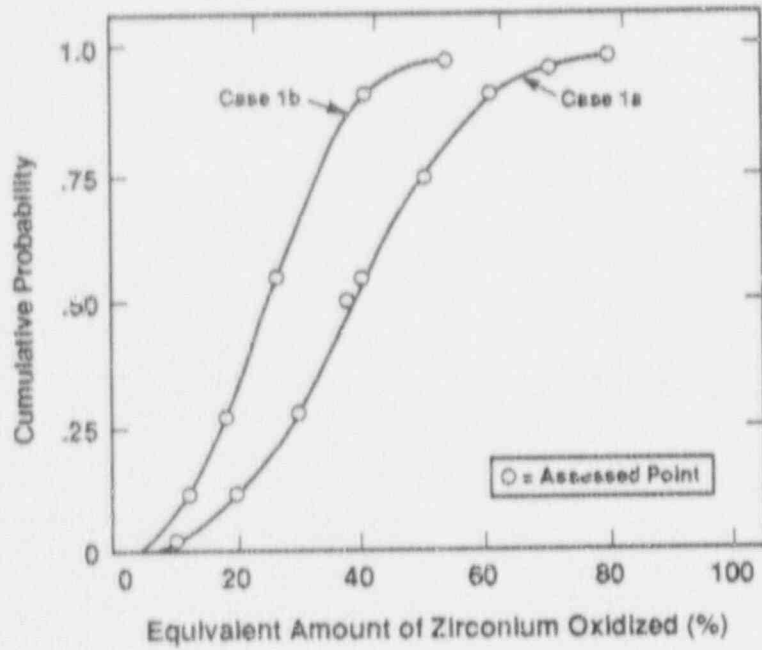
Figure C-2. Case 1a Assessments of Hydrogen Production for Expert C.
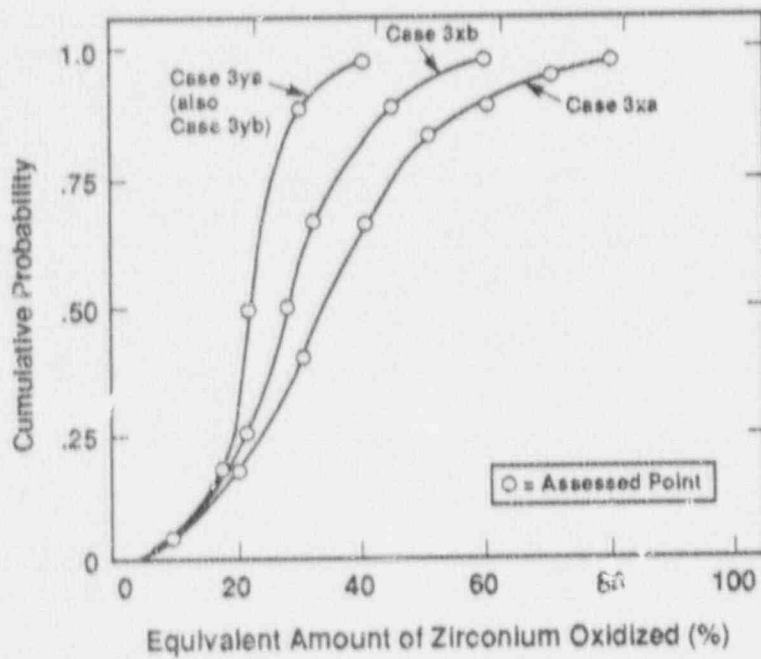
Figure C-3. Case 3 Assessments of Hydrogen Production for Expert C.
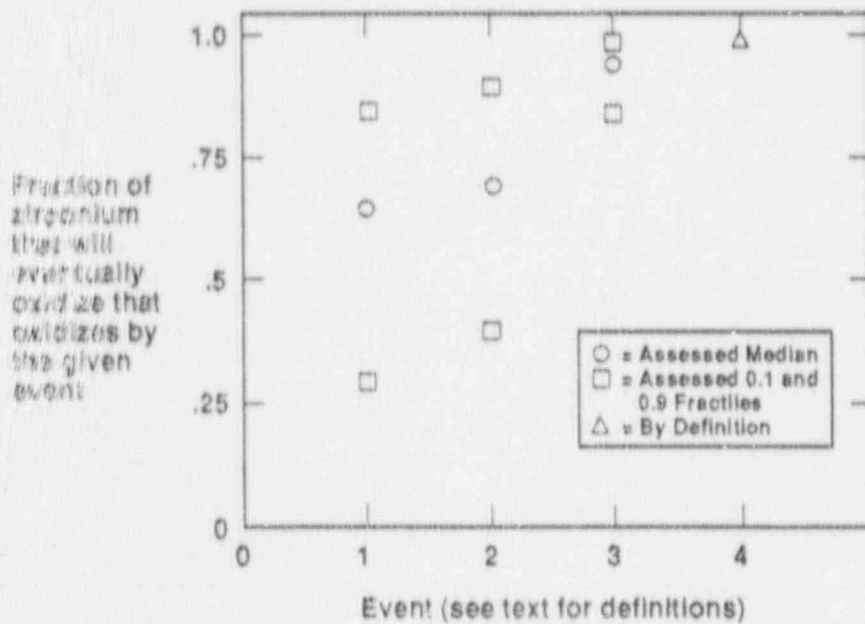
Figure C-4.   Timing of Hydrogen Production Using Judgments of Expert C for Case 1a.
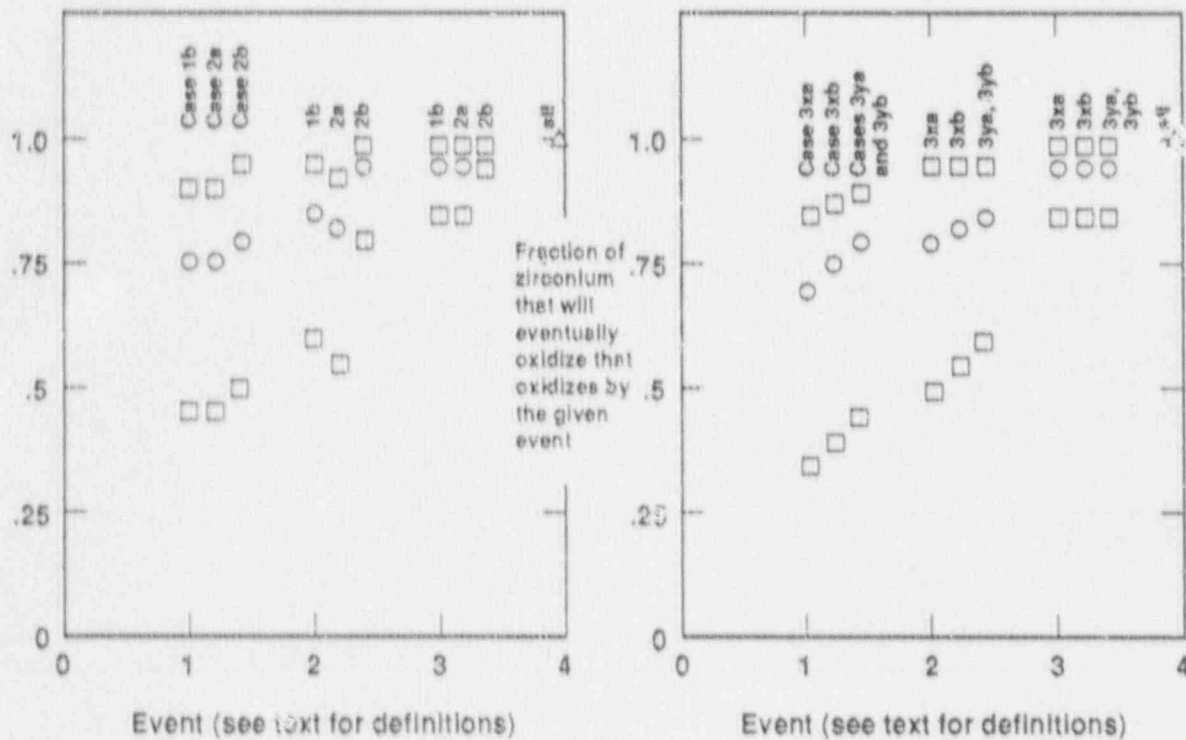
Figure C-5.   Timing of Hydrogen Production Using Judgments of Expert C. (○ assessed median; □ assessed 0.1 and c.1 fractiles; △ by definition)

Results of Expert C's Elicitation

The resulting cumulative probability distributions for hydrogen produced are shown in Figures C-1 through C-3. They indicate that Case 1a is likely to produce the most hydrogen whereas cases 2b and 3ya (which is the same as 3yb) are likely to produce the least amount of hydrogen. When all other factors are equivalent, there is a natural consistency in the assessments that high pressure meltdown produces more hydrogen than low pressure meltdown, that the recovery of the low pressure injection prior to the breach of the reactor pressure vessel results in the production of less hydrogen, and (for Case 3) when the water flow is sufficient to cover the core plate, there is less hydrogen produced.

Expert D's Elicitation

BWR In-Vessel Hydrogen Production

The Expert used several phases of extensive experience in degraded core modeling, including:

1. Detailed study of actual LWR-generic core degradation processes that occurred in TMI-2, and related in-reactor and ex-reactor experiments;

2. Directing the development of a detailed BWR core heatup and degradation code;

3. Making extensive use of this code (100s of runs);

4. Making comparative studies of existing industry and NRC core degradation codes; and

5. Using detailed studies of local core energy balances to provide guidance for the amount of hydrogen production that could be expected in the vessel before the core slumping into the head.

Separate assessments were made of the amount of hydrogen that would be produced in the reactor vessel as a result of the slumping into the bottom head.

Case Structure and Decomposition

Expert D used the same case structure as that proposed by the Sandia project team. However, as explained below, for cases 1b and 2b corresponding to when low pressure injection was recovered prior to the breach of the reactor pressure vessel, the resulting hydrogen produced was estimated to be the same. Expert D felt the estimates for the fraction of equivalent zircaloy oxidation produced at Peach Bottom could be used for the other BWRs. Hydrogen production in other BWRs would then be in proportion to the ratio of total core zircaloy inventories.

For the cases dealing with injection recovery, the elicitation considered only situations where the recovery was successful, implying that it was sufficiently early and adequate to prevent reactor vessel failure. Thus, the assessments with recovery (Cases 1b, 2b and 3b; Tables D-3, D-4 and D-5) are for the partial set where injection recovery is successful, meaning that it is in time to prevent vessel failure, but too late to avoid some hydrogen production.

Probability Distributions and Their Justifications

The assessments were done in two manners which were then compared and appraised to reach a final assessment. The first of these was a direct assessment of the cumulative distribution function for the amount of hydrogen produced that was developed by Expert D in preparation for the

elicitation session. The second assessment, during the elicitation, decomposed the production of hydrogen into two parts where hydrogen is first produced in-core and then produced in the bottom head. The results of combining these distributions to estimate the total hydrogen produced were then compared with the initial assessments. From these, which were quite consistent with each other, adjustments were made to reach a final distribution.

To illustrate the procedure, consider cases 1a and 3a (which Expert D considered as essentially identical). For this case, Expert D's distribution is shown in Table D-1 along with the initially assessed distribution and the calculated distribution. Specifically, Table D-1 shows the cumulative probabilities associated with different percentages of hydrogen being produced relative to the total amount of hydrogen that could be produced if all the zirconium were oxidized (equivalent fraction of zirconium oxidized).

The data determined in the assessment for the calculated estimates are shown in Figure D-1. Here, for instance, the percentage of hydrogen that could be produced in-core was between 0 to 30%. The probability of the production being between 0 to 10% was 0.15, between 10 and 20% was 0.60, and between 20 and 30% was 0.25. It was stated by Expert D that a reasonable assumption for the distributions within these ranges was uniform. Then, from Figure D-1, it is evident that the likely hydrogen production in the bottom head given that the in-core production was 0 to 10% is the following: a 0.30 probability of 0 to 10% hydrogen production in the bottom head and a 0.70 probability of 10 to 20% hydrogen production in the bottom head. The rest of the Figure is read similarly. Also, in the bottom head, it is assumed that the conditional probability distribution for the amount of hydrogen produced in each interval is uniform. Directly from the assessed information in Figure D-1, the calculated cumulative probability distribution indicated in Table D-1 can be determined. The final distribution indicated in Table D-1 was assessed directly by reconciling the initial and calculated assessments.

Table D-1
Cumulative Probability Distribution for the
Equivalent Amount of Zirconium Oxidized for Cases 1a and 3a

Percent of Zirconium Oxidized	0	10	20	30	40	50
Initial Cumulative Probability	0	0	0.10	0.55	0.95	1.0
Calculated Cumulative Probability	0	0.03	0.35	0.82	1.0	1.0
Final Cumulative Probability	0	0	0.2	0.65	0.95	1.0

| | In-Core Production | Bottom Head Production | |

0-10% (0.3)

0-10% (0.15)

10-20% (0.7)

0-10% (0.8)

10-20% (0.5)

10-20% (0.2)

0-10% (1.0)

20-30% (0.25)

10-20% (0)
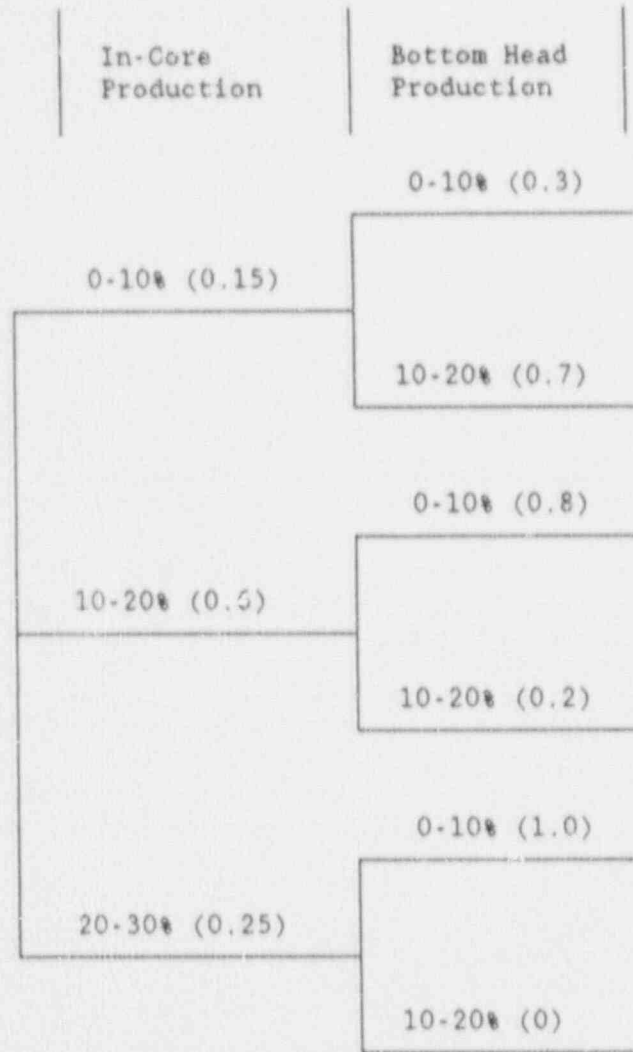
Figure D-1. Expert D's Hydrogen Production Estimate in Two Stages for Case 1a.

The initial assessments for Case 2a were done in the same way as those for cases 1a and 3a and are indicated in Table D-2.

Table D-2
Cumulative Probability Distribution for the
Equivalent Amount of Zirconium Oxidized for Case 2a

Percent of Zirconium Oxidized	0	10	20	30	40	50
Initial Cumulative Probability	0	0	0.10	0.45	0.90	1.0
Calculated Cumulative Probability	0	<0.01	0.17	0.57	0.90	1.0
Final Cumulative Probability	0	0	0.10	0.50	0.90	1.0

Table D-3 indicates the results of the assessments for reflood cases 1b and 2b before considering the very real situation where no hydrogen is produced as a result of successful injection recovery prior to vessel breach. These assessments were based on the assumption that the initiation of reflood is delayed for a sufficiently long period after the accident begins; otherwise, there is no hydrogen production. This is because hydrogen production cannot occur before there has been a sustained period when at least the upper approximately one-third of the core has been uncovered. For the purposes of this study, one-third uncovery was defined to occur at 30 minutes into the accident. However, the actual time delay from the start of the accident until the start of hydrogen production is highly variable and dependent upon the accident sequence; but the ensuing hydrogen production history, from the start of production onward, is much less variable. Therefore, only the relative times beyond 30 minutes in Figure D-2 have significant meaning. It is assumed that the likelihood that this recovery occurs prior to this time is 0.8, resulting in no hydrogen production.

The results for Case 3b are very similar to those for cases 1b and 2b. For Case 3b, there is a possible further decomposition that lends some insights about the implications for hydrogen production. For this case, it is assumed that the reflood occurs before some minimum amount of core damage, and hydrogen production has occurred. The minimum amount of core damage would be reached 10 to 20 minutes after start of hydrogen production (40 to 50 minutes after the start of the accident in the example shown in Figure D-2); otherwise, the vessel is lost. If the reflood occurs before hydrogen production begins (30 minutes after the accident began in this example), no hydrogen is produced. Hence, the percent of hydrogen caused by the reflood is considered to be strongly dependent on the percent of hydrogen produced (equivalent percent of total zirconium oxidized) up to the reflood time. The results of this dependency are shown in Table D-4. As an example, if there is 5% hydrogen production at reflood, it is then assumed that 3% additional hydrogen production would be caused by the reflood resulting in the total production of hydrogen of 8%. As can be seen, these results are quite consistent with those obtained directly for Case 3b assuming it is the same as cases 1b and 2b.

Table D-5 shows the final cumulative probability distributions for the percent of hydrogen produced for the three cases where low pressure injection is recovered prior to the breach of the reactor pressure vessel. These results take into account Expert D's judgment that there is an 80% likelihood that the capability to initiate reflood is recovered prior to the time when any hydrogen is produced and a 20% chance that it is recovered after some hydrogen is produced but prior to vessel breach. As such, the results in Table D-5 are the results in Table D-3 weighted by 0.2 with the additional 0.8 probability for the production of no hydrogen.

Table D-3
Cumulative Probability Distributions for the
Equivalent Amount of Zirconium Oxidized for Cases 1a
and 2b for the Partial Set Assuming That Hydrogen Is Produced

Percent of Zirconium Oxidized	0	5	10	15	20	25
Initial Cumulative Probability	0	0.30	0.80	0.95	1.0	1.0
Calculated Cumulative Probability	0	0.30	0.76	0.96	0.9975	1.0
Final Cumulative Probability	0	0.30	0.80	0.95	0.99	1.0
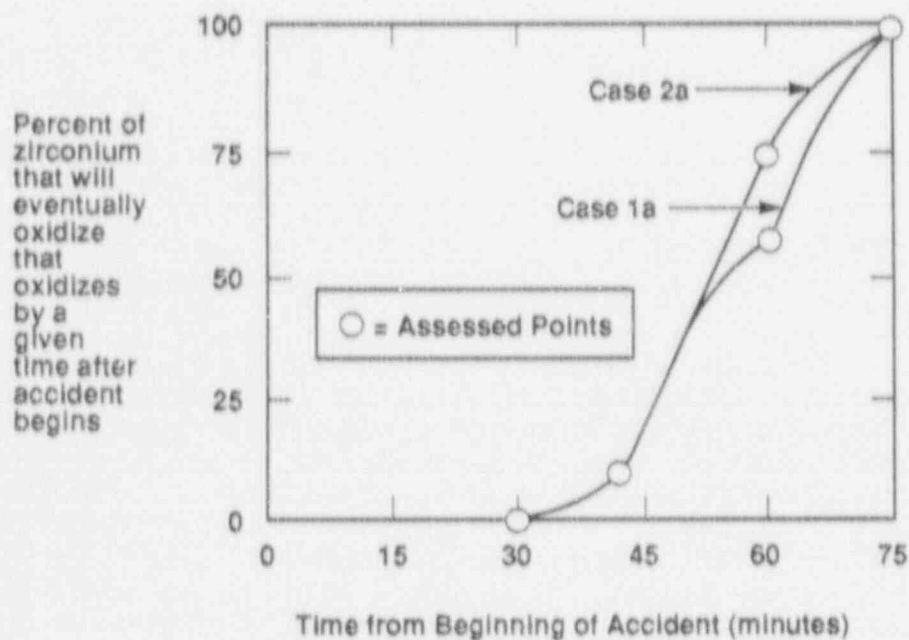
Figure D-2.   Timing of Hydrogen Production Using Judgments of Expert D.
Note: the only significance of absolute time in this example
is that hydrogen production is arbitrarily assumed to begin 30
minutes after the accident begins. However, relative time
from the time that hydrogen production begins does have
meaning as a general representation of the hydrogen production
history.

5.3-42

Table D-4

Relationship Between the Hydrogen Produced Prior to
Reflooding and then by Reflooding for Case 3b Measured in
Terms of the % of the Zirconium Oxidized

Percent Oxidized Prior to Reflood	Percent Oxidized By Reflooding	Total Zirconium Oxidized
0	0	0
1	0	1
3	1	4
5	3	8
10	10	20

Table D-5

Cumulative Probability Distribution for the
Equivalent Amount of Zirconium Oxidized for Cases 1b, 2b, 3b

Percent of Zirconium Oxidized	0	5	10	15	20	25
Final Cumulative Probability	0.8	0.86	0.96	0.99	0.998	1.0

Expert D provided an estimate for the percentage of the total hydrogen that
would be eventually produced as a function of the time from the start of
hydrogen production. As noted previously, in the example shown in Figure
D-2 the start of hydrogen production was arbitrarily set at 30 minutes; and
only relative times beyond 30 minutes have physical meaning. These
estimates, which were constructed for cases 1a and 2a only, are provided in
Figure D-2. For instance, in that figure the estimate of the percentage of
the total hydrogen produced in the first 10 minutes after the start of
hydrogen production is 10% for both Cases 1a and 2a. Within 30 minutes
after the start of hydrogen production, one expects 60% of the hydrogen to
be produced with Case 1a and 75% of the hydrogen to be produced with Case
2a.

There was no attempt to assess uncertainties about the percentage of the
hydrogen that would eventually be produced as a function of time. However,
at any given time, the estimate in Figure D-2 (e.g., 75% for Case 2a at 60
minutes) could be multiplied by the estimated percentages of equivalent
zirconium that would be oxidized (e.g., from Table D-2 for Case 2a) to
provide a cumulative probability distribution for the amount of equivalent
zirconium oxidized by a given time after initiation of the accident.

Figure D-3 shows the final cumulative probability distributions for the total hydrogen production for the six cases examined. These results are graphical representations of the final distributions in Table D-1 for Case 1a, and Table D-2 for Case 2a, and in Table D-5 for cases 1b, 2b, and 3b. Case 3a is essentially the same as Case 1a.
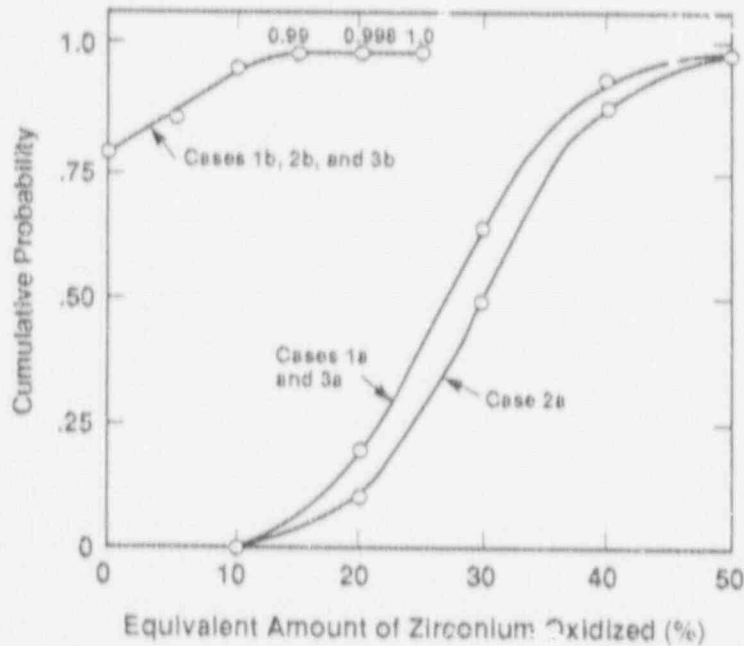
Figure D-3. Assessment for Hydrogen Production for Expert D.

Estimate of Hydrogen Production for BWRs and PWRs Following Reactor Vessel Lower Head Failure

Expert D's results are based upon the application of actual data from the meltdown accident at TMI-2 and on the understanding of generic LWR (both BWR and PWR) core degradation progression, through slumping and eventual collapse into the reactor vessel (RV) lower head. These results indicated that primary mobile molten material that would both cause RV lower head failure and be ejected immediately after that failure would be an essentially fully-oxidized ternary compound of $(U,Zr)O_2$, with varying but complementary fractions of uranium and zirconium.

Since this material has already exhausted virtually all of its oxidation potential, very little additional oxidation and hydrogen production would occur during the actual post RV failure ejection of this material. To bound this additional hydrogen production, an additional 0 to 5% equivalent zircaloy oxidation fraction is assigned, with equal weighting across that range, as the amount of hydrogen production during of molten core material following in either a BWR or a PWR system.

5.4   Issue 4: BWR Bottom Head Failure

Experts consulted. Michael Podowski, Rennselear Polytechnic Institute; Richard Hobbins, Idaho National Engineering Laboratory; Steve Hodge, Oak Ridge National Laboratory.

Rationale For Not Aggregating This Issue

This issue was not aggregated because the experts did not provide the project staff with enough information to complete the aggregation. The distributions used in the accident progression event tree (APET) were developed at Sandia and are documented in NUREG/CR-4551, Vol. 2, Part 6. The information provided by the experts was used, along with other information, to develop the distributions.

It is our conclusion from our discussions with the experts that this issue involves so much uncertainty that it was difficult to define self-consistent scenarios.

Issue Description

This issue relates to the pressure rise at vessel breach issue being assessed by the containment loads panel. In order for the containment loads panel to assess which phenomena can occur and the magnitude of the pressure rise, they need information as to the initial condition of the melt as it leaves the vessel. This information is provided by the results of Issue 4 elicitation.

Three different accident scenarios can be defined which determine the initial conditions leading up to core damage:

1. Short-term High-Pressure Meltdown.   This is a surrogate for any sequence where the automatic depressurization system (ADS) fails or the vessel repressurizes later due to high containment pressure, since the experts decided that variations in decay heat were not an important factor in determining the final melt conditions.

2. Short-term Low-Pressure Meltdown.   This is a surrogate for any sequence where ADS is successful or the vessel is depressurized due to a LOCA or stuck open SRV, since the experts decided that variations in decay heat were not an important factor in determining the final melt conditions.

3. High-Pressure Meltdown with CRD Injection.   This sequence represents an anticipated transient without scram (ATWS) sequence with inadequate makeup. This scenario will also be used to judge the effects of dumping water onto a melting core.

For each of the above cases, the experts were asked to define the characteristics and determine the probability of various scenarios relating to the mode of bottom head failure and the initial conditions of the melt. The three general scenarios which can be defined are:

1. Pressurized ejection of debris.

2. Gravity-driven pouring of molten debris at vessel breach.

3. Gravity-driven pouring of molten debris over an extended period following vessel breach.

Within each case the experts must assess all of the uncertainties associated with the in-vessel melt progression and define ranges for the parameters needed by the containment loads panel. These parameters were:

1. Mass of core ejected with time.

2. Temperature of ejected material with time.

3. Percent of ejected mass which is metal with time.

4. Percent of ejected mass which is molten with time.

Individual Elicitations for In-Vessel Issue 4

Expert A's Elicitation

Issue 4: BWR Bottom Head Failure

Description of Expert A's Rationale/Methodology

Expert A addressed Parts 1 and 3 of this issue in a similar fashion. He did not provide results for Part 2. For Parts 1 and 3 Expert A considered three possible scenarios for RPV failure:

1. High-pressure melt ejection (HPME) in which core debris is ejected, possibly through a penetration failure, into the pedestal area as a liquid jet driven by the gas pressure in the vessel.

2. Gravity pour (GP) in which the core debris flows under gravity into the pedestal area. The pour can contain entrained solids.

3. Dump (DMP) in which RPV failure occurs by creep-rupture allowing large quantities of debris to fall into the pedestal. The debris may be solid or may contain some liquid.

His assessment for Part 1 consists of identifying the probability of HPME. For Part 3 the probability of the other two scenarios was assessed, along with the other information requested relative to the state of the core debris for each of the three scenarios.

Expert A subdivided the three cases by the extent of in-vessel zircaloy oxidation. In essence, a high, medium, and low subcase was identified for each of the three cases described above. The three subcases were described as follows:

1. 30% zirconium oxidation. (Low, corresponding to oxidation of ≤ 30% of the core zirconium inventory.) The core debris contains large amounts of metallic material, dominated by phase zirconium. Debris melting temperatures will be approximately 2200 K.

2. 60% zirconium oxidation. (Medium, corresponding to oxidation of between 30 and 60% of the core zirconium inventory.) The debris melting temperature will be elevated to approximately 2700 K. Most of the zirconium will be involved in monotectic dissolution of UO_2.

3. 90% zirconium oxidation. (High, corresponding to oxidation of between 60 and 90% of the core zirconium inventory.) The debris contains almost solely oxides. A 2800 K melting temperature for the debris is the minimum expected.

   (Note that such high levels of zirconium oxidation were not assigned high probability by the experts considering that issue.)

A decomposition tree was constructed for this issue. This tree is shown in Figure A-1. Expert A considered five questions about the nature of the in-vessel melt progression in formulating this decomposition. These questions are discussed below.

Crust in Core

Examination of the core region of the Three Mile Island Unit 2 (TMI-2) reactor revealed that a crust of refrozen core material had formed within the core a meter or so above the core plate. This crust apparently allowed a region of hot debris to form within the core above that crust. Melting of debris in that hot region lead to a break-out of molten material which then flowed (apparently quite quickly) into the bottom head. Formation of a crust in the core was thus seen by Expert A to be a mechanism by which substantial quantities of molten debris could be formed. Without crust formation molten debris dribbles down from the melting fuel assemblies, collecting on the core plate.

Core Plate Failure

Expert A believed that the manner in which the core plate fails would affect the coolability of debris in the lower plenum. Massive failure, indicated by the upward branch in Figure A-1, would reduce the probability that the debris will quench in the lower plenum. Conversely, while localized failure of the core plate increases the likelihood of debris quenching, if the debris fails to quench, localized failure creates the condition under which there is a high likelihood that a jet of molten material will impinge on the lower head.

Debris Quench

For all the cases considered, the lower plenum contains water during core damage. Core debris penetrating the core plate can be quenched in this water. Expert A generally believed that quenching was likely (at least a 50% chance) and assigned higher probabilities for sequences in which there would be no massive failure of the core plate.

Penetration Failure or Jet Impingement Failure of the Head

Expert A considered localized failure of the bottom head (upward pathway in Figure A-1) versus a generalized failure (due to creep rupture) that would drop all the debris that had accumulated in the lower plenum out of the RPV essentially instantaneously. Localized failures could result either from melting of a bottom head penetration (control rod drive [CRD] or instrument tube) or by impingement of a jet of molten material falling from the core plate.

Molten Debris at Vessel Failure

Vessel failure by jet impingement or by gradual heating of debris that is initially quenched in the lower plenum could result in a substantial fraction of the debris in the lower head being molten when the vessel fails (upward path in Figure A-1). Expert A stated that thermal contact between debris in the lower plenum and the vessel wall was generally poor. Thus, while the vessel steel melts at a much lower temperature than the core debris, liquefaction and even superheating of the debris prior to bottom head failure was thought to be relatively likely.
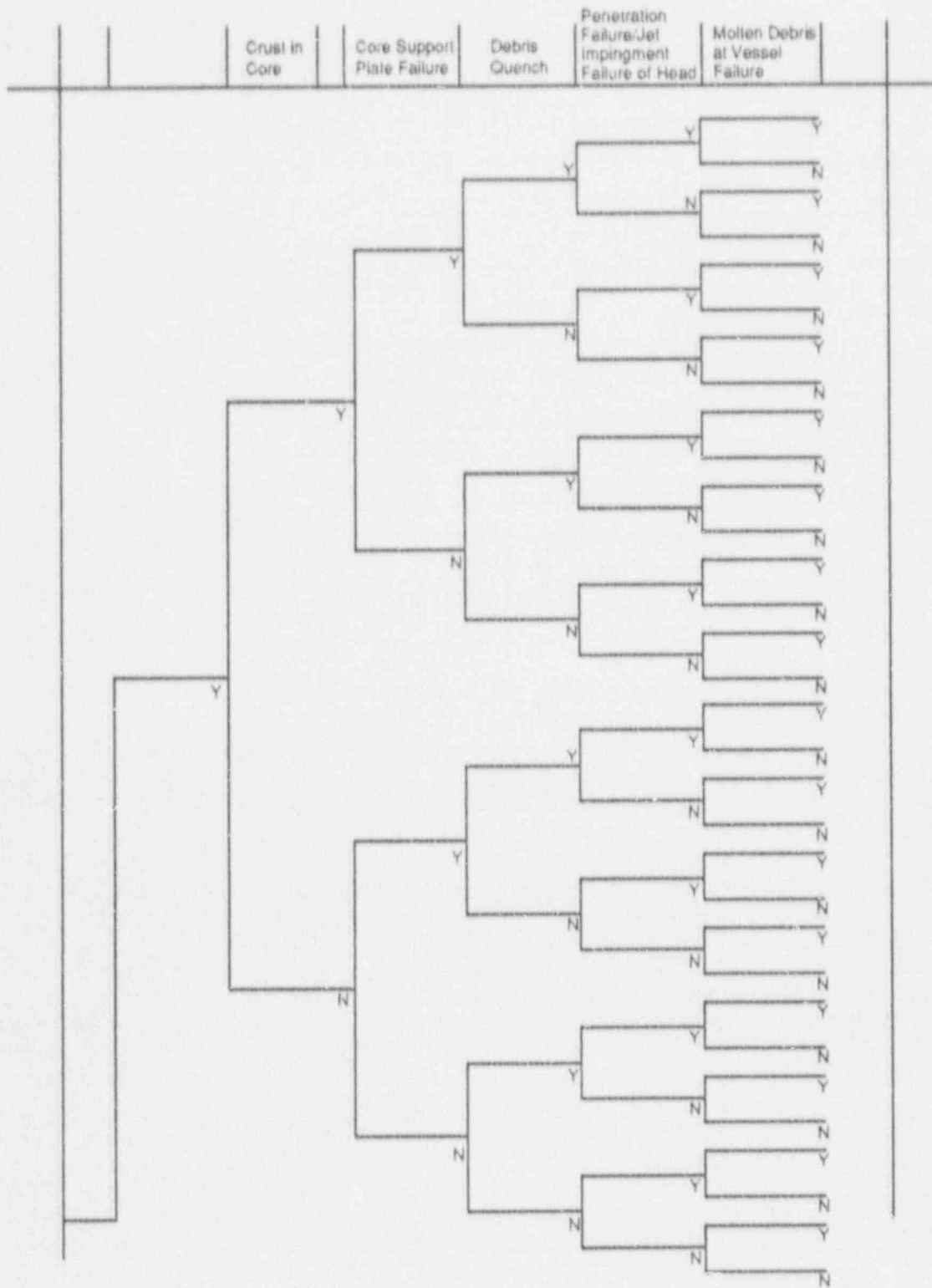
Figure A-1. Expert A's Decomposition Tree for BWR
Bottom Head Failure

Expert A used his judgment to evaluate each of the 31 probabilities in the decomposition tree for each of the nine subcases. The results were then aggregated according to the four scenarios (HPME, GP, Solid and Liquid DMP) defined above. Using the tree pathways for guidance, Expert A then constructed distributions for the core debris characteristics (timing, mass ejected, fraction of the ejected mass that is metallic, temperature, and superheat).

Results of the Expert's Elicitation

Table A-1 provides the probabilities inserted in the decomposition trees for each of the nine subcases formulated by Expert A. The probability for each scenario calculated by the tree is also provided in that table. From Table A-1 it is apparent that the level of in-vessel zircaloy oxidation is far more important than the distinction between Case 1 and Case 3 (both cases consider high RPV pressure). Thus, the results of Cases 1 and 3 have been combined and will be referred to as Case 1, RPV at high pressure.

Tables A-2 through A-7 provide the melt characteristics provided by Expert A for each of the six distinguishable cases. The distributions provided are essentially distributions on the debris temperature. Superheat and the fraction of the debris that is molten are completely correlated with the debris temperature.

The high-pressure scenarios were seen to have the potential to lead to lower temperature debris. The low end of the probability distribution for the high-pressure scenarios have significantly less superheat (150 K) than the low end for low-pressure scenarios. Similarly, the fraction of the debris that is liquid could be lower for high-pressure scenarios. These effects are the result of an expectation that the RPV will fail earlier when it is under pressure.

In general, Expert A believes that high temperature, predominantly liquid debris with substantial superheat (50 to 400 K) is to be expected. Little sensitivity to the specific accident scenario was expected. Distinctions between the cases considered are minor although a significant increase in the maximum debris temperature (500 K) was viewed to be possible if the level of in-vessel zircaloy oxidation were high. Significant probability (~0.6) was ascribed to dumping a large fraction of the core into the pedestal at RPV failure. Expert A placed a great deal of emphasis on the ability of core debris to form insulated layers both in the core and in the RPV bottom head. Insulating layers in the bottom head were seen to allow debris temperature to rise well above the melting temperature of the pressure vessel steel. In summary, Expert A gave a high probability to large quantities of hot, superheated, and (for in-vessel zirconium oxidation levels typically attributed by the review panel) substantially metallic (35 to 60%), debris.

Table A-1

Decomposition Tree Probabilities

Prob. Specified	Case 1			Case 2			Case 3		
Zr	Low Zr	Med. Zr	High Zr	Low Zr	Med. Zr	High Zr	Low Zr	Med. Zr	High Zr
P_1	0.5	--	--	--	--	--	--	--	--
P_2	0.8	--	--	--	--	--	--	--	--
P_3	0.9	--	--	--	--	--	--	--	--
P_4	0.5	--	--	--	--	--	--	--	--
P_5	0.8	--	--	--	--	--	--	--	--
P_6	0.5	--	--	--	--	--	--	--	--
P_9	0.9	--	--	--	--	--	--	--	--
P_{10}	0.8	--	--	--	--	--	--	--	--
P_{11}	0.9	--	--	--	--	--	--	--	--
P_{12}	0.8	--	--	--	--	--	--	--	--
P_{13}	0.9	--	--	--	--	--	--	--	--
P_{14}	0.8	--	--	--	--	--	--	--	--
P_{15}	0.9	--	--	--	--	--	--	--	--
P_{16}	0.4	--	--	--	--	--	--	--	--
P_{17}	0.5	--	--	--	--	--	--	--	--
P_{18}	0.7	--	--	--	--	--	--	--	--
P_{19}	0.6	--	--	--	--	--	--	--	--
P_{20}	0.4	--	--	--	--	--	--	--	--
P_{21}	0.5	--	--	--	--	--	--	--	--
P_{22}	0.7	--	--	--	--	--	--	--	--
P_{23}	0.6	--	--	--	--	--	--	--	--
P_{24}	0.4	--	--	--	--	--	--	--	--
P_{25}	0.5	--	--	--	--	--	--	--	--
P_{26}	0.7	--	--	--	--	--	--	--	--
P_{27}	0.6	--	--	--	--	--	--	--	--
P_{28}	0.4	--	--	--	--	--	--	--	--
P_{29}	0.5	--	--	--	--	--	--	--	--
P_{30}	0.7	--	--	--	--	--	--	--	--
P_{31}	0.6	--	--	--	--	--	--	--	--

Table A-1 (continued)

Prob. Specified	Case 1			Case 2			Case 3		
	Low Zr	Med. Zr	High Zr	Low Zr	Med. Zr	High Zr	Low Zr	Med. Zr	High Zr
HPME or Rapid Pour	0.46	0.39	0.31	0.42*	0.36*	0.29*	0.49	0.40	0.32
Gravity Pour	0.37	0.39	0.42	0.32	0.33	0.34	0.35	0.38	0.41
DMP	0.17	0.22	0.27	0.26	0.31	0.37	0.16	0.22	0.27

*Rapid pour, since HPME does not occur with RPV depressurized.

Table A-2

Melt Characteristics. Case 1A: High Pressure

Low Zr Oxidation (60% Metal in Debris)

Probability	Distribution Fractiles	Duration (min)	Melt Temperature (K)	Superheat (K)	Fraction Melted (%)
HPME Involving <40% of the Core					
0.38	0.05	0	1300	50	10
	0.50		2000	100	80
	0.95		2600	400	100
HPME Involving ≥40% of the Core					
0.10	0.05	0	1300	50	10
	0.50		2000	100	80
	0.95		2600	400	100
Gravity Pour					
0.36	0.05	10	1300	50	10
	0.50	200	2000	100	80
	0.95	450	2600	800	100
Dump Involving <40% of Core					
0.13	0.05	0	1300	50	10
	0.50		1800	100	50
	0.95		2300	200	90
Dump Involving ≥40% of Core					
0.03	0.05	0	1300	50	10
	0.50		1800	100	50
	0.95		2300	200	90

Table A-3
Melt Characteristics. Case 1B: High Pressure
Medium Zr Oxidation (35% Metal in Debris)

Probability	Distribution Fractiles	Duration (min)	Melt Temperature (K)	Superheat (K)	Fraction Melted (%)
HPME Involving <40% of the Core					
0.32	0.05	0	1300	50	10
	0.50		2400	100	80
	0.95		3100	400	100
HPME Involving ≥40% of the Core					
0.08	0.05		1300	50	10
	0.50		2400	100	80
	0.95	0	3100	400	100
Gravity Pour					
0.38	0.05	10	1300	50	10
	0.50	320	2400	100	80
	0.95	600	3100	800	100
Dump Involving <40% of Core					
0.18	0.05		1300	50	10
	0.50	0	2000	100	50
	0.95		2700	200	90
Dump Involving ≥40% of Core					
0.04	0.05		1300	50	10
	0.50	0	2000	100	50
	0.95		2700	200	90

Table A-4
Melt Characteristics. Case 1C: High Pressure
High Zr Oxidation (15% Metal in Debris)

Probability	Distribution Fractiles	Duration (min)	Melt Temperature (K)	Superheat (K)	Fraction Melted (%)
HPME Involving <40% of the Core					
0.25	0.05	0	1300	50	10
	0.50		2600	50	80
	0.95		3100	50	100
HPME Involving ≥40% of the Core					
0.06	0.05		1300	50	10
	0.50		2600	50	80
	0.95	0	3100	50	100
Gravity Pour					
0.42	0.05	10	1300	50	10
	0.50	320	2600	50	80
	0.95	600	3100	50	100
Dump Involving <40% of Core					
0.22	0.05		1300	50	10
	0.50	0	2200	50	50
	0.95		2800	50	90
Dump Involving ≥40% of Core					
0.05	0.05		1300	50	10
	0.50	0	2200	50	50
	0.95		2800	50	90

Table A-5
Melt Characteristics. Case 2A: Low Pressure
Low Zr Oxidation (60% Metal in Debris)

Probability	Distribution Fractiles	Duration (min)	Melt Temperature (K)	Superheat (K)	Fraction Melted (%)
HPME Involving <40% of the Core					
0.34	0.05	0	1500	200	10
	0.50		2000	100	80
	0.95		2600	400	100
HPME Involving ≥40% of the Core					
0.08	0.05		1500	200	10
	0.50		2000	100	80
	0.95	0	2600	400	100
Gravity Pour					
0.32	0.05	10	1500	200	10
	0.50	320	2000	100	80
	0.95	600	2600	200	100
Dump Involving <40% of Core					
0.21	0.05		1500	200	20
	0.50	0	1800	100	50
	0.95		2300	250	90
Dump Involving ≥40% of Core					
0.05	0.05		1500	200	20
	0.50	0	1800	100	50
	0.95		2300	250	90

Table A-6

Melt Characteristics. Case 2B: Low Pressure
Medium Zr Oxidation (35% Metal in Debris)

Probability	Distribution Fractiles	Duration (min)	Melt Temperature (K)	Superheat (K)	Fraction Melted (%)
HPME Involving <40% of the Core					
0.29	0.05	0	1500	200	20
	0.50		2400	100	80
	0.95		3100	450	100
HPME Involving ≥40% of the Core					
0.07	0.05		1500	200	20
	0.50		2400	100	80
	0.95	0	3100	400	100
Gravity Pour					
0.33	0.05	10	1500	50	10
	0.50	320	2400	100	80
	0.95	600	3100	400	100
Dump Involving <40% of Core					
0.25	0.05	0	1500	200	20
	0.50		2000	100	50
	0.95		2700	200	90
Dump Involving ≥40% of Core					
0.00	0.05	0	1500	200	20
	0.50		2000	100	50
	0.95		2700	200	90

Table A-7
Melt Characteristics. Case 2C: Low Pressure
High Zr Oxidation (15% Metal in Debris)

Probability	Distribution Fractiles	Duration (min)	Melt Temperature (K)	Superheat (K)	Fraction Melted (%)
HPME Involving <40% of the Core					
0.23	0.05	0	1500	200	20
	0.50		2600	100	80
	0.95		3100	50	100
HPME Involving ≥40% of the Core					
0.06	0.05		1500	200	20
	0.50		2600	100	80
	0.95	0	3100	50	100
Gravity Pour					
0.34	0.05	10	1500	50	10
	0.50	400	2600	100	80
	0.95	750	3100	50	100
Dump Involving <40% of Core					
0.30	0.05		1500	200	20
	0.50	0	2200	50	50
	0.95		2800	50	90
Dump Involving ≥40% of Core					
0.00	0.05		1500	200	20
	0.50	0	2200	50	50
	0.95		2800	50	90

Sources of Uncertainty

The branch points on the decomposition tree shown in Figure A-1 indicate the major sources of uncertainty for Expert A. Of these, the formation of a crust in the core contributed in the largest extent to this expert's conclusion. Quenching of the debris in the lower plenum contributed most to the uncertainty in the scenario for vessel failure.

Expert B's Elicitation

Issue 4: BWR Bottom Head Failure

Description of Expert B's Rationale/Methodology

The Expert began his analysis by reviewing the previous analyses and making a list of the important parameters or characteristics of the vessel or models which could impact the melt progression. This list was very extensive. The Expert then performed some computer runs using different and/or improved models in order to assess the effects of the uncertainties in the in-vessel models on the melt progression.

Three possibilities were given for state of debris at the lower head: (1) everything goes to bottom head and quenches so there are solid particles on the bottom; (2) due to densely packed materials in the lower plenum, freezing (i.e., candling) of materials flowing over solid walls occurs, reducing the amount of debris reaching the lower head; and (3) not all debris may quench and have cohesive debris, so that heat-up and reoxidation will be slower. The main difficulty with assessing this issue was in the ability to clearly define a unique set of conditions in order to discretize the possible melt progressions into a set of scenarios.

Results of Expert B's Elicitation

For each of the three cases, the Expert gave a probability of lower head failure within a specific time interval (A,B,C,D) and the mass of core ejected from the vessel vs. time after vessel breach (in metric tons), conditional on the lower head failing within the above specific time intervals. The Expert's uncertainty as to the type of melt progression and his evaluation of the effects of the uncertainties within a particular melt progression were used to define the time intervals and the pour characteristics.

Case 1

		Mass of Core (metric tons) vs Time			
	Prob	30 s	20 m	10 m	3 d
1A (0 to 2 h)	.05	5	10	15	80
1B (2 to 4 h)	.60	25	40	60	150
1C (4 h to 3 d)	.35	30	50	80	200
1D (no failure)	.01	0	0	0	0

Case 2

	Mass of Core (metric tons) vs Time				
	Prob	30s	2m	10m	3d
1A (0 to 2 h)	.2	2	5	20	100
1B (2 to 4 h)	.7	5	20	60	180
1C (4 h to 3 d)	.1	10	40	120	250
1D (no failure)	0	0	0	0	0

Case 3

	Mass of Core (metric tons) vs Time				
	Prob	30s	2m	10m	3d
1A (0 to 2 h)	.1	1	3	10	50
1B (2 to 4 h)	.1	5	15	30	100
1C (4 h to 3 d)	.2	5	20	60	150
1D* (no failure)	.6	0	0	0	0

* Strongly depends on CRD flow rate.

The Expert was unable to define more specifically certain core melt scenarios which would include some of the major differences in the melt progressions and to assign them weights. Also for the cases elicited, the Expert was unable to supply expected values for the parameters needed by the in-vessel group except for the mass of core ejected vs time from vessel breach (VB).

Sources of Uncertainty

The major sources of uncertainty for this analysis fall into two categories:

1. Initial Conditions. The initial conditions include such things as (a) the time of injection failure; (b) the initial water level in the core; (c) the level of decay heat at the start of boiloff; and (d) the initial power distribution.

5.4-19

2.   Modeling Uncertainties. These fall into two categories, (a) core configuration; and (b) process models. For (a), the level of detail of the core model and the various characteristics of the core which are included will result in substantial differences in the melt progression. For (b), the uncertainties in physical parameters, such as melting temperatures for eutectics, and accuracy of the physical models used can also result in substantial differences in the core melt progression.

Correlations with Other Variables

The output from this issue is correlated with the input variables to the containment loads issue on pressure rise after vessel breach and with such issues as the amount of fission products retained in vessel, and the probability of Direct Containment Heating (DCH) or ex-vessel steam explosions.

Suggested Methods for Reducing Uncertainty

In order to reduce the uncertainty in this issue, we need to understand how differences in the level of detail of the core models and the physical processes affect the details of the melt progression.

Expert C's Elicitation

Expert C provided the results of BWRSAR calculations which were used to develop the distributions ~d in the Accident Progression Event Tree (APET). No elicitation was pe..ormed.

5.5   Issue 5. PWR In-Vessel Hydrogen Generation

Summary of Expert Panel's Assessment of
In-Vessel Issue 5: PWR Hydrogen Generation

Experts consulted: Peter Bieniarz, Risk Management Associates; William
Camp, Sandia National Laboratories; Robert Lutz, Westinghouse Electric
Corporation; Garry Thomas, Electric Power Research Institute; Robert
Wright, Nuclear Regulatory Commission.

Issue Description

What distributions characterize the uncertainty in the extent of hydrogen
production prior to vessel breach? Hydrogen production is expressed in
terms of the fraction produced relative to that produced when all of the
zirconium in the core is oxidized.

Four cases were defined in the initial definition of the issue:

Case	RCS Pressure (psia)	Accumulators Discharged	UHI Discharged
1	2500	No	No
2	1000 to 1500	No	Partial
3	150 to 500	Partial	Yes
4	40 to 200	Yes	Yes

During the course of the meetings of the panel, the case structure was
discussed at some length. Some panel members expanded the initial case
structure, while others did not.

RCS pressure refers to the pressure when the water level drops below the
top of active fuel. The last two columns refer to discharge before the
onset of ceramic melting, and assume that the secondary system has not been
depressurized. UHI refers to the Upper Head Injection system, a feature
found only on Westinghouse reactors in ice condenser containments. Of the
three PWRs considered in this study, only Sequoyah has a UHI system. In
this regard, the Tennessee Valley Authority (TVA) received NRC's permission
to remove the UHI at the next refueling outage. The NRC has decided that
Sequoyah should be analyzed without UHI for this project, but this was not
decided until after the experts had completed their analyses. The consider-
ation of the UHI did not influence the expert results for this issue.

Summary of Experts' Rationale/Methodology

For each case, the amount of hydrogen produced for each point of the
aggregate was determined by averaging the values of the five members of the
panel who considered this issue. None of the experts provided a discrete
distribution for the original four cases, defined by the NUREG-1150
analysts.

Expert A based his conclusions primarily on the large number of code calculations that have been made. He concluded that MELPROG,[5-1] SCDAP,[5-2] and CORMLT[5-3] gave the most reasonable and realistic results. He considered the MARCH[5-4] results to be unrealistically high and the MAAP[5-5] results to be unrealistically low. Although Expert A used the results of all the codes, the results of the more mechanistic codes, MELPROG, SCDAP, and CORMLT, were weighted more heavily and were used to determine the mid-range of his distributions. Where results from these three codes were few or lacking altogether, Expert A made his distributions wider than they would have been if results from these codes had been available. Expert A provided plots giving the probability density as a function of the equivalent fraction of zirconium oxidized for Cases 1, 2, and 3. Values taken from these curves were used to form CDFs. Table 5-1 lists seven points from these CDFs, which are plotted in Figure 5-1. As Expert A provided no plot for Case 4, his results for Case 3 have been used for Case 4. Expert A derived his value for Case 2 by combining two other distributions. For Case 2, there is the question of whether the loop seal will clear in the loop with the break. Expert A's distribution for this case was formed by combining one curve for the subcase where the loop seal cleared with another curve, giving the hydrogen production when the seal did not clear.

Expert B based his analysis on the results of simulations with the various computer codes currently available. He felt that MELPROG-TRAC[5-6] and SCDAP-RELAP5[5-2] were the most accurate and trustworthy of these codes at this time. CORMLT has some very good constituent models and he utilized some CORMLT results, but he gave very little weight to MARCH and MAAP results. Expert B provided distributions for hydrogen generation for Cases 1 and 4. He deferred to another panel member for Case 2, and thought that Case 3 would be similar enough to Case 4 that his Case 4 results could be used. Expert B provided results for the 1, 10, 50, 90, and 99% points on a cumulative distribution. Interpolation, which somewhat smoothed the distribution, was used to obtain the values listed in Table 5-2, and shown in Figure 5-2. The values for Case 2 are taken from the Case 2 values for the other panel member.

Expert C based his conclusions on applicable test results, the TMI-2 accident, and the results of various code calculations. He saw the formation of a eutectic between the oxides of zirconium and uranium as the dominant phenomenon. Expert C did not link any of the points on his distributions directly to specific code or test results. Expert C divided Cases 1 and 2 into three subcases each, dependent upon the time of accumulator discharge. He also defined an additional case for that fraction of Case 2 where the break is in the cold leg and the loop seal clears. Expert C's distributions are listed in Table 5-3, and shown in Figure 5-3. Interpolation was used to obtain the 5 and 95% values.

Expert D based his conclusions primarily on a number of MAAP runs that were made for Ringhals 3 and Zion. Ringhals 3 is a three-loop plant with a NSSS similar to Surry's, and Zion is a four-loop plant with a NSSS similar to that of Sequoyah. Expert D considered Cases 2, 3, and 4 together, so he had only two cases. For each of these, however, he considered subcases which were defined by core blockage, core melt fraction of zirconium exposed, and relocation temperature, and status of accumulator dump. Eight

endpoints for each case were obtained. For each endpoint in his decomposition tree, Expert D assigned a distribution for hydrogen production based on specific MAAP[5-5] runs. He considered three sources of hydrogen: all the phenomena modeled in MAAP, extra hydrogen generated by accumulator discharge during core melt, and hydrogen resulting from stainless steel oxidation in the upper head. Utilizing Expert D's decomposition tree and the branching ratios he provided, the distributions for the sixteen endpoints were combined to get the final distributions for hydrogen production, shown in Table 5-4 and Figure 5-4.

Expert E based his analysis upon his work on the TMI-2 accident, MAAP calculations, and experience in comparing code results to the TMI-2 accident. Expert E provided distributions for the amount of hydrogen generated for two classes of accident. He lumped all accidents where the RCS pressure was above 200 psia into a blackout class, and all accidents where the RCS pressure was below 200 psia into a large break class. For each class, Expert E provided a distribution for zirconium oxidation in-core (before relocation) and additional distributions for oxidation in the lower head (after relocation). The distributions for oxidation in the lower head were conditional upon the amount of oxidation that occurred in-core. Thus the distributions for the two periods had to be convolved together to get the resultant distribution for the total hydrogen production in the vessel before breach. The resulting distributions were in terms of evenly spaced fraction of zirconium oxidized; interpolation was needed to obtain the values shown in Table 5-5 and Figure 5-5.

Method of Aggregation

The aggregate values for PWR hydrogen production are shown in Table 5-6 and Figure 5-6. The case and subcase structure of the expert who had the most cases and subcases was used to avoid losing information. The differences between Cases 1a and 1c, and between Cases 2a and 2c are very si. t. These cases will be combined for use in evaluating the APET, and Case 5 will probably be included with Cases 2a and 2c as well. It may also be possible to group Case 4 with Case 3a. Results for each subcase are listed in Tables 5-7 through 5-1t and shown in Figures 5-7 through 5-16.

The aggregate curves are very broad. This is a result of widely differing opinions among the panel members considering this issue. For example, consider Case 4. The difference between the 1% value and the 99% value is 103% equivalent zirconium oxidation. The difference between the highest value given for the 99% value (140% zirconium oxidation) and the lowest value given for the 99% value (35% zirconium oxidation) is 105% zirconium oxidation. Thus the range for the upper extreme value is greater than the entire range for the aggregate distribution.

For tabular display, the results of each expert were placed in common form: the seven values for the cumulative probability distribution as shown in Table 5-1 through 5-5. Only one of the five experts gave hydrogen production amounts for these seven points; for the others a manipulation, usually simple interpolation, was required to get the results in this form.

The aggregate of each case is formed by averaging over the percent of zirconium oxidized. That is, for each percent oxidized zirconium value for which one of the five experts has a value for the cumulative probability, an average is formed. As the other experts will probably not have given cumulative probabilities for that percent of zirconium oxidized, their values for the cumulative probability are formed by interpolation. For example consider Case 1a, Table 5-7. For 10% zirconium oxidized, Expert B has 1% cumulative probability, Expert C has 25% cumulative probability, and the other three experts have 0% cumulative probability. The aggregate cumulative probability for 10% zirconium oxidation is thus 26% divided by 5 or 5.2%. For 25% zirconium oxidation, Experts B, C, and D gave cumulative probabilities of 5, 75, and 5%, respectively. The values for Experts A and E are determined by interpolation, and then all five values are averaged to get the aggregate.

To illustrate the aggregation method, Tables 5-7 through 5-16 could have been recast in terms of cumulative probability values for every 5 or 10% zirconium oxidized. That way the aggregate would have been the average for each line. As three of the five experts gave zirconium oxidation percentages for fixed points on the cumulative probability distribution, however, adoption of this format would have required considerable interpolation. Thus, while Tables 5-7 through 5-16 present the experts' results in a form that better represents the form in which most of the experts gave their information, they are misleading in that the aggregate values are not the average of the five values directly above them in the tables.

The tails of the distributions would have been lost had the average been taken across the cumulative probabilities instead of across the percent zirconium oxidized. For example, in Case 1a, the average of the 99% zirconium oxidation percentages is 78.2%. Had we averaged this way, then only 1% of the sample members would have had zirconium oxidation values exceeding 78.2% and the upper tails of the distributions of Experts A and B would have been lost.

In Table 5-6 and Figure 5-6, the midpoint values may be observed to range from 30 to almost 50% zirconium oxidation. This is smaller than the range among the experts for several subcases. For example, the midpoint values for the five experts in Case 1a range from 15 to 65% zirconium oxidation. The differences among experts tend to be as large or larger than the differences between cases and subcases. This is especially true if the upper bound (95 and 99%) values are considered.

For Case 1, Expert C defined three subcases and Expert D defined two subcases. The other three experts did not define any subcases, so their entries are the same for Tables 5-7, 5-8, and 5-9. Expert D divided his subcases on whether the accumulators discharged during vessel breach; thus his entries in Tables 5-7 and 5-9 are identical. As Expert C's results for accumulator discharge before core melt and at vessel breach are very much the same, the aggregate distributions for Cases 1a and 1c are essentially identical. The two subcases will be considered together when the CET is evaluated.

For Case 2, Expert C also defined three subcases and Expert D also defined two subcases. The results for Case 2 are shown in Tables 5-10, 5-11, and 5-12. Since Expert C's results for accumulator discharge before core melt and at vessel breach are similar, the differences in the aggregate between Cases 2a and 2c are negligible, and the two subcases will be considered together when the CET is evaluated.

Expert C defined a Case 5, which is similar to Case 2c but has the break in the cold leg instead of the hot leg. Expert A defined his Case 2 to have the break in the cold leg, but made allowances for the possibility that the loop seal might not clear. The other two experts who gave distributions for Case 2 did not make distinctions as to break location or the time of accumulator discharge. It may be seen from Table 13 that Case 5 is identical to Case 2c except for the distribution of Expert C. The aggregate for Case 5 is very close to the aggregate distribution for Cases 2a and 2c.

The results for Case 3 are shown in Tables 5-14 and 5-15. While Expert C did not make a distinction for Case 3 for the time of accumulator discharge, Expert D did. Th differences in the aggregate values between Cases 3a and 3b border on being large enough to maintain the distinction between them. The results for Case 4 are shown in Table 5-16. None of the Experts defined subcases for Case 4. The differences in the aggregates for Case 4 and Case 3a are fairly small.

Following the tables and figures, each expert's elicitation is summarized.

<u>Aggregated Results</u>

Table 5-1
Amount of Hydrogen Generated
(percentage of zirconium oxidized)
Expert A

Case	RCS Pressure (psia)	Probability						
		1%	5%	25%	50%	75%	95%	99%
1	2500	20	27	39	47	57	78	96
2	1000-1500	8	16	24	30	40	62	80
3	150-500	13	23	56	66	84	106	140
4	40-200	13	23	56	66	84	106	140

Table 5-2
Amount of Hydrogen Generated
(percentage of zirconium oxidized)
Expert B

Case	RCS Pressure (psia)	Probability						
		1%	5%	25%	50%	75%	95%	99%
1	2500	10	25	50	65	90	125	140
2	1000-1500	8	16	24	30	40	62	80
3	150-500	10	20	45	65	85	103	110
4	40-200	10	20	45	65	85	103	110

Table 5-3
Amount of Hydrogen Generated
(percentage of zirconium oxidized)
Expert C

Case	RCS Pressure (psia)	Probability						
		1%	5%	25%	50%	75%	95%	99%
1a	2500 bCM*	5	6	10	15	25	45	50
1b	2500 dCM**	5	8	25	35	45	65	70
1c	2500 aVB***	5	6	10	18	30	55	60
2a	≈1200 bCM	5	7	20	32	40	57	60
2b	≈1200 dCM	5	10	30	40	48	75	80
2c	≈1200 aVB	5	8	25	35	42	57	60
3	150-500	10	14	30	40	60	75	80
4	40-200	10	13	25	35	50	78	85
5	≈1200 aVB	10	13	25	35	50	78	85

*bCM: before core melt
**dCM: during core melt
***aVB: after core melt

Table 5-4
Amount of Hydrogen Generated
(percentage of zirconium oxidized)
Expert D

Case	RCS Pressure (psia)	Probability						
		1%	5%	25%	50%	75%	95%	99%
1a	2500 nCM*	20	25	29	35	41	45	50
1b	2500 dCM**	25	31	44	59	68	74	80
2a	< 1500 nCM	13	17	20	24	28	31	35
2b	< 1500 dCM	18	23	34	48	56	61	66

*nCM: no core melt
**dCM: during core melt

Table 5-5
Amount of Hydrogen Generated
(percentage of zirconium oxidized)
Expert E

Case	RCS Pressure (psia)	Probability						
		1%	5%	25%	50%	75%	95%	99%
1-3	> 200	20	24	31	37	43	49	55
4	< 200	11	13	21	26	29	37	39

Table 5-6
PWR Hydrogen Generation (% zirconium oxidized)

Aggregate

	Cumulative Probability*						
	1%	5%	25%	50%	75%	95%	99%
Case 1a	6	10	28	39	50	96	125
Case 1b	8	20	34	45	62	93	125
Case 1c	6	10	28	39	52	96	125
Case 2a	7	14	23	30	39	57	73
Case 2b	8	17	27	36	47	64	78
Case 2c	7	15	24	30	40	57	73
Case 5	10	16	24	30	41	63	81
Case 3a	12	18	27	40	64	97	114
Case 3b	12	20	34	48	65	97	114
Case 4	11	15	24	33	63	97	114

*Cumulative Probability refers to the first row in the table. The numbers below that row are the values of the parameter defined in the table heading.

Table 5-7
PWR Hydrogen Generation (% zirconium oxidized)

Case 1a - RCS at 2500 psia, Accm. Dump before CM

	Cumulative Probability*						
	1%	5%	25%	50%	75%	95%	99%
Expert A	20	27	39	47	57	78	96
Expert B	10	25	50	65	90	125	140
Expert C	5	6	10	15	25	45	50
Expert D	20	25	29	35	41	45	50
Expert E	20	24	31	37	43	49	55
Aggregate	6	10	28	39	50	96	125

*Cumulative Probability refers to the first row in the table. The numbers below that row are the values of the parameter defined in the table heading.

Table 5-8
PWR Hydrogen Generation (% zirconium oxidized)

Case 1b - RCS at 2500 psia, Accm. Dump before CM

	Cumulative Probability*						
	1%	5%	25%	50%	75%	95%	99%
Expert A	20	27	39	47	57	78	96
Expert B	10	25	50	65	90	125	140
Expert C	5	8	25	35	45	65	70
Expert D	25	31	44	59	68	74	80
Expert E	20	24	31	37	43	49	55
Aggregate	8	20	34	45	62	93	125

*Cumulative Probability refers to the first row in the table. The numbers below that row are the values of the parameter defined in the table heading.

Table 5-9
PWR Hydrogen Generation (% zirconium oxidized)

Case 1c - RCS at 2500 psia, Accm. Dump before CM

	Cumulative Probability*						
	1%	5%	25%	50%	75%	95%	99%
Expert A	20	27	39	47	57	78	96
Expert B	10	25	50	65	90	125	140
Expert C	5	6	10	18	30	55	60
Expert D	20	25	29	35	41	45	50
Expert E	20	24	31	37	43	49	55
Aggregate	6	10	28	39	52	96	125

*Cumulative Probability refers to the first row in the table. The numbers below that row are the values of the parameter defined in the table heading.

Table 5-10
PWR Hydrogen Generation (% zirconium oxidized)

Case 2a - RCS at 1000 - 1500 psia, Accm. Dump before CM

	Cumulative Probability*						
	1%	5%	25%	50%	75%	95%	99%
Expert A	8	16	24	30	40	62	80
Expert B	8	16	24	30	40	62	80
Expert C	5	7	20	32	40	57	60
Expert D	13	17	20	24	28	31	35
Expert E	20	24	31	37	43	49	55
Aggregate	7	14	23	30	39	57	73

*Cumulative Probability refers to the first row in the table. The numbers below that row are the values of the parameter defined in the table heading.

Table 5-11
PWR Hydrogen Generation (% zirconium oxidized)

Case 2b - RCS at 1000 - 1500 psia, Accm. Dump before CM

	Cumulative Probability*						
	1%	5%	25%	50%	75%	95%	99%
Expert A	8	16	24	30	40	62	80
Expert B	8	16	24	30	40	62	80
Expert C	5	10	30	40	48	75	80
Expert D	18	23	34	48	56	61	66
Expert E	20	24	31	37	43	49	55
Aggregate	8	17	27	36	47	64	78

*Cumulative Probability refers to the first row in the table. The numbers below that row are the values of the parameter defined in the table heading.

Table 5-12
PWR Hydrogen Generation (% zirconium oxidized)

Case 2c - RCS at 1000 - 1500 psia, Accm. Dump before CM

	Cumulative Probability*						
	1%	5%	25%	50%	75%	95%	99%
Expert A	8	16	24	30	40	62	80
Expert B	8	16	24	30	40	62	80
Expert C	5	8	25	35	42	57	60
Expert D	13	17	20	24	28	31	35
Expert E	20	24	31	37	43	49	55
Aggregate	7	15	24	30	40	57	73

*Cumulative Probability refers to the first row in the table. The numbers below that row are the values of the parameter defined in the table heading.

Table 5-13
PWR Hydrogen Generation (% zirconium oxidized)

Case 5 - RCS at 1000 - 1500 psia, Cold Leg break,
Accm. Dump before CM

	Cumulative Probability*						
	1%	5%	25%	50%	75%	95%	99%
Expert A	8	16	24	30	40	62	80
Expert B	8	16	24	30	40	62	80
Expert C	10	13	25	35	50	78	85
Expert D	13	17	20	24	28	31	35
Expert E	20	24	31	37	43	49	55
Aggregate	10	16	24	30	41	63	81

*Cumulative Probability refers to the first row in the table. The numbers below that row are the values of the parameter defined in the table heading.

Table 5-14
PWR Hydrogen Generation (% zirconium oxidized)

Case 3a - RCS at 150 - 500 psia, No
Accm. Dump During CM

	Cumulative Probability*						
	1%	5%	25%	50%	75%	95%	99%
Expert A	13	23	56	66	84	106	140
Expert B	10	20	45	65	85	103	110
Expert C	10	14	30	40	60	75	80
Expert D	13	17	20	24	28	31	35
Expert E	20	24	31	37	43	49	55
Aggregate	12	18	27	40	64	97	114

*Cumulative Probability refers to the first row in the table. The numbers below that row are the values of the parameter defined in the table heading.

Table 5-15
PWR Hydrogen Generation (% zirconium oxidized)

Case 3b - RCS at 150 - 500 psia,
Accm. Dump During CM

	Cumulative Probability*						
	1%	5%	25%	50%	75%	95%	99%
Expert A	13	23	56	66	84	106	140
Expert B	10	20	45	65	85	103	110
Expert C	10	14	30	40	60	75	80
Expert D	18	23	34	48	56	61	66
Expert E	20	24	31	37	43	49	55
Aggregate	12	20	34	48	65	97	114

*Cumulative Probability refers to the first row in the table. The numbers below that row are the values of the parameter defined in the table heading.

Table 5-16
PWR Hydrogen Generation (% zirconium oxidized)

Case 4 - RCS at 40 - 200 psia

	Cumulative Probability*						
	1%	5%	25%	50%	75%	95%	99%
Expert A	13	23	56	66	84	106	140
Expert B	10	20	45	65	85	103	110
Expert C	10	13	25	35	50	78	85
Expert D	13	17	20	24	28	31	35
Expert E	11	13	21	26	29	37	39
Aggregate	11	15	24	33	63	97	114

*Cumulative Probability refers to the first row in the table. The numbers below that row are the values of the parameter defined in the table heading.
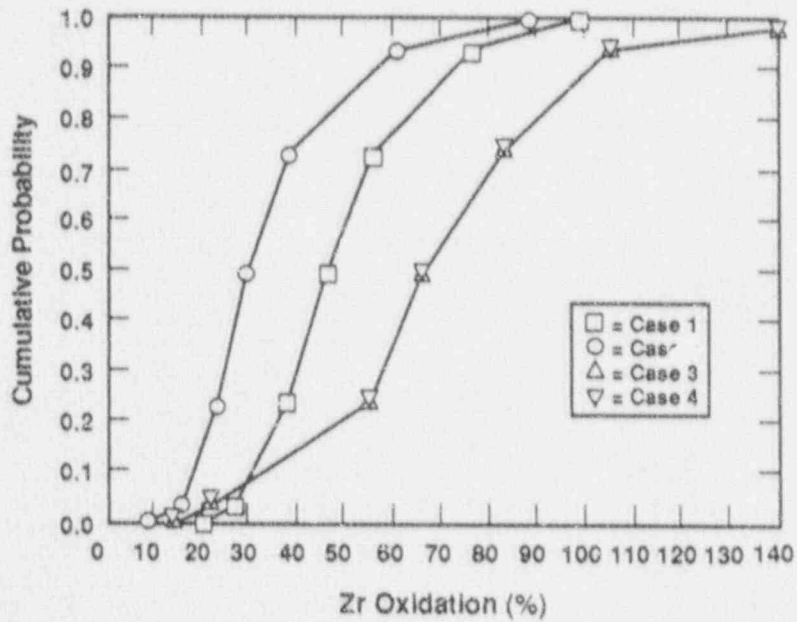
Figure 5-1.   Expert A: Percentage of Oxidized Zirconium.
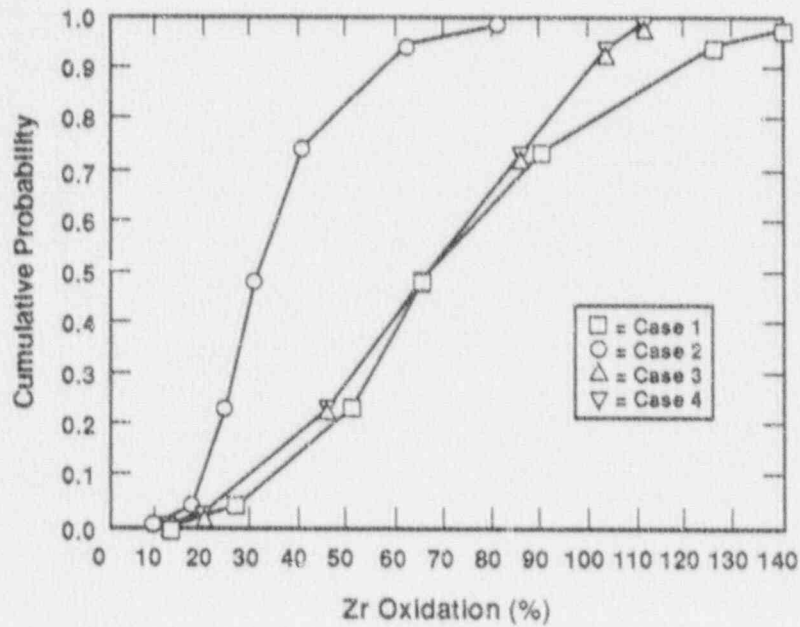
Figure 5-2.   Expert B: Percentage of Oxidized Zirconium.
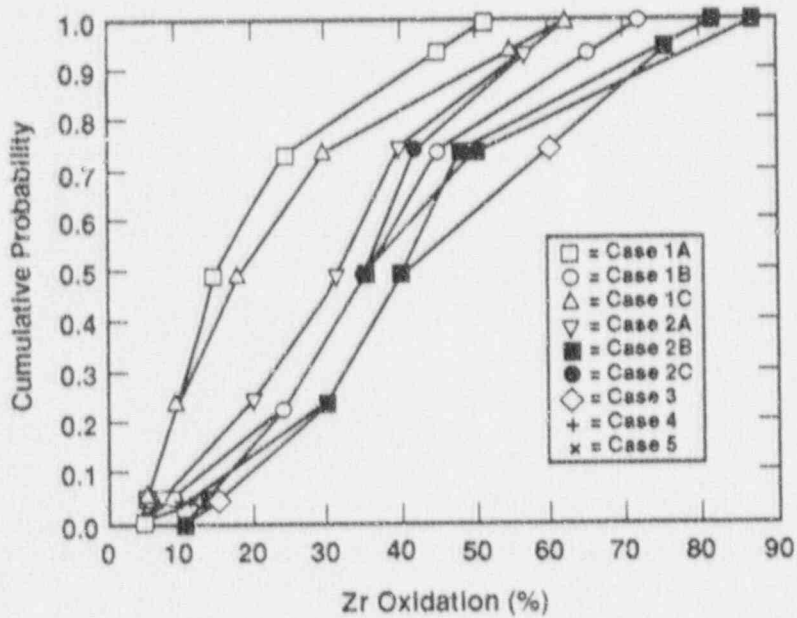
Figure 5-3.   Expert C: Percentage of Oxidized Zirconium.
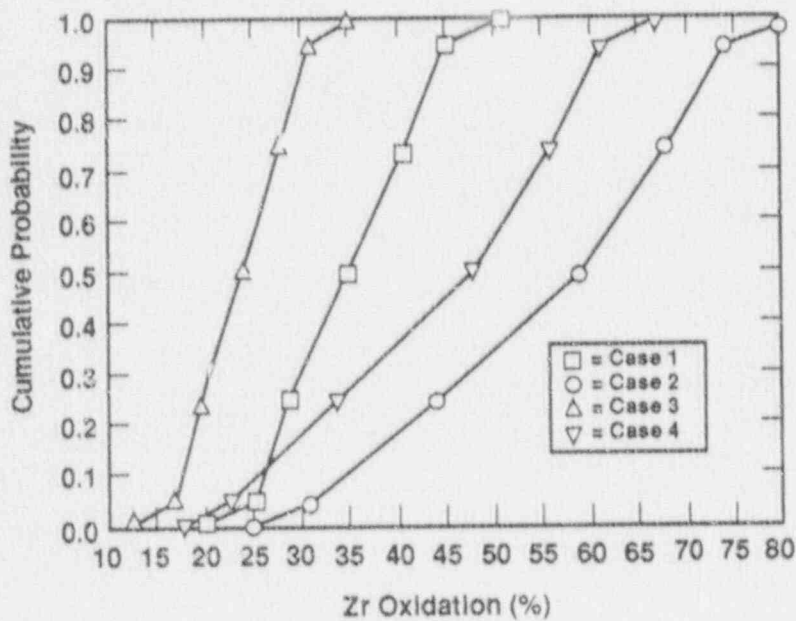
Figure 5-4.   Expert D: Percentage of Oxidized Zirconium.
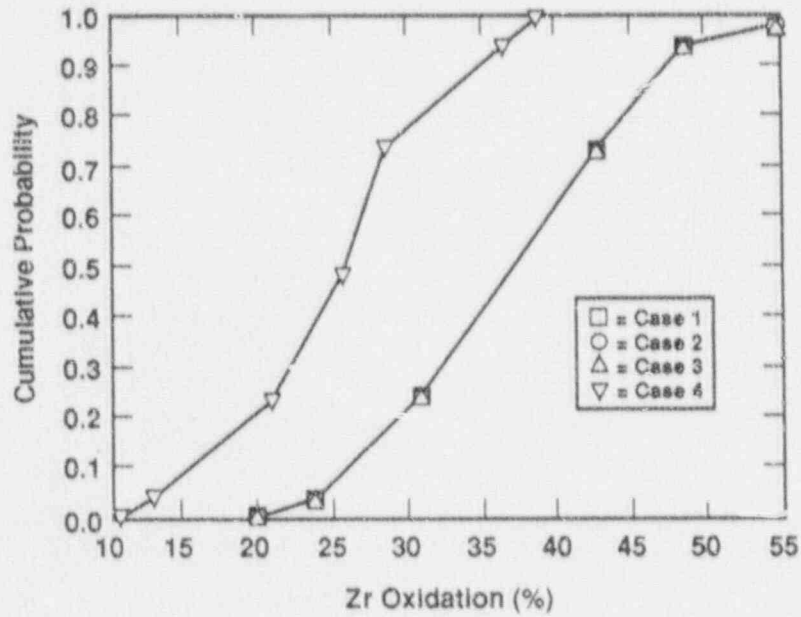
Figure 5-5. Expert E: Amount of Hydrogen Generated
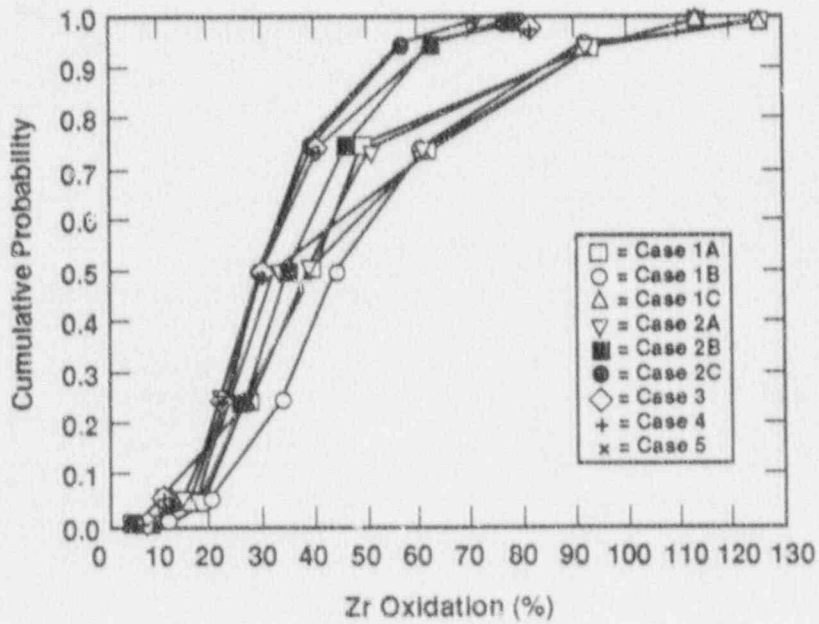
Figure 5-6. Aggregate of Oxidized Zirconium.
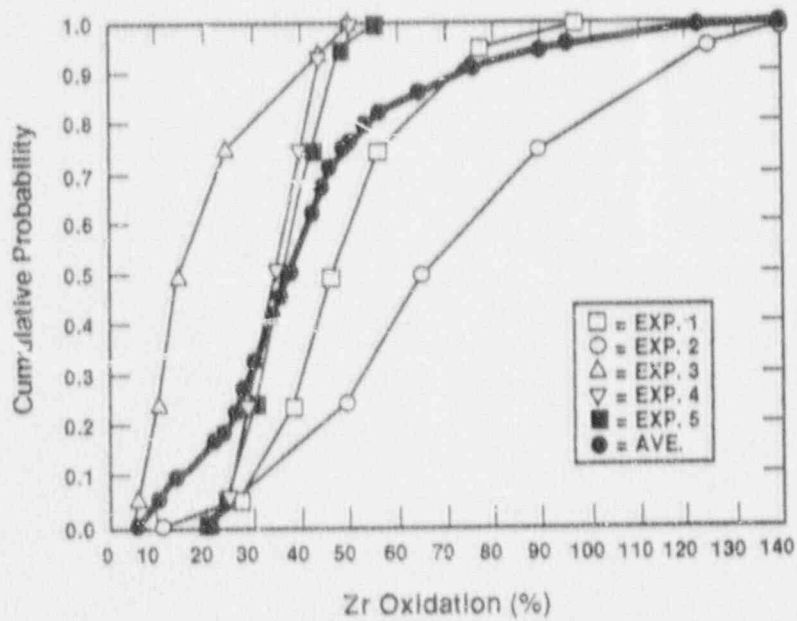
Figure 5-7.   Case 1a: RCS Percentage of Zirconium Oxidized When at 2500
psia.
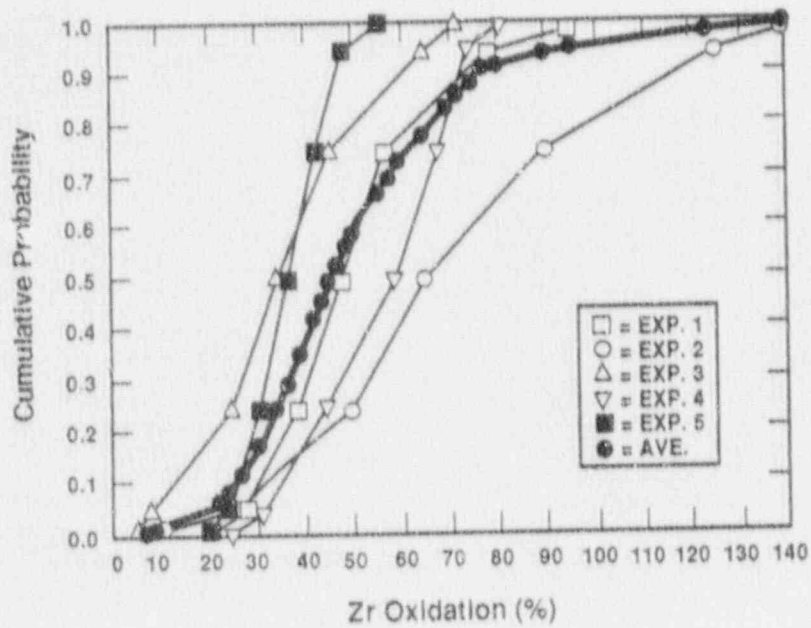
Figure 5-8.   Case 1b: RCS Percentage of Zirconium Oxidized When at 2500
psia.
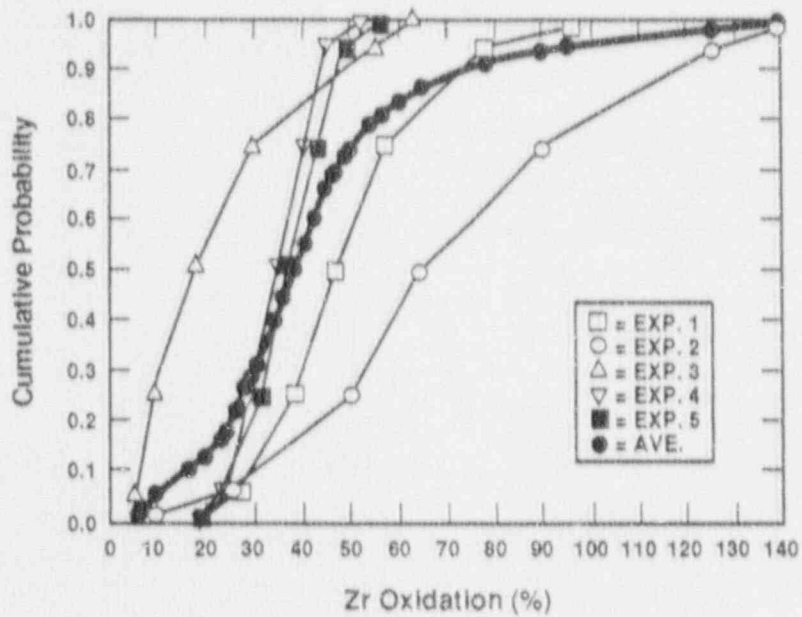
Figure 5-9.   Case 1c: RCS Percentage of Zirconium Oxidized When at 2500 psia.
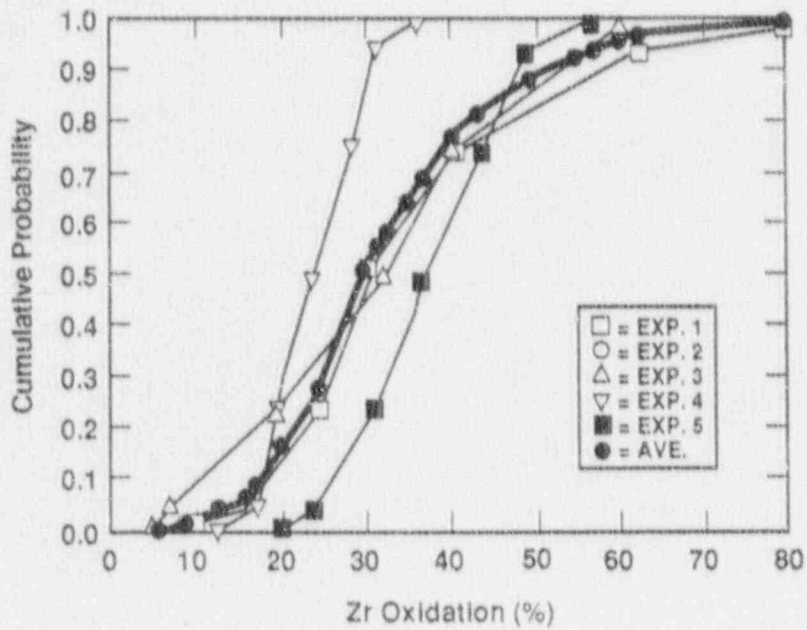
Figure 5-10.   Case 2a: RCS Percentage of Zirconium Oxidized When at 1000 to 1500 psia.
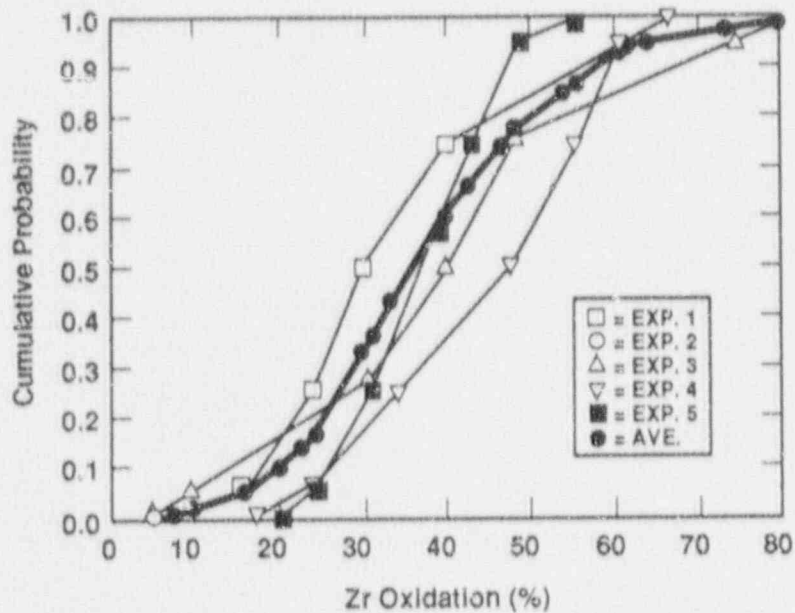
Figure 5-11. Case 2b: RCS Percentage of Zirconium Oxidized When at 1000 to 1500 psia.
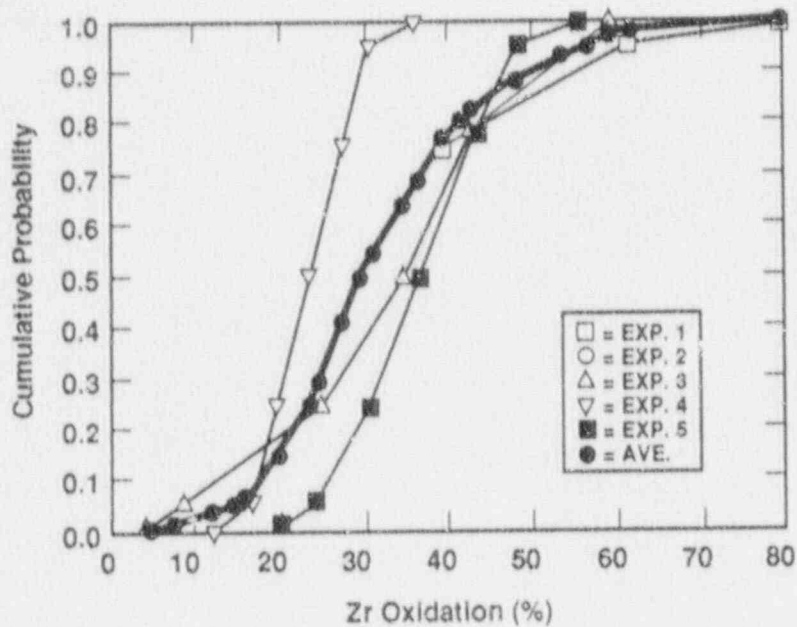
Figure 5-12. Case 2c: RCS Percentage of Zirconium Oxidized When at 1000 to 1500 psia.
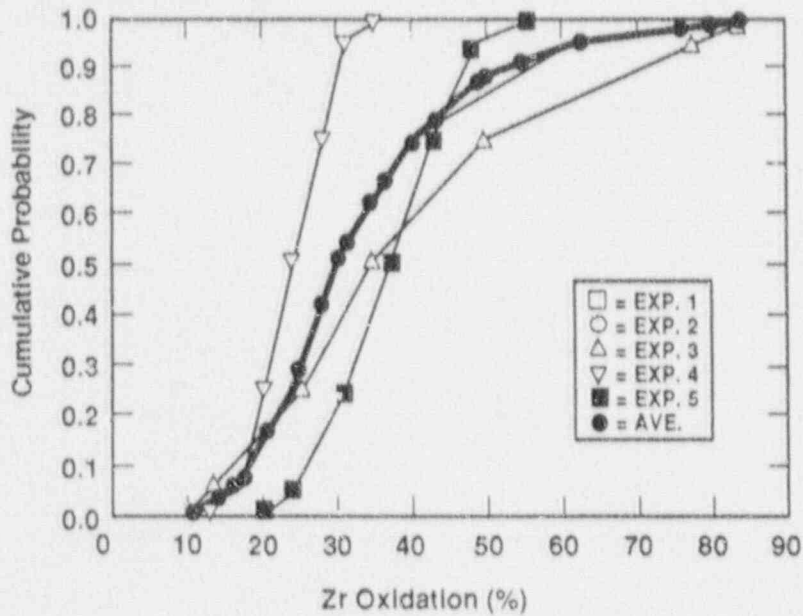
Figure 5-13. Case 3a: RCS Percentage of Zirconium Oxidized When at 150 to 500 psia.
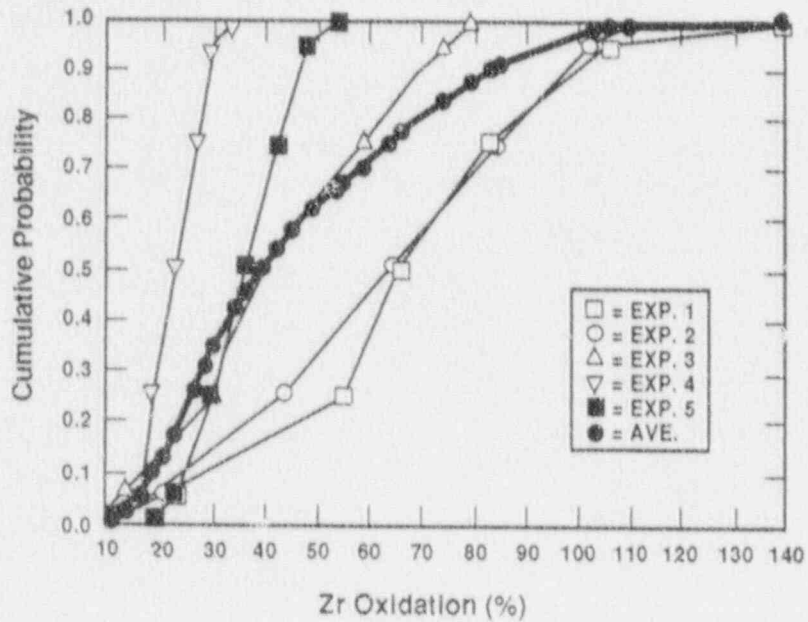
Figure 5-14. Case 3b: RCS Percentage of Zirconium Oxidized When at 150 to 500 psia.
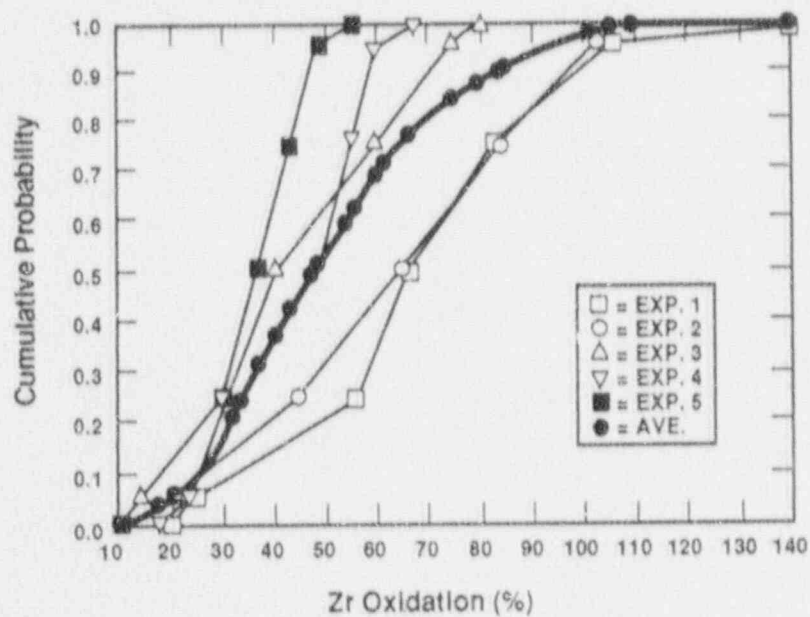
Figure 5-15. Case 4: RCS Percentage of Zirconium Oxidized When at 40 to 200 psia.
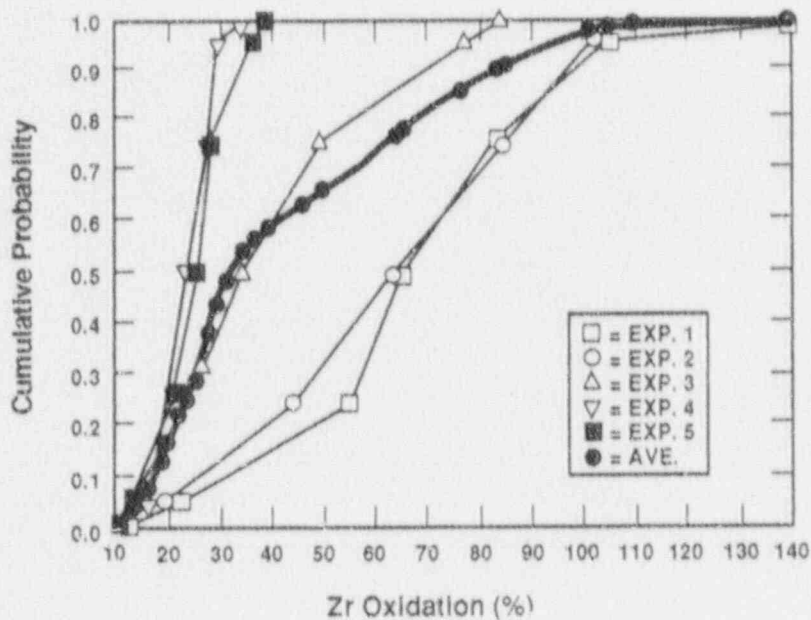
Figure 5-16. Case 5: RCS Percentage of Zirconium Oxidized When at 1000 to 1500 psia.

REFERENCES

5-1   J. E. Kelly et al., "MELPROG - PWR/MOD1 Analysis of a TMLB' Accident Consequence," NUREG/CR-4742, January 1987.

5-2   C. M. Allison et al., "SCDAP/RELAP5/MOD2 Code Manual," NUREG/CR-5273, EGG-2555, September 1989.

5-3   V. E. Denny, A. Mertol, and B. R. Sehgal, "CORMLT Modeling of Severe Fuel Damage in Postulated Accidents," Proceedings of National Heat Transfer Conference, Pittsburgh, PA, August 9 to 12, 1987.

5-4   J. A. Gieseke et al., "Radionuclide Release Under Specific LWR Accident Conditions," Vols. I - V, BMI-2104, Battelle Columbus Division, 1984.

5-5   Industry Degraded Core Rulemaking Program "Modular Accident Analysis Program (MAAP) User's Manual," IDCOR Technical Report on Subtasks 16.2 and 16.3, Fauske & Associates, Inc., for the Atomic Industrial Forum, Bethesda, MD, 1987.

5-6   B. E. Boyack, H. Stumpt, J. F. Lime, "TRAC User's Guide," NUREG/CR-4442, Los Alamos National Laboratory, Los Alamos, NM, November 1985.

Individual Elicitations for In-Vessel Issue 5

Expert A's Elicitation

Issue 5: PWR Hydrogen Generation

Description of Expert A's Rationale/Methodology

Expert A based his conclusions primarily on the large number of code calculations that have been made. He developed a decomposition, which took effective relocation temperature, post-relocation behavior, and the extent of stainless steel oxidation into account. However, he did not develop his hydrogen production distributions directly from this decomposition. Instead he determined which code calculations were appropriate for each endpoint on the tree which displayed his decomposition, and used this information to estimate the effects of varying the important phenomena on hydrogen production.

Expert A concluded that MELPROG,[A-1] SCDAP,[A-2] and CORMLT,[A-3] gave the most reasonable and realistic results. He considered the MARCH results[A-4] to be unrealistically high even though they did not include any hydrogen generation from stainless steel oxidation. He concluded that the MAAP results[A-5] were unrealistically low since MAAP assumed that blockage formation would prevent further oxidation above the blockage. It was Expert A's opinion that it was very unlikely that the blockage would be so complete.

When Expert A combined a high relocation temperature, conservative assumptions about post-relocation behavior, and extensive oxidation of stainless steel in the upper head, he obtained that hydrogen production equal to or exceeding 100% zirconium oxidation. Without stainless steel oxidation, these conservative assumptions give about 60% oxidation, which is typical of MARCH results. Making the most non-conservative assumptions, low relocation temperature, fast meltdown, and the MAAP assumptions on blockage formation and effectiveness, gives approximately 15% zirconium oxidation.

Although Expert A used the results of all the codes, the results of the more mechanistic codes, MELPROG, SCDAP, and CORMLT, were weighted more heavily and were used to determine the mid-range of Expert A's distributions. When results from these three codes were not available, Expert A made his distributions wider than they would have been if results from these codes had been available.

Results of Expert A's Elicitation

Expert A provided plots giving the probability density as a function of the equivalent fraction of zirconium oxidized for Cases 1, 2, and 3 (see Figures A-1, A-2, A-3). The results for Case 3 have been used for Case 4.

For Case 1, RCS at about 2500 psia, there are results available from all the codes. Considering these results, and the assumptions and constituent models in each code, Expert A drew a distribution from which the points for Case 1 were obtained. The mode is a little below 50% zirconium oxidation equivalent.
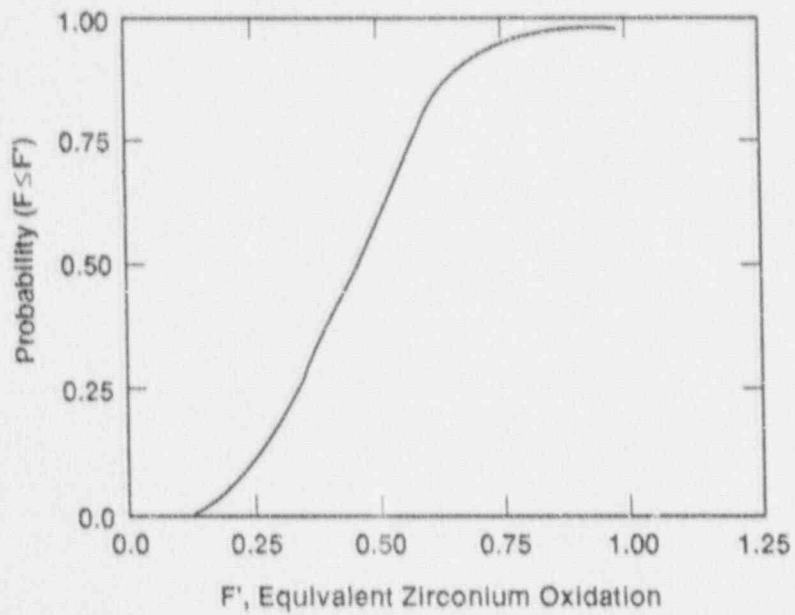
Figure A-1. Case 1.
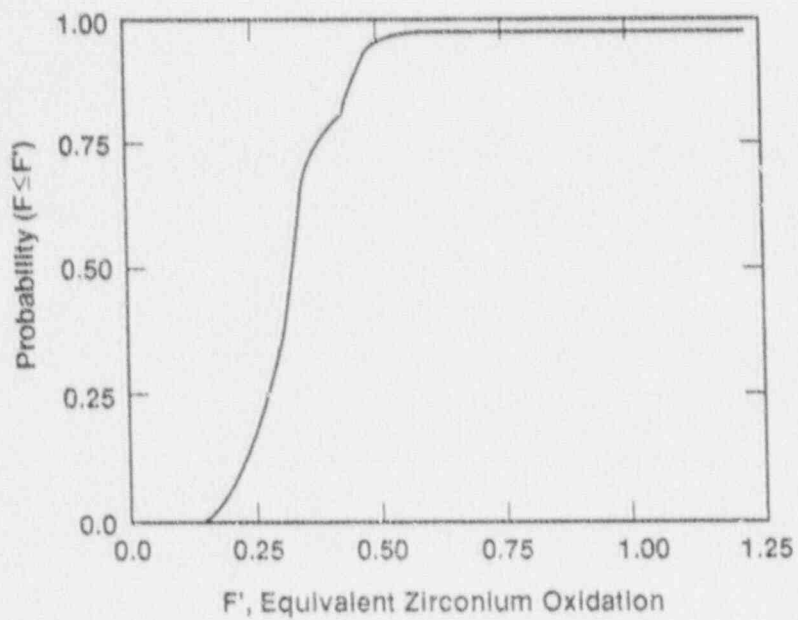
Figure A-2. Case 2.
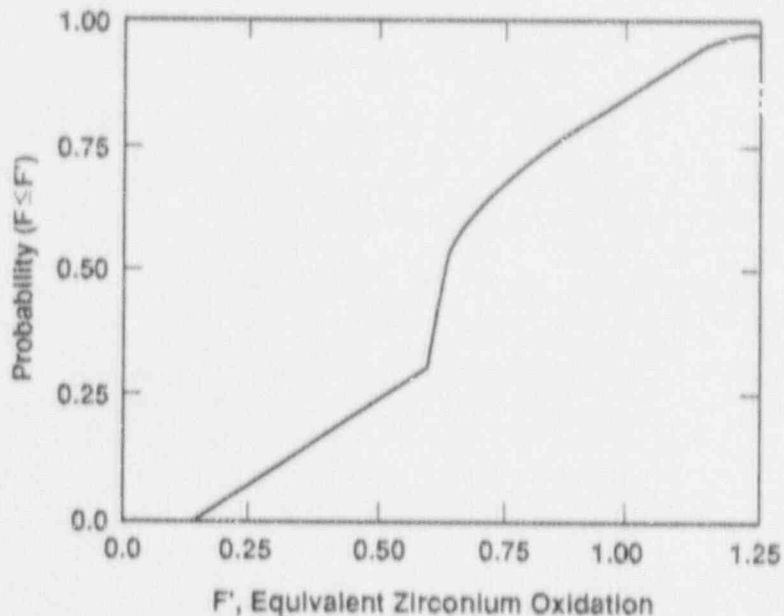
Figure A-3.   Case 3.

For Case 2, there is the question of whether the loop seal will clear in the loop with the break. Expert A's distribution for this case was a composite one. He took a fairly narrow distribution with the mode at 25% zirconium oxidation and combined it with the broader distribution for Case 1. The narrow distribution was given a relative weight of 75% and the Case 1 distribution a weight of 25%. The narrow distribution represents Expert A's distribution for the case where the loop seal clears, and the broad distribution represents his opinion for the case where the seal does not clear. While the typical case given to the expert panel for Case 2 was a pump seal break, there are other accidents to which this case applies that have the breaks in the hot leg and for which the seals will not clear. Expert A derived his Case 2 distribution in this manner to account for the uncertainty in the clearing of the loop seal for a pump seal break. In addition, it may be seen as a way of taking into account the accidents in this case that are due to hot leg breaks.

For Case 3, intermediate pressure (150 to 500 psia) in the RCS due to an S_2 break, Expert A found that there were considerably fewer calculations with MELPROG, SCDAP, and CORMLT than for the other cases. Using what results were available from these codes and utilizing what MARCH and MAAP results were available, he drew a distribution with a midpoint at about 65% zirconium oxidation. Since there would be steady steam flow through the core in this case, the amount of hydrogen produced is higher than for Case 1.

As Expert A did not give a distribution for Case 4, his distribution for Case 3 is being used for Case 4. Expert A has been asked to approve of this usage or provide a separate distribution for Case 4.

Sources of Uncertainty

Expert A felt that the largest source of uncertainty was in the mechanism and timing of clad failure. Experimental work and improved modeling that comes from better understanding will considerably reduce this uncertainty in the next few years. Oxidation kinetics, natural circulation, and blockage formation are relatively well understood, although the extent and effects of the blockage are still the source of considerable uncertainty.

REFERENCES

A-1. J. E. Kelly et al., "MELPROG - PWR/MOD1 Analysis of a TMLB' Accident Consequence," NUREG/CR-4742, January 1987.

A-2. C. M. Allison et al., "SCDAP/RELAP5/MOD2 Code Manual," NUREG/CR-5273, EGG-2555, September 1989.

A-3. V. E. Denny, A. Mertol, and B. R. Sehgal, "CORMLT Modeling of Severe Fuel Damage in Postulated Accidents," _Proceedings of National Heat Transfer Conference_, Pittsburgh, Pennsylvania, August 9 to 12, 1987.

A-4. J. A. Gieseke et al., "Radionuclide Release Under Specific LWR Accident Conditions," Vols. I - V, BMI-2104, Battelle Columbus Division, 1984.

A-5. Industry Degraded Core Rulemaking Program "Modular Accident Analysis Program (MAAP) User's Manual," IDCOR Technical Report on Subtasks 16.2 and 16.3, Fauske & Associates, Inc., for the Atomic Industrial Forum, Bethesda, MD, 1987.

Issue 5:   PWR Hydrogen Production

Description of Expert B's Rationale/Methodology

Expert B based his conclusions for early phase core melt progression primarily on the results of various computer codes MELPROG-TRAC,[B-1,B-2] RELAP-SCDAP,[B-3] and CORMLT[B-4] results   These codes give a general idea of how core degradation and melting progresses. Expert B divided the core melt into four stages:

1. The period up to the start of metallic relocation.   The core geometry is well known during this period, and most of the codes give similar results.   The largest uncertainty in this period is the effectiveness of natural circulation.

2. The period of metallic relocation. This period covers the melting and downward movement of the zircaloy cladding.   If metallic relocation ceases before ceramic relocation starts, then the period between them is included here.   This period is treated in most of the codes, but the details of this process are uncertain, so it is difficult to say whether the code treatments are good approximations.   The largest uncertainty during this period is the formation and effectiveness of a blockage across the lower fuel rods.   This blockage would consist of solidified zirconium containing dissolved UO_2.

3. The period of ceramic relocation.   This period covers the downward relocation of both solid and liquid ceramic material, including UO_2, ZrO_2, and mixtures thereof.   If ceramic relocation ceases before core slump, then the period between them is included here. The events in this period are poorly known, but the hydrogen production during this period is small compared with the two preceding periods, so this fact does not have a large effect.

4. The period of ceramic liquid drainage and solid material slumping. This period begins when a substantial fraction of the molten core relocates into the bottom head and continues until vessel breach. There are some experimental data on the events that may be expected during this period. The treatment in MELPROG is the most advanced one now available.   The largest uncertainty in this period is amount of material moving into the bottom head and its composition and temperature.   More than one drainage or slumping event may occur during this period.

The new CORE module in MELPROG is very good, and MELPROG has the best natural circulation model available.   There currently is no hydrogen blanketing model in MELPROG, but this is of low importance.   Recent Japanese data suggest that the old data were incorrect, and a new hydrogen blanketing model will be put into MELPROG soon. CORMLT has a reasonable hydrogen blanketing model, a good natural circulation model, and the best

available treatment of zircaloy relocation and blockage formation. MARCH[B-5] and MAAP[B-6] assume that the core is comprised of one homogenous material rather than treating the zirconium and the ceramic material (ZrO$_2$ and UO$_2$) separately. As the metal and the ceramic melt and relocate at different temperatures, such a treatment gives misleading results, and thus very little reliance has been placed on the results of these codes. Furthermore, the blockage model in MAAP is clearly incorrect, as shown by the Power Burst Facility (PBF) and MRV results.

Results of Expert B's Elicitation

Expert B provided 1, 10, 50, 90, and 99% probable values for the amount of hydrogen generated for two of the four cases. The amount of hydrogen generated is expressed as a fraction relative to that which would be produced if all the available zirconium in the core were oxidized. Values over 1.00 are possible since some stainless steel may be oxidized in addition to the zirconium. Expert B's views of PWR hydrogen production are given in the following table:

Case	RCS Pressure (psia)	Probability				
		1%	10%	50%	90%	99%
1	2500	0.10	0.40	0.65	1.10	1.40
2	1000-1500	-	-	-	-	-
3	150-500	-	-	-	-	-
4	40-200	0.10	0.30	0.65	0.95	1.10

A discussion of each case follows.

Case 1. This is the "classic" TMLB' case: meltdown at the PORV setpoint pressure with the reactor coolant system (RCS) pressure boundary intact until vessel breach. Expert B obtained his midpoint or best estimate from the SCDAP-RELAP5 results which showed the hydrogen produced was equivalent to a zirconium oxidation fraction of 0.38. To this value he added a fraction of 0.10 for late phase zirconium oxidation which is not modeled in the code, and he added 0.08 for hydrogen produced during quench or the melt-water reaction when the core slumps into the bottom head, which is also not modeled. He thus got a fraction of 0.56 for zirconium alone. He then added about 0.10 for stainless steel oxidation to get his midpoint or best estimate: a zirconium oxidation fraction of 0.65.

This reasoning is summarized in the following table, which is given in terms of zirconium oxidation fraction. The 10 and 90% values are shown in addition to the midpoint values just discussed.

Source of H_2	Probability		
	50%	90%	10%
Early Phase (SCDAP)	0.38	0.50	0.30
Late Phase	0.10	0.20	0.05
Melt-Water	0.08	0.15	0.05
Stainless Steel	0.09	0.25	0.00
Total Hydrogen	0.65	1.10	0.40

Expert B's reasoning for the 10 and 90% probable values is illustrated by the 90% probable case above. Expert B increased the zirconium oxidation fraction in the best estimate case (0.38) to 0.50 since this was an upper bound. He figured that 40% of what was unoxidized in the early phase would be oxidized in the late phase of the melt, and so obtained 0.20 for the late phase amount. And he figured that half of what was unoxodized in these periods would be oxidized in the melt-water reaction, thus getting 0.15 for that value.

Expert B compared his early phase amounts with the code results. MARCH[B-5] gave low, middle, and high zirconium fractions of about 0.43, 0.61, and 0.75. As MARCH tends to overestimate hydrogen production, he expected his values to be lower than MARCH. MAAP[B-6] gives zirconium oxidation fractions between 0.20 and 0.35 with blockage assumed, and between 0.50 and 0.70 with no blockage assumed. Older MELPROG runs with the two-dimensional PINS core module and natural circulation gave 0.55 for a relocation temperature of 2500 K, and 0.41 for a relocation temperature of 2200 K. With the one-dimensional model and no natural circulation, the zirconium oxidation fraction was 0.34. Considering all these models, Expert B thought that his 10, 50, and 90% probable early phase hydrogen amounts were about right.

The 1 and 99% hydrogen amounts were obtained by considering first principles, as there were no code runs which produced results at these extremes.

Case 2. This case has a very small break, either one which initiates the accident or one that develops during an accident initiated by a transient event. Having considered Cases 1 and 4 first, Expert B concluded that Case 2 would fall between them. As the differences in Cases 1 and 4 are slight, Expert B concluded that Case 2 would be very similar to Case 1, and did not provide separate amounts for hydrogen generation. The one exception is the pump seal break in the cold leg. MELPROG[B-1] results have shown that this sequence behaves very differently than if the break is in the hot leg since the loop seals clear. Expert B deferred to the other Expert on the panel who is most familiar with the MELPROG results for this subcase.

Case 3. This case has a small break, either one which initiates the accident or one that develops during an accident initiated by a transient event. Having considered Cases 1 and 4 first, Expert B concluded that Case 3 would fall between them. As the differences in Cases 1 and 4 are slight, Expert B concluded that Case 3 would be very similar to Case 4, and did not provide separate amounts for hydrogen generation. The one exception is the pump seal break in the cold leg. If this break is large enough to be in this class, then the discussion in Case 2 (above) applies.

Case 4. This case has a large initiating break; the RCS is at low pressure at the start of core melt and there is little blowdown or natural circulation during core melt. The uncertainties in this case are larger than they are in Case 1 since there has been much less study of this case, and there are few if any applicable calculations. Expert B obtained his midpoint or best estimate from the RELAP-SCDAP[B-3] results for TMLB' (Case 1). He reduced the early phase amount somewhat since there would be little or no effective natural circulation. He increased the late phase amount since there would be more zirconium left unoxidized after the first phase. As experiments have shown that 30% of the zirconium available is often oxidized in steam explosions that are likely at low pressure, he put the metal-water contribution at 0.15. No hydrogen was added for stainless steel oxidation, as the temperatures are thought to be low enough to preclude this source.

Expert B's reasoning is summarized in the following table, which is given in terms of zirconium oxidation fraction. The 10 and 90% values are shown in addition to the midpoint values just discussed.

Source of H_2	50%	90%	10%
Early Phase (SCDAP)	0.30	0.40	0.20
Late Phase	0.20	0.25	0.05
Melt-Water	0.15	0.20	0.05
Stainless Steel	0.00	0.10	0.00
Total Hydrogen	0.65	0.95	0.30

Sources of Uncertainty

Expert B concluded that there were many uncertainties in the entire core melt progression process. The largest uncertainties have been mentioned above for each phase of the melt progression. Other uncertainties are the fraction of the rods around the outside of the core which are not degraded, the strength and duration of natural circulation, the time and extent that core blockage forms (if it does) and the completeness of this blockage, and the effects of hydrogen blanketing. The effects of accumulator (and UHI) discharge are another large source of uncertainty. On one hand the water injection could produce more steam and increase zirconium oxidation markedly if the process were steam-starved before the accumulator discharge. On the other hand, the water could quench the core and shut off

5.5-33

zirconium oxidation altogether. The amount of stainless steel oxidation in the upper plenum is poorly known, and the effects of the Inconel grid spacers are not well understood.

REFERENCES

B-1   J. E. Kelly et al., "MELPROG - PWR/MOD1 Analysis of a TMLB' Accident
       Consequence," NUREG/CR-4742, January 1987.

B-2   B. E. Boyack, H. Stumpt, J. F. Lime, "TRAC User's Guide," NUREG/CR-
       4442, Los Alamos National Laboratory, Los Alamos, NM, November 1985.

B-3   C. M. Allison et al., "SCDAP/RELAP5/MOD2 Code Manual," NUREG/CR-5273,
       EGG-2555, September 1989.

B-4   V. E. Denny, A. Mertol, and B. R. Sehgal, "CORMLT Modeling of Severe
       Fuel Damage in Postulated Accidents," Proceedings of National Heat
       Transfer Conference, Pittsburgh, PA, August 9 to 12, 1987.

B-5   J. A. Gieseke et al., "Radionuclide Release Under Specific LWR
       Accident Conditions," Vols. I - V, BMI-2104, Battelle Columbus
       Division, 1984.

B-6   Industry Degraded Core Rulemaking Program, "Modular Accident Analysis
       Program (MAAP) User's Manual," IDCOR Technical Report on Subtasks
       16.2 and 16.3, Fauske & Associates, Inc., for the Atomic Industrial
       Forum, Bethesda, MD, 1987.

Issue 5: PWR Hydrogen Generation

Description of Expert C's Rationale/Methodology

Expert C based his conclusions on the test results, the analysis of TMI-2, and on the results of various computer codes. The test results include the PBF,[C-1] CORA,* and ACRR DFR[C-2] experiments. The code results used were mostly from MELPROG[C-3] and RELAP5/SCDAP[C-4] runs. He saw the most important phenomenon as the formation of a eutectic between the oxides of zirconium and uranium.

Expert C divided the degradation and melting of the core into six stages:

1. From core heatup to the start of geometry changes (ballooning);

2. From the start of fuel ballooning to the start of autocatalytic oxidation;

3. From the start of autocatalytic oxidation to the start of zircaloy relocation;

4. From the start of zircaloy relocation to rod collapse;

5. From rod collapse to support structure failure; and

6. The period of debris--water interaction in the lower plenum.

Expert C discussed each of these phases in some detail, including how each phase progressed for the four cases listed above. For Case 4, Expert C made a distinction between the cases where the break was the initiating event and those cases where the break occurred sometime after the start of the accident due to local overheating. The reason for this distinction is that in the second case a large amount of steam could be made available for zirconium oxidation during the core melt due to the flashing as the system depressurizes. If the break was the initiating event, very little steaming would be expected during core heatup and melting.

Phase 1: from core heatup to the start of geometry changes (ballooning). During this phase of the accident the generation rate of hydrogen is well defined by most codes. The uncovered fuel nodes commence heating up and significant zirconium oxidation commences when the temperature reaches 1500 K. As the temperature increases toward 1700 K, autocatalytic oxidation commences. The reaction kinetics of the oxidation reaction, as well as the rate limitations due to steam starvation, are well understood, and little uncertainty exists in calculating the hydrogen generation rate during this phase of the accident. The four cases behave much alike; the differences are in the rate of heatup.

---

*J. E. Kelly, Trip Report on the CORA Workshop Meeting, October 23, 1987.

Phase 2: from the start of fuel ballooning to the start of autocatalytic oxidation. The changes in core geometry that accompany fuel ballooning and bowing add uncertainty in that significant steam flow diversion may occur, resulting in localized steam-starved conditions. Moreover, in the open core lattice of PWRs, natural convection may be reduced, thus increasing core temperatures which in turn would affect the hydrogen generation rates.

The differences between cases during this phase are more pronounced than during the first stage. This is because the oxidation rates during this phase are substantially higher. In addition, for Case 1 and possibly Case 2, no rod ballooning would be expected because of the high pressure in the system. Natural circulation and PORV actuation are important in determining the rate and the extent of clad oxidation. For Cases 2 and 3, the continuous blowdown through the break reduces or eliminates natural convection and provides an abundant supply of steam for zirconium oxidation. Therefore, Expert C concluded that there would be less hydrogen production in this phase of the accident in Case 1 than in Cases 2 and 3. A possible exception to this conclusion may occur if depressurization of the system in Case 2 triggers the discharge of the "   m onto the heated core. This may have two possible outcomes.   that the discharge is sufficient to quench the core and te.m   .e _.e .idation. The second, probably more likely, is that the discharge of UHI results in quenching some of the fuel, but that the steam generated in doing so increases the pressure in the RCS which shuts off the UHI discharge. Several UHI discharges could occur, quenching the upper portions of the core. Overall, if the UHI system injects during this phase of oxidation, Expert C believed the effect would be to increase the total oxidation. This is because clad oxidation in the core would continue for a longer period of time.

For Case 3, the UHI and the accumulators would discharge well before their discharge could have any effect on oxidation rates. If an initiating large break (Case 4a) occurs, Expert C expects little oxidation during this phase unless the water level in the vessel is recovered. This is because very little or no steaming would be expected with the pressures so low, and the oxidation process requires steam. In Case 4b, where the accident turns into a low-pressure case during the core melt, the accident progression would depend upon the time of the break. If the break occurs early, Case 4b will be much like Case 4a. If the break occurs later, e.g., the hot leg fails due to thermal stresses during the period of rapid oxidation, the ensuing depressurization would result in vigorous flashing of water into steam and fueling of the steam-starved oxidation areas, thus increasing the metal-water reaction. Since it appeared that the thermally-induced hot leg (or surge line break) would occur fairly early in the accident progression, Expert C did not subdivide Case 4 when providing his results in numerical form.

Phase 3: from the start of autocatalytic oxidation to the start of zircaloy relocation. This phase of the accident is characterized by the very rapid oxidation of zirconium accompanied by the liberation of large amounts of energy which serves to further heat up the cladding and fuel. The uncertainty in hydrogen generation rates during this stage is greater than in the previous phase since the temperature of the cladding increases to

the range in which eutectics can begin to form. Two factors affect the uncertainty: (1) as the temperature increases, the applicability of the oxidation rate equations become less certain; and (2) the uncertainty in the temperature at which the fuel rod geometry changes take place impacts the oxidation rate of zirconium. Before the start of zircaloy relocation, the lower melting point materials comprising the control rods will most likely begin to melt and relocate downward. This relocation and quenching upon contact with water will result in the generation of substantial steam which may refuel steam-starved regions of the core and reinitiate vigorous oxidation. For PWRs, the silver-indium-cadmium control rods begin melting just as vigorous autocatalytic oxidation and localized steam starvation take place, i.e., about 1700 K. The melting silver and indium relocate downward and are likely to contact water in all cases except Case 4. The formation of eutectics at temperatures as low as 1500 K to 1750 K has been observed. The formation of these eutectics can result in early geometry changes which can lead to steam flow redistributions and can influence the oxidation rate early on.

The differences between the cases discussed in the previous phase apply to this phase as well, and the differences are likely o be more pronounced. During this phase, however, addition of steam to tr   tem by either UHI injection (in Case 2) or sudden system depressurizat   in Case 4b) could only increase the oxidation by supplying steam to those areas which had previously been steam starved. During this phase an important source of uncertainty is the early relocation of control rod materials.

Phase 4: from the start of zircaloy relocation to rod collapse. Hydrogen production during this phase of the accident is heavily dependent on the temperature at which the zircaloy relocates. The relocation removes the zirconium from the high temperature zone down to a low temperature zone, which reduces the oxidation in the high temperature region. Little if any zirconium oxidation occurs in the low temperature region. Obviously, if the zircaloy relocation occurs at a low temperature, low oxidation will result.

The downward moving zircaloy relocation may form a core blockage which would prevent the flow of steam to the unoxidized zirconium located above the blockage. The formation of this blockage would depend on the location of the water level. For Case 1, the blockage could be very extensive as in TMI-2 because the water level would be above the bottom of active fuel. The relocating $Zr-UO_2$ would solidify just above or at the water level. For Case 2, a similar situation could occur if the UHI system discharged prior to the zircaloy relocation; the water level in the vessel would be above the bottom of active fuel. For Cases 3 and 4a, the core blockage would probably not form, or if it did, it would form on the support structure.

For Case 4b, core blockage would not occur because the induced RCPB rupture would probably occur prior to the zircaloy relocation. The depressurization would drop the water level to about the core support plate or below, and therefore the relocating zircaloy would solidify on the core support plate or flow into the lower head. Of course if the depressurization were to occur during zircaloy relocation, the large pressure differential would probably blow through any blockage that had formed. Molten material might

be entrained in the rapidly flowing steam and hydrogen. The opening of flow paths as well as entrainment in the exit flow could contribute significantly to the overall hydrogen generation. Moreover, if melted material is indeed entrained in the gas flow, there exists a possibility of very rapid oxidation of the entrained material and the generation of large pressure spikes inside the reactor vessel.

Recent experimental evidence indicates that a nickel-zirconium eutectic may form where the Inconel grid spacers contact the fuel cladding. This eutectic ignites at a temperature below the autocatalytic temperature of the cladding. The autocatalytic oxidation of the grid spacers would generate sufficient energy to locally heat up the cladding which ignites in turn, initiating a burn front propagating downward which results in cladding relocation. This relocation removes the cladding from the hot areas and serves to further block the core, depriving the upper regions of the core of steam.

Phase 5: from rod collapse to support structure failure. Following the relocation of the zircaloy, the fuel pellets can conceivably remain standing in essentially their original locations. Eventually, these stacks begin to collapse and accumulate on the frozen relocated zircaloy and liquified fuel. In this manner, a rubble bed is formed which, if uncovered, as would be the case in all of the cases considered here, would begin to heat up and melt. At the time of this relocation, the water level in the vessel would probably be just below the core support plate and therefore little steaming would take place. This is true for all of the cases considered. During this phase, because of the low steaming rate, only a small additional amount of hydrogen would be generated.

Phase 6: the period of debris--water interaction in the lower plenum. During this phase, the relocating materials would interact with the lower plenum water resulting in the generation of large amounts of steam. Moreover, depending on the debris configuration and available zirconium, additional hydrogen would be evolved during this phase. Large surface areas of zirconium would have to be available for interaction with water in order to generate large amounts of hydrogen. But large surface areas imply small particles, which imply rapid quenching and thus cooling. Therefore from this standpoint, large amounts of hydrogen are not expected to be produced. However, the steam generated by the relocating material could fuel the steam-starved regions of the core still remaining in the core region; thus generating additional large amounts of hydrogen. Therefore the uncertainty in the relocation timing, (which indicates the amount of core still in the core region when the first relocation into the lower plenum occurs) is important.

The phenomenology of hydrogen production by the oxidation of the zirconium cladding is a complex interaction of many physical processes. During the course of an accident several of the phases described above may occur simultaneously so that separation of one phase from another is virtually impossible.

Results of Expert C's Elicitation

Expert C provided 1, 25, 50, 75, and 99% probable values for the amount of hydrogen generated for the four cases. He broke up Cases 1 and 2 into three subcases depending on the timing of the accumulator and UHI discharge. He also added a Case 5, which is similar to Case 2 except that the loop seals clear since the break is in the cold leg rather than the hot leg.

The amount of hydrogen generated is expressed as a fraction relative to that which would be produced if all the available zirconium in the core were oxidized. Values over 1.00 are possible since some stainless steel may be oxidized in addition to the zirconium, but Expert C had no values which exceeded 1.00. The times of accumulator and UHI discharge are abbreviated as follows: bCM for before core melt, dCM for during core melt, and aVB for at vessel breach.

Expert C's conclusions about PWR hydrogen production are given in the following table:

Case	RCS Pressure (psia)	Accm. Dis-charged	Probability				
			1%	25%	50%	75%	99%
1a	2500	bCM	0.05	0.10	0.15	0.25	0.50
1b	2500	dCM	0.05	0.25	0.35	0.45	0.70
1c	2500	aVB	0.05	0.10	0.175	0.30	0.60
2a	1000-1500	bCM	0.05	0.20	0.325	0.40	0.60
2b	1000-1500	dCM	0.05	0.30	0.405	0.475	0.80
2c	1000-1500	aVB	0.05	0.25	0.35	0.425	0.60
3	150-500		0.10	0.30	0.40	0.60	0.80
4	40-200		0.10	0.25	0.35	0.50	0.85
5	1000-1500		0.10	0.25	0.35	0.50	0.85

A discussion of each case follows:

Case 1a. This case applies if the RCS has been depressurized by operation of the auxiliary feedwater system before the onset of core melt. The accumulators discharge during this time. The RCS repressurizes before core melt starts since the only means of water loss is through the PORVs. As Expert C envisaged the accident progression, the water level drops gradually and stays below the melt front. A blockage forms which covers most of the core area above the water level. This blockage forces the escaping steam to flow around the melting core and minimizes H_2 production. The blockage, being cooled by the passing steam, would eventually be breached by the hot oxides it contains. The oxides would pour into the lower head as a jet.

Case 1b. In this case, meltdown at the PORV setpoint pressure proceeds until a break occurs in the RCS pressure boundary during core melt and

before vessel breach. The accumulators discharge during core melt. Expert C believes the accumulator discharge will generate a large amount of steam that will oxidize zirconium that otherwise would go unoxidized due to steam starvation. The quenching of the core caused by the accumulator discharge is only temporary and does not significantly alter the blockage formation described for Case 1a.

Case 1c. This is a meltdown at the PORV setpoint pressure with the RCS pressure boundary intact until vessel breach (TMLB'). The accumulators discharge at vessel breach. Expert C sees the core melt process proceeding much as it does in Case 1a. The discharge of the accumulators at vessel breach will quench the solid material left in the vessel after depressurization is complete.

Case 2a. This case has a very small break that initiated the accident. The accumulators have discharged before the onset of core melt. This occurred when the operators depressurized the RCS to a pressure below that which would occur due to the break alone. Expert C concluded that this case would proceed similarly to Case 1a. The hydrogen production probably will be a little higher than Case 1a because of the continuous steam flow through the core due to the existence of the break. The blockage formation will take place at the water level and move downward with it.

Case 2b. This case has a very small initiating break. A further failure of the pressure boundary during the core melt process causes the accumulators to discharge at that time. Expert C concluded that this case would proceed similarly to Case 1b, except that the hydrogen production probably will be a little higher because of the steady steam flow through the core caused by the break. The blockage will form at the water level elevation and move downward with it. The discharge of the accumulators will aid in forming and stabilizing the blockage. Once the water level reaches the support plates, the progression of events is the same as described for Cases 1a, 1b, and 1c.

Case 2c. This case has a very small break, either one which initiates the accident or one that develops during an accident initiated by a transient event. The pressure remains above the accumulator setpoint until vessel breach, and the accumulators discharge at vessel breach. Expert C concluded that this case would proceed similarly to Case 1c. The hydrogen production probably will be a little higher than Case 1c due to the continuous steaming.

Case 3. This case has a small break, either one which initiates the accident or one that develops during an accident initiated by a transient event. The break causes the pressure in the RCS to fall so low that the accumulators discharge before core melt starts. Expert C saw the core melt in this case proceeding in quite a different manner from the two cases described previously. Here the water level drops to below the core support plate fairly quickly. Consequently, the extensive blockage found in Cases 1 and 2 would not occur. Any core blockage that did develop would be localized. However, because the water level is below the core plate, little steaming would take place until some of the core starts dropping

into the water and quenching. This would start the oxidation of the zirconium, resulting in substantial H_2 production. The failure of the reactor head will be by thermal attack by the surrounding particle bed. The water in the lower head would have been evaporated by the lower temperature eutectic debris falling into the lower head. The higher temperature debris would fall on the partially quenched metallics and a mixture of oxides and metallic debris would be ejected from the vessel upon failure.

Case 4. This case has a large initiating break; the RCS is at low pressure at the start of core melt and there is little blowdown or natural circulation during core melt. The accumulators discharge before core melt commences. The behavior of the core and melt progression will proceed essentially the same way as for Case 3. The major difference from Case 3 is that the water level in the core is below the core plate when core melt begins. This limits the oxidation of zirconium during the early core heatup phase. Thus the H_2 production for this case will be a little less than for Case 3.

Case 5. This case is similar to Case 2c except that the break is in the cold leg so that the loop seals clear. The clearing of the loop seals results in establishing circulation through the steam generators, which limits the heating of the core. Expert C expects that the core temperatures will remain well below the temperatures at which significant zirconium oxidation occurs. The core would eventually melt but the amount of oxidation before the core slumps into the lower head would be very small. After core debris drops into the lower head, the steam generated by the quenching process would start the metal-water reaction and substantial zirconium oxidation would take place. The H_2 production and lower head failure would be very similar to Case 4.

Sources of Uncertainty

Expert C observed that there were many uncertainties in the entire core meltdown process. The largest uncertainty in hydrogen production occurs in the phase in which the zirconium relocates downward. The temperature at which the downward relocation of the zircaloy cladding begins is known only within wide limits. Whether this material freezes near the water level and forms a blockage in the center of the core is also uncertain. If an extensive blockage forms, it is likely to prevent steam from reaching the unoxidized zirconium directly above it. Experimental evidence indicates that blockage is not as crucial in PWRs as in BWRs. Since the PWR core has an open lattice geometry, the blockage would have to extend almost to the shroud in order to significantly affect the availability of steam to the bulk of the core.

REFERENCES

C-1   A. Cronenberg, R. Miller, and D. Osetek, "An Assessment of Hydrogen Generation for the PBF Severe Fuel Damage Scoping and 1-1 Tests," NUREG/CR-4866, EGG-2499, Idaho National Engineering Laboratory (EG&G Idaho, Inc.), Idaho Falls, ID, April 1987.

C-2   K. O. Reil et al., "Results of the ACRR DFR Experiments," Proceedings of the International ANS/ENS Topical Meeting on Thermal Reactor Safety, San Diego, CA, February 2-6, 1986.

C-3   J. E. Kelly et al., "MELPROG - PWR/MOD1 Analysis of a TMLB' Accident Consequence," NUREG/CR-4742, Sandia National Laboratories, Albuquerque, NM, January 1987.

C-4   P. D. Bayless, "Natural Circulation during a Severe Accident: Surry Station Blackout," EGG-SSRE-7858, Idaho National Engineering Laboratory, (EG&G Idaho, Inc.) Idaho Falls, ID, September 1987.

Expert D's Elicitation

Issue 5: PWR Hydrogen Generation

Description of Expert D's Rationale/Methodology

Expert D based his conclusions primarily on a number of MAAP runs that were
made for Ringhals 3[D-1] and Zion.[D-2] Some of the Ringhals results are
contained in a document prepared for Issues 1 and 2.[D-3] Ringhals 3 is a
three-loop plant with a NSSS similar to Surry's, and Zion is a four-loop
plant with a NSSS similar to that of Sequoyah. At Ringhals 3 and at
Surry, 100% zirconium oxidation corresponds to approximately 750 kg of
hydrogen, and 100% zirconium oxide' ', at Zion and at Sequoyah corresponds
to approximately 1000 kg of hydr.

The following table summarizes the MAAP runs for Ringhals 3:

Cumulative Hydrogen Production (kg) in MAAP for Ringhals 3

Case	Up to Relocation	Up to Vessel Failure	Total
TMLB'	100	140	170
TMLB' with EFW for 4 h	80	150	150
TMLB' with three PORVs open	180	195	
TMLB' with one PORV open	230	230	
TMLB' with EFW for 4 h & one PORV open	250	250	
TMLB' with "Hi" Relocation Temperature	90	220	

The interpretation of the three columns is as follows: for the base case
(first row) of the 170 kg of hydrogen produced during the entire accident,
100 kg had been produced by the time the core relocated and 140 kg had been
produced by the time the vessel failed. Only the first two cases were run
past the time of vessel failure.

The following table summarizes the MAAP runs for Zion:

Total Hydrogen Production (kg) in MAAP for Zion

Case	Total
TMLB'	210
TMLB' with loop seals cleared	140
TMLB' with two PORVs open	240

Opening the PORVs increases the hydrogen production significantly.

The MAAP models include the injection of accumulator water when the RCS depressurizes to the accumulator setpoint. However, if the accumulator water is injected after core relocation is underway, the models allow no cooling of the core debris. Nor do they include the production of hydrogen in the upper plenum by steam reacting with stainless steel. As some of the calculations have shown very high temperatures in the upper plenum, some oxidation of the stainless steel would be expected to occur in those cases. Furthermore, MAAP assumes that oxidation of a quantity of zirconium ceases when that quantity relocates.

Results of Expert D's Elicitation

Expert D's decomposition is depicted in Figure D-1. The first branch corresponds to the case structure and so does not have to be quantified. Expert D felt that there was a big difference between core melt at 2500 psia and core melt at pressures below 1500 psia (15 MPa). The upper path at the first branch is Case 1 above, and the lower branch is Cases 2, 3, and 4. Case 1 differs significantly from the other three cases because natural circulation is much more vigorous at 2500 psia than at the lower pressures. This comes about because the steam densities are so much higher at 2500 psia.

For the core blocked question, Expert D thought the "blocked" branch was more likely. The distribution he gave for this branching had a midpoint at 0.80 (for the "yes" branch) and a broad distribution. If the core is blocked, the amount of zirconium oxidized depends only on the amount of steam available, and was generally quite low. How much zirconium is exposed, and the relocation temperature, does not matter since the steam does not reach the zirconium.

For the zirconium-exposed or not-exposed question, Expert D favored a low amount of zirconium exposed: the midpoint of his distribution was 0.9 (for the "Lo" branch) and this distribution was also quite broad. If a high portion of the zirconium is exposed, the relocation temperature doesn't matter much since it will get oxidized before or after relocation. Thus there is no branching at the relocation temperature question for the path with the high exposed zirconium fraction. For the relocation temperature
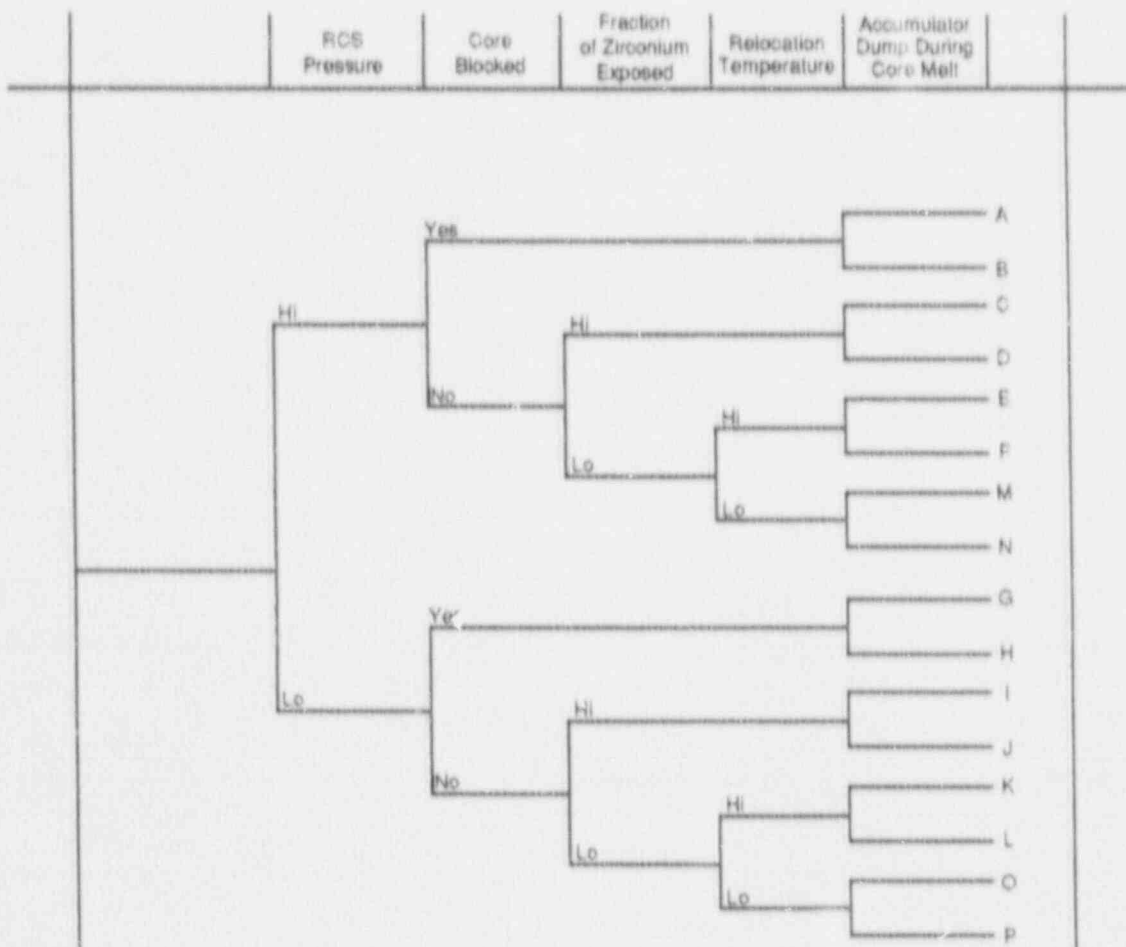
Figure D-1. Expert D's Decomposition

question, Expert D favored a low temperature; the midpoint of his distribution was 0.67 (for the "Lo" branch) and this distribution was extremely broad. Whether the accumulators discharge during the core melt is determined by the accident progression event tree, so this question does not have to be quantified.

For each of the endpoints on the tree, Expert D provided midpoint, 5%, and 95% values for the amount of hydrogen generated based on MAAP and other code runs. A summary of sources for the hydrogen production values is given in Table D-1 for the seven cases for which Expert D had analyses available. Table D-2 gives the 5, 50, and 95% values for all 16 endpoints on the tree. The amount of hydrogen produced is in kg for a plant the size of Ringhals 3 or Surry. The column entitled "Code H_2" contains the amount of hydrogen produced as calculated by MAAP (or another code). The next column shows what additional amount of hydrogen may be expected if the accumulators dump during core melt. Expert D's midpoint estimate for this amount was 150 kg, with a 5% probability of 25 kg and a 95% probability of 200 kg. These values remain the same for all cases where the accumulators discharge after zirconium oxidation has started. The fourth column is the additional amount of hydrogen produced by the oxidation of stainless steel in the upper plenum. The last two columns give the total amount of hydrogen produced in kilograms and in the fraction of the zirconium oxidized. The final column, applies to all three PWRs in this study. Each column has three entries, the 5, 50, and 95% probability values.

Table D-1
Summary of Analysis to Support Confidence Level
Assignments for the Logic Tree

End Point	Best Estimate Confidence Level	Supporting Analysis
A	0.99	Surry (Section 4.2)
B	0.90	Seabrook (Section 3.2.2)
		Ringhals (Section 3.5.1)
		Ringhals (Section 3.5.3)
C	0.95	Seabrook (Section 3.2.2)
		Ringhals (Section 3.5.1)
		Ringhals (Section 3.5.3)
		Ringhals (Section 3.5.2)
		Ringhals (Section 3.5.3)
		Surry (Section 4.1)
		Zion (Section 4.4)
D	0.99	Ringhals (Section 3.5.2)
		Ringhals (Section 3.5.3)
E	0.75	Seabrook (Section 3.2.1)
		Ringhals (Section 3.4.1)
		Ringhals (Section 3.4.2)
		Surry (Section 4.1)
		Zion (Section 4.4)

End Point	Best Estimate Confidence Level	Supporting Analysis
F	0.90	Seabrook (Section 3.2.1) Ringhals (Section 3.4.1) Ringhals (Section 3.5.2) Ringhals (Section 3.4.2) Surry (Section 4.1) Zion (Section 4.4)
G	0.95	Ringhals (Section 3.5.2)

Table D-2
PWR Hydrogen Production In-Vessel
In-Vessel Issue 5 (Expert D)

Case	Code H_2 (kg)	H_2 from Accm. Dump (kg)	H_2 from SS Ox. (kg)	Total H_2 Produced (kg)	Fraction of Zr Ox. (kg)
A	125-180-225	25-150-200	20-35-50	170-365-475	24-51-66
B	100-150-200	0	25-50-75	125-200-275	17-28-38
C	250-340-360	25-150-200	30-50-70	305-540-630	42-75-88
D	200-300-350	0	60-75-90	260-375-440	36-52-61
E	200-265-300	25-150-200	20-40-60	245-455-560	34-63-78
F	175-220-275	0	40-60-80	215-280-355	30-39-49
M	-240-	25-150-200	-20-	-410-	30-57-72
N	-200-	0	-40-	-240-	23-33-43
G	120-150-175	25-150-200	15-25-35	160-325-410	22-45-57
H	100-120-150	0	20-35-55	120-155-205	17-22-28
I	-230-	25-150-200	-40-	-420-	29-58-73
J	-200-	0	-55-	-250-	25-35-45
K	-180-	25-150-200	-50-	-360-	23-50-65
L	-150-	0	-30-	-190-	16-26-36
O	-160-	25-150-200	-20-	-330-	23-46-58
P	100-120-150	0	15-30-45	115-150-195	16-21-27

Expert D observed that an accident could not produce oxidation of 100% of the zirconium because some of the peripheral fuel assemblies were too cool to reach zirconium oxidation temperatures. Furthermore, the clad in the bottom third of the core often got up to oxidation temperatures only when the water level had dropped below bottom of active fuel, thus shutting off most of the steam supply. Considering that most accident progressions are steam limited, it is usually hard to get any code to give over 50% oxidation. Of course, most codes do not consider accumulator dump or steel oxidation.

Expert D concluded that significant stainless steel reaction with steam to produce hydrogen is only likely for cases with strong natural circulation flows. Analyses indicate that the reactor vessel internals above the core are heated to temperatures which can give SS water reactions only for TMLB' and similar events. Thus, no significant hydrogen from SS water reactions is expected for cases where the RCS pressure is below about 15 MPa (2500 psia) or cases in which the auxiliary feedwater is operating during core melt.

Sources of Uncertainty

If there is a supply of water to the core during core melt, hydrogen production can be expected to be considerably higher than if there is no such supply since there will be much more steam available. As these scenarios (in which AFW or ECC systems supply some water during core melt, but not enough to arrest the melt progression) are not very important, Expert D did not consider them further; however, the TMI-2 incident was just such an event as it had AFW flow, charging flow, and RCP start.

Depressurization of the RCS during core melt is also likely to cause more hydrogen production as lowering the pressure will cause flashing. If the water level has dropped below the bottom of active fuel, there is very little steam production since the water in the lower plenum is largely unaffected by the core melt progression. Flashing of this water would provide a source of steam during a period when the core is otherwise steam starved. The depressurization could come from a hot leg break or the opening of the PORVs by the operators.

The amount of core blockage and the exposure of the zirconium surfaces have been considered above, but the crude division into high and low branches is clearly a source of uncertainty. Other sources of uncertainty are the strength of natural circulation and clearing of the loop seals. These uncertainties were considered to be less important than those explicitly considered above, and their effects were not quantitatively included.

However, Expert D concluded that these uncertainties are relatively small compared with those accounted for by the variations in the analyses considered, and he did not take these factors into account explicitly.

Correlations With Other Variables

The core degradation model used in the computer code directly affects both the amount of hydrogen produced and the temperatures in the upper plenum of

the reactor vessel, and the temperatures in the upper plenum relate directly to the temperatures in the hot leg, surge line, and SG tubes. Since zirconium oxidation is exothermic, a high hydrogen production case is also a high hot leg temperature case. Thus, in the sampling, it would be inconsistent to take a low core temperature value for hot leg break (Issue 1) and a high zirconium oxidation value for hydrogen production (Issue 5).

Whether hot leg failure occurs has implications for hydrogen production and fission product behavior. If hot leg failure does occur, the steam flow rate in the core will increase. The amount of increase depends on how much core blockage is assumed. If the zirconium oxidation has been steam-limited up to this time, it may increase dramatically after the break due to the steam produced by flashing as the pressure drops. The same increased flow may also greatly reduce the amount of fission product deposition that occurs within the RCS, and thus may affect the source term.

REFERENCES

D-1. R.J. Lutz, Jr. et al., "Ringhals Unit 3 Severe Accident Analyses to support Development of Severe Accident Procedures," WCAP-11607, Westinghouse Nuclear Technology & Systems Division, Pittsburgh, PA, 1987.

D-2. Commonwealth Edison Co., "Zion Probabilistic Safety Analysis," Chicago, IL (no date identified in documents).

D-3. R. J. Lutz, Jr., "Creep Rupture Failure of Primary Coolant Piping prior to Reactor Vessel Failure for Severe Accidents," WCAP-11910, Westinghouse Nuclear Technology & Systems Division, Pittsburgh, PA, July 1988.

Expert E's Elicitation

PWR Hydrogen Production

Description of Expert E's Rationale/Methodology

The assessment of Expert E is based upon a considerable amount of TMl-2 accident investigative and analysis experience, leading the development of and making much use of two codes for evaluating severe core damage progression (one for PWRs and one for BWRs), a familiarity with the MAAP code,[E-1] and a large number of MAAP calculations. Expert E has had close involvement with comparison of code calculations to the actual TMI-2 post-accident findings, and has insight into code limitations and extrapolations of code calculations to real events. A few basic assumptions utilized in this assessment include the following:

1. Major movement of much of the remaining metallics (still unoxidized zirconium, iron, chromium, nickel, and control materials silver and indium) to places where they both become inactive and affect steam flow rates and flow patterns in the core (generally as a result of refreezing);

2. Consideration of the effects of the formation of local blockages in-vessel that alter natural circulation patterns;

3. Natural circulation patterns that are counter to core predictions. Inactive metallics are those which, as a result of the configuration in which they exist (location and physical state, e.g., relocated and refrozen), are unable to be oxidized within a timeframe that would affect reactor vessel failure and the ensuing primary phases of core-concrete interaction (CCI) or direct containment heating (DCH).

Expert E assumed that once hydrogen production has begun, a "unit of hydrogen production" is equivalent effectively to a "unit of core damage" because of energy deposition into the system. That is, the production of hydrogen from zirconium oxidation (the dominant oxidation process) leads to significant core damage resulting from the massive energy release associated with the zirconium oxidation. Thus, there is a direct relationship between accumulated hydrogen production and progress to vessel failure. The hydrogen production process was decomposed into two separate time regimes for the assessment. The first time regime covers the fraction of total zirconium oxidized in the core region while the core remained within its boundaries, and the second time regime considers the additional fraction oxidized both in the core and in the lower head (or in vessel) after relocation of a portion of the core into the lower head. Expert E's judgment is that at vessel breach there is little additional unoxidized zirconium or other metallics available (not active), on a practical time scale, to be oxidized.

Results of Expert E's Elicitation

Expert E's assessment consisted of two basic classes of accidents. The first is referred to as the station blackout class of accidents, and the second is the large-break LOCA class. The first class of accidents encompasses all system setpoint, high, and intermediate RCS pressure accidents, and covers Cases 1, 2 and 3. The second class of accidents is for low-pressure accidents caused by rapid depressurization only and covers Case 4.

Station Blackout Accident Class--Cases 1, 2, and 3

During the in-core H_2 production portion of this class, the median value is equivalent to about 25% total zirconium oxidation. Expert E judged that oxidation equivalent to 50% of the zirconium inventory oxidation is the absolute maximum of in-core oxidation, because as mentioned earlier, the system is overwhelmed by the energy release from oxidation. The core degrades and experiences gross relocation to the lower head well within the bounds of 50% equivalent zirconium oxidation. Early in the relocation process, it was judged that much of the remaining unoxidized metallics generally move to places where they become inactive (e.g., freezing at locations that will not result in their oxidation to any significant degree prior to vessel failure). The distribution provided for the equivalent fraction of core zirconium inventory oxidized in-core in the first time regime is as follows:

First Time Regime In-Core Equivalent* Zr Oxidation--Cases 1-3

Cumulative Probability	0	.05	.30	.70	.90	1.00
Equivalent % Zr Oxidized	0	10.00	20.00	30.00	40.00	50.00

Expert E determined a correlation between the amount of hydrogen produced in the second time regime (the time regime in which the debris is located to the bottom head) and the first time regime (the in-core time regime): higher values of in-core oxidation will result in lower values of in-vessel oxidation during the second time regime. As the in-core oxidation increases, there is both more total energy deposited in the core, causing imminent vessel failure, and less availability, because of both consumption and relocation of additional oxidizable metallics. This lower availability will decrease the later oxidation that results from processes arising from molten core material slumping into the reactor vessel lower head. Expert E provided distributions conditional upon 5 to 15, 25, 35, and 45% in-core oxidation values during the first time regime.

---

*Use of the word equivalent refers to the consideration of total energy release from all oxidation of all metallics as being from oxidation of the zircaloy inventory in the core region.

Additional Equivalent* Zr Oxidation During Second Time Regime--Cases 1-3

Cumulative Probability   0.0   .05   .50   .95

Prior in-core Production (equivalent % Zr oxidation)	Additional Oxidation Caused by Major Core Relocation into the Lower Head (equivalent % Zr oxidation)			
5-15%	-	10	20.0	30
25%	0	-	10.0	20
35%	0	-	5.0	10
45%	0	-	2.5	5

In order to estimate the total in-vessel hydrogen production, the in-core and lower head production portions are summed. The in-core portion is divided into ranges of 10% increments with, for lack of sufficient information, a uniform density assumed across the probability density function (pdf). The ranges for the in-core portion of the decomposition will be defined as follows: 0 to 10% = I_1, 10 to 20% = I_2, 20 to 30% = I_3, 30 to 40% = I_4, and 40 to 50% = I_5. The cumulative curves of the lower head production portion are approximated with straight lines using the .05 and .95 fractiles as bounds. This yields a convenient uniform conditional pdf for the lower head portion which can be easily convolved with the uniform pdf's for in-core production.

The result of the convolved pdf's is a family of triangular pdf's describing the total hydrogen production for each of the ranges given in the first portion of the assessment. For example, the convolved pdf for the 0 to 10% range is a triangle with the base ranging from 10 to 40% on the total hydrogen production axis and with its peak at the half-way point of 25%.

The probability for being within a total hydrogen production range is then computed. The ranges for the total hydrogen production will be defined as follows: 0 to 10% = T_1, 10 to 20% = T_2, 20 to 30% = T_3, 30 to 40% = T_4, 40 to 50% = T_5, and 50 to 55% = T_6. The probability value is obtained by summing the multiples of the probability of being within each in-core range by the probability of being within the total range for each in-core range:

$$Pr(T_j) = \Sigma_i \; Pr(I_i) * Pr(T_j/I_i)$$

where $Pr(T_j/I_i)$ is the fraction of the area of the triangle contained in the range T_j for the in-core range I_i. The values for T_1 - T_6 are computed as follows (zero values are not listed):

---

*Use of the word equivalent refers to the consideration of total energy release from all oxidation of all metallics as being from oxidation of the zircaloy inventory in the core region.

$Pr(T_1) = 0$

$Pr(T_2) = Pr(I_1) \ast Pr(T_2/I_1) = (.05) \ast (2/9) \approx .01$

$Pr(T_3) = Pr(I_1) \ast Pr(T_3/I_1) + Pr(I_2) \ast Pr(T_3/I_2) + Pr(I_3) \ast Pr(T_3/I_3)$
$\quad\quad = (.05) \ast (5/9) + (.25) \ast (2/9) + (.4) \ast (2/9) \approx .18$

$Pr(T_4) = Pr(I_1) \ast Pr(T_4/I_1) + Pr(I_2) \ast Pr(T_4/I_2) + Pr(I_3) \ast Pr(T_4/I_3)$
$\quad\quad + Pr(I_4) \ast Pr(T_4/I_4)$
$\quad\quad = (.05) \ast (2/9) + (.25) \ast (5/9) + (.4) \ast (5/9) + (.2) \ast (1/2) \approx .47$

$Pr(T_5) = Pr(I_2) \ast Pr(T_5/I_2) + Pr(I_3) \ast Pr(T_5/I_3) + Pr(I_4) \ast Pr(T_5/I_4)$
$\quad\quad + Pr(I_5) \ast Pr(T_5/I_5)$
$\quad\quad = (.25) \ast (2/9) + (.4) \ast (2/9) + (.2) \ast (1/2) + (.1) \ast (7/9) \approx .32$

$Pr(T_6) = Pr(I_5) \ast Pr(T_6/I_5) = (.1) \ast (2/9) \approx .02$

The resultant cumulative probability distribution for total hydrogen production based on equivalent % zirconium oxidized is:

Cumulative Probability Distribution for Total In-Vessel Equivalent Zirconium Oxidation--Cases 1-3

Cumulative Probability	0.0	0.10	0.19	0.66	0.98	1.00
Equivalent % Zr Oxidized	0.0	20.00	30.00	40.00	50.00	55.00

Large Break LOCA Accident Class--Case 4

The main difference between the station blackout case and the large-break LOCA case is that in the blackout case, zirconium oxidation is the most dominant mechanism for energy transfer to the system and subsequent core degradation, whereas, for the large-break case, decay heat relatively has a much larger effect in core heatup and melting. Also in Case 4, there is less water in the system, and therefore less potential for zirconium oxidation. So, for the in-core portion during the first time regime, the values Expert E supplied in the distribution were lower than for the blackout case:

First Time Regime In-Core Equivalent Zirconium Oxidation--Case 4

Cumulative Probability	0.0	0.20	0.70	1.00
Equivalent % Zr Oxidized	0.0	10.00	20.00	30.00

For the lower head portion, Expert E utilized the same type of correlation and reasoning as for the blackout case. Distributions were provided conditional upon 5, 15, and 25% in-core oxidation values:

Cumulative probability	0.0	0.05	0.50	0.95
Previous In-Core Production (equivalent % Zr oxidation)	Additional Oxidation Caused by Major Core Relocation into the Lower Head (equivalent % Zr oxidation)			
5%	-	10	15	20
15%	-	5	10	15
25%	0	-	5	10

Again, using the same process for convolving, and the same range values for I_1 to I_5 and T_1 to T_6 as outlined above, the results are as follows:

$Pr(T_1) = 0$

$Pr(T_2) = (.2)*(1/2) + (.5)*(1/8) \approx .16$

$Pr(T_3) = (.2)*(1/2) + (.5)*(3/4) + (.3)*(1/2) \approx .63$

$Pr(T_4) = (.5)*(1/8) + (.3)*(1/2) \approx .21$

$Pr(T_5) = 0$

$Pr(T_6) = 0$

In addition the value for 25% Zr oxidation for Case 4 can be calculated:

$Pr(0-25\%) = (.2)*(7/8) + (.5)*(1/2) + (.3)*(1/8) \approx .46$.

The resultant cumulative probability distribution for total hydrogen production based on equivalent % zirconium oxidized is:

Cumulative Probability Distribution for Total In-Vessel Equivalent Zr Oxidation--Case 4

Cumulative probability	0	0.16	0.46	0.79	1.00
Equivalent % Zr oxidized	0	20.00	25.00	30.00	40.00

Sources of Uncertainty

The primary sources of uncertainty Expert E denoted in this assessment deal with the core relocation processes. Another uncertainty is how much of the metallics becomes inactive after relocation. Uncertainties arise as to the timing of the relocation with respect to in-core zirconium oxidation. Considering the time span to vessel failure and the ensuing primary ramifications of that failure, uncertainties in how much of the relocated unoxidized metallics remain inactive and for how long affect the outcome. Also, the amount of steam that is actually available to the metallics that still have the potential to oxidize (are still potentially active) provides additional uncertainties.

Suggested Methods for Reducing Uncertainty

The TMI-2 core and reactor vessel examinations already have provided unique and highly appropriate data on both full-scale reactor core melting, and slump'g progression and hydrogen production during in-core zirconium oxida. on (the first time regime). Completion of this examination, including the further characterization of the slumped core materials in the reactor vessel lower head and damage caused to the lower head and its components, will provide invaluable data on the effects of gross core slumping out of the core boundaries (the second time regime).

It is of paramount importance that this TMI-2 data base be more completely used in improving core melt progression modeling. Since zirconium oxidation/H_2 production is the dominant force in core melt progression, such use of TMI-2 data therefore improves H_2 production modeling.

The OECD LOFT-LP-FP-2 experiment[8-2] is the second most important (after TMI-2) data base for improving core melt (H_2 production) modeling. The data from this experiment are extremely appropriate for making core melt progression modeling improvements.

The many small-scale experiments, such as the NRC Severe Fuel Damage experiments in the PBF, ACRR, NRU reactors and the German out-of-pile CORA experiments, offer very limited appropriate data that must be used with extreme care and with great selectivity to avoid modeling assumptions in core melt progression that represent small-scale systems and do not apply to light water reactor (LWR) cores.

REFERENCES

E-1. Industry Degraded Core Rulemaking Program, "Modular Accident Aanalysi
      Program (MAAP) User's Manual," IDCOR Technical Report on Subtasks
      16.2 and 16.3, Fauske & Associates, Inc., for the Atomic Industrial
      Forum, Bethesda, MD, 1987.

E-2   A. Sharon, "Simulation of LOFT Experiment LP-FP-2 Using the Modular
      Accident Analysis Program (MAAP) Version 3, FAI/86-27 (Revision 1),
      Fauske & Associates, Inc., June 1987.

5.6   Issue 6: PWR Bottom Head Failure

Summary and Aggregation of In-Vessel Issue 6
PWR Bottom Head Failure

Experts Consulted: Richard R. Hobbins, EG&G Idaho, Inc., (Idaho National
Engineering Laboratory); Garry R. Thomas, Electric Power Research
Institute; Peter Bieniarz, Risk Management Associates; William Camp, Sandia
National Laboratories.

Issue Description

What is the probability that temperature-induced failure of the bottom head
in PWRs will result in the pressurized ejection of the molten core debris
rather than a gravity pour? Also important is the consideration whether
the vessel fails by formation of a large hole, such as a penetration
failure by formation of a large hole. Throughout the description of this
issue, the hole size refers to the initial size not the ablated size.

In addition to the probability of failure mode, the Containment Loads
Expert Panel requested information about mass ejected as a function of
time, the temperature of the melt, the unoxidized metallic fraction of the
ejected material, ε ᆌ the fraction of ejected material which is molten.

Initially, three cas‿   ⌐ defined for this issue:

Case	RCS Pressure (psia)	Accumulators Discharged	UHI Discharged
1	2500	No	No
2	2000	No	Partial
3	200 to 1200	Partial	Yes

The state of RCS pressure, the state of the accumulators, and the state of
the upper head injection (UHI) defined in the case structure apply to the
time of vessel failure. The reference scenario representing Case 1 has no
break in the RCS pressure boundary until the vessel fails and the entire
meltdown takes place at the PORV setpoint pressure. In Case 2, there is an
S_3-size break as defined in NUREG/CR-4550 in the pressure boundary. Much
of the core melt may take place at 1200 to 1500 psia, but in the reference
scenario the RCS repressurizes to around 2000 psia shortly before vessel
failure. In Case 3, there is an S_2-size break in the pressure boundary.
Most of the core melt is expected to occur below 600 psia, but some
repressurization may occur before vessel breach. Most simulations of core
meltdowns with S_2 breaks show complete or nearly complete discharge of the
accumulators before vessel failure.

The pressures at vessel breach listed above can result from many different
scenarios. There are numerous variations on the cases listed above, and
they cannot all be considered here. Operation of the auxiliary feedwater
system, especially when the secondary system is depressurized, may lower

the pressure at vessel breach significantly, and will affect the timing of accumulator discharge. There is no case for vessel failure at 200 psia or less since gravity pour is assured for those cases.

UHI refers to the upper head injection system, a feature found only on Westinghouse reactors in ice condenser containments. Of the three PWRs considered in this study, only Sequoyah has a UHI system. In this regard, TVA has received NRC permission to physically remove the UHI at the next refueling outage. The NRC has decided that Sequoyah should be analyzed without UHI for this project, but this information was received only after most of the experts had completed their assessments.

Summary of Experts' Rationale/Methodology

Four members of the panel considered the issue of the mode of failure of the vessel for PWRs; their conclusions are shown in Tables 6-1 and 6-2.

Expert A based his analysis upon his work on the TMI-2 accident, MAAP calculations, and experience in comparing code results to the TMI-2 accident. Expert A treated all three cases together since he felt there would be no significant differences between them. He believed that vessel failure will always be a penetration failure. The initial hole size will be about 1 or 2 square inches, and will ablate rapidly. No more than 60% of the core can be ejected, and the portion that is ejected will all escape in about a minute.

Expert B based his analysis primarily on the accident at Three Mile Island (TMI). He has spent most of the past few years analyzing the data that has been developed as the core at TMI-2 has been dismantled and removed. Expert B divided PWR bottom head failures into three types: high pressure melt ejection (HPME), gravity pour, and dump. (He uses the term 'dump' to denote a massive creep-rupture failure of the vessel.) Expert B concluded that the vessel failure mode depended directly on the amount of zirconium oxidation in vessel, and divided the zirconium oxidation into three ranges. To obtain his split fractions for vessel failure mode, Expert B decomposed the problem on the basis of: crust formation, lower support plate failure, debris quench in bottom head, penetration failure or vessel failure by jet impingement, and fraction molten at vessel failure. His split fractions for HPME ranged from 17 to 31%, for gravity pour from 23 to 27%, and for dump from 46 to 58%.

Expert C based his conclusions primarily on MELPROG calculations and on experimental results. Expert C felt he could not distinguish subcases on the basis of zirconium oxidized in-vessel. For Cases 1 and 3, his assessment was that the vessel would always fail at a penetration, resulting in HPME. For Case 2, he felt that 75% of the time the loop seals would clear and that the debris in the bottom head would be rich in unoxidized metals, which would fail the vessel by eutectic formation with the steel. The other 25% of the time he felt the loop seals would not clear and Case 2 would behave like Case 1.

Expert D based his conclusions on the experiments, the analysis of TMI-2, and on the results of various computer codes. He concluded that the high pressure sequences would probably result in vessel failure due to the impingement of an oxidic jet. Thus the material initially ejected would be largely oxidic and contain only a small fraction of unoxidized metal. As the vessel fails relatively early in this mode, only the material already in the bottom head at the time of failure is available for expulsion. If the impinging jet did not fail the bottom head, then the accumulating debris would fail it somewhat later, and the debris ejected initially would still be largely oxidic, but with a higher metallic fraction. The low pressure sequences would result in the accumulation of core debris in the bottom head, and the most likely failure mechanism would be thermal attack and a large local failure. The ejected material would be highly metallic.

There was a wide difference of opinion for the mode of vessel breach. One expert was certain that vessel failure would always be by failure of a penetration, resulting in HPME all the time for all three cases. Another expert concluded that HPME would occur only about 25% of the time for all three cases. Only Expert B thought that a "dump" or gross bottom head failure was possible. Expert B also provided failure mode split fractions for three ranges of in-vessel zirconium oxidation while none of the others did. Since his results for the three oxidation ranges were not markedly different from each other, in the aggregate there is no significant dependence on the fraction of zirconium oxidized in-vessel. Thus, Expert B's failure mode fractions for the 30 to 60% zirconium oxidation range were used to obtain Table 6-3.

Method of Aggregation

None of the experts gave all the information requested about the melt ejection process. While each expert provided some of the requested information, there was no common form for what information was received. Thus it was very difficult to derive the information requested by the Loads Panel. The steps taken to put some of the information in a common form are described in this section.

For the mode of vessel failure, the fractions were averaged across the four experts. Expert B gave failure mode split fractions as a function of the amount of in-vessel zirconium oxidation (see Table 6-2). As none of the other experts considering this issue felt the failure mode depended in a known way on the amount of zirconium oxidation in-vessel, when an aggregate was formed that preserved the dependence on zirconium oxidation, it was not significant. This follows from the fact that the failure mode split fractions provided by Expert B for the three ranges of zirconium oxidation were fairly similar, especially compared to the conclusions of the other experts. Thus, no dependency on zirconium oxidation is shown in Table 6-3. As the values of Expert B for 30 to 60% zirconium oxidation were very close to the average of his three ranges, those failure mode split fractions were used in the averaging performed to obtain Table 6-3.

To aggregate the results for the core fraction ejected promptly, several inferences had to be drawn from the material provided by the experts in the elicitation sessions. Expert A provided a probability density distribution which was summed to give a cumulative distribution. Expert B said only that he was 80% confident that less than 40% of the core would be ejected. To obtain endpoints for his distribution, it was inferred from his discussion that not less than 10% of the core would be ejected, nor more than 60%. This gave the three points for Expert B shown in Figure 6-1. Expert C provided relative weights for four ranges of temperature and total mass in the bottom head at vessel failure. From his statement that all of the molten material plus 20 to 30 tons of the solid material would be ejected promptly, the first table in Section 6.2 was used to form the following table, based on a total core mass of 176 tons.*

Region	Temperature (K)	Weight (%)	In Lower Head		Ejected Material	
			Total Mass (Tons)	Fraction Molten (%)	(Tons)	(%)
1	2600 to 2900	16	150	45	98	55
2	2450 to 2600	32	140	40	84	48
3	2250 to 2450	31	120	30	61	35
4	2210 to 2250	21	100	15	35	20

The total mass and fraction molten refer to all the material in the bottom head. The last column gives the promptly ejected material as a fraction of the entire core (mass basis). These values were used with the relative weights to construct a probability density function, from which was derived the cumulative distribution for Expert C shown in Figure 6-1.

The information that Expert D provided indicated that the minimum fraction ejected was 14%, and the maximum was 27%. These two points were used as the endpoints for a straightline distribution.

Aggregated Results

The range of information about the fraction of core material ejected is very broad and covers the entire range of plausible values. Figure 6-1 shows the distributions provided by the four experts and the aggregate distribution for the fraction of the core ejected promptly. The maximum fraction of the core ejected is about 60%. The midpoint value for the aggregate distribution is about 30%. Several assumptions had to be made to get a distribution for the fraction of the core ejected for some of the experts. There is not enough information for the other properties of the ejected debris to make plotting distributions worthwhile.

---

*This is not the current core mass for the Surry case. The Expert, however, carried out all of his calculations with an oversize core so that the percentages provided are current.

Experts A and B thought that there was a direct relationship between the amount of zirconium oxidation in-vessel and the temperature of the ejected material. Expert A expected the ejecta to be between 2000 and 2800 K. Expert B gave temperatures ranging from 1300 K to 3100 K which depended on the amount of zirconium oxidized before vessel failure. For the HPME failure mode, he provided three points for each of the oxidation ranges:

Zr Oxidation	5% Prob.	50% Prob.	95% Prob.
< 30%	1300 K	2000 K	2600 K
30 to 60%	1300 K	2400 K	3100 K
> 60%	1300 K	2600 K	3100 K

Expert C concluded that the ejecta would have a temperature between 2200 K and 2900 K. He placed 63% of his weighting on temperatures between 2250 K and 2600 K, which were the central two regions of the four he defined. It is difficult to say what Expert D intended, but it is inferred from the information he provided that he expects the ejected core debris to have a temperature around 2800 K.

For the fraction of the ejected core debris that is unoxidized metal, Expert A provided a number of distributions which were convolved together to obtain a distribution for the fraction of the total zirconium which is both unoxidized and ejected. The range of this distribution is from 0% to 17.5%. If the maximum fraction is applied strictly to the zirconium then the ejecta is about 4% unoxidized metal. It may also be argued that the metal in the core other than zirconium should behave in much the same way. If the 17.5% is applied to the total metal in the core, then about 12% of the debris is unoxidized metal.

Expert B gave a single value for the fraction of unoxidized metal in the ejecta for each of his zirconium oxidation ranges: 15% metal for > 60% oxidation, 35% metal for 30 to 60% oxidation, and 60% metal for < 30% oxidation.

From the information provided by Expert C, the fraction of unoxidized metal can be calculated for Case 1:

			In Lower Head		In Ejecta
Region	Temperature (K)	Weight (%)	Total Mass* (Tons)	Fraction Molten (%)	Metal Fraction (%)
1	2600 to 2900	16	150	40	41
2	2450 to 2600	32	140	40	48
3	2250 to 2450	31	120	20	33
4	2210 to 2250	21	100	10	29

*This is not the current core mass for the Surry case. The Expert, however, carried out all of his calculations with an oversize core so that the percentages provided are current.

As in the table for Expert C on the previous page, the total mass and metal mass refer to the material in the bottom head just before vessel failure. The metal fraction is the fraction in the ejected debris. It may be noted that the fraction molten is highest for the range which has the second highest fraction ejected. In deriving the metal fraction in the ejected core debris it was assumed that all the metal was molten at the time of vessel failure. (Expert C stated that all the molten debris plus 20 to 30 tons of the solid material was ejected at vessel failure.)

Expert D did not give a fraction for unoxidized metal in the ejected debris, however, it appears from his tables that he expects the unoxidized metal to constitute about one quarter of the ejected material for the high pressure cases.

The experts were asked to estimate the time for the melt ejection and the time for the gas blowdown following the melt ejection. The information obtained in the elicitations is as follows:

Expert	HPME (s)	Gas Blowdown (s)
A	≈ 60	N.A.
B	< 60	N.A.
C	4	60
D	30	20
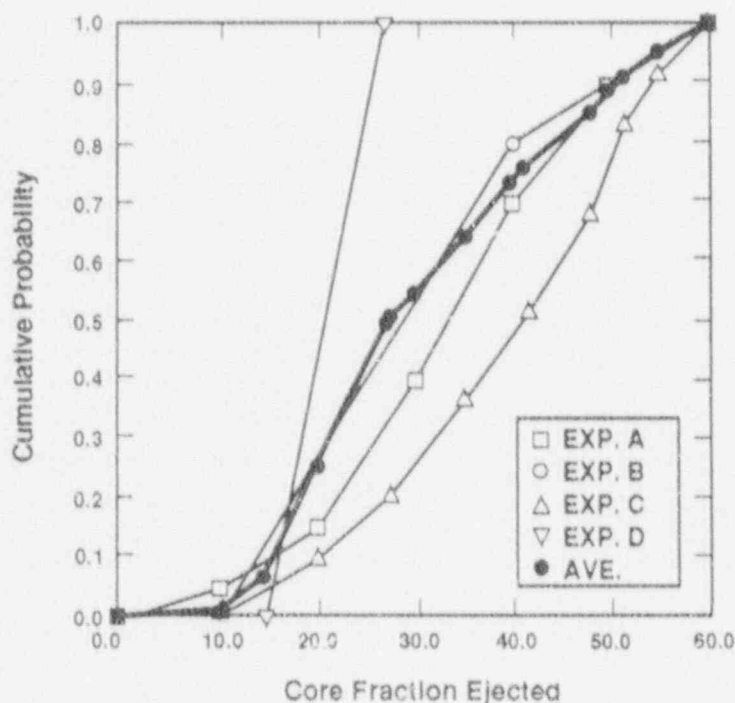
Figure 6-1. Core Fraction Ejected.

Table 6-1
Experts A, C, and D
Mode of Bottom Head Failure

Case	RCS Pres. (psia)	Expert A		Expert C		Expert D	
		HPME	Pour	HPME	Pour	HPME	Pour
1	2500	100%	0%	100%	0%	90%	10%
2	2000	100%	0%	25%	75%	90%	10%
3	200-1200	100%	0%	100%	0%	20%	80%

Table 6-2
Expert B; Mode of Bottom Head Failure

Case	RCS Pres. (psia)	Zirconium Oxidation	Failure Mode		
			HPME	Pour	Dump
1	2500	< 30%	31%	23%	46%
1	2500	30 to 60%	25%	23%	52%
1	2500	> 60%	21%	23%	56%
2	2000	< 30%	28%	25%	47%
2	2000	30 to 60%	23%	24%	53%
2	2000	> 60%	20%	23%	57%
3	200 to 1200	< 30%	25%	27%	48%
3	200 to 1200	30 to 60%	21%	26%	53%
3	200 to 1200	> 60%	17%	25%	58%

Table 6-3
Aggregate; Mode of Bottom Head Failure

Case	RCS Pres. (psia)	Failure Mode		
		HPME	Pour	Dump
1	2500	79%	8%	13%
2	2000	60%	27%	13%
3	200 to 1200	60%	27%	13%

Individual Elicitations for In-Vessel Issue 6

Expert A's Elicitation

Issue 6: PWR Bottom Head Failure

Description of Expert A's Rationale/Methodology

For this assessment, Expert A's judgment is based upon extensive involvement in the TMI-2 accident[A-1] investigation, including many detailed analyses of the core damage phases of the accident up through the slumping of 10 to 20 tons of molten core material into the TMI-2 vessel lower head. Also, the assessment is based on long-time familiarity and utilization of the MAAP code[A-2, to A-5] and its preceding model for lower vessel head failure developed as part of the Zion safety study.[A-6] Expert A has been involved with detailed comparisons of code calculations to the actual TMI-2 post-accident findings,[A-7] and has insight into code limitations and extrapolations of code calculations to real events.

A basic assumption used in this assessment is the relatively early and major slumping movement of unoxidized metallics (still unoxidized zirconium, iron, nickel, chromium, and control materials such as silver and indium) within the reactor vessel during core relocation. Specifically, the impact of the refreezing of these metallics upon both components of the lower core and vessel internals, as occurred at TMI-2, is taken into account. This process effectively separates many of the still potentially unoxidizable metallics from the later slumping of a large portion of the core mass into the reactor vessel lower head. The slumping core material then would be composed primarily of (uranium, zirconium) O_2, i.e., composed mainly of a fully oxidized material. Most of these separated metallics then can be considered to be inactive (unoxidizable) within the timeframe of vessel lower head failure.

Expert A believes that lower head failure will always be local and initially small, e.g., at a penetration ($\sim 1/2$ in^2), with follow-on ablation of the hole as the molten core is ejected from the vessel; failure time would be delayed for only a short time (<<10 minutes) following major core slumping into the lower head. The post-failure ejection time would be about o.. minute (i.e., several tens of seconds), and constant rate of ejection can be assumed across the time span for practical purposes.

Results of Expert A's Elicitation

Expert A did not differentiate between the three cases supplied, a single distribution was provided for all three cases, since the overall progression of core melting (i.e., the overall thermodynamic state of the partially molten core) in these cases would be similar if evaluated at the point where there would be major core slumping into the lower head. As the first part of the elicitation, the fraction of core mass that is ejected at vessel failure is provided. The upper bound of this mass is 60% because some of the core (probably at least 40%) is judged either not yet melted

(primary) or to be refrozen upon reactor vessel internals (secondary) prior to gross core slumping into the lower head. The distribution provided for the fraction of core mass ejected is as follows:

Fraction of Core Mass Ejected Upon Lower Head Failure

Cumulative probability:	0.0	.05	.15	.40	.70	.90	1.0
% Core ejected:	0	10	20	30	40	50	60

The median value is at about 33%. The fraction of core mass ejected from the vessel would be directly correlated to the amount of hydrogen produced in-vessel; but, due to several effects such as refreezing (even in the lower plenum of the vessel), the correlation holds only to the first order.

The next step was to determine the fraction of equivalent total zirconium that is both unoxidized and ejected from the vessel at failure. This value includes metals other than zirconium (e.g., iron, chromium, and nickel) treated as equivalent zirconium. In general, as noted above, Expert A believes that most of the still unoxidized metal will be held up in-vessel where it will have never melted (e.g., in both the outer periphery and the lowest portion of the core) or will have "moved and refrozen" in the lower core or on vessel structures as is directly supported by TMI-2 evidence. In Expert A's judgment--based directly on chemical analysis of the core material in the lower head of TMI-2--if vessel breach had occurred during the TMI-2 accident, the metallic content of the ejected molten core would have been totally "inactive." That is to say, virtually all of the metal in the ejected core would already have been oxidized, and most, if not virtually all, of the remaining unoxidized metals would have been held up in vessel.

Of course, a limited amount of unoxidized metallics, primarily components of steel and stainless steel (iron, chromium, and nickel), would have been entrained in the ejected material as a result of the limited ablation of both lower core support structures along the slumping core pathway and the vessel head at the failure locations. These metallics contribute much less potential exothermic energy upon oxidation than an equivalent mass of zirconium and are therefore of notably less importance in determining ensuing core-concrete interactions and any direct containment heating effects.

There are correlations between the amount of core available to be ejected (i.e., molten and mobile) and both unoxidized metal in the ejected melt and the temperature of the melt at ejection. For a given temperature at ejection, if there is a small amount of core available to be ejected, there will be relatively small amounts of unoxidized metal in the ejected melt. If there is a high amount of core ejected, there will be relatively higher amounts of oxidized metals, but relatively low amounts of unoxidized metal. The intermediate values of ejected mass probably will possess the highest relative amounts of unoxidized metal.

The absolute amounts of equivalent unoxidized zirconium are strongly dependent upon the temperature of the core mass at ejection, with less

equivalent unoxidized zirconium available as temperature increases.
Expert A therefore initially provided the amount of unoxidized equivalent
zirconium in the ejected core melt for levels of about 10 to 20%, 30 to
40%, and 50 to 60% core mass ejected at an initial ejection temperature
of 2000 K. The effect of increasing the initial temperature of the
ejected mass will be discussed later.

Equivalent Amount of Unoxidized Zr Ejected as a Function of Ejected Core Mass if Ejected Core Material is at 2000 K

Cumulative Probability: 0.0   .10   .75   .90   .98

Core fraction ejected at 2000 K:	Equivalent % unoxidized Zr in melt				
10% to 20%	0	-	1.5	-	2.0	
30% to 40%		-	5.0	7.5	12.0	15.0
50% to 60%		-	3.0	6.0	9.0	-

To obtain the fraction of core zirconium that is both unoxidized and
ejected at a temperature of 2000 K and at failure, the two distributions
must be convolved. Discrete ranges for fraction of core ejected are
selected in 10% increments as follows $F_1 = 0\text{-}10\%$, $F_2 = 10\text{-}20\%$, ..., F_6
$= 50\text{-}60\%$. Discrete ranges for % of unoxidized equivalent zirconium in
the ejected melt are then selected in 2.5% increments: $Z_1 = \leq2.5\%$, $Z_2 =$
$\leq5\%$, ..., $Z_7 = \leq17.5\%$. Probabilities associated with each of the core
ejection ranges is then multiplied by the probability that the zirconium
value is less than or equal to Z_j and summed for each core ejection
range, $i = 1$ through 6:

$$Pr(Z_j) = \Sigma_i\ Pr(F_i)*Pr(Z_j/F_i)$$

Where $Pr(Z_j/F_i)$ is the probability that the zirconium value is less than
or equal to Z_j for the core ejection range F_i. The values for Z_1 through
Z_7 are computed as follows:

$Pr(Z_1) = Pr(F_1)*Pr(Z_1/F_1) + Pr(F_2)*Pr(Z_1/F_2) + ... + Pr(F_6)*Pr(Z_1/F_6)$
$= (.05)(1)+(.1)(1)+(.25)(0)+(.3)(0)+(.2)(0)+(.1)(0) = .15$

$Pr(Z_2) = Pr(F_1)*Pr(Z_2/F_1) + Pr(F_2)*Pr(Z_2/F_2) + ... + Pr(F_6)*Pr(Z_2/F_6)$
$= (.05)(1)+(.1)(1)+(.25)(.1)+(.3)(.1)+(.2)(.6)+(.1)(.6) \approx .39$

$Pr(Z_3) = Pr(F_1)*Pr(Z_3/F_1) + Pr(F_2)*Pr(Z_3/F_2) + ... + Pr(F_6)*Pr(Z_3/F_6)$
$= (.15)(1)+(.55)(.75)+(.3)(.85) \approx .82$

$Pr(Z_4) = ... \approx (.15)(1)+(.55)(.85)+(.3)(1) \approx .92$

$Pr(Z_5) = ... \approx (.15)(1)+(.55)(.9)+(.3)(1) \approx .95$

$Pr(Z_6) = ... \approx (.15)(1)+(.55)(.98)+(.3)(1) \approx .99$

$Pr(Z_7) = ... = 1$

The resulting distribution for the equivalent fraction of core zirconium that is both unoxidized and ejected from the vessel at 2000 K is:

Equivalent Amount of Unoxidized Zr Ejected if Ejected Core Material is at 2000 K

Cumulative probability:	0.0	.15	.39	.82	.92	.95	.99	1.0
% equivalent zirconium unoxidized and ejected:	0.0	2.5	5.0	7.5	10.0	12.5	15.0	17.5

It is then necessary to consider the effect of melt ejection temperature. Expert A judged that the ejected melt temperature would range from 2000 to 2800 K, with temperature increasing with increased oxidation of the molten core material that will be ejected. That is to say, Expert A believes that there is a direct relation between the amount of unoxidized metal in the melt and its temperature; the higher the temperature, the lower the fraction of unoxidized zirconium contained in the melt.

The distribution of equivalent unoxidized zirconium in the ejected material is given in the following table as a function of ejection temperature. Note that the variable in the table is expressed as a fraction of equivalent unoxidized zirconium in the melt at 2000 K. For example, if the 2000 K ejected material contains 10.0% equivalent unoxidized zirconium (cumulative probability of 92% from the table above), then an ejected mass at 2400 K would contain 0.7 (from the table below) times 10.0%, or 7.0% equivalent unoxidized zirconium.

Effect of Initial Temperature of Ejected Core Material on Ejected Fraction of Equivalent Unoxidized Zirconium

Melt ejection temperature (K)	2000	2200	2400	2600	2800
Fraction of equivalent unoxidized Zr at ejection	1.0	0.9	0.7	0.4	0.05

Sources of Uncertainty

The major source of uncertainty arises from determining the combined amount of core material that has not melted prior to vessel failure and that has refrozen in-vessel. Another source of uncertainty is the amount and types of unoxidized metals that are frozen in the vessel--i.e., it is believed, based upon TMI-2 experience and logical sequencing of core melt progression, that an effective zone refining is occurring as the core melts, resulting in a relatively efficient separation of unoxidized metallics from the primary material that is ejected upon vessel failure. Very high temperature (> 2200 K) oxidation kinetics are additional uncertainties.

Suggested Methods for Reducing Uncertainty

A careful evaluation of the data that has been and will be obtained from TMI-2 regarding both the slumping of molten core material into the TMI-2 vessel lower head and the damage caused to the head and its components (e.g., the in-core instrumentation penetrations) should provide the basis for a well-defined problem of lower head damage caused by a slumping molten core. Applying existing models for such events to this problem will enable checking and improvement of these models.

The inferred core melt progression and effective zone refining of unoxidized metallics that occurred in the TMI-2 case must be accounted for in core melt progression models. For example, data show that the upper core debris bed and both the large nearly homogeneous once-molten region in the lower core and the virtually identical (chemically) relocated mass in the lower head are notably deficient of zirconium (about 50% and approximately 30 to 40% missing, respectively). The latter material, as represented by the relocated material in the lower head is essentially 100% oxidized--i.e., no remaining unoxidized metallics.

REFERENCES

A-1. Electric Power Research Institute, "Analysis of Three Mile Island - Unit 2 Accident," NSAC-1, March 1980.

A-2. Industry Degraded Core Rulemaking Program, "In-Vessel Core Melt Progression Phenomena," IDCOR Technical Report 15.1A, July 1983.

A-3. Industry Degraded Core Rulemaking Program, "Analysis of In-Vessel Core Melt Progression," IDCOR Technical Report 15.1B, September 1983.

A-4. A. Sharon, "Simulation of the TMI-2 Accident Using the MAAP Modular Accident Analysis Program," Version 2.0, EPRI NP-4292, Electric Power Research Institute, Palo Alto, CA, January 1986.

A-5. M. A., Kenton, R. E. Henry, and G. R. Thomas, "Simulation of the TMI-2 Accident Using the Modular Accident Analysis Program," _Proceedings of the International ANS/ENS Topical Meeting on Thermal Reactor Safety_, San Diego, CA, February 2-6, 1986, Paper XXIII.3.

A-6. Fauske & Associates, Inc., "Simulation of LOFT Experiment LP-FP-2 Using the Modular Accident Analysis Program (MAAP) Version 3," FAI/86-27 (Revision 1), Fauske & Associates, Inc., June 1987.

A-7. A. Sharon et al., "Simulation of the TMI-2 Accident Phases 1 and 2 (to 174 minutes into the Accident) Using the Modular Accident Analysis Program (MAAP) Version 3B and the MAAP 2.0 Plant Parameter File," Electric Power Research Institute, 1988.

Expert B's Elicitation

Issue 6: PWR Bottom Head Failure

Description of Expert B's Rationale/Methodology

Expert B based his assessment primarily on the evidence obtained from the accident at Three Mile Island 2.[B-1 to B-7] He has had extensive experience analyzing this accident, and applying information from this accident and the PBF tests[B-8 to B-10] to reactor accidents in general.

Expert B felt that the failure of the bottom head would proceed similarly for the PWRs and the BWRs. For the PWRs, he divided the failures into three classes:

1. HPME,
2. Gravity Pour, and
3. Dump.

The HPME failure mode implies both a relatively small hole and high enough pressure in the RCS at the time of failure to eject the core material. The gravity pour failure mode implies either a hole large enough that HPME does not occur or insufficient driving pressure in the vessel. Expert B uses the term 'dump' to denote a massive creep-rupture failure of the vessel.

Expert B concluded that the vessel failure mode depended directly on the amount of zirconium oxidation in vessel, and divided the zirconium oxidation into three ranges. Below 30% zirconium oxidation, there would be lots of unoxidized metal present in the core material in the bottom head, and eutectics would form readily. The alpha form of zirconium dominates, with melting temperatures around 2200 K. Between 30 and 60% zirconium oxidation in-vessel, there is less unoxidized metal available. The monotectic dissolution of of UO_2 by zirconium implies a melting temperature around 2700 K. Above 60% zirconium oxidation, the material in the bottom head is largely oxidic, and the temperature of the core material will be above 2800 K.

To obtain his split fractions for vessel failure mode, Expert B decomposed the problem on the basis of:

1. Crust formation,
2. Lower support plate failure,
3. Debris quench in bottom head,
4. Penetration failure or vessel failure by jet impingement, and
5. Fraction molten at vessel failure.

Expert B quantified an event tree containing these five questions for the three levels of zirconium oxidation for each of the three cases (nine trees in all). Each of the 32 endpoints in the tree was assigned to one of the three failure modes listed above. Evaluation of the tree gave the fraction for each failure mode for each of the nine combinations of case (RCS pressure) and subcase (fraction of zirconium oxidized in-vessel).

Results of Expert B's Elicitation

Expert B provided failure mode information for three levels of zirconium oxidation for each of the three cases. He did not provide durations for the gas blowdown following melt expulsion, nor did he provide values for gas temperature at vessel breach. The nine cases and subcases are:

Case	RCS Pres. (psia)	Zr Ox.	Failure Mode		
			HPME	Pour	Dump
1	2500	< 30%	31%	23%	46%
1	2500	30-60%	25%	23%	52%
1	2500	> 60%	21%	23%	56%
2	2000	< 30%	28%	25%	47%
2	2000	30-60%	23%	24%	53%
2	2000	> 60%	20%	23%	57%
3	200 to 1200	< 30%	25%	27%	48%
3	200 to 1200	30-60%	21%	26%	53%
3	200 to 1200	> 60%	17%	25%	58%

For each of the three values of zirconium oxidation for each case, Expert B provided a table of ejection mode and probability, mass ejected, melt temperature and superheat, and fraction molten for different portions of the debris ejection. The meaning of the first two columns for HPME and Dump is that the essentially all of the core that leaves the vessel at all will leave the vessel is less than one minute. For the Pour failure mode in Table B-1, Expert B expects 5% of the core that leaves the vessel at all to have escaped in 5 minutes, 50% to have escaped in 100 minutes, and 95% to have escaped in 225 minutes. Note that these percentages are of the core that escapes; the amount that escapes is given in columns 3 and 4. According to Expert B, the probability is 80% that less than 40% of the core will escape at vessel failure, for all cases and subcases. The next three columns provide the 5%, 50%, and 95% values of the melt temperature distribution for each subcase. The last two columns give corresponding values for the fraction of metal in the melt and fraction of the ejected material which is molten.

Table B-1
Information for Each of the Three Values of Zirconium Oxidation

---

RCS at 2500 psia - Zr Oxidation < 30%

| Time | | Melt Ejected | | Temperature | | Super | Metal | Molten |
| Prob. | (min) | Prob. | Core | Prob. | Melt | -heat | in Melt | Fraction |
(%)		(%)	(%)	(%)	(K)	(K)	(%)	(%)
31% - High Pressure Melt Ejection								
100	0	80	< 40	5	1300	50	60	10
		20	> 40	50	2000	100	60	80
				95	2600	400	60	100
23% - Gravity Pour								
5	5	80	< 40	5	1300	50	60	10
50	100	20	> 40	50	2000	100	60	80
95	225			95	2600	400	60	100
46% - Dump								
100	0	80	< 40	5	1300	50	60	10
		20	> 40	50	1800	100	60	50
				95	2300	200	60	90

RCS at 2500 psia - 30% < Zr Oxidation < 60%

| Time | | Melt Ejected | | Temperature | | Super | Metal | Molten |
| Prob. | (min) | Prob. | Core | Prob. | Melt | -heat | in Melt | Fraction |
(%)		(%)	(%)	(%)	(K)	(K)	(%)	(%)
25% - High Pressure Melt Ejection								
100	0	80	< 40	5	1300	50	35	10
		20	> 40	50	2400	100	35	80
				95	3100	400	35	100
23% - Gravity Pour								
5	5	80	< 40	5	1300	50	35	10
50	160	20	> 40	50	2000	100	35	80
95	300			95	2600	400	35	100
52% - Dump								
100	0	80	< 40	5	1300	50	35	10
		20	> 40	50	2000	100	35	50
				95	2700	200	35	90

RCS at 2500 psia - 60% < Zr Oxidation

| Time | | Melt Ejected | | Temperature | | Super | Metal | Molten |
| Prob. (min) | | Prob. | Core | Prob. | Melt | -heat | in Melt | Fraction |
(%)		(%)	(%)	(%)	(K)	(K)	(%)	(%)
21% - High Pressure Melt Ejection								
100	0	80	< 40	5	1300	50	15	10
		20	> 40	50	2600	50	15	80
				95	3100	50	15	100
23% - Gravity Pour								
5	5	80	< 40	5	1300	50	15	10
50	200	20	> 40	50	2600	50	15	80
95	375			95	2600	50	15	100
56% - Dump								
100	0	80	< 40	5	1300	50	15	10
		20	> 40	50	2200	50	15	50
				95	2800	50	15	90

RCS at 2000 psia - Zr Oxidation < 30%

| Time | | Melt Ejected | | Temperature | | Super | Metal | Molten |
| Prob. (min) | | Prob. | Core | Prob. | Melt | -heat | in Melt | Fraction |
(%)		(%)	(%)	(%)	(K)	(K)	(%)	(%)
28% - High Pressure Melt Ejection								
100	0	80	< 40	5	1300	50	60	10
		20	> 40	50	2000	100	60	80
				95	2600	400	60	100
25% - Gravity Pour								
5	5	80	< 40	5	1300	50	60	10
50	100	20	> 40	50	2000	100	60	80
95	225			95	2600	400	60	100
47% - Dump								
100	0	80	< 40	5	1300	50	60	10
		20	> 40	50	1800	100	60	50
				95	2300	200	60	90

RCS at 2000 psia - 30% < Zr Oxidation < 60%

Time Prob. (min) (%)		Melt Ejected Prob. Core (%) (%)		Temperature Prob. Melt (%) (K)		Super -heat (K)	Metal in Melt (%)	Molten Fraction (%)

23% - High Pressure Melt Ejection

100	0	80	< 40	5	1300	50	35	10
		20	> 40	50	2400	100	35	80
				95	3100	400	35	100

24% - Gravity Pour

5	5	80	< 40	5	1300	50	35	10
50	160	20	> 40	50	2000	100	35	80
95	300			95	2600	400	35	100

53% - Dump

100	0	80	< 40	5	1300	50	35	10
		20	> 40	50	2000	100	35	50
				95	2700	200	35	90

RCS at 2000 psia - 60% < Zr Oxidation

Time Prob. (min) (%)		Melt Ejected Prob. Core (%) (%)		Temperature Prob. Melt (%) (K)		Super -heat (K)	Metal in Melt (%)	Molten Fraction (%)

20% - High Pressure Melt Ejection

100	0	80	< 40	5	1300	50	15	10
		20	> 40	50	2600	50	15	80
				95	3100	50	15	100

24% - Gravity Pour

5	5	80	< 40	5	1300	50	15	10
50	200	20	> 40	50	2600	50	15	80
95	375			95	3100	50	15	100

53% - Dump

100	0	80	< 40	5	1300	50	15	10
		20	> 40	50	2200	50	15	50
				95	2800	50	15	90

RCS at 200-1200 psia - Zr Oxidation < 30%

Time		Melt Ejected		Temperature				
Prob. (%)	(min)	Prob. (%)	Core (%)	Prob. (%)	Melt (K)	Super -heat (K)	Metal in Melt (%)	Molten Fraction (%)

25% - High Pressure Melt Ejection

100	0	80	< 40	5	1300	50	60	10
		20	> 40	50	2000	100	60	80
				95	2600	400	60	100

27% - Gravity Pour

5	5	80	< 40	5	1300	50	60	10
50	100	20	> 40	50	2000	100	60	80
95	225			95	2600	400	60	100

48% - Dump

100	0	80	< 40	5	1300	50	60	10
		20	> 40	50	1800	100	60	50
				95	2300	200	60	90

RCS at 200-1200 psia - 30% < Zr Oxidation < 60%

Time		Melt Ejected		Temperature				
Prob. (%)	(min)	Prob. (%)	Core (%)	Prob. (%)	Melt (K)	Super -heat (K)	Metal in Melt (%)	Molten Fraction (%)

21% - High Pressure Melt Ejection

100	0	80	< 40	5	1300	50	35	10
		20	> 40	50	2400	100	35	80
				95	3100	400	35	100

26% - Gravity Pour

5	5	80	< 40	5	1300	50	35	10
50	160	20	> 40	50	2000	100	35	80
95	300			95	2600	400	35	100

53% - Dump

100	0	80	< 40	5	1300	50	35	10
		20	> 40	50	2000	100	35	50
				95	2700	200	35	90

RCS at 200-1200 psia - 60% < Zr Oxidation

Time		Melt Ejected		Temperature		Super	Metal	Molten
Prob. (min) (%)		Prob. (%)	Core (%)	Prob. (%)	Melt (K)	-heat (K)	in Melt (%)	Fraction (%)

17% - High Pressure Melt Ejection

100	0	80	< 40	5	1300	50	15	10
		20	> 40	50	2600	50	15	80
				95	3100	50	15	100

25% - Gravity Pour

5	5	80	< 40	5	1300	50	15	10
50	200	20	> 40	50	2600	50	15	80
95	375			95	2600	50	15	100

58% - Dump

100	0	80	< 40	5	1300	50	15	10
		20	> 40	50	2200	50	15	50
				95	2800	50	15	90

Sources of Uncertainty

Expert B observed that there were many uncertainties in the entire core meltdown process. The largest uncertainties in determining the mode of bottom head failure are the composition and temperature of the molten debris, the mechanical behavior of the penetrations and their welds, and of the head itself.

REFERENCES

B-1. A. W. Cronenberg, S. R. Behling, and J. M. Broughton, "Assessment of Damage Potential to the TMI-2 Lower Head due to Thermal Attack by Core Debris," EGG-TMI-7222, Idaho National Engineering Laboratory, (EG&G Idaho, Inc.), June 1986.

B-2. D. W. Akers, E. R. Carlson, B. A. Cook, S. A. Ploger, and J. O. Carlson, "TMI-2 Core Debris Grab Samples--Examination and Analysis," Part 1, GEND-INF-075, Idaho National Engineering Laboratory, (EG&G Idaho, Inc.), September 1986.

B-3. R. R. Hobbins, A. W. Cronenberg, S. Langer, D. E. Owen, and D. W. Akers, "Insights on Severe Accident Chemistry from TMI-2," NUREG/CP-0078, _Proceedings of the American Chemical Society Symposium on Chemical Phenomena Associated with Radioactivity Released during Severe Nuclear Plant Accidents, Anaheim, CA_, Sept. 9-12, 1986.

B-4. E. L. Tolman, J. P. Adams, J. L. Anderson, P. Kuan, R. K. McCardle, and J. M. Broughton, "TMI-2 Accident Scenario Update," EGG-TMI-7489, Idaho National Engineering Laboratory, (EG&G Idaho, Inc.), December 1986.

B-5. M. Epstein and H. K. Fauske, "The TMI-2 Core Relocation - Heat Transfer and Mechanism," EGG-TMI-7956, Idaho National Engineering Laboratory, (EG&G Idaho, Inc.), July 1987.

B-6. R. L Moore, "TMI-2 Reactor Vessel Lower Head Heatup Calculations," EGG-TMI-7784, Idaho National Engineering Laboratory, (EG&G Idaho, Inc.), August 1987.

B-7. A. W. Cronenberg and E. L. Tolman, "Thermal Interaction of Core Melt Debris with the TMI-2 Baffle, Core-Former, and Lower Head Structures," EGG-TMI-7811, Idaho National Engineering Laboratory, (EG&G Idaho, Inc.), September 1987.

B-8. A. D. Knipe, S. A. Ploger, and D. J. Osetek, "PBF Severe Fuel Damage Scoping Test--Test Results Report," NUREG/CR-4683, August 1986.

B-9. Z. R. Martinson, D. A. Petti, and B. A. Cook, "PBF Severe Fuel Damage Test 1-1--Test Results Report," Vol. 1, NUREG/CR-4684, October 1986.

B-10. D. J. Osetek, "Results of the Four PBF Severe Fuel Damage Tests," _Fifteenth Water Reactor Safety Information Meeting, Gaithersburg, MD_, October 26-30, 1987, NUREG/CP-0090.

Expert C's Elicitation

Issue 6: PWR Bottom Head Failure

Description of Expert C's Rationale/Methodology

Expert C based his conclusions primarily on the large number of code calculations that have been made. He was of the opinion that MELPROG,[C-1] SCDAP,[C-2] and CORMLT,[C-3] gave the most reasonable and realistic results. He also took into account experimental results and the TMI-2 accident. Expert C concluded that he would be unable to distinguish between low and high oxidation of zirconium in the vessel before breach. Thus his results apply to all levels of in-vessel metal oxidation. He began his assessment by considering what constituted reasonable ranges for important parameters for Case 1 just before the failure of the vessel. His results were (for Surry):

Mass in lower head	100 to 150 tons
Temperature of debris	2100 to 2600 K
Mass of metal in debris	10 to 40 tons
Liquid fraction	15 to 40%

For converting to core fractions, the initial composition of the core for Surry is:

Uranium dioxide	101.1 tons
Zirconium	23.1 tons
Other metal	8.7 tons
Grids	43.1 tons
Total	176.0 tons*

He next considered what could prevent the material from being ejected, and considered that the formation of sintered material or hard dense crusts would suffice.

To determine the hole size, he relied on experimental data and calculations. Although the SPIT, HIPS, and Surtsey experiments are not strictly applicable since all the material is molten, they form the best data available. It was Expert C's assessment that the hole size is independent of the RCS pressure. For 17 MPa (2500 psia), he expects core ejection to take about 4 s, with gas blowdown continuing for another 60 s. At 2 MPa (290 psia), core ejection should take about 10 s, with gas blowdown continuing for another 30 s.

To determine the composition of the ejecta, Expert C divided the continuum of possible states into four regions based on temperature. He concluded that the failure mode would always be a penetration failure, which would rapidly ablate to about 0.4 m in diameter.

———— ——————————

*This is not the current core mass for the Surry case. The Expert, however, carried out all of his calculations with an oversize core so that the percentages provided are correct.

Expert C thought that his distribution for Case 1 was large enough to be applied to Case 3 as well. For Case 2, the situation is quite different because the S_3 break in the example case is a pump seal failure, and this failure causes the loop seals to clear. There is little oxidation of zirconium because the steam is less available.

It was Expert C's assessment that reasonable ranges for important parameters for Case 2 just before the failure of the vessel were:

Mass in lower head	20 to 70 tons
Temperature of debris	Not given
Mass of metal in debris	15 to 60 tons
Liquid fraction	Not given

If the break is in the hot leg, or if the code results are wrong and pump seal failure does not cause the loop seals to clear, then Case 2 will be much like Case 1. To account for this possibility, Expert C combined two distributions, one for the seals-clear case and one for the seals-not-clear case. For Case 2, Expert C concluded that a gravity pour was probable as the MELPROG calculation showed the pressure to be about 40 bars (600 psia) and decreasing rapidly at the time of vessel failure. Further, for Case 2 the large amount of unoxidized metal in the debris in the bottom head will form a eutectic with the steel in the vessel wall and melt through the wall forming a large hole.

Expert C observed that it might be possible for radiation heat transfer and conduction through the vessel wall to quench the debris in the bottom head in the absence of water. If the maximum amount of mass is in the bottom head, the probability of quenching is small enough to be ignored. For the minimum amount of debris in the bottom head, the probability of quenching is about 40%. This quenching is not permanent, however. Large amount of UO_2 will later come down on top of the quenched material and eventually reheat it to the melting point. This quenching delays vessel failure considerably.

Results of Expert C's Elicitation

For Case 1 (RCS at 2500 psia), Expert C divided the possible states into four regions based on temperature. For each region he provided a weight or probability, the total mass of material in the lower head at the time of vessel failure, the mass of unoxidized metal in the lower head at the time of vessel failure, and the fraction of the total mass which is molten.

Region	Temperature (K)	Weight (%)	Total Mass (Tons)	Metal Mass (Tons)	Fraction Molten (%)
1	2600 to 2900	16	150	40	45
2	2450 to 2600	32	140	40	40
3	2250 to 2450	31	120	20	30
4	2210 to 2250	21	100	10	15

The weights give Expert C's estimate of the likelihood that each of the four regions would be observed. Expert C concluded that all vessel failures for Case 1 would be penetration failures and would result in high pressure melt ejection (HPME). The results from mechanistic code calculations almost always fall in the three lower regions. The material promptly ejected would be all of the molten material plus 20 to 30 tons of solid material.

For Case 2, there is the question of whether the loop seal will clear in the loop with the break. Expert C's distribution for this case was a composite one. If the loop seals do not clear, the results for Case 1 (above) apply. He gave this scenario a weight of 25%. If the loop seals clear, which has a 75% weight, then the following describes the molten material in the bottom head at the time of vessel failure:

	Lower Bound	Upper Bound
Temperature	1800 K	2200 K
Zr metal	10 tons	15 tons
ZrO_2	2 tons	12 tons
Steel	5 tons	50 tons
Control rods	5 tons	5 tons
U metal	2 tons	6 tons

Expert C thought that a log-uniform distribution between the lower and upper bounds would be appropriate. At vessel failure, all the molten material plus 20 tons of solid material will come out. The failure mode will be a gravity pour.

For Case 3, the information given for Case 1 is appropriate as the distribution is wide enough to include the effects of lower pressure.

Expert C noted that after the prompt ejection or pour, most of the remaining material in the bottom head will eventually come out. However, there will be some peripheral fuel rods which never melt, and some material frozen on the vessel wall or on remaining support structures which never remelts.

Sources of Uncertainty

Expert C felt that essentially all the phenomena involved are uncertain; there is very little in any of the proposed scenarios that can be considered robust. The behavior of the core before relocation from its initial location is much better understood than the behavior of the debris in the bottom head. More is known about Case 1 than about the lower pressure cases, and very little is known about Case 1. The SPIT, HIPS, and Surtsey tests are not directly applicable since almost all the material was molten in those experiments. The uncertainty in the temperature and timing of clad failure mean that the timing of the relocation is uncertain, and the path and final location of the relocating material is also uncertain. There is little or no evidence for the location and extent of crust formation. The result is that there is an uncertainty of several hundred degrees (K) in the melt temperature at vessel failure.

REFERENCES

C-1.   J. E. Kelly et al., "MELPROG - PWR/MOD1 Analysis of a TMLB' Accident Consequence," NUREG/CR-4742, January 1987.

C-2   C. M. Allison et al., "SCDAP/RELAP5/MOD2 Code Manual," NUREG/CR-5273, EGG-2555, September 1989.

C-3   V. E. Denny, A. Mertol, and B. R. Sehgal, "CORMLT Modeling of Severe Fuel Damage in Postulated Accidents," _Proceedings of National Heat Transfer Conference_, Pittsburgh, PA, August 9 to 12, 1987.

Expert D's Elicitation

Issue 6: PWR Bottom Head Failure

Description of Expert D's Rationale/Methodology

The bottom head of a PWR contains numerous penetrations of different sizes. When the bottom head contains high temperature core debris, the welds securing these penetrations could fail. Alternatively, the high temperature core debris could heat up the bottom head so that the strength of the steel decreases appreciably. The load of the debris plus the internal pressure could then exceed the strength of the vessel resulting in the formation of a hole or even gross failure of the bottom head.

Usually the bottom head contains water at the time when the core debris relocates into the bottom head. Thermal attack is likely to be either jet impingement on a penetration or a slower temperature rise due to heat transfer from the debris in the bottom head. The water in the bottom head at the time of relocation could conceivably quench the debris to temperatures below those which threaten the integrity of the vessel, although this appears to be unlikely to Expert D. However, should this happen, the debris can be cooled indefinitely if it is in a coolable configuration and water continues to be supplied. Particle size and porosity determine whether the debris bed is coolable.

If the debris bed is not in a coolable configuration, or if there is no make-up of water to the vessel, the debris will eventually reheat and start thermal attack of the vessel. This could result in penetration failure, localized failure of the vessel shell, or shell failure near the point where the top of the debris contacts the vessel wall.

The different modes of thermal attack complicate quantification of the mode of vessel failure and the characterization of the debris in the bottom head at the time of vessel failure. If a penetration fails due to jet impingement, only the molten material actually in the bottom head would be available for immediate discharge. After it had been forced out, the blowdown of the remaining water and gases would depressurize the RCS. The bulk of the core debris might then exit the vessel over a considerable period under the influence of gravity alone. The amount released from the vessel this way would depend upon the amount of core involved in the original relocation jet which failed the vessel.

If the vessel fails by the slower mechanism of increasing temperature due to accumulated core debris in the bottom head, a substantial portion of the core could be ejected at high pressure. This would be true whether the failure was at a penetration or was a larger localized shell failure. In this failure mode also, the ejection of the molten debris would be followed by a blowdown of water and gas, which in turn would be followed by gravity pouring of core debris that was not in the bottom head at the time of failure.

If the vessel failed near the contact of the upper surface of the debris and the wall, Expert D felt the failure would be localized in an 'aneurism' on the side of the vessel. As the rupture location is above the bulk of the molten material in the bottom head, only a small portion of the molten corium would be ejected under pressure before the blowdown of water and gas. The bulk of the molten corium would pour out later, driven by gravity alone, after a penetration or other local failure occurred near the bottom of the head.

Thermal attack of the lower head may depend upon the rate and amount of metallic oxidation in the lower head. However, Expert D does not believe that much oxidation will occur in the lower head, so he does not expect oxidation to significantly influence the mode of vessel failure.

In summary, Expert D identified three failure modes:

1. Jet impingement,
2. Direct thermal attack by accumulated debris, and
3. Side failure.

In the written material accompanying his elicitation on In-Vessel Issue 5, PWR Hydrogen Production, Expert D divided the degradation and melting of the core into six stages:

1. Core heatup to the start of geometry changes (ballooning),

2. From the start of fuel ballooning to the start of autocatalytic oxidation,

3. From the start of autocatalytic oxidation to the start of zircaloy relocation,

4. From the start of zircaloy relocation to rod collapse,

5. From rod collapse to support structure failure, and

6. The period of debris--water interaction in the lower plenum.

Expert D's discussion of each of these phases in detail is not reproduced here, but may be consulted in the summary of his elicitation for Issue 5. In those discussions, Expert D concluded that the high pressure sequences would probably result in vessel failure due to the impingement of an oxidic jet. Thus the material initially ejected would be largely oxidic and contain only a small fraction of unoxidized metal. If the impinging jet did not fail the bottom head, then the accumulating debris probably would fail it somewhat later. If the vessel failed in this way, then the debris ejected initially would still be largely oxidic, but with a higher metallic fraction than if it failed earlier due to jet impingement.

The low pressure sequences would result in the accumulation of core debris in the bottom head, which would boil off the remaining water and reheat. The primary failure mechanism would be thermal attack resulting in local failure. The ejected material would be highly metallic. For the low

pressures cases, it is possible, but unlikely, that the initial relocation of core debris into the bottom head would fail the vessel by jet impingement. The composition of the ejected core debris in that case would be even more metallic than if the head failed later due to thermal attack.

In all cases sufficient zirconium leaves the vessel unoxidized to result in significant zirconium oxidation during the core-concrete interaction. Thus the dependency on the unoxidized metal content of the ejected corium is not particularly important.

Results of Expert D's Elicitation

Expert D grouped the two higher pressure cases together, and provided jet impingement and debris accumulation (thermal attack) scenarios for the two remaining cases.

Case	RCS Pres. (psia)	Failure Mechanism	Prob- ability	Blowdown Duration	Gas Temp.
1&2	2000 to 2500	Jet Imp.	90%	20 s	1400 K
1&2	2000 to 2500	Debris Accm.	10%	20 s	1400 K
3	200 to 1200	Jet Imp.	20%	N.A.	700 K
3	200 to 1200	Debris Accm.	80%	N.A.	700 K

That is, for his high pressure case, Expert D envisaged vessel failure by jet impingement occurring 90% of the time, resulting in an initial small hole in the vessel. The other 10% of the time for his high pressure case, Expert D thought that a large hole would result from thermal attack. For the low pressure case, Expert D thought that a large hole resulting from general thermal attack was more likely.

For each of the four scenarios above, Expert D provided a table of mass ejected, melt temperature, and fraction molten for different portions of the debris ejection.

High Pressure; Jet Impingement

Time	Percent of Melt Ejected		Temperature (K)		Percent Molten	
	Oxide	Metal	Oxide	Metal	Oxide	Metal
0 to 30 s	20-40	5-10	3000	2100	75 to 100	100
30 s to 1 h	40-50	10-30	3000	1900	75 to 100	100
1 to 4 h	50-55	30-60	2900	1800	75 to 90	100
4 to 10 h	55-65	60-80	2900	1800	70	100
10 to 24 h	65-75	80-85	2800	1800	70	100

High Pressure; Debris Accumulation

Time	Percent of Melt Ejected		Temperature (K)		Percent Molten	
	Oxide	Metal	Oxide	Metal	Oxide	Metal
0 to 30 s	20-40	20-30	3000	2200	75 to 90	100
30 s to 1 h	40-50	30-50	3000	2100	75 to 90	100
1 to 4 h	50-55	50-60	3000	1900	75 to 90	100
4 to 10 h	55-65	60-80	2900	1800	70	100
10 to 24 h	65-75	80-85	2800	1800	70	100

Low Pressure; Jet Impingement

Time	Percent of Melt Ejected		Temperature (K)		Percent Molten	
	Oxide	Metal	Oxide	Metal	Oxide	Metal
0 to 10 min	2- 5	15-25	2600	2700	100	100
10 min to 1 h	5-30	25-50	3000	1900	75 to 90	100
1 to 4 h	30-50	50-70	2800	1900	75 to 90	100
4 to 10 h	50-60	70-80	2800	1800	75 to 90	100
10 to 24 h	60-80	80-85	2800	1800	75 to 90	100

Low Pressure; Debris Accumulation

Time	Percent of Melt Ejected		Temperature (K)		Percent Molten	
	Oxide	Metal	Oxide	Metal	Oxide	Metal
0 to 10 min	5-10	20-40	3000	2100	75	100
10 min to 1 h	10-30	40-60	3000	1900	75 to 90	100
1 to 4 h	30-50	60-70	2800	1900	75 to 90	100
4 to 10 h	50-60	70-80	2800	1800	75 to 90	100
10 to 24 h	60-80	80-85	2800	1800	75 to 90	100

The percent of the mass ejected is cumulative, but the temperature and percent molten columns refer to the material ejected during the time period indicated.

Sources of Uncertainty

Expert D observed that there were many uncertainties in the entire core meltdown process. The largest uncertainty in determining the mode of bottom head failure is the specific composition of the melt and its associated temperature. This factor influences the time and rate of release from the melt.

References

Regarding references, Expert D writes: "No specific references can be cited on this issue as very little is available. My thinking was mostly deductive and guided by the work which Marty Pilch presented, 'Modes of Lower Head Failure,' at the meeting on November 13, 1987, and Garry Thomas' presentation on the TMI accident progression at the meeting on December 17, 1987."

APPENDIX A

Probabilistic Model for Induced Rupture of
Steam Generator Tubes

Walter B. Murfin

1. Inspection of Steam Generator Tubes

References 1 through 3 report steam generator tube defects for 1981
through 1984. The table below summarizes data taken from those
references ("Fraction defective" is the fraction of tubes inspected
which were plugged or otherwise removed from service; this may be taken
as a proxy for tubes having defects exceeding 40% of wall thickness).

Table 1

Year	Fraction of Tubes Inspected	Fraction Defective
1981	19.8%	0.30%
1982	26.1%	0.20%
1983	21.8%	0.18%
1984	26.8%	0.16%
----	----	----
Averages	23.6%	0.21%

The average interval bewteen inspections is the inverse of the fraction
inspected per year, or 4.237 years. If defects grow linearly with
time, and if the "oldest" tubes are inspected each time, the average
rate of defect growth is 4.96×10^{-4} x (number of tubes) per calendar
year. The average number of defects at any time, anywhere in the steam
generators, is 0.1055%, assuming that all tubes defective are caught
when inspected. There are thus, on the average, about 11 "uncaught"
defective tubes at Surry and about 14 at Sequoyah and Zion.

2. Frequency Distrubution for Number of Defective Tubes.

Historical data show that about half of all defects in tubes are at or
near the inlet tube sheet. The rate for defects near the inlet plenum
is thus half the total rate, or 5.27E-4. With this as a true rate and
with a total number of tubes as 10,164, the cumulative probability
distribution for the number of defective tubes near the inlet plenum at
any time at Surry (assuming a binomial distribution) is shown in Table
2.

Table 2

N	Prob(No. defects ≤ N)
0	0.0047
1	0.030
2	0.097
3	0.218
4	0.379
5	0.553
6	0.708
7	0.826
8	0.906
9	0.953
10	0.979
11	0.991
12	0.996
13	0.999
14	1.000

3. Rupture of Defective Tubes

The analysis by J. Miller (attached) for creep rupture of a tube with 2400 psid differential pressure indicates equivocal failure for a hemispherical defect 0.030" deep (0.020" wall remaining) at 1000K. A 50% failure probability is assigned to defects of this depth. With 50% less wall (0.010" remaining) failure is virtually certain. With 50% more wall (0.030" remaining) failure would be extremely unlikely. Assume a straight line cumulative failure probability, 0.0 probability of failure at 0.030" wall (0.020" defect depth), 0.5 probability of failure at 0.020" wall (0.030" defect depth) and 1.0 probability of failure at 0.010" wall (0.040" defect depth).

The distribution of defect depths is not well known; however, tubes would not be taken out of service with less than 40% wall thickness defects. Assume a triangular probability density function with a peak at 0.020" depth, dropping to zero at 0.040" depth. (If there were many defects with depths of 0.040" or more, leaks would be common in ordinary service.)

A Monte Carlo simulation was run using these distributions. The calculated probability of at least N tubes rupturing is shown on Table 3.

Table 3.
Cumulative probability distribution for number of tubes ruptured
at 1000 K.

N. Number of tubes.	Probability that number of tubes ruptured is less than or equal to N.
0	0.431
1	0.792
2	0.952
3	0.993
4	0.999
5	1.000

Stated another way, at 1000K there is a probability of 0.569 of rupturing at least one tube.

We do not have an analysis for a tube temperature other than 1000K. At 800K the yield strength of the material is approximately 30% higher than at 1000K. The defect depth distribution was scaled down by a factor of 1.3, and a similar Monte Carlo analysis was carried out. The cumulative distribution function for number of tubes failed at 800K is shown in Table 4.

Table 4.
Cumulative probability distribution for number of tubes ruptured at 800 K.

N, Number of tubes.	Probability that number of tubes ruptured is less than or equal to N.
0	0.779
1	0.978
2	0.999
3	1.000

Stated another way, the probability of rupturing at least one tube at 800K is 0.221.

The yield strength of the material is 30% lower at 1060K. The defect depth distribution was scaled up by a factor of 1.3 for 1060K, and the Monte Carlo simulation was rerun. Table 5 shows the cumulative distribution function for number of tubes failed at 1060K

Table 5
Cumulative probability distribution for number of tubes ruptured at 1060K.

N, Number of tubes	Probability that number of tubes ruptured is less than or equal to N.
0	0.053
1	0.211
2	0.470
3	0.736
4	0.911
5	0.982
6	0.998
7	1.000

There is thus a probability of 0.947 of rupturing at least one tube at 1060K.

At 600K the yield strength of the material is about 50% higher than at 1000K. The probability of rupturing at least one tube, at least with the distributions assumed here, is essentially zero.

If the steam generators are not depressurized, or do not remain depressurized on the secondary side, there is very low probability of rupturing any tubes at any temperature below about 1040K.

These CDFs do not include the probability that the tubes are at the temperature indicated; the probabilities must be conditioned by the probability of being at temperature. On the other hand, the containment event tree already precedes the question on occurrence of SGTR by a question on induced hot leg LOCA. The probabilities should not be conditioned by the probability of hot leg LOCAs.
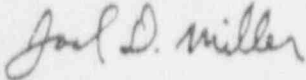
References

1. Tatone, O. S. & Pathania, R. S. (1984). Steam generator tube performance: Experience with water-cooled nuclear power reactors during 1981. Nuclear Safety, 25, No. 3: 373-398.

2. Tatone, O. S. & Pathania, R. S. (1985). Steam generator tube performance: Experience with water-cooled nuclear power reactors during 1982. Nuclear Safety, 26, No. 5: 623-639.

3. Tatone, O. S., Meindl, P. & Taylor, G. F. (1987). Steam generator tube performance: Experience with water-cooled nuclear power reactors during 1983 and 1984. Nuclear Safety, 28, No. 3: 374-390.

APPENDIX B

oate March 10, 1988

to. W. B. Murfin, 6413

[signature]

from. J. D. Miller, 1521

subject: Stress Analysis of an Inconel 600 Steam Generator Tube

INTRODUCTION

Risk assessment analyses for nuclear reactors must account for many different possible modes of failure. One of those modes has been postulated to be failure of tubes in a reactor's steam generator under severe accident conditions. Steam generator tubes are inspected regularly. during periodic scheduled maintenance, so some statistics are available concerning defects which develop in these tubes under ordinary operating conditions. At your request. a structural analysis has been performed which investigates the possibility of failure. due to the existence of defects, for steam generator tubes under severe accident conditions. The purpose of the structural analysis is to assess whether this is a viable failure mode which should be included in a risk analyst ..

Under severe accident conditions. high temperatures and pressures will be present within the reactor. The survival or failure of steam generator tubes will depend on the creep rupture strength of the material from which they are made. The structural analysis addressed a specific defect and tube geometry under specified accident conditions. with the objective of identifying the length of time the tube may be expected to survive before rupturing. In particular. can the tube survive for one hour?

The steam generator tube analyzed is made of Inconel 600 alloy. A spherically shaped indentation is assumed to exist on the outside surface of the tube. This defect was specified to be a void of diameter 0.060 inch anu depth 0.030 inch. thus extending over halfway through the 0.050 inch wall thickness of the 0.875 inch outside diameter Inconel tube. The tube is bent around a radius at its midpoint so that it resembles a large letter l. The defect is located near the midlength of one of the legs of the l. Under the specified accident conditions. the tube is assumed to be at a temperature of 1,000 K (1,340 °F) and to have a pressure loading of 2,500 psi internally and 100 psi externally.

FINITE ELEMENT MODEL

Since the tube is relatively long and free to expand axially due to its overall l-shape, and the assumed defect location is far away from the constrained ends of the tube. a finite

element model of a small section of the tube near the defect could be used in the analysis. A three-dimensional finite element mesh was constructed with PATRAN 1, and is shown in Figures 1 and 2. In order to reduce the total number of elements, to increase the computation speed, and yet retain fineness of the mesh in the vicinity of the defect, the geometry was assumed to be octosymmetric. Although this assumption implies that two defects exist on opposite sides of the tube, the results of the analysis should be identical whether there is one defect or two present; no interaction in the hoop, meridional, or radial stresses and strains would occur between defects on opposite sides of the tube because of their spacing apart and small sizes in relation to the circumferential dimension of the tube. The modeled section therefore extended 90 degrees around the circumference of the tube.

Boundary conditions on the model were consistent with the assumptions of symmetry. The origin of the model was located at the center (origin) of the spherical void, with the Cartesian X-dimension extending toward the center of the tube and the Y-dimension along the length of the tube. Thus the X-Y plane passes through the radial-longitudinal cross-section of the tube and forms the boundary at the defect, and the X-Z plane cuts through the circumferential cross-section, forming another boundary. A plane parallel to the Y-Z plane, at X=0.4375 inch, forms the boundary at 90 degrees. Geometric constraints were placed on the nodes of the mesh lying on these planes such that they were allowed to displace within but not off of the plane. The top boundary of the model, at Y=0.5 inch, was assigned a uniformly distributed traction corresponding to the meridional membrane stress in a cylinder with internal pressure, which in this case was 9,900 psi based on net internal pressure of 2,400 psi.

Pressure loads were distributed along both the inner and outer surfaces of the model, rather than as a net internal pressure. This explicitly accounts for the effects of pressure acting on the surfaces of the spherical void. Since the meridional and circumferential stresses due to the net internal pressure are tensional, the pressure on the surfaces of the void will add to the tension stresses, in effect tending to expand the defect. A pressure load of 2,500 psi was distributed along the inner surface of the model and a pressure of 100 psi was distributed normal to each element face on the outside surface, including those exposed in the spherical void.

The three-dimensional version of the static structural analysis code JAC 2, JAC3D was used to calculate the stresses in the model due to the pressure loading. While the pressure loads were ramped up from zero to their full magnitudes, the effect of temperature was included by assuming that the entire model was a constant 1,000 K. This was accomplished by using appropriate material properties for the Inconel 600 at that temperature. These properties 3-6 are listed in Table 1, in which E is the modulus of elasticity, ν is Poisson's ratio, E_T is the hardening modulus, σ_y is the yield stress, and σ_u is the ultimate strength. Since stress-strain data on the post-yield hardening behavior of Inconel 600 at high temperature was not available, a total of five calculations were made, for variations of bilinear elastic-plastic behavior ranging from purely linear elastic to elastic with perfect plasticity.

Property	@ 1,000 K
E (psi)	18.0×10^6
ν	0.3
E_T/E	0-1
σ_y (psi)	20.65×10^3
σ_u (psi)	39.2×10^3

Table 1: Mechanical Material Properties of Inconel 600

FINITE ELEMENT RESULTS

The results from JAC3D are summarized in Table 2, in which the peak values of the effective and principal stresses are listed for each of the five calculations. The resulting stresses in the tube section are highly dependent on the value chosen for the ratio of post-yield hardening modulus to the elastic modulus, shown in Table 2 as the hardening ratio. It is unlikely, however, that the behavior of Inconel 600 is either purely elastic or perfectly plastic, so the true result is probably closer to one of the three middle, non-bounding calculations. As the hardening ratio approaches 1.0 (linear elastic behavior) the resulting stresses become more severe, since plasticity allows redistribution of stress which in effect lessens the extent of the stress concentration created by the presence of the void. Complete results for the case of hardening ratio equal to 0.1 are shown in the form of contour plots of stress in Figures 3 through 6.

Hardening Ratio E_T/E	Effective Stress σ_{VM}	Hoop Stress σ_{MAX}	Radial Stress σ_{MIN}	Axial Stress σ_y
0.0 (perfect plasticity)	19.25	27.02	3.59	17.39
0.001	20.68	27.02	3.58	17.40
0.01	20.95	27.07	3.57	17.54
0.1	22.95	29.12	3.40	18.48
1.0 (purely elastic)	32.39	35.36	2.58	19.73

Table 2: JAC3D Peak Stress Results, psi $\times 10^3$

DISCUSSION

Because the objective of the analysis was to determine the length of time the steam generator tube could last without rupturing from its assumed loading, calculated values of the effective or von Mises stress must be compared to published values of the creep

rupture strength of Inconel 600. Available creep rupture data are reproduced in Figures 7 5 and 8 6 . The published data were empirically derived and shows how much time, in hours, specimens of Inconel 600 survived at certain temperatures under certain amounts of uniaxial tensile stress. Unfortunately, most of the data at the temperature of interest was collected for lower stress levels than were calculated in this analysis, so the curves were published with minimum times of at least ten hours. In addition, the fabrication or work harder   tories of both the creep rupture data specimens and the actual tube are either un   or unknown, so this effect cannot be accounted for. Nonetheless, linear extrapolation of the published curves (for 1,350 °F) back to one hour results in a possible range of values of the rupture stress between about 23,000 psi to 32,000 psi. These values would be slightly greater at 1,340 °F (1,000 K). The calculated peak values of effective stress range between 19,000 to 32,000 psi depending on the assumption made for post-yield hardening. It is therefore impossible to tell whether the tube would definitely last for an hour under the stated accident conditions.

A further consideration is that the defect was assumed to be a perfectly spherical void of completely specified dimensions, in an otherwise ideal tube. In reality of course, any actual defect in an actual tube would probably not be perfectly spherical and possibly not even smooth surfaced. The rounded defect assumption results in a stress concentration in the tube wall, but any more sharply delineated void for which the cross-section of the tube wall changes more abruptly would increase the severity of the stress concentration. The tube must also have been manufactured within a range of tolerances for both wall thickness and overall roundness, which might make an actual void extend relatively deeper through the tube wall.
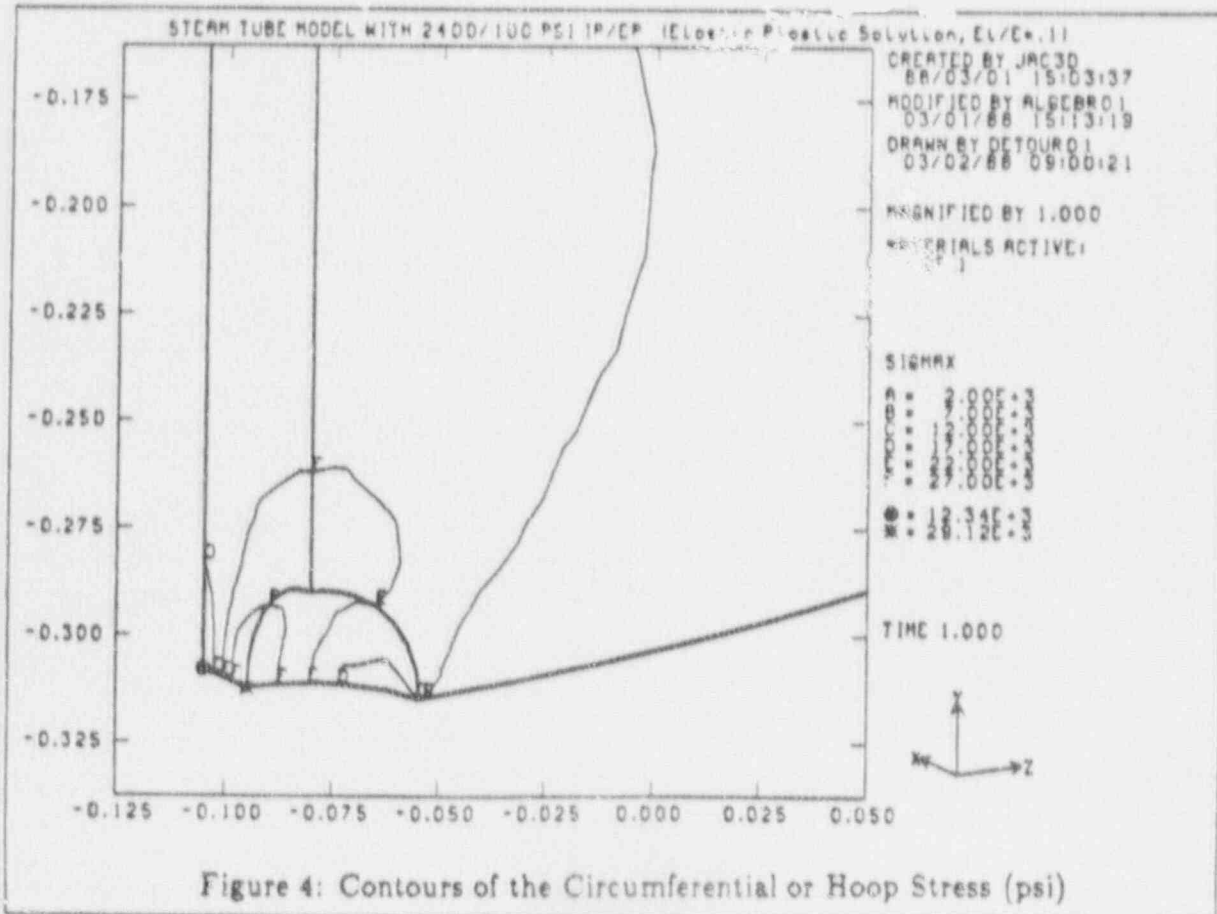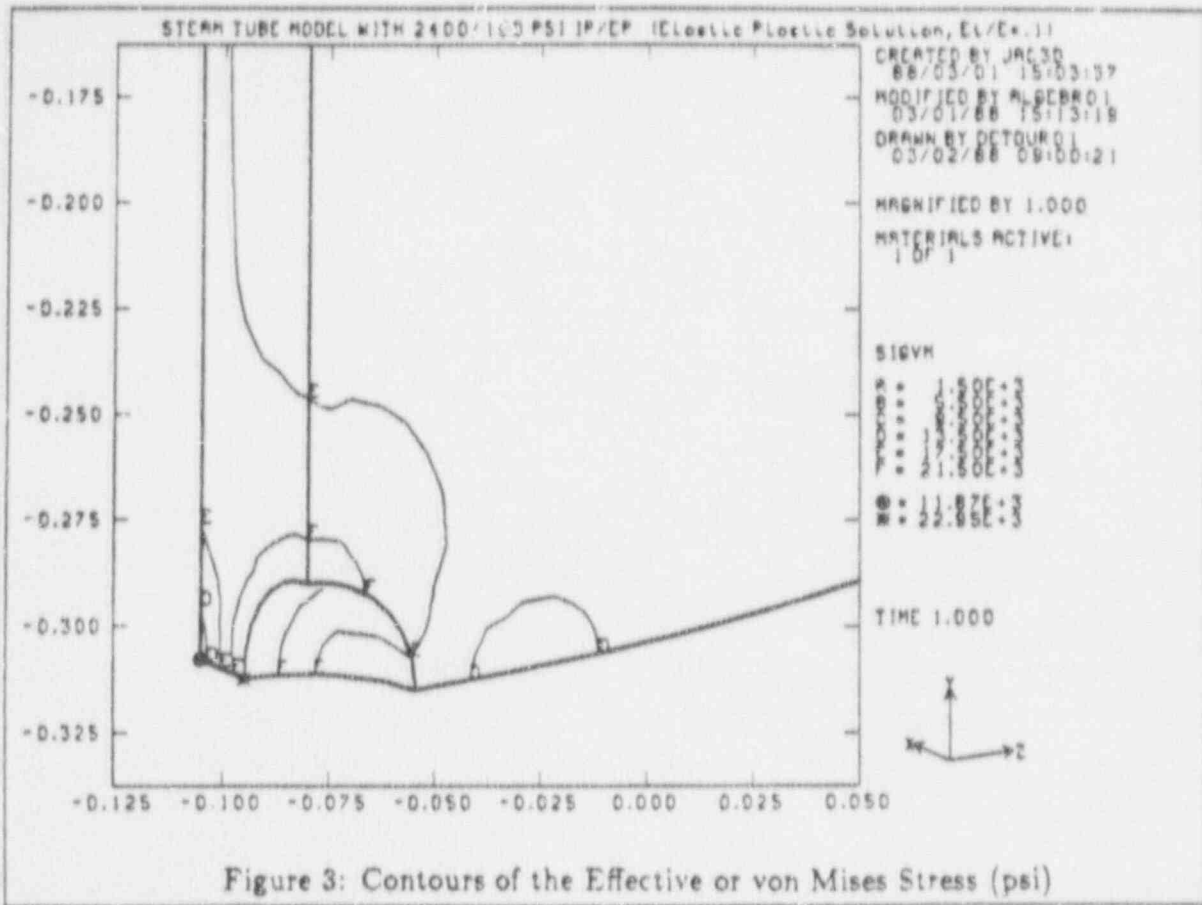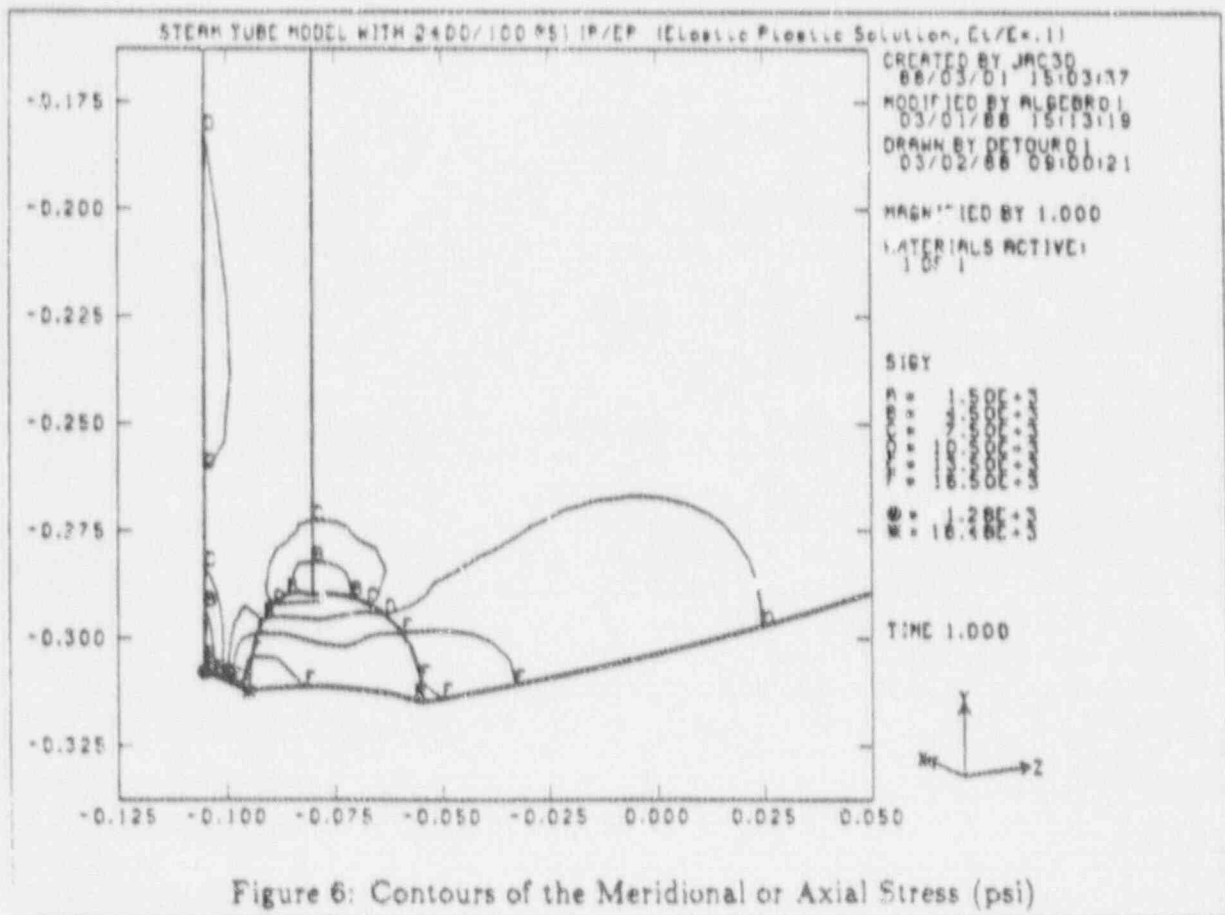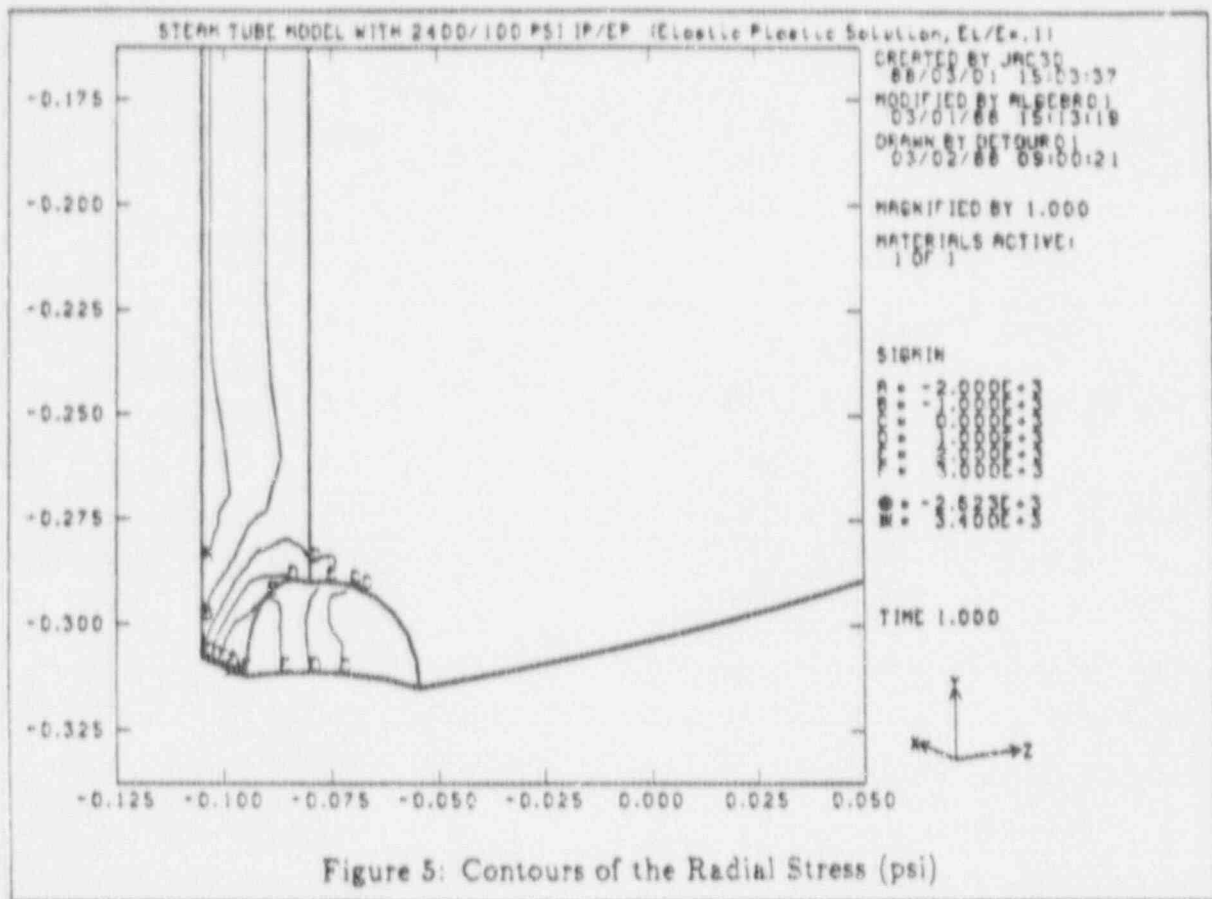
CONCLUSIONS

Finite element analysis of an Inconel 600 steam generator tube with an assumed defect in the shape of a spherical void on the outside surface of the tube and subjected to high temperature and pressure loads shows that a significant stress concentration arises due to the defect. Although an ideal tube without defects would probably survive this loading for several hours, the question as to how long the defective tube would last cannot be answered with certainty. The rise in stress due to the defect is enough to yield the Inconel and cause stress redistribution, but published material properties for Inconel are not complete enough to allow calculation of more than a possible range of resulting stress values. In addition, the failure limits of the material concerning creep rupture at very short times, such as one hour, are also not well characterized, which again results in identification of a range of possible values. Since the two ranges, that of stress in the material and that of failure limits for the material, overlap significantly, it is impossible to tell whether the tube would survive for one hour at 1,000 K with an internal pressure of 2,500 psi and an external pressure of 100 psi. It would be conservative to assume at this point that the tube will fail.

REFERENCES

1. "PATRAN II—The Complete Engineering Software System. User's Guide, Version 2.2," PDA Engineering. Software Products Division, Santa Ana, California, November 1985.

2. Biffle, J. H., "JAC—A Two-Dimensional Finite Element Computer Program for the Nonlinear Quasistatic Response of Solids with the Conjugate Gradient Method." Report SAND81-0998, Sandia National Laboratories, Albuquerque, New Mexico, April 1984.

3. *Inconel 600 Technical Bulletin*, International Nickel Co., Inc., 5th Edition, 1978.

4. "Metallic Materials and Elements for Aerospace Vehicle Structures. Volume 2," MIL-HDBK-5E. Department of Defense, Washington, D.C., June 1987.

5. "Metals Handbook: Properties and Selection of Metals, Volume 1," American Society for Metals, Metals Park, Ohio, 1961.

6. "Aerospace Structural Metals Handbook, Volume 4," Material Properties Data Center, Battelle Columbus Laboratories, Columbus, Ohio, 1984.
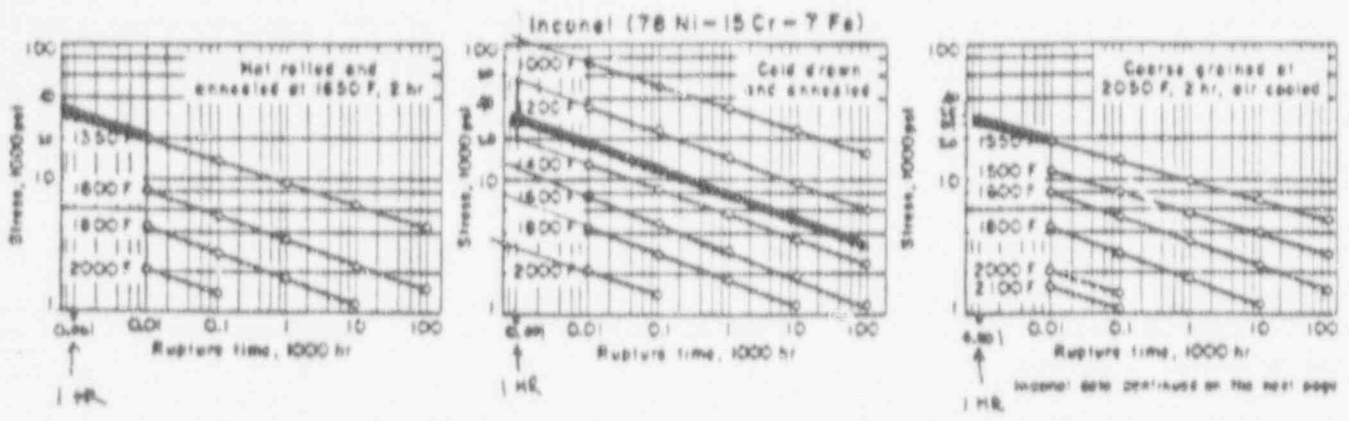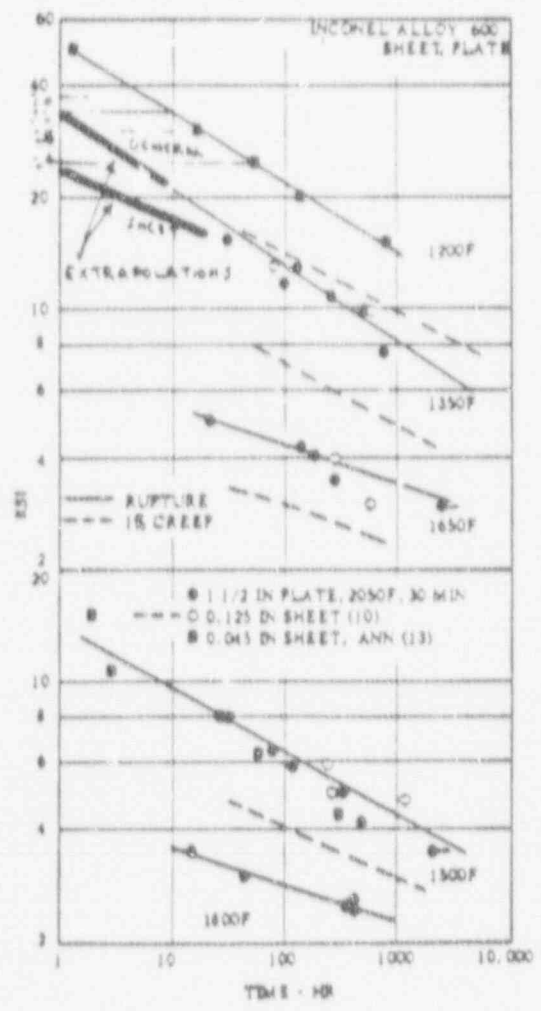
Figure 1: Finite Element Mesh Used in JAC3D

Figure 2: Close-up View of the Mesh Around the Defect

Figure 3: Contours of the Effective or von Mises Stress (psi)

Figure 4: Contours of the Circumferential or Hoop Stress (psi)

CREATED BY JAC3D
88/03/01 15:03:37
MODIFIED BY ALGEBRA I
03/01/88 15:13:19
DRAWN BY DETOUR II
03/02/88 09:00:21

MAGNIFIED BY 1.000

MATERIALS ACTIVE:
1 OF 1

SIGRIN

A: -2.000E+3
B: -1.000E+3
C: 0.000E+0
D: 2.000E+3
F: 3.000E+3

@: -3.523E+3
#: 3.400E+3

TIME 1.000

Figure 5: Contours of the Radial Stress (psi)

CREATED BY JAC3D
88/03/01 15:03:37
MODIFIED BY ALGEBRA I
03/01/88 15:13:19
DRAWN BY DETOUR II
03/02/88 09:00:21

MAGNIFIED BY 1.000

MATERIALS ACTIVE:
1 OF 1

SIGY

A: 1.50E+3
B: 4.50E+3
C: 7.50E+3
D: 10.50E+3
F: 13.50E+3
G: 16.50E+3

@: 1.28E+3
#: 16.48E+3

TIME 1.000

Figure 6: Contours of the Meridional or Axial Stress (psi)

Figure 7: Creep Rupture Data for Inconel 600 [5]

Figure 8: Creep Rupture Data for Inconel 600 [6]

DISTRIBUTION

1510 J. W. Nunziato
1520 C. W. Peterson
1521 R. D. Krieg
1522 R. C. Reuter
1523 J. H. Biffle
1524 A. K. Miller
1530 L. W. Davison
1550 R. C. Maydew
6413 E. D. Gorham-Bergeron
1521 J. D. Miller

APPENDIX C

LIST OF DOCUMENTS PROVIDED TO IN-VESSEL EXPERT PANEL
November 11-13, 1987
(Revised 3-3-88)

1. Attendee List -- Expert Review Panel Meeting November 11-13, 1987. HANDOUT
2. Welcome and introduction, N. R. Ortiz, Sandia. COPIES OF VIEWGRAPHS
3. Normative training, Steve Hora, University of Hawaii at Hilo. Set 1, COPIES OF VIEWGRAPHS
4. Normative training, Steve Hora, University of Hawaii at Hilo. Set 2, COPIES OF VIEWGRAPHS
5. Overview of NUREG-1150 backend methodology, Fred Harper, Sandia. COPIES OF VIEWGRAPHS
6. Introduction to technical issues, Eric Haskin, Sandia. COPIES OF VIEWGRAPHS
7. Temperature induced hot leg failure (PWR): Context in NUREG-1150 analysis, Walt Murfin, Technadyne. COPIES OF VIEWGRAPHS
8. In-Vessel Melt Progression: PWR Hot Leg Failure Issue, John Kelly, Sandia. COPIES OF VIEWGRAPHS
9. Presentation, Bob Lutz, Westinghouse. COPIES OF VIEWGRAPHS
10. Presentation, Vern Denny, SAIC. COPIES OF VIEWGRAPHS
11. Second Day Agenda. HANDOUT
12. Temperature induced steam generator tube rupture (PWRs): Context in NUREG-1150 analysis, Walt Murfin, Technadyne. COPIES OF VIEWGRAPHS
13. Presentation, Bob Lutz, Westinghouse. COPIES OF VIEWGRAPHS
14. IDCOR Calculations and Perspectives on the Potential for Induced Steam Generator Tube Rupture, Mark Kenton, FAI. COPIES OF VIEWGRAPHS
15. In vessel hydrogen production (BWRs): Context in NUREG-1150 analysis, Chris Amos, SAIC. COPIES OF VIEWGRAPHS
16. Richard Hobbins, INEL. COPIES OF VIEWGRAPHS
17. In-Vessel Hydrogen Production (BWRs) MELCOR Perspective, Randy Summers, Sandia. COPIES OF VIEWGRAPHS
18. Modeling of Core Heatup/Degradation and Metal-Water Reaction in APRIL.MOD2, Mike Podowski, RPI. COPIES OF VIEWGRAPHS
19. Hydrogen Source Term for Recoverable BWR Degraded Core Accidents, Garry Thomas, EPRI. COPIES OF VIEWGRAPHS
20. TMI-2 Lower Core Damage Transition Zones, G. R. Thomas, EPRI. COPIES OF VIEWGRAPHS
21. IDCOR Perspective on In-Vessel Hydrogen Production in BWRs, Ariel Sharon, FAI. COPIES OF VIEWGRAPHS
22. Perspectives on BWR In-Vessel Hydrogen Production, Observational Evidence from the DF-4 Control Blade/Channel Box Experiment, R. O. Gauntt, Sandia. COPIES OF VIEWGRAPHS and
23. SUMMARY PAPER WITH SAME TITLE.
24. Boiling Water Reactor Severe Accident Response (BWRSAR) Approach to In-Vessel Hydrogen Production, Steve Hodge, ORNL COPIES OF VIEWGRAPHS
25. BWR Temperature-Induced Bottom Head Failure Mode: The Issue and Its Context, C. N. Amos, SAIC. COPIES OF VIEWGRAPHS

26. Boiling Water Reactor Severe Accident Response (BWRSAR)
Approach to Bottom Head Penetration Failure, Steve Hodge, ORNL.
COPIES OF VIEWGRAPHS
27. IDCOR Work on the Mode of Vessel Failure, Marc A. Kenton,
FAI. COPIES OF VIEWGRAPHS
28. Modeling of BWR Lower Plenum Failure Modes, Michael
Podowski, RPI. COPIES OF VIEWGRAPHS
29. In-Vessel Hydrogen Production (PWR's): Context in NUREG-1150
Analysis, Sandia. COPY OF VIEWGRAPH
30. In-Vessel Melt Progression: Pwr Hydrogen Generation Issue,
John. E. Kelly, Sandia. COPIES OF VIEWGRAPHS
31. STCP In-Vessel Hydrogen Generation, Peter Cybulskis, BCL.
COPIES OF VIEWGRAPHS
32. IDCOR Perspective and Results on Core Melt Progression
Modelling, Marc A. Kenton, FAI. COPIES OF VIEWGRAPHS
33. Modes of Lower Head Failure, Marty Pilch, Sandia. COPIES OF
VIEWGRAPHS
34. TMI-2 Presentation, Richard Hobbins, INEL. COPIES OF
VIEWGRAPHS

PAPERS MADE AVAILABLE BY MIKE PODOWSKI:
35. "The Modeling of Reactor Pressure Vessel Failure Modes
During Core Meltdown Accidents of BWRs, D. H. Kim, M. Z.
Podowdski, R. T. Lahey, Jr." PAPER
36. "An Analysis of BWR-Core Degradation and Meltdown
Progression Using the MELRPI Computer Code", S. H. Kim, M. Z.
Podowski, and R. T. Lahey, Jr." PAPER
37. "A Study of Using Simulant Materials to Model Core Meltdown
Accidents", M. Z. Podowski, S. Kasprzak, and R. T. Lahey, Jr.
PAPER
38. "The Modeling of BWR Thermal-Hydraulics for Severe Accidents
Analysis, B. R. Koh, M. Z. Podowski and R. T. Lahey, Jr." PAPER

HANDOUTS FROM NRC:
39. Bibliography of work produced by SERI or HCOG for use in
addressing degraded core rulemaking.
40. Summaries of three ESEERCO Source Term Reports.
41. Draft of Summary Description of Cooland Boilaway and Damage
Progression Program Severe Accident Research at PNL, F. E.
Panisko, Pacific Northwest Laboratory.
42. Summary of The ACRR DF-4 BWR Control Blade/Channel Box Fuel
Damage Experiment, R. O. Gaunt, Sandia National Laboratories
(This paper appears to be identical the paper handed out at the
meeting by Randy.)

HANDOUTS FROM FAI
43. "Analysis of the PBF-SFD Fuel Bundle and LWR Cahnnel
Behavior in Degraded Conditions", Ariel Sharon, Fauske and
Associates, Inc.

HANDOUTS PROVIDED BY SANDIA
44. Position papers on all the issues.
45. NUREG-1150 Appendix J
46. NUREG-1150 Appendix L

47. "Advanced Severe Accident Response Models for BWR Application", L. J. Ott, ORNL
48. "Steam Generator Tube Performance: Experience with Water-Cooled Nuclear Power Reactors During 1981", O. S. Tatone and R. S. Pathania, Nuclear Safety, 25, May-June 1984.
49. "Surry Source Term and Consequence Analysis", EPRI NP-4096, June 1985.
50. "Natural Circulation During A Severe Accident: Surry Station Blackout", P. D. Bayless, EGG-SSRE-7858, September 1987.
51. "MELPROG-PWR/MOD1 Analysis of a TMLB' Accident Sequence", J. E. Kelly, R. J. Henninger, J. F. Dearing, NUREG/CR-4742, January 1987.
52. "Effects of Natural Convection Flows on PWR System Temperatures During Severe Accidents", B. R. Sehgal, W. A. Stewart, V. E. Denny, R. C-J Chen, 1985 National Heat Transfer Conference.
53. PWR Primary System Temperatures During Postulated Severe Addicents, V. Denny, B. R. Sehgal, American Nuclear Society Transactions, Vol. 47 (1984).
54. "Roll of Natural Circulation in Severe Accident Analysis", V. Denny, SAIC.
55. "Natural Circulation in Reactor Coolant System", J. T. Han, NUREG-1265, Chapter 2.
56. "Steam Generators", Nuclear Power Experience, Vol. PWR-2, Section D.
57. "Uncertainty Papers on Severe Accident Source Terms", NUREG-1265:
    2. Natural Circulation in Reactor Coolant System, Han
    3. In-Vessel Core Melt Progression and Hydrogen Generation, Wright
    4. High-Pressure Melt Ejection (Direct Containment Heating), Lee
    6. Hydrogen Combustion, Worthington
    7.
58. Hydrogen Generation in BWR Degraded Core Accidents, BWR Core Heatup Code Modeling Basis and Features, Garry Thomas, EPRI. COPIES OF VIEWGRAPHS
59. Hydrogen Generation in BWR Degraded Core Accidents, Summary of EPRI Scoping Study, Garry Thomas, EPRI. COPIES OF VIEWGRAPHS
60. "An Assessment of Hydrogen Generation for the PBF Severe Fuel Damage Scoping and 1-1 Tests", A. Cronenberg, R. Miller and D. Osetek, NUREG/CR-4866, April 1987.
61. Description of accident sequences belonging to cases under consideration for the PWR In-Vessel Hydrogen Production and Mode of Vessel Failure Issues. Walt Murfin, Technadyne
62. Description of additional details of cases being considered for Hot-Leg Failure. Walt Murfin, Technadyne

HANDOUTS PROVIDED BY INEL
63. "Zircaloy Oxidation Behavior in BWR Fuel Bundles Under Severe Accident Conditions", A. W. Cronenberg
64. " Zircaloy Oxidation and Hydrogen Generation Behavior During Severe Accidents", A. W. Cronenberg, ESA, INC.

PROVIDED BY EPRI
65. MAAP User's Manual, Volumes 1 and 2.

PROVIDED BY BNL
66. Letter detailing Zion-Specific accident sequences belonging
to cases under consideration for the (PWR) In-Vessel Hydrogen
Production and Mode of Vessel Failure Issues. Steve Unwin, BNL,
November 17, 1987.

MAILED AFTER THE INITIAL MEETING:

67. Graph provided by Jocelyn Mitchell, NRC, comparing relative
axial power assumed for calculations by MARCH, MELPROG, SCDAP AND
MAAP.
68. Copy of a letter from Peter Cybulskis(Battelle) to Chris
Amos(SAIC) explaining how MARCH keeps track of %Zr oxidyzed in
the vessel.
69. A list, compiled by Sandia analysists of the amount of Zr
contained in the vessels of the five plants considered in the
NUREG-1150 study.
70. A list of additional references. The list was assembled by
the NRC.
71. A letter and attachments from Gary Thomas. It outlines
corrections to a handout provided at the first panel meeting.
72. To all panel members except Steve Hodge considering mode of
vessel breach and hydrogen production in Peach Bottom,
photographs of the core plate and bottom head penetrations from
the Limerick and Peach Bottom plants. They were provided by Greg
Krueger of Philadelphia Electric Company.
73. To all panel members except Steve Hodge, Bob Wright and
Peter Bieniarz, a report on APRIL code modeling.
74. Additional information about the Zion accident sequences
from Steve Unwin at Brookhaven.
75. Reference material for the Temperature Induced Hot Leg and
Steam Generator Tube Rupture issues from R. J. Lutz, Jr. at
Westinghouse Electric Corporation.
76. Comments on the Consideration of Operator Actions in Back-
end Severe Accident Analyses from R. J. Lutz, Jr. at Westinghouse
Electric Corportation.
77. "Sequenced for PWR In-vessel Hydrogen Production Surry and
Sequoyah"
78. List of "Natural Circulation" references, from NRC.
79. To Bill Camp, Bob Lutz and Vern Denny from Roj Sehgal,
"copies of some publications and of a presentation made by Dr. W.
Stewart on the Natural Convection Flows experiments at
Westinghouse R&D Laboratories.
80. To Peter Bieniarz from John Kelly, "Trip Report for CORA
Workshop Meeting", October 23, 1987.
81. By Stone & Webster, E. A. Warman et al, "Fission Product
Transport and Retention in PWR REactor Coolant and Containment
Systems", CSNI/OECD Meeting, Karlsruhe, FRG, Sept. 4, 1984, pp
2-5.

82.   Available at elicitation meeting: M. Donahue et al, "Analysis of Retention Revaporization in a BWR Mark II Power Plant", IAEA Meeting, Columbus, Ohio, Oct. 28-Nov. 1, 1985.
83.   Available at elicitation meeting: P. B. Bieniarz, "Report on the Analysis of TCI Sequence for Fitzpatrick Nuclear Station, December 31, 1987.

DISTRIBUTION:

Frank Abbe,
U. K. Atomic Ere   Authority
Wigshaw Lane, Co...neth
Warrington, Cheshire, WA3 4NE
ENGLAND

Kiyoharu Abe
Department of Reactor Safety
  Research
Nuclear Safety Research Center
ToKai Research Establishment
JAERI
Tokai-mura, Naga-gun
Ibaral.i-ken,
JAPAN

Ulvi Adalioglu
Nuclear Engineering Division
Cekmece Nuclear Research and
  Training Centre
P.K.1, Havaalani
Istanbul
TURKEY

Bharat Agrawal
USNRC-RES/AEB
MS: NL/N-344

Kiyoto Iizawa
Safety Research Group
Reactor Research and Development
  Project
PNC
9-13m 1-Chome Akasaka
Minatu-Ku
Tokyo
JAPAN

Oguz Akalin
Ontario Hydro
700 University Avenue
Toronto, Ontario
CANADA M5G 1X6

David Aldrich
Science Applications International
  Corporation
1710 Goodridge Drive
McLean, VA 22102

Agustin Alonso
University Politecnica De Madrid
J Gutierrez Abascal, 2
28006 Madrid
SPAIN

Christopher Amos
Science Applications International
  Corporation
2109 Air Park Road SE
Albuquerque, NM 87106

Richard C. Anoba
Project Ergr., Corp. Nuclear Safety
Carolina Power and Light Co.
P. O. Box 1551
Raleigh, NC 27602

George Apostolakis
UCLA
Boelter Hall, Room 5532
Los Angeles, CA 90024

James W. Ashkar
Boston Edison Company
800 Boylston Street
Boston, MA 02199

Donald H. Ash n.
Bechtel Power Corporation
P.O. Box 2166
Houston, TX 77252-2166

J.   Assuncao
Cab. ce de Proteccao e Seguranca
  Nuclear
Secretario de Estado de Energia
Ministerio da Industria
av. da Republica, 45-6°
1000 Lisbon
PORTUGAL

Mark Averett
Florida Power Corporation
P.O. Box 14042
St. Petersburg, FL 33733

Raymond O. Bagley
Northeast Utilities
P.O. Box 270
Hartford, CT 06141-0270

Juan Bagues
Consejo de Seguridad Nucleare
Sarangela de la Cruz 3
28020 Madrid
SPAIN

George F. Bailey
Washington Public Power Supply
 System
P. O. Box 968
Richland, WA 99352

H. Bairiot
Belgonucleaire S A
Rue do Champ de Mars 25
B-1050 Brussels
BELGIUM

Louis Baker
Reactor Analysis and Safety
 Division
Building 207
Argonne National Laboratory
9700 South Cass Avenue
Argonne, IL 60439

H-P. Balfanz
TUV-Norddeutschland
Grosse Bahnstrasse 31,
2000 Hamburg 54
FEDERAL REPUBLIC OF GERMANY

Patrick Baranowsky
USNRC-NRR/OEAB
MS: 11E-22

H. Bargmann
Dept. de Mecanique
Inst. de Machines Hydrauliques
 et de Mecaniques des Fluides
Ecole Polytechnique de Lausanne
CH-1003 Lausanne
M.E. (ECUBLENS)
CH. 1015 Lausanne
SWITZERLAND

Robert A. Bari
Brookhaven National Laboratory
Building 130
Upton, NY 11973

Richard Barrett
USNRC-NRR/PRAE
MS. 10A-2

Kenneth S. Baskin
S. California Edison Company
P.O. Box 800
Rosemead, CA 91770

J. Basselier
Belgonucleaire S A
Rue du Champ de Mars 25, B-1050
Brussels
BELGIUM

Werner Bastl
Gesellschaft Fur Reaktorsicherheit
Forschungsgelande
D-8046 Garching
FEDERAL REPUBLIC OF GERMANY

Anton Bayer
BGA/ISH/ZDB
Postfach 1108
D-8042 Neuherberg
FEDERAL REPUBLIC OF GERMANY

Ronald Bayer
Virginia Electric Power Co.
P. O. Box 26666
Richmond VA 23261

Eric S. Beckjord
Director
USNRC-RES
MS: NL/S-007

Bruce B. Beckley
Public Service Company
P.O. Box 330
Manchester, NH 03105

William Beckner
USNRC-RES/SAIB
MS: NL/S-324

Robert M. Bernero
Director
USNRC-NMSS
MS: 6A-4

Ronald Berryman [2]
Virginia Electric Power Co.
P. O. Box 26666
Richmond, VA 23261

Robert C. Bertucio
NUS Corporation
1301 S. Central Ave, Suite 202
Kent, WA 98032

John H. Bickel
EG&G Idaho
P.O. Box 1625
Idaho Falls, ID 83415

Peter Bieniarz
Risk Management Association
2309 Dietz Farm Road, NW
Albuquerque, NM 87107

Adolf Birkhofer
Gesellschaft Fur Reaktorsicherheit
Forschungsgelande
D-8046 Garching
FEDERAL REPUBLIC OF GERMANY

James Blackburn
Illinois Dept. of Nuclear Safety
1035 Outer Park Drive
Springfield, IL 62704

Dennis C. Bley
Pickard, Lowe & Garrick, Inc.
2260 University Drive
Newport Beach, CA 92660

Roger M. Blond
Science Applications Int. Corp.
20030 Century Blvd., Suite 201
Germantown, MD 20874

Simon Board
Central Electricity Generating
  Board
Technology and Planning Research
  Division
Berkeley Nuclear Laboratory
Berkeley Gloucestershire, GL139PB
UNITED KINGDOM

Mario V. Bonace
Northeast Utilities Service Company
P.O. Box 270
Hartford, CT 06101

Gary J. Boyd
Safety and Reliability Optimization
  Services
9724 Kingston Pike, Suite 102
Knoxville, TN 37922

Robert J. Breen
Electric Power Research Institute
3412 Hillview Avenue
Palo Alto, CA 94303

Charles Brinkman
Combustion Engineering
7910 Woodmont Avenue
Bethesda, MD 20814

K. J. Brinkmann
Netherlands Energy Res. Fdtn.
P.O. Box 1
17_.__ Petten NH
NETHERLANDS

Allan R. Brown
Manager, Nuclear Systems and
  Safety Department
Ontario Hydro
700 University Ave.
Toronto, Ontario M5G1X6
CANADA

Robert G. Brown
TENERA L.P.
1340 Saratoga-Sunnyvale Rd.
Suite 206
San Jose, CA 95129

Sharon Brown
EI Services
1851 So. Central Place, Suite 201
Kent, WA 98031

Ben Buchbinder
NASA, Code QS
600 Maryland Ave. SW
Washington, DC 20546

R. H. Buchholz
Nutech
6835 Via Del Oro
San Jose, CA 95119

Robert J. Budnitz
Future Resources Associates
734 Alameda
Berkeley, CA 94707

Gary R. Burdick
USNRC-RES/DSR
MS: NL/S-007

Arthur J. Buslik
USNRC-RES/PRAB
MS: NL/S-372

M. Bustraan
Netherlands Energy Res. Fdtn.
P.O. Box 1
1755ZG Petten NH
NETHERLANDS

Nigel E. Buttery
Central Electricity Generating
  Board
Booths Hall
Chelford Road, Knutsford
Cheshire, WA168QG
UNITED KINGDOM

Jose I. Calvo Molins
Probabilistic Safety Analysis
  Group
Consejo de Seguridad Nuclear
Sor Angela de la Cruz 3, Pl. 6
28020 Madrid
SPAIN

J. F. Campbell
Nuclear Installations Inspectorate
St. Peters House
Balliol Road, Bootle
Merseyside, L20 3LZ
UNITED KINGDOM

Kenneth S. Canady
Duke Power Company
422 S. Church Street
Charlotte, NC 28217

Lennart Carlsson
IAEA A-1400
Wagramerstrasse 5
P.O. Box 100
Vienna, 22
AUSTRIA

Annick Carnino
Electricite de France
32 Rue de Monceau 8EME
Paris, F5008
FRANCE

G. Caropreso
Dept. for Envir. Protect. & Hlth.
ENEA Cre Casaccia
Via Anguillarese, 301
00100 Roma
ITALY

James C. Carter, III
TENERA L.P.
Advantage Place
308 North Peters Road
Suite 280
Knoxville, TN 37922

Eric Cazzoli
Brookhaven National Laboratory
Building 130
Upton, NY 11..

John G. Cesare
SERI
Director Nuclear Licensing
5360 I-55 North
Jackson, MS 39211

S. Chakraborty
Radiation Protection Section
Div. De La Securite Des Inst. Nuc.
5303 Wurenlingen
SWITZERLAND

Sen-I Chang
Institute of Nuclear Energy
  Research
P.O. Box 3
Lungtan, 325
TAIWAN

J. R. Chapman
Yankee Atomic Electric Company
1671 Worcester Road
Framingham, MA 01701

Robert F. Christie
Tennessee Valley Authority
400 W. Summit Hill Avenue, W10D190
Knoxville, TN 37902

T. Cianciolo
BWR Assistant Director
ENEA DISP TX612167 ENEUR
Rome
ITALY

Thomas Cochran
Natural Resources Defense Council
1350 New York Ave. NW, Suite 300
Washington, D.C.   20005

Frank Coffman
USNRC-RES/HFB
MS: NL/N-316

Larry Conradi
NUS Corporation
16835 W. Bernardo Drive
Suite 202
San Diego, CA 92127

Peter Cooper
U.K. Atomic Energy Authority
Wigshaw Lane, Culcheth
Warrington, Cheshire, WA3 4NE
UNITED KINGDOM

C. Allin Cornell
110 Coquito Way
Portola Valley, CA 94025

Michael Corradini
University of Wisconsin
1500 Johnson Drive
Madison, WI 53706

E. R. Corran
Nuclear Technology Division
ANSTO Research Establishment
Lucas Heights Research Laboratories
Private Mail Bag 7
Menai, NSW 2234
AUSTRALIA

James Costello
USNRC-RES/SSEB
MS: NL/S-217A

George R. Crane
1570 E. Hobble Creek Dr.
Springville, UT 84663

Mat Crawford
SERI
5360 I-55 North
Jackson, MS 39211

Michael C Cullingford
Nuclear Safety Division
IAEA
Wagramerstrasse, 5
P.O. Box 100
A-1400 Vienna
AUSTRIA

Garth Cummings
Lawrence Livermore Laboratory
L-91, Box 808
Livermore, CA 94526

Mark A. Cunningham
USNRC-RES/PRAB
MS: NL/S-372

James J. Curry
7135 Salem Park Circle
Mechanicsburg, PA 17055

Peter Cybulskis
Battelle Columbus Division
505 King Avenue
Columbus, OH 43201

Peter R. Davis
PRD Consulting
1935 Sabin Drive
Idaho Falls, ID 83401

Jose E. DeCarlos
Consejo de Seguridad Nuclear
Sor Angela de la Cruz 3, Pl. 8
28016 Madrid
SPAIN

M. Marc Decreton
Department Technologie
CEN/SCK
Boeretang 200
B-2400 Mol
BELGIUM

Richard S. Denning
Battelle Columbus Division
505 King Avenue
Columbus, OH 43201

Vernon Denny
Science Applications Int. Corp.
5150 El Camino Real, Suite 3
Los Altos, CA 94303

J. Devooget
Faculte des Sciences Appliques
Universite Libre de Bruxelles
av. Franklin Roosevelt
B-1050 Bruxelles
BELGIUM

R. A. Diederich
Supervising Engineer
Environmental Branch
Philadelphia Electric Co.
2301 Market St.
Philadelphia, PA 19101

Raymond DiSalvo
Battell Columbus Division
505 Ki s Avenue
Columbus, OH 43201

Mary T. Drouin
Science Applications International
  Corporation
2109 Air Park Road S.E.
Albuquerque, NM 87106

Andrzej Drozd
Stone and Webster
  Engineering Corp.
243 Summer Street
Boston, MA 02107

N. W. Edwards
NUTECH
145 Martinville Lane
San Jose, CA 95119

Ward Edwards
Social Sciences Research Institute
University of Southern California
Los Angeles, CA 90089-1111

Joachim Ehrhardt
Kernforschungszentrum Karlsruhe/INR
Postfach 3640
D-7500 Karlsruhe 1
FEDERAL REPUBLIC OF GERMANY

Adel A. El-Bassioni
USNRC-NRR/PRAB
MS: 10A-2

J. Mark Elliott
International Energy Associates,
  Ltd., Suite 600
600 New Hampshire Ave., NW
Washington, DC 20037

Farouk Eltawila
USNRC-RES/AEB
MS: NL/N-344

Mike Epstein
Fauske and Associates
P. O. Box 1625
16W070 West 83rd Street
Burr Ridge, IL 60521

Malcolm L. Ernst
USNRC-RGN II

F. R. Farmer
The Long Wood, Lyons Lane
Appleton, Warrington
WA4 5ND
UNITED KINGDOM

P. Fehrenback
Atomic Energy of Canada, Ltd.
Chalk River Nuclear Laboratories
Chalk River Ontario, K0J1P0
CANADA

P. Ficara
ENEA Cre Casaccia
Department for Thermal Reactors
Via Anguillarese, 301
00100 ROMA
ITALY

A. Fiege
Kernforschungszentrum
Postfach 3640
D-7500 Karlsruhe
FEDERAL REPUBLIC OF GERMANY

ohn Flack
SNRC-RES/SAIB
MS: NLS-324

George F. Flanagan
Oak Ridge National Laboratory
P.O. Box Y
Oak Ridge, TN 37831

Karl N. Fleming
Pickard, Lowe & Garrick, Inc.
2260 University Drive
Newport Beach, CA 92660

Terry Foppe
Rocky Flats Plant
P. O. Box 464, Building T886A
Golden, CO 80402-0464

Joseph R. Fragola
Science Applications International
 Corporation
274 Madison Avenue
New York, NY 10016

Wiktor Frid
Swedish Nuclear Power Inspectorate
Division of Reactor Technology
P. O. Box 27106
S-102 52 Stockholm
SWEDEN

James Fulford
NUS Corporation
910 Clopper Road
Gaithersburg, MD 20878

Urho Pulkkinen
Technical Research Centre of
Finland
Electrical Engineering Laboratory
Otakaari 7 B
SF-02150 Espoo 15
FINLAND

J. B. Fussell
JBF Associates, Inc.
1630 Downtown West Boulevard
Knoxville, TN 37919

John Garrick
Pickard, Lowe & Garrick, Inc.
2260 University Dri e
Newport Beach, CA 92660

John Gaunt
British Embassy
3100 Massachusetts Avenue, NW
Washington, DC 20008

Jim Gieseke
Battelle Columbus Division
505 King Avenue
Columbus, OH 43201

Frank P. Gillespie
USNRC-NRR/PMAS
MS: 12G-18

Ted Ginsburg
Department of Nuclear Energy
Building 820
Brookhaven National Laboratory
Upton, NY 11973

James C. Glynn
USNRC-RES/PRAB
MS: NL/S-372

P. Govaerts
Departement de la Surete Nucleaire
Association Vincotte
avenue du Roi 157
B-1060 Bruxelles
BELGIUM

George Greene
Building 820M
Brookhaven National Laboratory
Upton, NY 11973

Carrie Grimshaw
Brookhaven National Laboratory
Building 130
Upton, NY 11973

H. J. Van Grol
Energy Technology Division
Energieonderzoek Centrum Nederland
Westerduinweg 3
Postbus 1
NL-1755 Petcen ZG
NETHERLANDS

Sergio Guarro
Lawrence Livermore Laboratories
P. O. Box 808
Livermore, CA 94550

Mike Hitchler
Westinghouse Electric Corp.
Savanna River Site
Aiken, SC 29808

Richard Hobbins
EG&G Idaho
P. O. Box 1625
Idaho Falls, ID 83415

Steven Hodge
Oak Ridge National Laboratory
P.O. Box Y
Oak Ridge, TN 37831

Lars Hoegberg
Office of Regulation and Research
Swedish Nuclear Power Inspectorate
P. O. Box 27106
S-102 52 Stockholm
SWEDEN

Lars Hoeghort
IAEA A-1400
Wagranerstraase 5
P.O. Box 100
Vienna, 22
AUSTRIA

Edward Hofer
Giesellschaft Fur Reaktorsicherheit
Forschurgsgelande
D-8046 Garching
FEDERAL REPUBLIC OF GERMANY

Peter Hoffmann
Kernforschingszentrum Karlsruhe
Institute for Material
  Und Festkorperforsching I
Postfach 3640
D-7500 Karlsruhe 1
FEDERAL REPUBLIC OF GERMANY

N. J. Holloway
UKAEA Safety and Reliability
  Directorate
Wigshaw Lane, Culcheth
Warrington, Cheshire, WA34NE
UNITED KINGDOM

Stephen C. Hora
University of Hawaii at Hilo
Division of Business Administration
  and Economics
College of Arts and Sciences
Hilo, HI 96720-4091

J. Peter Hoseman
Swiss Federal Institute for
  Reactor Research
CH-5303, Wurenlingen
SWITZERLAND

Thomas C. Houghton
KMC, Inc.
1747 Pennsylvania Avenue, NW
Washington, DC 20006

Dean Houston
USNRC-ACRS
MS: P-315

Der Yu Hsia
Taiwan Atomic Energy Council
67, Lane 144, Keelung Rd.
Sec. 4
Taipei
TAIWAN

Alejandro Huerta-Bahena
National Commission on Nuclear
  Safety and Safeguards (CNSNS)
Insurgentes Sur N. 1776
Col. Florida
C. P. 04230 Mexico, D.F.
MEXICO

Kenneth Hughey [2]
SERI
5360 I-55 North
Jackson, MS 39211

Won-Guk Hwang
Kzunghee University
Yongin-Kun
Kyunggi-Do 170-23
KOREA

Michio Ichikawa
Japan Atomic Energy Research
  Institute
Dept. of Fuel Safety Research
Tokai-Mura, Naka-Gun
Ibaraki-Ken, 319-1
JAPAN

Sanford Israel
USNRC-AEOD/ROAB
MS: MNBB-9715

Krishna R. Iyengar
Louisiana Power and Light
200 A Huey P. Long Avenue
Gretna, LA 70053

Jerry E. Jackson
USNRC-RES
MS: NL/S-302

R. E. Jaquith
Combustion Engineering, Inc.
1000 Prospect Hill Road
M/C 9490-2405
Windsor, CT 06095

S. E. Jensen
Exxon Nuclear Company
2101 Horn Rapids Road
Richland, WA 99352

Kjell Johannson
Studsvik Energiteknik AB
S-611 82, Nykoping
SWEDEN

Richard John
SSM, Room 102
927 W. 35th Place
USC, University Park
Los Angeles, CA 90089-0021

D. H. Johnson
Pickard, Lowe & Garrick, Inc.
2260 University Drive
Newport Beach, CA 92660

W. Reed Johnson
Department of Nuclear Engineering
University of Virginia
Reactor Facility
Charlottesville, VA 22901

Jeffery Julius
NUS Corporation
1301 S. Central Ave, Suite 202
Kent, WA 98032

H. R. Jun
Korea Adv. Energy Research Inst.
P.O. Box 7, Daeduk Danju
Chungnam 300-31
KOREA

Peter Kafka
Gesellschaft Fur Reaktorsicherheit
Forschungsgelande
D-8046 Garching
FEDERAL REPUBLIC OF GERMANY

Geoffrey D. Kaiser
Science Application Int. Corp.
1710 Goodridge Drive
McLean, VA 22102

William Kastenberg
UCLA
Boelter Hall, Room 5532
Los Angeles, CA 90024

Walter Kato
Brookhaven National Laboratory
Associated Universities, Inc.
Upton, NY 11973

M. S. Kazimi
MIT. 24-219
Cambridge, MA 02139

Ralph L. Keeney
101 Lombard Street
Suite 704W
San Francisco, CA 94111

Henry Kendall
Executive Director
Union of Concerned Scientists
Cambridge, MA

Frank King
Ontario Hydro
700 University Avenue
Bldg. H11 G5
Toronto
CANADA M5G1X6

Oliver D. Kingsley, Jr.
Tennessee Valley Authority
1101 Market Street
GN-38A Lookout Place
Chattanooga, TN 37402

Stephen R. Kinnersly
Winfrith Atomic Energy
  Establishment
Reactor Systems Analysis Division
Winfrith, Dorchester
Dorset DT2 8DH
ENGLAND

Ryohel Kiyose
University of Tokyo
Dept. of Nuclear Engineering
7-3-1 Hongo Bunkyo
Tokyo 113
JAPAN

George Klopp
Commonwealth Edison Company
P.O. Box 767, Room 35W
Chicago, IL 60690

Klaus Koberlein
Gesellschaft Fur Reaktorsicherheit
Forschungsgelande
D-8046 Garching
FEDERAL REPUBLIC OF GERMANY

E. Kohn
Atomic Energy Canada Ltd.
Candu Operations
Mississauga
Ontario, L5K 1B2
CANADA

Alan M. Kolaczkowski
Science Applications International
  Corporation
2109 Air Park Road, S.E.
Albuquerque, NM 87106

S. Kondo
Department of Nuclear Engineering
Facility of Engineering
University of Tokyo
3-1, Hongo 7, Bunkyo-ku
Tokyo
JAPAN

Herbert J. C. Kouts
Brookhaven National Laboratory
Building 179C
Upton, NY 11973

Thomas Kress
Oak Ridge National Laboratory
P.O. Box Y
Oak Ridge, TN 37831

W. Kroger
Institut fur Nukleare
  Sicherheitsforschung
Kernforschungsanlage Julich GmbH
Postfach 1913
D-5170 Julich 1
FEDERAL REPUBLIC OF GERMANY

Greg Krueger [?]
Philadelphia Electric Co.
2301 Market St.
Philadelphia, PA 19101

Bernhard Kuczera
Kernforschungzentrum Karlsruhe
LWR Safety Project Group (PRS)
P. O. Box 3640
D-7500 Karlsruhe 1
FEDERAL REPUBLIC OF GERMANY

Jeffrey L. LaChance
Science Applications International
  Corporation
2109 Air Park Road S.E.
Albuquerque, NM 87106

H. Larsen
Riso National Laboratory
Postbox 49
DK-4000 Roskilde
DENMARK

Wang L. Lau
Tennessee Valley Authority
400 West Summit Hill Avenue
Knoxville, TN 37902

Timothy J. Leahy
EI Services
1851 South Central Place, Suite 201
Kent, WA 98031

John C. Lee
University of Michigan
North Campus
Dept. of Nuclear Engineering
Ann Arbor, MI 48109

Tim Lee
USNRC-RES/RPSB
MS: NL/N-353

Mark T. Leonard
Science Applications International
  Corporation
2109 Air Park Road, SE
Albuquerque, NM 87106

Leo LeSage
Director, Applied Physics Div.
Argonne National Laboratory
Building 208, 9700 South Cass Ave.
Argonne, IL 60439

Milton Levenson
Bechtel Western Power Company
50 Beale St.
San Francisco, CA 94119

Librarian
NUMARC/USCEA
1776 I Street NW, Suite 400
Washington, DC 80006

Eng Lin
Taiwan Power Company
242, Roosevelt Rd., Sec. 3
Taipei
TAIWAN

N. J. Liparulo
Westinghouse Electric Corp.
P. O. Box 355
Pittsburgh, PA 15230

Y. H. (Ben) Liu
Department of Mechanical
  Engineering
University of Minnesota
Minneapolis, MN 55455

Bo Liwnang
IAEA A-1400
Swedish Nuclear Power Inspectorate
P.O. Box 27106
S-102 52 Stockholm
SWEDEN

J. P. Longworth
Central Electric Generating Board
Berkeley Gloucester
GL13 9PB
UNITED KINGDOM

Walter Lowenstein
Electric Power Research Institute
3412 Hillview Avenue
P. O. Box 10412
Palo Alto, CA 94303

William J. Luckas
Brookhaven National Laboratory
Building 130
Upton, NY 11973

Hans Ludewig
Brookhaven National Laboratory
Building 130
Upton, NY 11973

Robert J. Lutz, Jr.
Westinghouse Electric Corporation
Monroeville Energy Center
EC-E-371, P. O. Box 355
Pittsburgh, PA 15230-0355

Phillip E. MacDonald
EG&G Idaho, Inc.
P.O. Box 1625
Idaho Falls, ID 83415

Jim Mackenzie
World Resources Institute
1735 New York Ave. NW
Washington, DC 20006

Richard D. Fowler
Idaho Nat. Engineering Laboratory
P.O. Box 1625
Idaho Falls, ID 83415

A. P. Malinauskas
Oak Ridge National Laboratory
P.O. Box Y
Oak Ridge, TN 37831

Giuseppe Mancini
Commission European Comm.
CEC-JRC Eraton
Ispra Varese
ITALY

Lasse Mattila
Technical Research Centre of
  Finland
Lonnrotinkatu 37, P. O. Box 169
SF-00181 Helsinki 18
FINLAND

Roger J. Mattson
SCIENTECH Inc.
11821 Parklawn Dr.
Rockville, MD 20852

Donald McPherson
USNRC-NRR/DONRR
MS: 12G-18

Jim Metcalf
Stone and Webster Engineering
  Corporation
245 Summer St.
Boston, MA 02107

Mary Meyer
A-1, MS F600
Los Alamos National Laboratory
Los Alamos, NM 87545

Ralph Meyer
USNRC-RES/AEB
MS: NL/N-344

Charles Miller
8 Hastings Rd.
Momsey, NY 10952

Joseph Miller
Gulf States Utilities
P. O. Box 220
St. Francisville, LA 70775

William Mims
Tennessee Valley Authority
400 West Summit Hill Drive.
W10D199C-K
Knoxville, TN 37902

Jocelyn Mitchell
USNRC-RES/SAIB
MS: NL/S-324

Kam Mohktarian
CBI Na-Con Inc.
800 Jorie Blvd.
Oak Brook, IL 60521

James Moody
P.O. Box 641
Rye, NH 03870

S. Mori
Nuclear Safety Division
OECD Nuclear Energy Agency
38 Blvd. Suchet
75016 Paris
FRANCE

Walter B. Murfin
P.O. Box 550
Mesquite, NM 88048

Joseph A. Murphy
USNRC-RES/DSR
MS: NL/S-007

V. I. Nath
Safety Branch
Safety Engineering Group
Sheridan Park Research Community
Mississauga, Ontario L5k 1B2
CANADA

Susan J. Niemczyk
1545 18th St. NW, #112
Washington, DC 20036

Pradyot K. Niyogi
USDOE-Office of Nuclear Safety
Washington, DC 20545

Paul North
EG&G Idaho, Inc.
P. O. Box 1625
Idaho Falls, ID 83415

Edward P. O'Donnell
Ebasco Services, Inc.
2 World Trade Center, 89th Floor
New York, NY 10048

David Okrent
UCLA
Boelter Hall, Room 5532
Los Angeles, CA 90024

Robert L. Olson
Tennessee Valley Authority
400 West Summit Hill Rd.
Knoxville, TN 37902

Simon Ostrach
Case Western Reserve University
418 Glennan Bldg.
Cleveland, OH 44106

D. Paddleford
Westinghouse Electric Corporation
Savanna River Site
Aiken, SC 29808

Robert L. Palla, Jr.
USNRC-NRR/PRAB
MS: 10A-2

Chang K. Park
Brookhaven National Laboratory
Building 130
Upton, NY 11973

Michael C. Parker
Illinois Department of Nuclear
  Safety
1035 Outer Park Dr.
Springfield, IL 62704

Gareth Parry
NUS Corporation
910 Clopper Road
Gaithersburg, MD 20878

J. Pelce
Departement de Surete Nucleaire
IPSN
Centre d'Estudes Nucleaires du CEA
B.P. no. 6, Cedex
F-92260 Fontenay-aux-Roses
FRANCE

J. Petrangeli
ENEA Nuclear Energy ALT Disp
Via V. Brancati, 48
00144 Rome
ITALY

Marty Plys
Fauske and Associates
16W070 West 83rd St.
Burr Ridge, IL 60521

Mike Podowski
Department of Nuclear Engineering
  and Engineering Physics
RPI
Troy, NY 12180-3590

Robert D. Pollard
Union of Concerned Scientists
1616 P Street, NW, Suite 310
Washington, DC 20036

R. Potter
UK Atomic Energy Authority
Winfrith, Dorchester
Dorset, DT2 8DH
UNITED KINGDOM

William T. Pratt
Brookhaven National Laboratory
Building 130
Upton, NY 11973

M. Preat
Chef du Service Surete Nucleaire et
  Assurance Qualite
TRACTEBEL
Bd. du Regent 8
B-100 Bruxells
BELGIUM

David Pyatt
USDOE
MS: EH-332
Washington, DC 20545

William Raisin
NUMAEC
1726 M St. NW
Suite 904
Washington, DC 20036

Joe Rashid
ANATECH Research Corp.
3344 N. Torrey Pines Ct.
Suite 1320
La Jolla, CA 90237

Dale M. Rasmuson
USNRC-RES/PRAB
MS: NL/S-372

Ingvard Rasmussen
Riso National Laboratory
Postbox 49
DK-4000, Roskilde
DENMARK

Norman C. Rasmussen
Massachusetts Institute of
  Technology
77 Massachusetts Avenue
Cambridge, MA 02139

John W. Reed
Jack R. Benjamin & Associates, Inc.
444 Castro St., Suite 501
Mountain View, CA 94041

David B. Rhodes
Atomic Energy of Canada, Ltd.
Chalk River Nuclear Laboratories
Chalk River, Ontario K0J1P0
CANADA

Dennis Richardon
Westinghouse Electric Corporation
P.O. Box 355
Pittsburgh, PA 15230

Doug Richeard
Virginia Electric Power Co.
P.O.Box 26666
Richmond, VA 23261

Robert Ritzman
Electric Power Research Institute
3412 Hillview Avenue
Palo Alto, CA 94304

Richard Robinson
USNRC-RES/PRAB
MS: NL/S-372

Jack E. Rosenthal
USNRC-AEOD/ROAB
MS: MNBB-9715

Denwood F. Ross
USNRC-RES
MS: NL/S-007

Frank Rowsome
9532 Fern Hollow Way
Gaithersburg, MD 20879

Wayne Russell
SERI
5360 I-55 North
Jackson, MS 39211

Jorma V. Sandberg
Finnish Ctr. Rad. Nucl. and Safety
Department of Nuclear Safety
P.O. Box 268
SF-00101 Helsinki
FINLAND

G. Saponaro
ENEA Nuclear Engineering Alt.
Zia V Brancati 4B
00144 ROME
ITALY

M. Sarran
United Engineers
P. O. Box 8223
30 S 17th Street
Philadelphia, PA 19101

Marty Sattison
EG&G Idaho
P. O. Box 1625
Idaho Falls, ID 83415

George D. Sauter
Electric Power Research Institute
3412 Hillview Avenue
Palo Alto, CA 94303

Jorge Schulz
Bechtel Western Power Corporation
50 Beale Street
San Francisco, CA 94119

B. R. Sehgal
Electric Power Research Institute
3412 Hillview Avenue
Palo Alto, CA 94303

Subir Sen
Bechtel Power Corp.
15740 Shady Grove Road
Location 1A-7
Gaithersburg, MD 20877

S. Serra
Ente Nazionale per l'Energia
  Electtrica (ENEL)
via G. B. Martini 3
Rome
ITALY

Bonnie J. Shapiro
Science Applications International
  Corporation
360 Bay Street
Suite 200
Augusta, GA 30901

H. Shapiro
Licensing and Risk Branch
Atomic Energy of Canada Ltd.
Sheridan Park Research Community
Mississauga, Ontario L5K 1B2
CANADA

Dave Sharp
Westinghouse Savannah River Co.
Building 773-41A, P. O. Box 616
Aiken, SC 29802

John Sherman
Tennessee Environmental Council
1719 West End Avenue, Suite 227
Nashville, TN 37203

Brian Sheron
USNRC-RES/DSR
MS: NL/N-007

Rick Sherry
JAYCOR
P. O. Box 85154
San Diego, CA 92138

Steven C. Sholly
MHB Technical Associates
1723 Hamilton Avenue, Suite K
San Jose, CA 95125

Louis M. Shotkin
USNRC-RES/RPSB
MS: NL/N-353

M. Siebertz
Chef de la Section Surete' des
  Reacteurs
CEN/SCK
Boeretang, 200
B-2400 Mol
BELGIUM

Melvin Silberberg
USNRC-RES/DE/WNB
MS: NL/S-260

Gary Smith
SERI
5360 I-55 North
Jackson, MS 39211

Gary L. Smith
Westinghouse Electric Corporation
Hanford Site
Box 1970
Richland, WA 99352

Lanny N. Smith
Science Applications International
  Corporation
2109 Air Park Road SE
Albuquerque, NM 87106

K. Soda
Japan Atomic Energy Res. Inst.
Tokai-Mura Naka-Gun
Ibaraki-Ken 319-11
JAPAN

David Sommers
Virginia Electric Power Company
P. O. Box 26666
Richmond, VA 23261

Herschel Spector
New York Power Authority
123 Main Street
White Plains, NY 10601

Themis P. Speis
USNRC-RES
MS: NL/S-007

Klaus B. Stadie
OECD-NEA, 38 Bld. Suchet
75016 Paris
FRANCE

John Stetkar
Pickard, Lowe & Garrick, Inc.
2216 University Drive
Newport Beach, CA 92660

Wayne L. Stiede
Commonwealth Edison Company
P.O. Box 767
Chicago, IL 60690

William Stratton
Stratton & Associates
2 Acoma Lane
Los Alamos, NM 87544

Soo-Pong Suk
Korea Advanced Energy Research
 Institute
P. O. Box 7
Daeduk Danji, Chungnam 300-31
KOREA

W. P. Sullivan
GE Nuclear Energy
175 Curtner Ave., M/C 789
San Jose, CA 95125

Tony Taig
U.K. Atomic Energy Authority
Wigshaw Lane, Culcheth
Warrington, Cheshire, WA3 4NE
UNITED KINGDOM

John Taylor
Electric Power Research Institute
3412 Hillview Avenue
Palo Alto, CA 94303

Harry Teague
U.K. Atomic Energy Authority
Wigshaw Lane, Culcheth
Warrington, Cheshire, WA3 4NE
UNITED KINGDOM

Technical Library
Electric Power Research Institute
P.O. Box 10412
Palo Alto, CA 94304

Mark I. Temme
General Electric, Inc.
P.O. Box 3508
Sunnyvale, CA 94088

T. G. Theofanous
University of California, S.B.
Department of Chemical and Nuclear
 Engineering
Santa Barbara, CA 93106

David Teolis
Westinghouse-Bettis Atomic Power
 Laboratory
P. O. Box 79, ZAP 34N
West Mifflin, PA 15122-0079

Ashok C. Thadani
USNRC-NRR/SAD
MS: 7E-4

Garry Thomas
L-499 (Bldg. 490)
Lawrence Livermore National
 Laboratory
7000 East Ave.
P.O. Box 808
Livermore, CA 94550

Gordon Thompson
Institute for Research and
 Security Studies
27 Ellworth Avenue
Cambridge, MA 02139

Grant Thompson
League of Women Voters
1730 M. Street, NW
Washington, DC 20036

Arthur Tingle
Brookhaven National Laboratory
Building 130
Upton, NY 11973

Rich Toland
United Engineers and Construction
30 S. 17th St., MS 4V7
Philadelphia, PA 19101

Brian J. R. Tolley
DG/XII/D/1
Commission of the European
 Communities
Rue de la Loi, 200
B-1049 Brussels
BELGIUM

David R. Torg
Atomic Energy of Canada Ltd.
Whiteshell Nuclear
  Research Establishment
Pinawa, Manitoba, ROE 1LO
CANADA

Alfred F. Torri
Pickard, Lowe & Garrick, Inc.
191 Calle Magdalena, Suite 290
Encinitas, CA 92024

Klau Trambauer
Gesellschaft Fur Reaktorsicherheit
Forschungsgelande
D-8046 Garching
FERERAL REPUBLIC OF GERMANY

Nicholas Tsoulfanidis
Nuclear Engineering Dept.
University of Missouri-Rolla
Rolla, MO 65401-0249

Chao-Chi Tung
c/o H.B. Bengelsdorf
ERC Environmental Services Co.
P. O. Box 10130
Fairfax, VA 22030

Brian D Turland
UKAEA Culham Laboratory
Abingdon, Oxon OX14 3DB
ENGLAND

Takeo Uga
Japan Institute of Nuclear Safety
Nuclear Power Engineering Test
  Center
3-6-2, Toranomon
Minato-ku, Tokyo 108
JAPAN

Stephen D. Unwin
Battelle Columbus Division
505 King Avenue
Columbus, OH 43201

A. Valeri
DISP
ENEA
Via Vitaliano Brancati, 48
I-00144 Rome
ITALY

Harold VanderMolen
USNRC-RES/PRAB
MS: NL/S-372

G. Bruce Varnado
ERC International
1717 Louisiana Blvd. NE, Suite 202
Albuquerque, NM 87110

Jussi K. Vaurio
Imatran Voima Oy
Loviisa NPS
SF-07900 Loviisa
FINLAND

William E. Vesely
Science Applications International
  Corporation
2929 Kenny Road, Suite 245
Columbus, OH 43221

J. I. Villadoniga Tallon
Div. of Analysis and Assessment
Consejo de Seguridad Nuclear
c/ Sor Angela de la Cruz, 3
28020 Madrid
SPAIN

Willem F. Vinck
Kapellestract 25
1980
Tervuren
BELGIUM

R. Virolainen
Office of Systems Integration
Finnish Centre for Radiation and
  Nuclear Safety
Department of Nuclear Safety
P.O. Box 268
Kumpulantie 7
SF-00520 Helsinki
FINLAND

Raymond Viskanta
School of Mechanical Engineering
Purdue University
West Lafayette, IN 47907

S. Visweswaran
General Electric Company
175 Curtner Avenue
San Jose, CA 95125

Truong Vo
Pacific Northwest Laboratory
Battelle Blvd.
Richland, WA 99352

Richard Vogel
Electric Power Research Institute
P. O. Box 10412
Palo Alto, CA 94303

G. Volta
Engineering Division
CEC Joint Research Centre
CP No. 1
I-21020 Ispra (Varese)
ITALY

Ian B. Wall
Electric Power Research Institute
3412 Hillview Avenue
Palo Alto, CA 94303

Adolf Walser
Sargent and Lundy Engineers
55 E. Monroe Street
Chicago, IL 60603

Edward Warman
Stone & Webster Engineering Corp.
P.O. Box 2325
Boston, MA 02107

Norman Weber
Sargent & Lundy Co.
55 E. Monroe Street
Chicago, IL 60603

Lois Webster
American Nuclear Society
555 N. Kensington Avenue
La Grange Park, IL 60525

Wolfgang Werner
Gesellschaft Fur Reaktorsicherheit
Forschungsgelande
D-8046 Garching
FEDERAL REPUBLIC OF GERMANY

Don Wesley
IMPELL
1651 East 4th Street
Suite 210
Santa Ana, CA 92701

Detlof von Winterfeldt
Institute of Safety and Systems
  Management
University of Southern California
Los Angeles, CA 90089-0021

Pat Worthington
USNRC-RES/AEB
MS: NL/N-344

John Wreathall
Science Applications International
  Corporation
2929 Kenny Road, Suite 245
Columbus, OH 4322.

D. J. Wren
Atomic Energy of Canada Ltd.
Whiteshell Nuclear Research
  Establishment
Pinawa, Manitoba, ROE 1LO
CANADA

Roger Wyrick
Inst. for Nuclear Power Operations
1100 Circle 75 Parkway, Suite 1500
Atlanta, GA 30339

Kun-Joong Yoo
Korea Advanced Energy Research
  Institute
P. O. Box 7
Daeduk Danji, Chungnam 300-31
KOREA

Faith Young
Energy People, Inc.
Dixou Springs, TN 37057

Jonathan Young
R. Lynette and Associates
15042 Northeast 40th St.
Suite 206
Redmond, WA 98052

C. Zaffiro
Division of Safety Studies
Directorate for Nuclear Safety and
  Health Protection
Ente Nazionale Energie Alternative
Via Vitaliano Brancati, 48
I-00144 Rome
ITALY

Mike Zentner
Westinghouse Hanford Co.
P. O. Box 1970
Richland, WA 99352

X. Zikidis
Greek Atomic Energy Commission
Agia Paraskevi, Attiki
Athens
GREECE

Bernhard Zuczera
Kernforschungszentrum
Postfach 3640
D-7500 Karlsruhe
FEDERAL REPUBLIC OF GERMANY

1521 J. R. Weatherby
3141 S. A. Landenberger [5]
3151 W. I. Klein
5214 D. B. Clauss
6344 E. D. Gorham
6411 D. D. Carlson
6411 R. J. Breeding
6411 D. M. Kunsman
6400 D. J. McCloskey
6410 D. A. Dahlgren
6412 A. L. Camp
6412 S. L. Daniel
6412 T. M. Hake
6412 L. A. Miller
6412 D. B. Mitchell
6412 A. C. Payne, Jr.
6412 T. T. Sype
6412 T. A. Wheeler
6412 D. W. Whitehead
6413 T. D. Brown
6413 F. T. Harper [2]
6415 R. M. Cranwell
6415 W. R. Cramond [3]
641. R. L. Iman
6418 J. E. Kelly
6418 K. J. Maloney
6419 M. P. Bohn
6419 J. A. Lambright
6422 D. A. Powers
6424 K. D. Bergeron
6424 J. J. Gregory
6424 D. R. Bradley
6424 D. C. Williams
6425 S. S. Dosanjh
6453 J. S. Philbin

6460 J. V. Walker
6463 M. Berman
6463 M. P. Sherman
6471 L. D. Bustard
6473 W. A. von Riesemann
8524 J. A. Wackerly

U.S. NUCLEAR REGULATORY COMMISSION

BIBLIOGRAPHIC DATA SHEET

(See instructions on the reverse)

2. TITLE AND SUBTITLE

Evaluation of Severe Accident Risks:
Quantification of Major Input Parameters

Expert Opinion Elicitation on In-Vessel Issues

3. DATE REPORT PUBLISHED

MONTH	YEAR
December	1990

4. FIN OR GRANT NUMBER

A1322

5. AUTHOR(S)

F.T. Harper, R.J. Breeding, T.D. Brown, J.J. Gregory,
A.C. Payne, E.D. Gorham, C.N. Amos*

* Science Applications International Corporation

6. TYPE OF REPORT

Technical

7. PERIOD COVERED *(Inclusive Dates)*

8. PERFORMING ORGANIZATION — NAME AND ADDRESS *(If NRC, provide Division, Office or Region, U.S. Nuclear Regulatory Commission, and mailing address; if contractor, provide name and mailing address.)*

Sandia National Laboratories
P. O. Box 5800
Albuquerque, NM 87185

10. SUPPLEMENTARY NOTES

11. ABSTRACT *(200 words or less)*

In support of the Nuclear Regulatory Commission's (NRC's) assessment of the risk
from severe accidents at commercial nuclear power plants in the U.S. reported in
NUREG-1150, the Severe Accident Risk Reduction Program (SARRP) has completed a
revised calculation of the risk to the general public from severe accidents at
five nuclear power plants: Surry, Sequoyah, Zion, Peach Bottom and Grand Gulf.

The emphasis in this risk analysis was not on determining a "so-called" point
estimate of risk. Rather, it was to determine the distribution of risk, and to
discover the uncertainties that account for the breadth of this distribution.
Off-site risk initiation by events, both internal to the power station and external
to the power station were assessed.

Much of the important input to the logic models was generated by expert panels.
This document presents the distributions and the rationale supporting the
distributions for the questions posed to the In-Vessel Expert Panel.

12. KEY WORDS/DESCRIPTORS *(List words or phrases that will assist researchers in locating the report.)*

Probabilistic Risk Assessment, Reactor Safety, Severe Accidents,
In-Vessel Accident Progression, Bottom Head Failure, In-Vessel
Hydrogen Generation, Hot Leg Failure, Steam Generator Tube
Rupture

13. AVAILABILITY STATEMENT

Unlimited

14. SECURITY CLASSIFICATION

(This Page)

Unclassified

(This Report)

Unclassified

15. NUMBER OF PAGES

16. PRICE